TECHNISCHE UNIVERSITÄT MÜNCHEN
Fakultät für Elektrotechnik und Informationstechnik
Professur für Methoden der Signalverarbeitung

Reduced-Entropy Signals in MIMO Communication Systems

Christoph A. Hellings

Vollständiger Abdruck der von der Fakultät für Elektrotechnik und Informationstechnik der Technischen Universität München zur Erlangung des akademischen Grades eines

Doktor-Ingenieurs

genehmigten Dissertation.

Vorsitzende: Prof. Dr.-Ing. Sandra Hirche
Prüfende der Dissertation:
1. Prof. Dr.-Ing. Wolfgang Utschick
2. Prof. Dr.-Ing. Eduard Jorswieck

Die Dissertation wurde am 14.06.2017 bei der Technischen Universität München eingereicht und durch die Fakultät für Elektrotechnik und Informationstechnik am 16.11.2017 angenommen.

Abstract

Unlike in single-user systems, where maximum-entropy signals are optimal, transmission with reduced entropy can be beneficial in multiuser communication systems with interference. This work proposes a mathematical framework that allows for a unified treatment of different kinds of entropy reduction, such as coding across carriers or so-called improper signals. It is then studied for various multiantenna systems (MIMO systems, i.e., multiple-input multiple-output) with interference whether or not reduced-entropy signals can bring gains and how transmit strategies based on such signals can be optimized.

Acknowledgments

First of all, I am deeply grateful to my supervisor Professor Wolfgang Utschick, who found the perfect balance between giving me the freedom to pursue my own research ideas and contributing to the success of this work with the right comments and ideas at the right time. Moreover, in his research group on signal processing methods at Technische Universität München, he has managed to create an inspiring atmosphere of friendship, openness for discussions and collaborations, and eagerness to jointly work on a better understanding of fundamental aspects of signal processing and communications. This was an ideal environment for working on this thesis. I also would like to express my gratitude to Professor Eduard Jorswieck, not only for volunteering as second examiner, but also for being a great partner for scientific discussions whenever we met throughout the last years, as well as to Professor Sandra Hirche for organizing and chairing the examination.

My gratitude also goes to all the colleagues in the signal processing methods group at Technische Universität München for having been great friends and office partners throughout the last years, and for having contributed to this work either formally as collaborators and coauthors of the various prepublications or informally by always being available for interesting and fruitful discussions and by sharing their expert knowledge on various aspects of signal processing. Moreover, I am happy to have been the supervisor of many talented students, some of which significantly influenced my research with the interesting ideas they contributed.

Contents

Chapter 1

Introduction

While the data rate requirements will continue to increase drastically in future wireless communication networks, the available frequency spectrum is naturally a scarce resource. Accordingly, one of the most important challenges for researchers and system developers is to significantly increase the overall spectral efficiency of the systems, i.e., the total data rate that can be achieved normalized by the bandwidth used for the transmission.

Among the various approaches towards this goal, we find ideas such as a denser reuse of frequencies in nearby cells or a paradigm shift from an exclusive assignment of resources to users towards a more flexible scheduling, where several users may share a resource. In both cases, the new challenge is to deal with interference, namely from neighboring cells or from co-channel users that are sharing the same resource.

A promising technology to handle this interference are so-called multiple-input multiple-output (MIMO) systems, where multiple antennas are deployed at the transmitters and receivers. The joint preprocessing of the signals that are sent via the individual elements of a transmit antenna array, as well as the joint processing of the signals that are received at multiple receive antennas, allow for additional filtering in the spatial domain. This can be used to suppress interference from other users or from other data streams of the same user, so that multiple users can be served on the same resource and/or multiple data streams per user can be supported simultaneously.

In addition to suppressing interference by spatial filtering, advanced multiuser encoding or decoding techniques allow to partially cancel out interference by means of coding. Provided that an interfering signal is known to the transmitter, it is possible to encode a signal such that the same data rate as in the interference-free case can be decoded by the receiver. On the other hand, an interfering signal that is known to the receiver can readily be suppressed by subtracting it from the received signal. In some multiuser settings, these principles can be exploited in successive encoding or decoding schemes which reduce the number of interfering signals and thus increase the system throughput.

However, despite decades of research, there are still many aspects of communication systems with interference that are not fully understood even if abstract information theoretic models

Some of the results presented in this work are also contained in [1–28].

of the systems are considered. For the simple example of a single-input/single-output (SISO) interference channel consisting of two transmitter-receiver pairs with a single antenna at each terminal, the capacity region is still unknown apart from some special cases. Even if we ignore the problem of deciding for an optimal multiuser coding scheme and assume simpler single-user codes instead, there is in general still no way to find the optimal input distribution for each user. Nevertheless, the recent information theoretic literature continuously makes further steps towards a better understanding of such interference networks.

One of the most interesting insights of the past years is that some paradigms that are well-known from single-user communication systems not necessarily hold in interference-limited systems. For instance, the capacity-achieving input distribution in a single-user system with additive proper Gaussian noise is proper Gaussian as well [29].[1] It was revealed in [30] that this no longer needs to be the case in the presence of interference, and many further publications showing gains by improper signaling in other scenarios with interference followed (e.g., [31–38]).

A second example is that the capacity of a single-user multicarrier system can be achieved by separate coding on each carrier (e.g., [39, Sec. 5.3] for single-antenna systems; a formal proof for multiantenna systems is included in Section 4.2). Again, this paradigm was shown to not necessarily hold in systems with interference [40], and many further examples where coding across carriers can be beneficial were found (e.g., [41–44]).

On the other hand, there are system models in which improper signaling cannot bring any gains despite the fact that interference is present. The most prominent examples are multiple access channels (multipoint-to-point transmission) and broadcast channels (point-to-multipoint transmission) [45, 46]. Interestingly, it can be shown for exactly the same system models that coding across carriers cannot bring any gains either [47–50]. This suggests that there should be some kind of connection between these two concepts, and that the study of new transmit paradigms for communication systems with interference should be conducted in a more general way.

The common point that we identify and analyze in this work is that both concepts reduce the amount of information—measured by the so-called differential entropy—contained in the individual transmit signals as compared to conventional transmission schemes. For the sake of a unified treatment, we make use of the notion of maximum-entropy signals, which include proper signals and separate coding on each carrier as special cases, and the notion of reduced-entropy signals, which include improper signals and coding across carriers.

After deriving a mathematical framework that allows for a unified treatment of various kinds of maximum-entropy signals, we apply this new framework to understand in which kinds of systems maximum-entropy signals are optimal and, conversely, in which kinds of systems reduced-entropy signals can be beneficial. Intuitively speaking, reducing the differential entropy of the transmit signal decreases the amount of information that this signal can carry, and thus the achievable data rate. Therefore, maximum-entropy transmission turns out to be optimal in interference-free systems (point-to-point transmission). However, in systems with interference, a trade-off occurs. While the entropy reduction decreases the rate that is achievable for the transmission to the intended receiver, it makes the signal at the same time less harmful for

[1] For Gaussian random vectors, the term *proper* is equivalent to the term *circularly symmetric*, see Section 2.9.1. Conversely, for *improper* Gaussian vectors, the term *asymmetric complex* Gaussian is also used (e.g., [30]).

other receivers where it is observed as interference. This gives an intuitive explanation for the gains by reduced-entropy transmission in interference channels (multipoint-to-multipoint transmission) that have been revealed in the abovementioned studies.

Our main attention lies on an intermediate case between these two extremes, namely on downlink systems (point-to-multipoint transmission). It turns out that such systems—known as *broadcast channels* in the information theoretic literature—can indeed behave like either of the two cases depending on which assumptions we make about the employed transmit strategies. In addition, we present results for an example of a relay-aided transmission, which turns out to behave in some regard similar as a downlink scenario. To obtain a complete overview, we compare our findings with results on interference channels from the existing literature and with observations that can be made in the case of point-to-point transmission. Moreover, we study some aspects of algorithm design and provide results on additional topics such as worst-case noise and uplink-downlink duality.

The details of the various system models that we consider as well as an overview of the related literature are in each case provided in the respective chapter.

1.1 Overview

In this section, we give an overview of the structure and the contributions of this work. Subsequently, in the remainder of the introduction, we introduce the fundamentals of multiuser MIMO communications systems, the notions of maximum-entropy and reduced-entropy signals, and some notational conventions.

The purpose of Chapter 2 is to set the mathematical foundation for our studies. After briefly revisiting some results from the mathematical literature that are needed for our derivations, we introduce the concept of *power shaping spaces*, and we derive a comprehensive collection of equations and statements related to such spaces. This new approach is a generalization of the parameterization of covariance matrices proposed in [6, 7], which we thus present as a special case.

In Chapter 3, we formulate the mathematical models for multiuser MIMO communication systems, and we demonstrate how the concept of power shaping spaces can be applied to study improper signaling and coding across carriers. Moreover, we discuss how the simultaneously achievable rates of the various users can be described by a rate region and how we can find Pareto-optimal points of such a region under various assumptions on the allowed transmit strategies.

The first communication system we study is a MIMO system without interference, which we consider in Chapter 4. Even though no surprising new insights are obtained in this chapter, it is worthwhile to see the functioning of the new framework in a simple setting before turning our attention to the more complicated scenarios with interference. Moreover, some statements about the optimal input distributions and about the worst-case noise, which we show in that chapter, might seem intuitively clear, but have not been proven formally in the related literature.

After that, we turn our attention to systems with interference. In Chapters 5 and 6, we consider the *MIMO multiple access channel* and the *MIMO broadcast channel*, where part of the interference is eliminated by means of the coding schemes. We generalize results about the optimality of proper signaling [45, 46] and of separate coding on each carrier [47–50] from

settings with sum power constraints to the case of more general covariance constraints, and we derive the properties of the worst-case noise. These chapters contain results that were shown in [21, 25, 28], but unlike therein, we now obtain them as special cases of the more general framework of maximum-entropy signals and reduced-entropy signals.

Despite the fact that interference is present, the multiuser settings considered up to this point behave quite similar to the single-user MIMO channel: maximum-entropy transmission is optimal in case of maximum-entropy noise. However, this changes significantly if a highly complex multiuser encoding for interference-suppression is avoided and all interference in the MIMO broadcast channel is instead treated as additional noise. This setting is studied in Chapter 7. After extending existing results on uplink-downlink duality [16, 51] in a way that they can be used to study maximum-entropy transmission, we provide a variety of examples that show that the optimality of maximum-entropy signals observed in the previous chapters does not hold any longer. In addition to previous results on the benefits of improper signaling (see also [5, 16]) and about gains obtained by coding across carriers (see also [1, 4, 15, 18, 52]), this chapter contains several new results on both topics and establishes a connection between these two types of entropy reduction. For instance, we show that improper signaling and coding across carriers are not interchangeable: there are situations where gains can be achieved by one of the techniques, but not by the other. Finally, we study the question how transmit strategies involving reduced-entropy transmission can be optimized. To this end, we generalize considerations from [11, 20, 23, 53] to the new framework of power shaping spaces.

In Chapter 8, we turn our attention to *interference channels* where multiple transmitter-receiver pairs share a common medium. For this scenario, various kinds of performance gains by means of coding across carriers (e.g., [40, 42]) or improper signaling (e.g., [30–36]) have been reported in the existing literature. We summarize these results, put them in the more general context of reduced-entropy transmission, and compare them with our findings in broadcast channels. In addition, we discuss the special case of a so-called *one-sided interference channel (Z-interference channel)*, where we extend recent studies on improper signaling [37, 38] to the case of time-sharing (see also [8]).

The last system that we consider is the *MIMO relay channel* under the assumption that the partial decode-and-forward scheme (e.g., [54, Sec. 9.4.1], [55, Sec. 16.6]) is employed. It turns out that the arising subproblems in the optimization of the achievable data rate can be related to rate maximization problems in multiple access channels and broadcast channels that are known from Chapters 5 and 6. We can exploit this to prove optimality of maximum-entropy transmission and to derive a worst-case noise theorem. These results are presented in Chapter 9 as a generalization of results from [6, 22].

In Chapter 10, we give some concluding remarks and we finally turn our attention to the possibility of transmitting non-Gaussian signals, which is excluded in the other chapters. When combined with existing insights from [56], our findings point to an interesting topic for future research: reduced-entropy transmission by means of non-Gaussian signals.

1.2 MIMO Communication Systems

A multiuser MIMO system consists of a set of *nodes* (*terminals*) $\mathrm{T} \in \mathcal{T}$ equipped with m_{T} antennas, which can act as transmitters, as receivers, or as relays. In this work, we consider

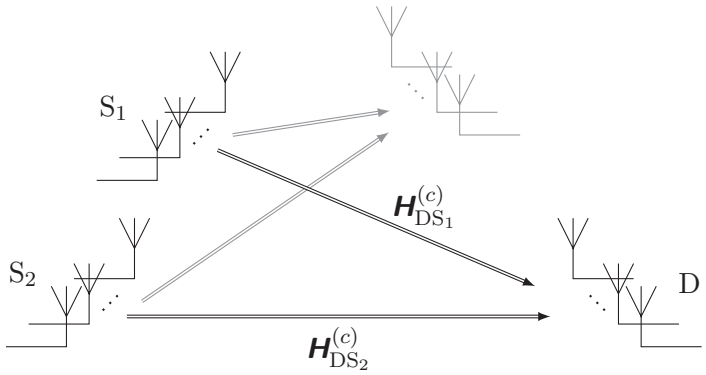

Figure 1.1: Illustration of the data transmission (1.1) *on carrier c of a multiuser MIMO system. The black receiver* D *may either be interested in both signals (e.g., in an uplink system, see Chapter 5), or one of the signals can be considered as undesirable interference (e.g., in an interference channel, see Chapter 8). If another receiver is present in the system (indicated in gray), a description analogous to* (1.1) *can be written down for the second receiver.*

various types of such systems, namely a single-user system (point-to-point), uplink and downlink systems (multipoint-to-point and point-to-multipoint), interference channels (multipoint-to-multipoint), as well as a simple relaying scenario. For each of the considered system models, we specify the details at the beginning of the respective chapter.

We assume that transmission takes place over C orthogonal resources, such as carriers in a multicarrier system, orthogonal codes, disjoint time intervals, fading states of a fading channel, etc. (see, e.g., [39, 49]). For simplicity, we use the term carrier, keeping in mind that other types of orthogonal resources are possible as well. In the information theoretic literature, such a scenario is also referred to as *parallel channels* (e.g., [40]).

We assume that the channels are frequency-flat within each carrier, which is a sensible assumption if the carriers are sufficiently narrow or if they are obtained by using orthogonal frequency division multiplexing (OFDM, e.g., [39, Sec. 3.4.4]). The transmission from a transmitter (*source*) S to a receiver (*destination*) D on carrier c can then be modeled as a multiplication by a matrix $\boldsymbol{H}_{\mathrm{DS}}^{(c)} \in \mathbb{C}^{m_{\mathrm{D}} \times m_{\mathrm{S}}}$, where m_{T} denotes the number of antennas at terminal T. The received signal $\boldsymbol{y}_{\mathrm{D}}^{(c)} \in \mathbb{C}^{m_{\mathrm{D}}}$ on carrier c can be a superposition of signals originating from several transmitters, i.e.,[2]

$$\boldsymbol{y}_{\mathrm{D}}^{(c)} = \sum_{\mathrm{S} \in \mathcal{S}_{\mathrm{D}}} \boldsymbol{H}_{\mathrm{DS}}^{(c)} \boldsymbol{x}_{\mathrm{S}}^{(c)} + \boldsymbol{\eta}_{\mathrm{D}}^{(c)}, \quad c = 1, \ldots, C \tag{1.1}$$

where $\mathcal{S}_{\mathrm{D}}$ is the set of transmitters whose signals $\boldsymbol{x}_{\mathrm{S}}^{(c)} \in \mathbb{C}^{m_{\mathrm{S}}}$ are received by node D, and $\boldsymbol{\eta}_{\mathrm{D}}^{(c)} \in \mathbb{C}^{m_{\mathrm{D}}}$ is additive noise, which is independent of the transmit signals and independent of the noise vectors at other receivers. In this work, we only consider Gaussian MIMO systems, meaning that the noise is always assumed to be Gaussian. Further assumptions on the noise are stated in Section 1.4.3.

Whenever several signals are received in a superimposed manner (see the illustration in Figure 1.1), we have to distinguish between useful signals and interfering signals. For instance in an uplink scenario (see Chapter 5), all received signals may be considered as useful. However,

[2]For details on the notation, see Section 1.5.

in other situations such as in an interference channel (see Chapter 8), we are only interested in one of the signals and all other signals are considered as interference. The various strategies to handle such an interference range from trying to decode and subtract the interference to simply treating the interference as noise. For each of the systems considered in the various chapters of this work, we clarify how the interference is handled when we introduce the respective system model.

We assume throughout this work that all coefficients in the channel matrices are perfectly known. Even though this assumption is not realistic, it is useful for studying fundamental properties of the considered systems. Extending our results to scenarios with imperfect channel knowledge is left open for future research.

We use a discrete-time complex baseband model (e.g., [39]), and we assume that the noise does not have any temporal correlations. For all system models we consider, we can find so-called single-letter characterizations (see, e.g., [57, 58]) in the information theoretic literature, which enable us to characterize achievable rates without writing down time-dependent expressions that describe all symbols over which a codeword spans. Therefore, all signals are written without a time-index as already done in (1.1).

1.3 Achievable Rates as Performance Criterion

All considerations in this work are based on so-called *achievable rates* in the sense of Shannon [59], i.e., on data rates at which a transmission is possible with an arbitrarily small probability of error. We use discrete-time representations of the systems, so that all data rates are given in bits per channel use.

Achievable rates enable us to study the limitations of communication systems from an information theoretic point of view, yielding benchmarks for any practical system. Moreover, using a so-called signal-to-noise ratio (SNR) gap approximation (e.g., [60]), achievable rates can be used to obtain approximative results on the data rates of systems that apply practical coding and modulation schemes.

In MIMO systems, where users might be served with multiple data streams, achievable rates play a particularly important role. While other performance measures, such as the signal-to-interference-and-noise ratio (SINR), the mean square error (MSE), and the bit error rate (BER), are only meaningful for a single data stream per user, leading to various competing definitions for extensions to the multistream case (see, e.g., the examples in [61, Sec. 3.4] and the references therein), achievable rates indisputably extend to the case of multiple data streams per user and are, therefore, an adequate performance measure for MIMO communications. Further details on achievable rates are introduced in Section 3.2.

1.4 Maximum-Entropy Signals and Reduced-Entropy Signals

To calculate achievable rates in a communication system, we have to study the so-called *mutual information* (see Section 2.1.3) between transmitted and received signals, which is closely related to the entropies of the involved signals and of the noise. The entropy of a signal can be intuitively understood as a measure for its randomness and is related to the amount of information that a signal can carry. As we consider continuous-valued signals, we have to make

use of a slightly different measure (see [59]), which is commonly referred to as *differential entropy* [62]. If it is clear from the context that *differential* entropies are considered, the shorter term *entropy* is sometimes still used for the sake of brevity. The mathematical definition of the differential entropy is given in Section 2.1.3.

As it is a measure for the randomness, the differential entropy is not influenced by the mean value of a signal, but the mean has an influence on the signal power. We adopt the common assumption that the noise has mean zero, and we note that this should hold for transmit signals as well since a nonzero mean would lead to a higher transmit power requirement without having an influence on the differential entropy [29]. Due to the assumption that the mean of all random vectors is zero, there is a direct relation between power and variance. In particular, the total signal power of a zero-mean random vector is the sum of the individual variances of the components.

In information theoretic studies, we are often interested in so-called maximum-entropy distributions (e.g., [62]), i.e., distributions that maximize the differential entropy under given constraints on the statistical properties of the signals. We restrict all our considerations to constraints on the second-order properties, i.e., on variances, correlations, and related quantities. When keeping the second-order properties fixed, the differential entropy of a random vector is maximized if all components are jointly Gaussian distributed [59, 62]. In this sense, a Gaussian signal with some given second-order properties is a maximum-entropy signal. Note that all signals we consider in this work are assumed to be Gaussian random vectors or scalars. For an outlook to non-Gaussian signals, see Chapter 10.

If we fix only parts of the second-order properties, we can obtain further statements about maximum-entropy signals. The following statements, which can be verified mathematically by means of the definitions given in Chapter 2, are meant to give a first impression about statistical properties that have an influence on the differential entropy of a Gaussian signal.

Since a correlation between the components leads to a reduction of the differential entropy compared to the case where the components are uncorrelated, a Gaussian random vector with uncorrelated components is the maximum-entropy signal among all signals with fixed individual variances. If we fix only the total power, i.e., the sum of the variances, a maximum-entropy signal must in addition have the same variance for all components. Any power imbalance between the components reduces the differential entropy. When allowing the total power to lie in some interval, the differential entropy is maximized by using the highest feasible power.

An additional aspect has to be considered for complex random vectors, where the differential entropy is reduced if (strictly linear) correlations[3] between the signal and its complex conjugate are present [29, 63]. In the literature, signals for which this is the case are called *improper* in contrast to so-called *proper* signals (e.g., [63, 64]). To distinguish between these two kinds of signals, we can consider the so-called *pseudocovariance matrix* [63] (see Section 2.9.1). For a given covariance matrix, the maximum-entropy signal is the one whose pseudocovariance matrix is zero, i.e., it is a proper signal [29, 63].

The above overview shows that we can obtain different notions of maximum-entropy signals depending on which statistical properties we consider to be given or, equivalently, among which set of possible signals we can choose. Whenever it is clear from the context which set of

[3]Correlations in the sense of only the first equation in Definition 2.9.4. Clearly, a signal is always correlated with its conjugate if the stricter notion of uncorrelatedness based on both equations in Definition 2.9.4 is used.

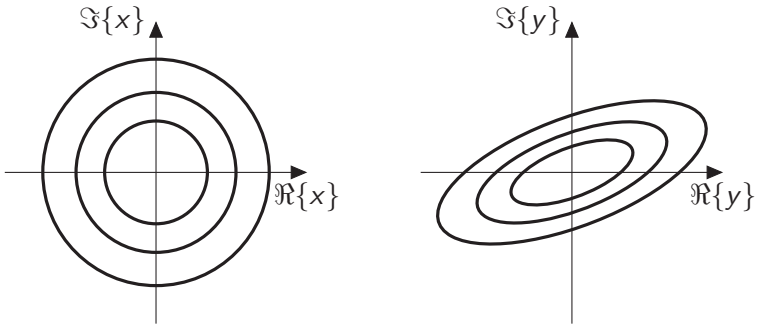

Figure 1.2: Contour lines of the probability density functions of a proper Gaussian random variable x (left) and an improper Gaussian random variable y (right).

possible signals is considered, we use the term *maximum-entropy signal* if the free parameters are chosen such that the differential entropy becomes as large as possible. Conversely, if a different choice is made for the free parameters, we have a *reduced-entropy signal*.

When speaking about maximum-entropy signals and reduced-entropy signals in the following chapters, we always assume that the total power belongs to the given parameters. It then needs to be specified which other aspects of the second-order properties are considered as given, and which ones can be freely adapted to maximize the entropy. To this end, we introduce the concept of *power shaping spaces* in Chapter 2, and we give a formal definition of *maximum-entropy signals with respect to a power shaping space* in Definition 2.5.1. By means of this mathematical framework, many derivations can be performed in a general manner, i.e., independently of which parameters will finally be considered as given or free.

In the remainder of this section, we briefly describe the two most important kinds of entropy reduction we consider, namely improper signaling and correlations across carriers. Moreover, we briefly discuss typical assumptions on the noise in communication systems, and how they are related to the notion of maximum-entropy signals.

1.4.1 Proper, Improper, and General Complex Signaling

As mentioned before, it was shown in various publications that the system performance in communication systems with interference can be improved by transmitting improper signals, which can be interpreted as an example for a type of reduced-entropy transmission. Mathematical details on proper and improper signals are given in Section 2.9. An illustration for the special case of a scalar complex Gaussian random variable is given in Figure 1.2. A scalar proper random variable has uncorrelated real and imaginary parts with equal variance, which leads to a circularly symmetric probability density function in case of the Gaussian distribution.

Most of the results on proper signals and improper signals that we discuss are obtained by studying the considered systems from the more general perspective of maximum-entropy signals and reduced-entropy signals. Nevertheless, even though the new framework proposed in Chapter 2 lets improper signaling appear as nothing but a special case, it is a case of particular importance, as can be seen from the large number of recent publications on this subject (e.g., the literature reviewed in Section 8.2). Considering this special case is thus an integral part of all chapters.

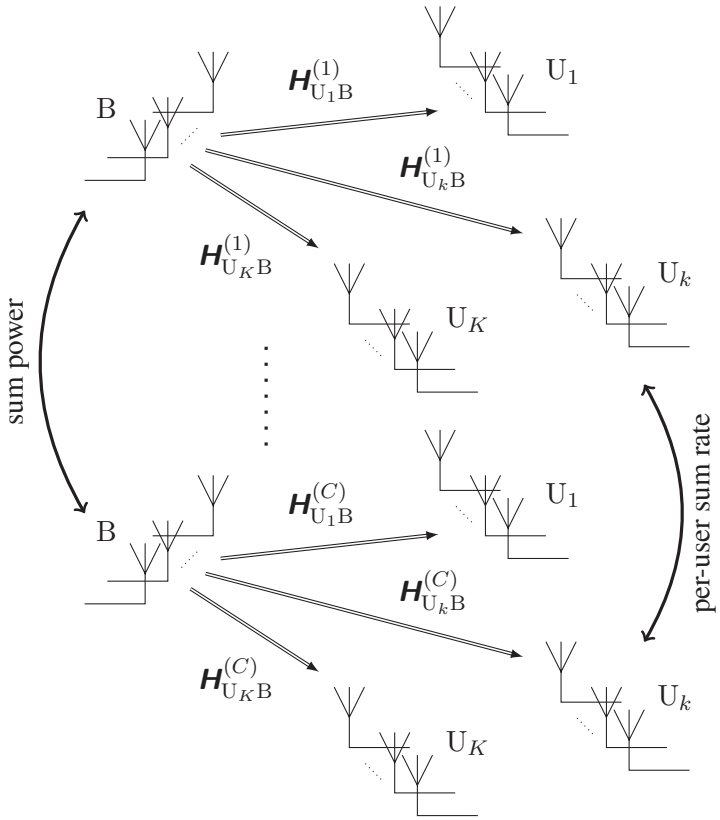

Figure 1.3: Illustration of CN transmission for the example of a MIMO broadcast channel (see Chapters 6 and 7). With CN transmission, the system can be treated as C separate systems, which are only coupled via a constraint on, e.g., the sum transmit power and via the sum rates of the users.

The following terminology is used. We say that a transmit strategy makes use of *improper signaling* if at least one of the input signals is improper. Conversely, *proper signaling* refers to the case where all input signals are proper. The term *general complex signals* includes proper and improper signals as special cases. In case of multiple carriers, we say that a multicarrier signal is proper if the per-carrier signals are jointly proper (see Definition 2.9.3).

1.4.2 Carrier-Cooperative Transmission and Coding Across Carriers

As a second special case of reduced-entropy transmission, we consider signals that are correlated across carriers. Using such signals in a communication system is called *carrier-cooperative (CC) transmission* (e.g., [11,43,65]). In this case, the signal corresponding to an encoded data stream is spread across several carriers, which can be described as *coding across carriers* [39] (or *joint encoding* [40]). On the other hand, if *separate encoding* [39,40] on each carrier is performed, we do not have any correlations between the carriers, which is called *carrier-noncooperative (CN) transmission* (e.g., [11,43,65]). An illustration is given in Figure 1.3.

Additional care must be taken in multihop scenarios with relaying, where CN transmission does not imply separate coding on all carriers (see Section 9.5.2). However, in single-hop systems, the terms CN transmission and separate coding are used interchangeably.

The decision to use CN transmission can simplify both the transceiver optimization process

and the actual operation of a system (e.g., [1]). Therefore, one of our aims is to study in which cases CN transmission can be applied without any performance loss compared to CC transmission. Systems where this is the case are called *separable* in the literature (e.g., [40, 42]).

For the sake of brevity, we use the acronyms CC and CN also for signals that do not have an interpretation as a transmit strategy, e.g., for the noise. The acronym CC may thus be understood in a wider sense as *carriers correlated*, and we use the term *CC signal* for any multicarrier signal whose components on the various carriers are correlated. Accordingly, CN can be understood as *carriers not correlated*, and we call any signal consisting of uncorrelated per-carrier signals a *CN signal* (Definition 3.3.2). Note that the terms uncorrelated and independent can be used as synonyms as long as we consider only Gaussian signals.

1.4.3 Properties of the Noise

We adopt the common assumption that the additive noise that occurs in the transmission (1.1) is Gaussian with full-rank covariance matrix. This can be justified from a practical perspective by the composite effect of many independent noise sources [66, 67], and from a theoretical perspective by the fact that Gaussian noise is the worst-case noise in general wireless networks under very mild assumptions [66, 67]. Note that the latter result is related to the abovementioned maximum-entropy property of the Gaussian distribution. This connection between worst-case noise and maximum differential entropy suggests that it should be possible to show that maximum-entropy noise is the worst-case noise also if a different kind of maximum-entropy signals is considered (see the examples in Section 1.4). Indeed, this is done in several worst-case noise theorems, which are proven in the various chapters (e.g., Theorem 4.4.1).

If a model with complex signals is used, it is often assumed that the noise is not only Gaussian, but also proper. This is a sensible assumption since it is the case for the complex baseband representation at the demodulator output of a bandpass system with real wide-sense stationary noise [63]. Note that proper noise is the maximum-entropy signal among all complex Gaussian noise signals with fixed covariance matrix [29, 63].

In multicarrier systems, it additionally makes sense to assume that the Gaussian noise is uncorrelated across carriers (e.g., [39, Sec. 5.3.3]), i.e., we have CN noise. This is the maximum-entropy signal if the second-order statistical properties of the noise within each carrier are fixed (see Section 3.4.3).

Due to all these properties, we may assume in many cases that the noise in a communication system is a maximum-entropy signal in several respects. By carefully choosing appropriate power shaping spaces at the receivers, this can be formalized mathematically (see Section 3.4.4) and exploited in the study of communication systems. For example, we observe for a MIMO system without interference as studied in Chapter 4 that whenever the noise belongs to a certain kind of maximum-entropy signals, the transmit signal should belong to the same kind. On the other hand, it turns out that a reduced-entropy transmit signal can be beneficial in case of reduced-entropy noise. For systems with interference, by contrast, it needs to be investigated in detail (see Chapters 5 through 9) whether reduced-entropy transmit signals can be beneficial even if the noise is a maximum-entropy signal.

1.5 Notation

In this work, vectors are typeset in boldface lowercase letters, and matrices in boldface uppercase letters. Whenever a matrix or vector is described in parallel by a complex representation and a real-valued representation, we use sans-serif font (A or x) for the complex representation and serif font with additional accents ($\grave{\boldsymbol{A}}$ or $\breve{\boldsymbol{x}}$) for the real-valued representation (see Section 2.9). On the other hand, in equations that are valid no matter whether the considered matrices and vectors are complex or real, serif font ($\boldsymbol{A}$ or $\boldsymbol{x}$) is used throughout. Note that the conjugate-transpose operator in this kind of equations becomes equivalent to the conventional transpose if real matrices and vectors are plugged in.

We use the following special matrices, vectors, scalars, and sets. In addition, notations for further special sets are introduced in Section 2.1.1.

$\mathbf{0}$	zero matrix or vector of appropriate size
$\mathbf{1}$	all-ones vector of appropriate length
$\mathbf{e}_i$	ith canonical unit vector of appropriate length
$\mathbf{I}_L$	identity matrix of size L
$\boldsymbol{d}(\boldsymbol{A})$	vector containing the diagonal elements of the matrix $\boldsymbol{A}$
$\boldsymbol{\lambda}(\boldsymbol{A})$	vector containing the eigenvalues of the matrix $\boldsymbol{A}$
$\boldsymbol{C}_{\boldsymbol{x}}$	covariance matrix of a random vector $\boldsymbol{x}$
$\boldsymbol{C}_{\boldsymbol{x},\boldsymbol{y}}$	cross-covariance matrix of the random vectors $\boldsymbol{x}$ and $\boldsymbol{y}$
$\mathrm{diag}(\alpha_i)$	diagonal matrix with diagonal elements α_i
$\mathrm{blkdiag}(\boldsymbol{A}^{(c)})$	block-diagonal matrix with diagonal blocks $\boldsymbol{A}^{(1)}, \ldots, \boldsymbol{A}^{(C)}$
$\mathrm{stack}(\boldsymbol{a}^{(c)})$	stacked vector $[\boldsymbol{a}^{(1),\mathrm{T}}, \ldots, \boldsymbol{a}^{(C),\mathrm{T}}]^{\mathrm{T}}$
a_i	ith element of a vector $\boldsymbol{a}$
e	Euler's number
j	imaginary unit
$\mathbb{R}^N_{0,+}$	closed positive orthant of $\mathbb{R}^N$, i.e., $\mathbb{R}^N_{0,+} = \{\boldsymbol{x} \in \mathbb{R}^N \colon x_i \geq 0,\ \forall i\}$

The following operators are used.

$\boldsymbol{A}^{\mathrm{T}}$	transpose of a matrix or vector
$\boldsymbol{A}^{\mathrm{H}}$	conjugate-transpose of a matrix or vector
$\boldsymbol{A}^*$	complex conjugation
$\Re(\bullet)$	real part
$\Im(\bullet)$	imaginary part
$\grave{\Re}(\mathsf{A})$	real representation of a complex matrix, see Section 2.9.5
$\breve{\Re}(\mathsf{a})$	real representation of a complex vector, see Section 2.9.2
$\boldsymbol{A}^{-1}$	inverse of a matrix
$\boldsymbol{A}^{+}$	Moore-Penrose pseudoinverse of a matrix
$\boldsymbol{A}^{\frac{1}{2}}$	matrix square root of a positive-semidefinite matrix
$\mathrm{tr}[\boldsymbol{A}]$	trace of a matrix
$\det \boldsymbol{A}$	determinant of a matrix
$\mathrm{rank}\,[\boldsymbol{A}]$	rank of a matrix
$\mathrm{null}[\boldsymbol{A}]$	null space of a matrix

$\operatorname{range}[\boldsymbol{A}]$	column space of a matrix
$\langle \boldsymbol{A}, \boldsymbol{B} \rangle$	(Frobenius) inner product of $\boldsymbol{A}$ and $\boldsymbol{B}$, see Section 2.1.1
$f \circ g$	function composition
$\mathrm{E}[\bullet]$	expectation
$\mathrm{h}\left(\boldsymbol{x}\right)$	differential entropy of a random vector $\boldsymbol{x}$, see Section 2.1.3
$\mathrm{h}\left(\boldsymbol{x} \,\middle|\, \boldsymbol{y}\right)$	conditional differential entropy of $\boldsymbol{x}$ conditioned on $\boldsymbol{y}$
$\mathrm{I}\left(\boldsymbol{x}; \boldsymbol{y}\right)$	mutual information between the random vectors $\boldsymbol{x}$ and $\boldsymbol{y}$, see Section 2.1.3
$\mathrm{I}\left(\boldsymbol{x}; \boldsymbol{y} \,\middle|\, \boldsymbol{z}\right)$	conditional mutual information of $\boldsymbol{x}$ and $\boldsymbol{y}$ conditioned on $\boldsymbol{z}$
$\lvert a \rvert$	absolute value of a
$\lvert \mathcal{X} \rvert$	cardinality of a set $\mathcal{X}$
$\mathcal{X} \cap \mathcal{Y}$	intersection of the sets $\mathcal{X}$ and $\mathcal{Y}$
$\bigcup_{i \in \mathcal{I}} \mathcal{X}_i$	union of the sets $\mathcal{X}_i$ for all $i \in \mathcal{I}$
$\mathcal{X} \setminus \mathcal{Y}$	set difference of the sets $\mathcal{X}$ and $\mathcal{Y}$
$\mathcal{X} \times \mathcal{Y}$	Cartesian product of the sets $\mathcal{X}$ and $\mathcal{Y}$
$\bigotimes_{i \in \mathcal{I}} \mathcal{X}_i$	Cartesian product of the sets $\mathcal{X}_i$ for all $i \in \mathcal{I}$
$\operatorname{conv} \mathcal{X}$	convex hull of the set $\mathcal{X}$
$\operatorname{proj}_{\mathcal{A}}(\bullet)$	projection to a subspace $\mathcal{A}$
$\mathcal{A}^{\perp_{\mathcal{V}}}$	orthogonal complement of a subspace $\mathcal{A}$ in a vector space $\mathcal{V}$
$\mathcal{A} + \mathcal{B}$	sum of the subspaces $\mathcal{A}$ and $\mathcal{B}$, i.e., $\{A + B \mid A \in \mathcal{A},\ B \in \mathcal{B}\}$
$\mathcal{A} \oplus \mathcal{B}$	orthogonal sum of the subspaces $\mathcal{A}$ and $\mathcal{B}$, i.e., the same as $\mathcal{A} + \mathcal{B}$, but with the implication that $\mathcal{A}$ and $\mathcal{B}$ are orthogonal

Expressions involving variables with a superscript index and an exponent (or an exponent-like operator), are written in the form $\boldsymbol{A}^{(i),k}$ for $(\boldsymbol{A}^{(i)})^k$ and $\boldsymbol{A}^{(i),\mathrm{H}}$ for $(\boldsymbol{A}^{(i)})^{\mathrm{H}}$. Moreover, we use shorthand notations of the forms

- $(a_k)_{\forall k} = (a_k)_{k=1,\ldots,K} = (a_1, \ldots, a_K)$,
- $(a^{(c)})_{\forall c} = (a^{(c)})_{c=1,\ldots,C} = (a^{(1)}, \ldots, a^{(C)})$,
- $(a)_{\forall c} = (a)_{c=1,\ldots,C} = (a, \ldots, a)$ (tuple with C elements),
- $(\boldsymbol{C}_{\boldsymbol{x}_{\mathrm{S}}})_{\mathrm{S} \in \mathcal{S}} = (\boldsymbol{C}_{\boldsymbol{x}_{\mathrm{S}_1}}, \ldots, \boldsymbol{C}_{\boldsymbol{x}_{\mathrm{S}_{|\mathcal{S}|}}})$ where $\mathcal{S} = (\mathrm{S}_1, \ldots, \mathrm{S}_{|\mathcal{S}|})$,
- $\{a_k\}_{k \in \mathcal{K}} = \{a_{k_1}, \ldots, a_{k_{|\mathcal{K}|}}\}$, where $\mathcal{K} = \{k_1, \ldots, k_{|\mathcal{K}|}\}$.

Finally, we make use of the following partial orderings and preorderings.

$\boldsymbol{a} \geq \boldsymbol{b}$	$\boldsymbol{b} \leq \boldsymbol{a}$	$a_i \geq b_i$ for all components $i = 1, \ldots, N$ ($\boldsymbol{a}, \boldsymbol{b} \in \mathbb{R}^N$)
$\boldsymbol{a} \succ \boldsymbol{b}$	$\boldsymbol{b} \prec \boldsymbol{a}$	$\boldsymbol{b}$ is majorized by $\boldsymbol{a}$, see Section 2.1.2
$\boldsymbol{A} \succ \boldsymbol{0}$	$\boldsymbol{0} \prec \boldsymbol{A}$	$\boldsymbol{A}$ is positive-definite
$\boldsymbol{A} \succeq \boldsymbol{0}$	$\boldsymbol{0} \preceq \boldsymbol{A}$	$\boldsymbol{A}$ is positive-semidefinite (psd)
$\boldsymbol{A} \succeq \boldsymbol{B}$	$\boldsymbol{B} \preceq \boldsymbol{A}$	$\boldsymbol{A} - \boldsymbol{B}$ is positive-semidefinite (psd)
$\mathcal{X} \supseteq \mathcal{Y}$	$\mathcal{Y} \subseteq \mathcal{X}$	$\mathcal{Y}$ is a subset of $\mathcal{X}$ or equal to $\mathcal{X}$
$\mathcal{X} \supset \mathcal{Y}$	$\mathcal{Y} \subset \mathcal{X}$	$\mathcal{Y}$ is a strict subset of $\mathcal{X}$

Chapter 2

Power Shaping Spaces and Maximum-Entropy Signals

As already mentioned in Section 1.4, the concept of so-called *power shaping spaces* can be used to formally describe maximum-entropy signals, i.e., signals which have the highest differential entropy within a certain family of signals. In this chapter, we introduce this framework, which is the mathematical foundation of many derivations in this work. After revisiting some mathematical preliminaries, we give a brief motivation and the formal definition of a power shaping space. Then, we derive fundamental properties of such spaces, and we give examples of power shaping spaces including those that are particularly relevant for the investigations that follow.

2.1 Mathematical Preliminaries

In addition to the notational conventions introduced in Section 1.5, the following definitions and results are needed for our derivations.

2.1.1 Vector Spaces of Matrices

We make intensive use of the fact that the space of complex $N \times M$ matrices $\mathbb{C}^{N\times M}$ and the space of real $N \times M$ matrices $\mathbb{R}^{N\times M}$ with the Frobenius inner product (e.g., [68, Sec. 5.2])

$$\langle \boldsymbol{A}, \boldsymbol{B} \rangle = \mathrm{tr}[\boldsymbol{B}^{\mathrm{H}}\boldsymbol{A}] \tag{2.1}$$

are Hilbert spaces. Note that $\mathrm{tr}[\boldsymbol{B}^{\mathrm{H}}\boldsymbol{A}] = \mathrm{tr}[\boldsymbol{A}\boldsymbol{B}^{\mathrm{H}}]$, which turns out to be useful in many derivations. For spaces of tuples of matrices $(\boldsymbol{A}_k)_{\forall k}$, $(\boldsymbol{B}_k)_{\forall k}$, we use the inner product $\langle (\boldsymbol{A}_k)_{\forall k}, (\boldsymbol{B}_k)_{\forall k} \rangle = \sum_{k=1}^{K} \mathrm{tr}[\boldsymbol{B}_k^{\mathrm{H}}\boldsymbol{A}_k]$.

It is easy to verify that the spaces of Hermitian matrices

$$\mathbb{H}^M = \{\boldsymbol{S} \in \mathbb{C}^{M\times M} \mid \boldsymbol{S} = \boldsymbol{S}^{\mathrm{H}}\} \subset \mathbb{C}^{M\times M} \tag{2.2}$$

and real symmetric matrices

$$\mathbb{S}^M = \{\boldsymbol{S} \in \mathbb{R}^{M\times M} \mid \boldsymbol{S} = \boldsymbol{S}^{\mathrm{T}}\} \subset \mathbb{R}^{M\times M} \tag{2.3}$$

are linear subspaces, i.e., they are vector spaces themselves. Within $\mathbb{H}^M$ (and thus also in $\mathbb{S}^M \subset \mathbb{H}^M$), the definition of the inner product simplifies to $\langle \boldsymbol{A}, \boldsymbol{B} \rangle = \mathrm{tr}[\boldsymbol{B}\boldsymbol{A}]$.

We use the following notation for spaces of block-diagonal matrices.

Definition 2.1.1. *Let $\mathcal{L} = (\ell_1, \ldots, \ell_C) \in \mathbb{N}^C$ and $\mathcal{M} = (m_1, \ldots, m_C) \in \mathbb{N}^C$ be tuples of natural numbers. We use $\mathbb{C}^{\mathcal{L}\times\mathcal{M}}$ (or $\mathbb{R}^{\mathcal{L}\times\mathcal{M}}$) to denote the space of complex (or real-valued) block-diagonal matrices where the diagonal blocks are matrices with sizes $\ell_1 \times m_1 \ldots, \ell_C, \times m_C$. Accordingly, the notation $\mathbb{H}^{\mathcal{M}}$ (or $\mathbb{S}^{\mathcal{M}}$) is used for the space of Hermitian (or real symmetric) block-diagonal matrices with block sizes $m_1 \times m_1, \ldots, m_C \times m_C$.*

2.1.2 Majorization Theory

Majorization theory has been used to study various aspects of wireless communication systems, as summarized, e.g., in [61, 69], and it is also an important ingredient for establishing the framework of power shaping spaces. In line with the existing literature (e.g., [61, 68–71]), we introduce the following definition.

Definition 2.1.2. *Let $a_{\downarrow i}$ denote the ith largest component of a vector $\boldsymbol{a}$. Then, a vector $\boldsymbol{x} \in \mathbb{R}^M$ is majorized by a vector $\boldsymbol{y} \in \mathbb{R}^M$, denoted by $\boldsymbol{x} \prec \boldsymbol{y}$, if*

$$\sum_{i=1}^{m} x_{\downarrow i} \leq \sum_{i=1}^{m} y_{\downarrow i} \tag{2.4}$$

for all $m = 1, \ldots, M$ with equality for $m = M$.

Intuitively speaking, $\boldsymbol{x} \prec \boldsymbol{y}$ means that the entries of $\boldsymbol{y}$ are more spread out than those of $\boldsymbol{x}$ while the sum over all components is the same for both vectors. According to [70, Sec. 1.A.3], we have $\boldsymbol{x} \prec \boldsymbol{y}$ if and only if $\sum_{i=1}^{M} |x_i - a| \leq \sum_{i=1}^{M} |y_i - a|, \ \ \forall a \in \mathbb{R}$. The following Lemma is a direct consequence of this equivalence.

Lemma 2.1.1. *If $\boldsymbol{x}_j \prec \boldsymbol{y}_j$ for all pairs of vectors $\boldsymbol{x}_j, \boldsymbol{y}_j \in \mathbb{R}^{M_j}$, $j = 1, \ldots, J$, then $[\boldsymbol{x}_1^{\mathrm{T}}, \ldots, \boldsymbol{x}_J^{\mathrm{T}}]^{\mathrm{T}} \prec [\boldsymbol{y}_1^{\mathrm{T}} \ldots, \boldsymbol{y}_J^{\mathrm{T}}]^{\mathrm{T}}$.*

Below, we provide some further statements about majorization, which are helpful for the derivations that follow in the next sections.

Lemma 2.1.2 ([70, Sec. 1.A])**.** *For any given vector $\boldsymbol{x} \in \mathbb{R}^M$ with $\sum_{i=1}^{M} x_i = \alpha$, it holds that $\frac{\alpha}{M}\mathbf{1} \prec \boldsymbol{x} \prec \alpha \mathbf{e}_m$, $m \in \{1, \ldots, M\}$.*

Lemma 2.1.3 ([70, Th. 9.B.1])**.** *For any Hermitian matrix $\boldsymbol{S} \in \mathbb{H}^M$, we have $\boldsymbol{d}(\boldsymbol{S}) \prec \boldsymbol{\lambda}(\boldsymbol{S})$, i.e., the vector of diagonal elements is majorized by the vector of eigenvalues.*

So-called Schur-convex and Schur-concave functions preserve the preordering of majorization [70]. We make use of the following definitions and properties.

Definition 2.1.3 (cf. [70, Definition 3.A.1])**.** *A function $f : \boldsymbol{x} \mapsto f(\boldsymbol{x})$ is said to be Schur-convex (or Schur-concave) on a set $\mathcal{X} \subseteq \mathbb{R}^M$ if $\boldsymbol{x} \prec \boldsymbol{y}$ with $\boldsymbol{x}, \boldsymbol{y} \in \mathcal{X}$ implies that $f(\boldsymbol{x}) \leq f(\boldsymbol{y})$ (or that $f(\boldsymbol{x}) \geq f(\boldsymbol{y})$, respectively). The function is said to be strictly Schur-convex (or strictly Schur-concave) in case that equality $f(\boldsymbol{x}) = f(\boldsymbol{y})$ holds only if $\boldsymbol{y}$ is a permuted version of $\boldsymbol{x}$.*

Lemma 2.1.4 ([70, Propositions 3.C.1 and 3.C.1.a]). *If $g : x \mapsto g(x)$ is convex (or concave) for $x \geq 0$, the function $f : \boldsymbol{x} \mapsto f(\boldsymbol{x}) = \sum_{i=1}^{M} g(x_i)$ is Schur-convex (or Schur-concave, respectively) for $\boldsymbol{x} \in \mathbb{R}_{0,+}^{M}$. If g is strictly convex (or strictly concave), then f is strictly Schur-convex (or strictly Schur-concave, respectively).*

Lemma 2.1.5 ([70, Proposition 3.F.1]). *The function $f : \boldsymbol{x} \mapsto f(\boldsymbol{x}) = \prod_{i=1}^{M} x_i$ is Schur-concave for $\boldsymbol{x} \in \mathbb{R}_{0,+}^{M}$.*

2.1.3 Differential Entropy of Gaussian Random Vectors

Throughout this work, all random vectors are assumed to be Gaussian with mean zero unless otherwise stated. A real-valued or proper complex random vector $\boldsymbol{z}$ can thus be described exhaustively by specifying the *covariance matrix*

$$\boldsymbol{C}_{\boldsymbol{z}} = \mathrm{E}[(\boldsymbol{z} - \mathrm{E}[\boldsymbol{z}])(\boldsymbol{z} - \mathrm{E}[\boldsymbol{z}])^{\mathrm{H}}] = \mathrm{E}[\boldsymbol{z}\boldsymbol{z}^{\mathrm{H}}] \tag{2.5}$$

where we have plugged in the zero-mean assumption $\mathrm{E}[\boldsymbol{z}] = \boldsymbol{0}$. The description of improper complex random vectors is discussed in Section 2.9.

The *differential entropy* of a continuous random vector $\boldsymbol{z}$ is defined as [59, 62]

$$\mathrm{h}\left(\boldsymbol{z}\right) = -\,\mathrm{E}[\log_2 f_{\boldsymbol{z}}(\boldsymbol{z})] \tag{2.6}$$

where $f_{\boldsymbol{z}}$ is the probability density function of $\boldsymbol{z}$. For a real-valued or proper Gaussian random vector $\boldsymbol{z}$, we have [29, 59, 62, 63].

$$\mathrm{h}\left(\boldsymbol{z}\right) = \mu \log_2 \det\left(\frac{1}{\mu}\pi \mathrm{e} \boldsymbol{C}_{\boldsymbol{z}}\right) \tag{2.7}$$

where $\mu = \frac{1}{2}$ if $\boldsymbol{z}$ is real [59, 62] and $\mu = 1$ is $\boldsymbol{z}$ is proper complex [29, 63].

If the differential entropy $\mathrm{h}\left(\boldsymbol{y}\right)$ and the *conditional differential entropy* of $\boldsymbol{y}$ conditioned on $\boldsymbol{x}$ [59, 62]

$$\mathrm{h}\left(\boldsymbol{y} \,|\, \boldsymbol{x}\right) = -\,\mathrm{E}[\log_2 f_{\boldsymbol{y}|\boldsymbol{x}}(\boldsymbol{y}|\boldsymbol{x})] \tag{2.8}$$

(calculated based on the conditional probability density function $f_{\boldsymbol{y}|\boldsymbol{x}}$ with the expectation taken in terms of both $\boldsymbol{x}$ and $\boldsymbol{y}$) are both finite, we can obtain the *mutual information* (e.g., [62]) between two continuous random vectors $\boldsymbol{x}$ and $\boldsymbol{y}$ from

$$\mathrm{I}\left(\boldsymbol{x}; \boldsymbol{y}\right) = \mathrm{h}\left(\boldsymbol{y}\right) - \mathrm{h}\left(\boldsymbol{y} \,|\, \boldsymbol{x}\right). \tag{2.9}$$

Note that $\mathrm{I}\left(\boldsymbol{x}; \boldsymbol{y}\right) = \mathrm{I}\left(\boldsymbol{y}; \boldsymbol{x}\right)$. Finally, we can calculate *conditional mutual information* expressions of the form [62]

$$\mathrm{I}\left(\boldsymbol{x}; \boldsymbol{y} \,|\, \boldsymbol{z}\right) = \mathrm{h}\left(\boldsymbol{y} \,|\, \boldsymbol{z}\right) - \mathrm{h}\left(\boldsymbol{y} \,|\, \boldsymbol{x}, \boldsymbol{z}\right). \tag{2.10}$$

2.2 Motivation

By means of the equation for the differential entropy of Gaussian random vectors (2.7), we can formulate the considerations from Section 1.4 mathematically as can be seen in the following example. Let

$$\boldsymbol{A} = \begin{bmatrix} 1 & \\ & 1 \end{bmatrix} \qquad \boldsymbol{B} = \begin{bmatrix} 1 & \\ & -1 \end{bmatrix} \qquad \boldsymbol{C} = \begin{bmatrix} & 1 \\ 1 & \end{bmatrix}. \tag{2.11}$$

Now consider a real-valued Gaussian random vector $\boldsymbol{x} = [x_1, x_2]^{\mathrm{T}}$ with covariance matrix $\boldsymbol{C}_{\boldsymbol{x}} = \boldsymbol{A} + \beta\boldsymbol{B} + \gamma\boldsymbol{C}$ with β and γ such that $\boldsymbol{C}_{\boldsymbol{x}}$ is a valid covariance matrix, i.e., a positive-semidefinite matrix. Note that the total signal power $\mathrm{tr}[\boldsymbol{C}_{\boldsymbol{x}}]$ is the same for any β and γ, but choosing $\beta \neq 0$ introduces a power imbalance between the two components x_1 and x_2 while choosing $\gamma \neq 0$ introduces a correlation.

From $\det \boldsymbol{C}_{\boldsymbol{x}} = 1 - \beta^2 - \gamma^2$, it is easy to see that $\det \boldsymbol{A} > \det(\boldsymbol{A} + \beta\boldsymbol{B}) > \det(\boldsymbol{A} + \beta\boldsymbol{B} + \gamma\boldsymbol{C})$ for any $\beta \neq 0$, $\gamma \neq 0$. Apparently, the power imbalance reduces $\det \boldsymbol{C}_{\boldsymbol{x}}$, and thus the differential entropy (2.7), and the correlation reduces it further. Similarly, we have $\det \boldsymbol{A} > \det(\boldsymbol{A} + \gamma\boldsymbol{C}) > \det(\boldsymbol{A} + \beta\boldsymbol{B} + \gamma\boldsymbol{C})$.

We can thus interpret a Gaussian random vector $\boldsymbol{x}'$ with covariance matrix $\boldsymbol{C}_{\boldsymbol{x}'} = \boldsymbol{A}$ as maximum-entropy signal among the vectors with the same total power. On the other hand, the vector $\boldsymbol{x}_\beta$ with covariance matrix $\boldsymbol{C}_{\boldsymbol{x}_\beta} = \boldsymbol{A} + \beta\boldsymbol{B}$ is a maximum-entropy signal among the vectors with the same fixed individual powers (but arbitrary correlations). Finally, among the vectors with fixed total power and fixed correlations (but arbitrary individual powers), the vector $\boldsymbol{x}_\gamma$ with covariance matrix $\boldsymbol{C}_{\boldsymbol{x}_\gamma} = \boldsymbol{A} + \gamma\boldsymbol{C}$ is the maximum-entropy signal.

2.3 Definition

Considerations as in the previous example become more involved in higher dimensions, where much more possibilities for entropy reductions exist. The aim of this chapter is to establish a framework which allows for similar considerations in more general settings.

The three matrices in (2.11) form an orthogonal basis of the space of 2×2 symmetric matrices $\mathbb{S}^2$. By setting one of the scalar parameters β or γ to zero in order to obtain a maximum-entropy signal, we restrict the covariance matrix to lie in a linear subspace of $\mathbb{S}^2$. This motivates a formal definition of subspaces which contain covariance matrices of maximum-entropy signals. Note that the relation to maximum-entropy signals does not directly become clear from the following definition, but is shown later in Section 2.5.

Definition 2.3.1. *Let $\mathbb{S}$ be the space of Hermitian matrices or real symmetric matrices of size $M_{\mathbb{S}} \times M_{\mathbb{S}}$, i.e., $\mathbb{S} = \mathbb{H}^{M_{\mathbb{S}}}$ or $\mathbb{S} = \mathbb{S}^{M_{\mathbb{S}}}$. A subspace $\mathcal{P} \subseteq \mathbb{S}$ which fulfills*

$$\boldsymbol{P}_1\boldsymbol{P}_2\boldsymbol{P}_1 \in \mathcal{P} \qquad \forall \boldsymbol{P}_1, \boldsymbol{P}_2 \in \mathcal{P} \tag{2.12}$$

$$\mathbf{I}_{M_{\mathbb{S}}} \in \mathcal{P} \tag{2.13}$$

is called power shaping space. *The orthogonal complement of $\mathcal{P}$ in $\mathbb{S}$ with respect to the Frobenius inner product* (2.1) *is then called* entropy reduction space *and is denoted by $\mathcal{N} = \mathcal{P}^{\perp_{\mathbb{S}}}$.*

The proposed names for $\mathcal{P}$ and $\mathcal{N}$ are clarified when we study the relation to differential entropies in Section 2.5. Since $\mathcal{P}$ and $\mathcal{N}$ are linear subspaces of the real vector space $\mathbb{H}^{M_{\mathbb{S}}}$, it is clear that

$$\alpha_1\boldsymbol{P}_1 + \alpha_2\boldsymbol{P}_2 \in \mathcal{P} \qquad \forall \boldsymbol{P}_1, \boldsymbol{P}_2 \in \mathcal{P}, \forall \alpha_1, \alpha_2 \in \mathbb{R} \tag{2.14}$$

$$\alpha_1\boldsymbol{N}_1 + \alpha_2\boldsymbol{N}_2 \in \mathcal{N} \qquad \forall \boldsymbol{N}_1, \boldsymbol{N}_2 \in \mathcal{N}, \forall \alpha_1, \alpha_2 \in \mathbb{R}. \tag{2.15}$$

Moreover, as $\mathcal{P}$ and $\mathcal{N}$ are orthogonal, we have

$$\mathrm{tr}[\boldsymbol{P}\boldsymbol{N}] = \langle \boldsymbol{P}, \boldsymbol{N} \rangle = 0 \quad \forall \boldsymbol{P} \in \mathcal{P},\ \forall \boldsymbol{N} \in \mathcal{N} \tag{2.16}$$

and we can decompose any $\boldsymbol{S} \in \mathbb{S}$ uniquely into

$$\boldsymbol{S} = \boldsymbol{P} + \boldsymbol{N} \quad \text{with} \quad \boldsymbol{P} = \mathrm{proj}_{\mathcal{P}}(\boldsymbol{S}) \in \mathcal{P},\ \boldsymbol{N} = \mathrm{proj}_{\mathcal{N}}(\boldsymbol{S}) \in \mathcal{N}. \tag{2.17}$$

Remark 2.3.1. *If $\mathcal{P}$ and $\bar{\mathcal{P}}$ are power shaping spaces such that $\mathcal{P} \subseteq \bar{\mathcal{P}} \subseteq \mathbb{H}^{M_{\mathbb{S}}}$, we may replace $\mathbb{S} = \mathbb{H}^{M_{\mathbb{S}}}$ in the above definition by $\mathbb{S} = \bar{\mathcal{P}}$, i.e., we may decide to consider $\mathcal{N} = \mathcal{P}^{\perp_{\bar{\mathcal{P}}}}$ as the corresponding entropy reduction space (instead of $\mathcal{N} = \mathcal{P}^{\perp_{\mathbb{S}}}$). If this more general definition is used, the results derived below are still valid.*

2.4 Basic Properties

In addition to the desired behavior in terms of differential entropy (to be derived in Section 2.5), Definition 2.3.1 leads to further useful properties, which are shown in the following.

Proposition 2.4.1. $\mathrm{tr}[\boldsymbol{N}] = 0 \quad \forall \boldsymbol{N} \in \mathcal{N}$.

Proof. Since any $\boldsymbol{N} \in \mathcal{N}$ must be orthogonal to $\mathbf{I}_{M_{\mathbb{S}}}$, we have $0 = \mathrm{tr}[\mathbf{I}_{M_{\mathbb{S}}}\boldsymbol{N}] = \mathrm{tr}[\boldsymbol{N}],\ \forall \boldsymbol{N} \in \mathcal{N}$. □

Using the product property (2.12), we can derive a product rule for entropy reduction matrices $\boldsymbol{N} \in \mathcal{N}$.

Proposition 2.4.2. $\boldsymbol{P}\boldsymbol{N}\boldsymbol{P} \in \mathcal{N},\ \forall \boldsymbol{P} \in \mathcal{P}, \forall \boldsymbol{N} \in \mathcal{N}$.

Proof. For any $\boldsymbol{P}' \in \mathcal{P}$, we have $\mathrm{tr}[\boldsymbol{P}\boldsymbol{N}\boldsymbol{P}\boldsymbol{P}'] = \mathrm{tr}[\boldsymbol{P}\boldsymbol{P}'\boldsymbol{P}\boldsymbol{N}] = \mathrm{tr}[\boldsymbol{P}''\boldsymbol{N}] = 0$ since $\boldsymbol{P}'' = \boldsymbol{P}\boldsymbol{P}'\boldsymbol{P} \in \mathcal{P}$ due to (2.12), i.e., $\boldsymbol{P}\boldsymbol{N}\boldsymbol{P}$ is orthogonal to any $\boldsymbol{P}' \in \mathcal{P}$. □

The following lemma about the kth powers $\boldsymbol{P}^k,\ k \in \mathbb{N}_0$ of power shaping matrices $\boldsymbol{P} \in \mathcal{P}$ and the subsequent theorem are very useful as they imply that any power shaping space $\mathcal{P}$ is closed under a wide variety of operations including matrix square roots and matrix inversion.

Lemma 2.4.1. $\boldsymbol{P}^k \in \mathcal{P},\ \forall \boldsymbol{P} \in \mathcal{P}, \forall k \in \mathbb{N}_0$.

Proof. Obviously, $\boldsymbol{P}^0 = \mathbf{I}_{M_{\mathbb{S}}} \in \mathcal{P}$ by (2.13) and $\boldsymbol{P}^1 = \boldsymbol{P} \in \mathcal{P}$. For $k \geq 2$, (2.12) yields $\boldsymbol{P}^k = \boldsymbol{P}\boldsymbol{P}^{k-2}\boldsymbol{P} \in \mathcal{P}$ by induction using $\boldsymbol{P}^{k-2} \in \mathcal{P}$. □

Theorem 2.4.1. *Let $\boldsymbol{\Lambda} = \mathrm{diag}(\lambda_i)$ be obtained from the eigenvalue decomposition $\boldsymbol{U}\boldsymbol{\Lambda}\boldsymbol{U}^{\mathrm{H}} = \boldsymbol{P}$ of $\boldsymbol{P} \in \mathcal{P}$, and let $\boldsymbol{\Psi} = \mathrm{diag}(f(\lambda_i))$ for an arbitrary scalar function $f : \mathbb{R} \to \mathbb{R}$. Then, $\boldsymbol{U}\boldsymbol{\Psi}\boldsymbol{U}^{\mathrm{H}} \in \mathcal{P}$.*

Proof. Let $D \leq M_{\mathbb{S}}$ be the number of distinct eigenvalues of $\boldsymbol{P}$. We can find a polynomial p of degree at most $D-1$ with real coefficients such that $f(\lambda_i) = p(\lambda_i)$ for $i = 1, \ldots, M_{\mathbb{S}}$ (e.g., [68, Sec. 0.9.11]). Then, $\boldsymbol{\Psi} = \mathrm{diag}(p(\lambda_i)) = p(\boldsymbol{\Lambda})$ and $\boldsymbol{U}\boldsymbol{\Psi}\boldsymbol{U}^{\mathrm{H}} = \boldsymbol{U}\,\mathrm{diag}(p(\lambda_i))\boldsymbol{U}^{\mathrm{H}} = p(\boldsymbol{P})$, i.e., the polynomial p applied to the matrix $\boldsymbol{P}$ (see, e.g., [68, Prob. 1.3.P3]). Due to (2.14) and Lemma 2.4.1, we have $p(\boldsymbol{P}) \in \mathcal{P}$. □

Corollary 2.4.1. *For any $\boldsymbol{P} \in \mathcal{P}$ with $\boldsymbol{P} \succeq \mathbf{0}$, the positive-semidefinite square root $\boldsymbol{P}^{\frac{1}{2}} \succeq \mathbf{0}$ is element of $\mathcal{P}$.*

Proof. Apply Theorem 2.4.1 with $f(\lambda) = \sqrt{\lambda}$. □

Corollary 2.4.2. *The pseudoinverse $\boldsymbol{P}^+$ of any $\boldsymbol{P} \in \mathcal{P}$ is element of $\mathcal{P}$. The same holds for the inverse $\boldsymbol{P}^{-1}$ if it exists.*

Proof. Apply Theorem 2.4.1 with $f(\lambda) = \frac{1}{\lambda}$ for $\lambda \neq 0$ and $f(\lambda) = 0$ otherwise. □

Corollary 2.4.3. *For any $\boldsymbol{P} \in \mathcal{P}$, the projection matrix $\boldsymbol{P}^+\boldsymbol{P}$ is element of $\mathcal{P}$.*

Proof. Apply Theorem 2.4.1 with $f(\lambda) = \lambda \cdot \frac{1}{\lambda} = 1$ for $\lambda \neq 0$ and $f(\lambda) = \lambda \cdot 0 = 0$ otherwise. □

Finally, we show that the intersection of two power shaping spaces is again a power shaping space.

Proposition 2.4.3. *Let $\mathcal{A} \subseteq \mathbb{S}$ and $\mathcal{B} \subseteq \mathbb{S}$ be two power shaping spaces. Then, $\mathcal{P} = \mathcal{A} \cap \mathcal{B}$ is a power shaping space as well.*

Proof. For all $\boldsymbol{P}_1, \boldsymbol{P}_2 \in \mathcal{P}$, we have $\boldsymbol{P}_1, \boldsymbol{P}_2 \in \mathcal{A} \;\Rightarrow\; \boldsymbol{P}_1\boldsymbol{P}_2\boldsymbol{P}_1 \in \mathcal{A}$ and $\boldsymbol{P}_1, \boldsymbol{P}_2 \in \mathcal{B} \;\Rightarrow\; \boldsymbol{P}_1\boldsymbol{P}_2\boldsymbol{P}_1 \in \mathcal{B}$. Thus, $\boldsymbol{P}_1\boldsymbol{P}_2\boldsymbol{P}_1 \in \mathcal{A} \cap \mathcal{B}$. Moreover, $\mathbf{I}_{M_\mathbb{S}} \in \mathcal{A}$ and $\mathbf{I}_{M_\mathbb{S}} \in \mathcal{B}$ imply $\mathbf{I}_{M_\mathbb{S}} \in \mathcal{A} \cap \mathcal{B}$. This shows that (2.12) and (2.13) hold for $\mathcal{P} = \mathcal{A} \cap \mathcal{B}$. □

2.5 Power Shaping Spaces and Differential Entropy

The following fundamental result is the basis for establishing a relation between the definition of a power shaping space in Definition 2.3.1 and the concept of differential entropy, which is the aim of this section.

Theorem 2.5.1. *For any $\boldsymbol{P} \in \mathcal{P}$ and any $\boldsymbol{N} \in \mathcal{N}$, we have $\boldsymbol{\lambda}(\boldsymbol{P}) \prec \boldsymbol{\lambda}(\boldsymbol{P} + \boldsymbol{N})$.*

Proof. Consider the sorted eigenvalue decomposition $\boldsymbol{U}\boldsymbol{\Lambda}\boldsymbol{U}^{\mathrm{H}} = \boldsymbol{P}$ with

$$\boldsymbol{\Lambda} = \operatorname{diag}(\lambda_i) = \begin{bmatrix} \lambda_{(1)}\mathbf{I}_{|\mathcal{I}_1|} & & \\ & \ddots & \\ & & \lambda_{(L)}\mathbf{I}_{|\mathcal{I}_L|} \end{bmatrix} \tag{2.18}$$

where $\lambda_{(\ell)},\ \ell = 1, \ldots, L$ are the distinct eigenvalues, and $\mathcal{I}_\ell,\ \ell = 1, \ldots, L$ are disjoint index sets containing the indices of the corresponding eigenvectors $\boldsymbol{u}_i,\ i \in \mathcal{I}_\ell$. Let $\boldsymbol{d}_\ell \in \mathbb{R}^{|\mathcal{I}_\ell|}$ be a vector with elements $d_i = \mathbf{e}_i^{\mathrm{T}}\boldsymbol{U}^{\mathrm{H}}(\boldsymbol{P} + \boldsymbol{N})\boldsymbol{U}\mathbf{e}_i,\ i \in \mathcal{I}_\ell$, where we can write $d_i = \lambda_{(\ell)} + \varphi_i$ with $\varphi_i = \mathbf{e}_i^{\mathrm{T}}\boldsymbol{U}^{\mathrm{H}}\boldsymbol{N}\boldsymbol{U}\mathbf{e}_i = \boldsymbol{u}_i^{\mathrm{H}}\boldsymbol{N}\boldsymbol{u}_i$.

Let $\boldsymbol{J}_\ell = \sum_{i \in \mathcal{I}_\ell} \boldsymbol{u}_i\boldsymbol{u}_i^{\mathrm{H}}$. We can express $\boldsymbol{J}_\ell$ as[1] $\boldsymbol{J}_\ell = \boldsymbol{U}\operatorname{diag}(f_\ell(\lambda_i))\boldsymbol{U}^{\mathrm{H}}$, where f_ℓ is an indicator function which takes the value $f_\ell(\lambda) = 1$ if $\lambda = \lambda_{(\ell)}$ and $f_\ell(\lambda) = 0$ otherwise. Due to Theorem 2.4.1, we have that $\boldsymbol{J}_\ell \in \mathcal{P}$. Therefore,

$$\sum_{i \in \mathcal{I}_\ell} \varphi_i = \sum_{i \in \mathcal{I}_\ell} \boldsymbol{u}_i^{\mathrm{H}}\boldsymbol{N}\boldsymbol{u}_i = \sum_{i \in \mathcal{I}_\ell} \operatorname{tr}[\boldsymbol{u}_i\boldsymbol{u}_i^{\mathrm{H}}\boldsymbol{N}] = \operatorname{tr}[\boldsymbol{J}_\ell\boldsymbol{N}] = 0 \tag{2.19}$$

so that $\sum_{i \in \mathcal{I}_\ell} d_i = \lambda_{(\ell)}|\mathcal{I}_\ell|$. Thus, $\lambda_{(\ell)}\mathbf{1} \prec \boldsymbol{d}_\ell,\ \ell = 1, \ldots, L$ by Lemma 2.1.2.

[1]The notation $\operatorname{diag}(f_\ell(\lambda_i))$ has to be understood in the sense that the ith diagonal element equals $f_\ell(\lambda_i)$ for a fixed value of ℓ.

Noting that $\boldsymbol{\lambda}(\boldsymbol{P})$ is the concatenation of all vectors $\lambda_{(\ell)}\mathbf{1} \prec \boldsymbol{d}_\ell, \quad \ell = 1, \dots, L$ and that $\boldsymbol{d}(\boldsymbol{U}^{\mathrm{H}}(\boldsymbol{P}+\boldsymbol{N})\boldsymbol{U})$ is the concatenation of all vectors $\boldsymbol{d}_\ell, \quad \ell = 1, \dots, L$, we can apply Lemmas 2.1.1 and 2.1.3 to obtain

$$\boldsymbol{\lambda}(\boldsymbol{P}) \prec \boldsymbol{d}(\boldsymbol{U}^{\mathrm{H}}(\boldsymbol{P}+\boldsymbol{N})\boldsymbol{U}) \prec \boldsymbol{\lambda}(\boldsymbol{U}^{\mathrm{H}}(\boldsymbol{P}+\boldsymbol{N})\boldsymbol{U}) \tag{2.20}$$

where $\boldsymbol{\lambda}(\boldsymbol{U}^{\mathrm{H}}(\boldsymbol{P}+\boldsymbol{N})\boldsymbol{U}) = \boldsymbol{\lambda}(\boldsymbol{P}+\boldsymbol{N})$. □

As in (2.17), any covariance matrix $\boldsymbol{C}_{\boldsymbol{x}}$ can be uniquely decomposed into $\boldsymbol{C}_{\boldsymbol{x}} = \boldsymbol{P}+\boldsymbol{N}$ with $\boldsymbol{P} \in \mathcal{P}$ and $\boldsymbol{N} \in \mathcal{N}$. Conversely, any matrix $\boldsymbol{P}+\boldsymbol{N}$ can be interpreted as the covariance matrix of some random vector if it is positive-semidefinite. As shown in the following, this can only be the case if the power shaping component $\boldsymbol{P}$ is positive-semidefinite and if a condition on the fundamental subspaces induced by $\boldsymbol{P}$ and $\boldsymbol{N}$ is fulfilled.

Proposition 2.5.1. *If* $\boldsymbol{P}+\boldsymbol{N} \succeq \mathbf{0},\ \boldsymbol{P} \in \mathcal{P},\ \boldsymbol{N} \in \mathcal{N}$*, then* $\boldsymbol{P} \succeq \mathbf{0}$*,* $\mathrm{null}[\boldsymbol{P}] \subseteq \mathrm{null}[\boldsymbol{N}]$*, and* $\mathrm{rank}\,[\boldsymbol{N}] \leq \mathrm{rank}\,[\boldsymbol{P}]$.

Proof. Since the eigenvalues of $\boldsymbol{P}+\boldsymbol{N}$ are more spread out than those of $\boldsymbol{P}$ (due to Theorem 2.5.1), we have $\lambda_{\min}(\boldsymbol{P}) \geq \lambda_{\min}(\boldsymbol{P}+\boldsymbol{N})$, where $\lambda_{\min}$ denotes the smallest eigenvalue. As $\lambda_{\min}(\boldsymbol{P}+\boldsymbol{N}) \geq 0$ if $\boldsymbol{P}+\boldsymbol{N} \succeq \mathbf{0}$, we obtain $\lambda_{\min}(\boldsymbol{P}) \geq 0$ so that $\boldsymbol{P} \succeq \mathbf{0}$. If $\boldsymbol{P}+\boldsymbol{N} \succeq \mathbf{0}$, it must also hold that $\boldsymbol{A}(\boldsymbol{P}+\boldsymbol{N})\boldsymbol{A}^{\mathrm{H}} \succeq \mathbf{0}$ for any $\boldsymbol{A}$ [68, Observation 7.1.8.a]. Let $\boldsymbol{A} = \mathbf{I}_{M_{\mathbb{S}}} - \boldsymbol{P}^{+}\boldsymbol{P}$, so that $\boldsymbol{A}\boldsymbol{P}\boldsymbol{A} = \mathbf{0}$ and $\boldsymbol{A}\boldsymbol{N}\boldsymbol{A} = \boldsymbol{A}(\boldsymbol{P}+\boldsymbol{N})\boldsymbol{A} \succeq \mathbf{0}$. Since $\boldsymbol{A} \in \mathcal{P}$ (Corollary 2.4.3), we have $\boldsymbol{A}\boldsymbol{N}\boldsymbol{A} \in \mathcal{N}$ (Proposition 2.4.2). As $\boldsymbol{A}\boldsymbol{N}\boldsymbol{A} \succeq \mathbf{0}$, the fact that $\mathrm{tr}[\boldsymbol{A}\boldsymbol{N}\boldsymbol{A}] = 0$ (due to Proposition 2.4.1) implies that $\boldsymbol{A}\boldsymbol{N}\boldsymbol{A} = \mathbf{0}$. For $\boldsymbol{x} \in \mathrm{null}[\boldsymbol{P}]$, we have $\boldsymbol{A}\boldsymbol{x} = \boldsymbol{x}$, and thus $\boldsymbol{x}^{\mathrm{H}}\boldsymbol{N}\boldsymbol{x} = \boldsymbol{x}^{\mathrm{H}}\boldsymbol{A}\boldsymbol{N}\boldsymbol{A}\boldsymbol{x} = 0$. Due to $\boldsymbol{P}+\boldsymbol{N} \succeq \mathbf{0}$, we must have $\boldsymbol{z}^{\mathrm{H}}(\boldsymbol{P}+\boldsymbol{N})\boldsymbol{z} \geq 0$ for any vector $\boldsymbol{z}$. Setting $\boldsymbol{z} = \boldsymbol{y}+\alpha\boldsymbol{x}$ with $\alpha \in \mathbb{R}$ and $\boldsymbol{y} \notin \mathrm{null}[\boldsymbol{N}]$, we must have

$$0 \leq (\boldsymbol{y}+\alpha\boldsymbol{x})^{\mathrm{H}}(\boldsymbol{P}+\boldsymbol{N})(\boldsymbol{y}+\alpha\boldsymbol{x}) = \boldsymbol{y}^{\mathrm{H}}(\boldsymbol{P}+\boldsymbol{N})\boldsymbol{y} + 2\alpha\Re(\boldsymbol{y}^{\mathrm{H}}\boldsymbol{N}\boldsymbol{x})$$

but we can always find an α such that the right hand side becomes negative unless $\boldsymbol{x} \in \mathrm{null}[\boldsymbol{N}]$. This proves $\mathrm{null}[\boldsymbol{P}] \subseteq \mathrm{null}[\boldsymbol{N}]$, and $\mathrm{rank}\,[\boldsymbol{N}] \leq \mathrm{rank}\,[\boldsymbol{P}]$ is a direct consequence. □

We are now ready to establish the connection between power shaping spaces and the differential entropy of Gaussian random vectors.

Theorem 2.5.2. *Let* $\boldsymbol{C}_{\boldsymbol{x}}$ *be the covariance matrix of a real-valued or proper complex Gaussian random vector* $\boldsymbol{x}$*. For any fixed power shaping component* $\boldsymbol{P} = \mathrm{proj}_{\mathcal{P}}(\boldsymbol{C}_{\boldsymbol{x}})$*, the differential entropy of* $\boldsymbol{x}$ *is maximized if* $\boldsymbol{N} = \mathrm{proj}_{\mathcal{N}}(\boldsymbol{C}_{\boldsymbol{x}}) = \mathbf{0}$.

Proof. The differential entropy of $\boldsymbol{x}$ is given by (2.7). We thus need to show that $\det \boldsymbol{P} \geq \det(\boldsymbol{P}+\boldsymbol{N})$. Note that $\boldsymbol{P}+\boldsymbol{N} = \boldsymbol{C}_{\boldsymbol{x}} \succeq \mathbf{0}$ implies $\boldsymbol{P} \succeq \mathbf{0}$ due to Proposition 2.5.1. For $\boldsymbol{X} \succeq \mathbf{0}$, $\det \boldsymbol{X}$ is the product of the nonnegative eigenvalues of $\boldsymbol{X}$ and thus Schur-concave in $\boldsymbol{\lambda}(\boldsymbol{X})$ (see Lemma 2.1.5 and Definition 2.1.3). Thus, the inequality is a consequence of Theorem 2.5.1. □

Due to this result, we can interpret a random vector with $\boldsymbol{N} = \mathbf{0}$ as a maximum-entropy signal, and we can call $\boldsymbol{N}$ the *entropy reduction matrix*. In Section 1.4, we stated that we always assume the total power to belong to the set of given parameters when speaking about maximum-entropy signals and reduced-entropy signals. This is reflected in Proposition 2.4.1,

which ensures that varying the entropy reduction matrix $\boldsymbol{N}$ can never change the total power $\mathrm{tr}[\boldsymbol{C}_{\boldsymbol{x}}] = \mathrm{tr}[\boldsymbol{P} + \boldsymbol{N}] = \mathrm{tr}[\boldsymbol{P}]$.

The matrix $\boldsymbol{P}$ determines the total signal power, but it may, depending on which power shaping space we consider, also specify how this power is shaped, e.g., in the spatial domain in a multiantenna system or in the sense of spectral shaping in multicarrier systems (see Section 3.4.2). This motivates the name *power shaping matrix*. For further interpretations of the shaping of signals in MIMO communication systems, see, e.g., [72].

The above observations lead to the following formal definition of a maximum-entropy signal.

Definition 2.5.1. *A real-valued or proper Gaussian vector $\boldsymbol{x}$ is called* maximum-entropy signal *with respect to a power shaping space $\mathcal{P}$ if its covariance matrix $\boldsymbol{C}_{\boldsymbol{x}}$ lies in $\mathcal{P}$, i.e., if the entropy reduction matrix $\mathrm{proj}_{\mathcal{N}}(\boldsymbol{C}_{\boldsymbol{x}})$ is zero.*

We will see later that there are many data transmission scenarios in which the worst-case Gaussian noise vectors are maximum-entropy signals. The following proposition is the mathematical basis for results of this kind (e.g., for the one in Section 4.4).

Proposition 2.5.2. *For all $\boldsymbol{P} \in \mathcal{P},\ \boldsymbol{N} \in \mathcal{N}$ such that $\boldsymbol{P} + \boldsymbol{N} \succeq \boldsymbol{0}$, we have*

$$0 \leq \det(\mathbf{I}_{M_{\mathbb{S}}} + \boldsymbol{P}^{-1}) \leq \det(\mathbf{I}_{M_{\mathbb{S}}} + (\boldsymbol{P} + \boldsymbol{N})^{-1}). \tag{2.21}$$

Proof. Note that $\boldsymbol{P} + \boldsymbol{N} = \boldsymbol{C}_{\boldsymbol{x}} \succeq \boldsymbol{0}$ implies $\boldsymbol{P} \succeq \boldsymbol{0}$ due to Proposition 2.5.1. Since $g(x) = \log_2(1+x^{-1})$ is convex for $x \geq 0$, the function $\log_2 \det(\mathbf{I}_{M_{\mathbb{S}}} + \boldsymbol{X}^{-1}) = \sum_{i=1}^{M_{\mathbb{S}}} \log_2(1+\lambda_i(\boldsymbol{X})^{-1})$ is a Schur-convex function of the vector of eigenvalues $\boldsymbol{\lambda}(\boldsymbol{X}) \geq \boldsymbol{0}$ (see Lemma 2.1.4 and Definition 2.1.3). Thus, the inequality is a consequence of Theorem 2.5.1. □

2.6 Transformations between Power Shaping Spaces

If a random vector $\boldsymbol{x}$ is transformed to a different vector space by a linear mapping $\boldsymbol{x} \mapsto \boldsymbol{y} = \boldsymbol{H}\boldsymbol{x}$, the covariance matrix of the transformed random vector is given by $\boldsymbol{C}_{\boldsymbol{y}} = \boldsymbol{H}\boldsymbol{C}_{\boldsymbol{x}}\boldsymbol{H}^{\mathrm{H}}$. In this section, we commence by considering transformation matrices with orthonormal columns. More general transformations are discussed in the next section.

Proposition 2.6.1. *For a matrix $\boldsymbol{U}$ with $\boldsymbol{U}^{\mathrm{H}}\boldsymbol{U} = \mathbf{I}_{M_{\mathbb{S}'}}$, let $\mathbb{S}' = \{\boldsymbol{S}' \mid \boldsymbol{S}' = \boldsymbol{U}^{\mathrm{H}}\boldsymbol{S}\boldsymbol{U},\ \boldsymbol{S} \in \mathbb{S}\}$. If $\boldsymbol{U}\boldsymbol{U}^{\mathrm{H}} \in \mathcal{P}$, the set $\mathcal{P}' = \{\boldsymbol{P}' \mid \boldsymbol{P}' = \boldsymbol{U}^{\mathrm{H}}\boldsymbol{P}\boldsymbol{U},\ \boldsymbol{P} \in \mathcal{P}\} \subseteq \mathbb{S}'$ is a power shaping space. The corresponding entropy reduction space in $\mathbb{S}'$ is $\mathcal{N}' = \{\boldsymbol{N}' \mid \boldsymbol{N}' = \boldsymbol{U}^{\mathrm{H}}\boldsymbol{N}\boldsymbol{U},\ \boldsymbol{N} \in \mathcal{N}\}$.*

Proof. $\mathcal{P}'$ is a vector space since $\alpha_1(\boldsymbol{U}^{\mathrm{H}}\boldsymbol{P}_1\boldsymbol{U}) + \alpha_2(\boldsymbol{U}^{\mathrm{H}}\boldsymbol{P}_2\boldsymbol{U}) = \boldsymbol{U}^{\mathrm{H}}(\alpha_1\boldsymbol{P}_1 + \alpha_2\boldsymbol{P}_2)\boldsymbol{U} \in \mathcal{P}'$ for all $\boldsymbol{P}_1, \boldsymbol{P}_2 \in \mathcal{P}$. Moreover, $\mathbf{I}_{M_{\mathbb{S}'}} = \boldsymbol{U}^{\mathrm{H}}\mathbf{I}_{M_{\mathbb{S}}}\boldsymbol{U} \in \mathcal{P}'$ since $\mathbf{I}_{M_{\mathbb{S}}} \in \mathcal{P}$, and we have for all $\boldsymbol{P}_1, \boldsymbol{P}_2 \in \mathcal{P}$ that $\boldsymbol{U}^{\mathrm{H}}\boldsymbol{P}_1\boldsymbol{U}\boldsymbol{U}^{\mathrm{H}}\boldsymbol{P}_2\boldsymbol{U}\boldsymbol{U}^{\mathrm{H}}\boldsymbol{P}_1\boldsymbol{U} = \boldsymbol{U}^{\mathrm{H}}\boldsymbol{P}_1\tilde{\boldsymbol{P}}\boldsymbol{P}_1\boldsymbol{U} \in \mathcal{P}'$ with $\tilde{\boldsymbol{P}} = \boldsymbol{U}\boldsymbol{U}^{\mathrm{H}}\boldsymbol{P}_2\boldsymbol{U}\boldsymbol{U}^{\mathrm{H}} \in \mathcal{P}$ and $\boldsymbol{P}_1\tilde{\boldsymbol{P}}\boldsymbol{P}_1 \in \mathcal{P}$.

The space $\mathcal{N}'$ is orthogonal to $\mathcal{P}'$ since $\mathrm{tr}[\boldsymbol{U}^{\mathrm{H}}\boldsymbol{P}\boldsymbol{U}\boldsymbol{U}^{\mathrm{H}}\boldsymbol{N}\boldsymbol{U}] = \mathrm{tr}[\tilde{\boldsymbol{P}}\boldsymbol{N}] = 0$ due to $\tilde{\boldsymbol{P}} \in \mathcal{P}$, and we note that any matrix $\boldsymbol{S}' \in \mathbb{S}'$ can be represented as $\boldsymbol{S}' = \boldsymbol{U}^{\mathrm{H}}\boldsymbol{S}\boldsymbol{U} = \boldsymbol{U}^{\mathrm{H}}(\boldsymbol{P} + \boldsymbol{N})\boldsymbol{U} = \boldsymbol{U}^{\mathrm{H}}\boldsymbol{P}\boldsymbol{U} + \boldsymbol{U}^{\mathrm{H}}\boldsymbol{N}\boldsymbol{U}$, where $\boldsymbol{U}^{\mathrm{H}}\boldsymbol{P}\boldsymbol{U} \in \mathcal{P}'$ and $\boldsymbol{U}^{\mathrm{H}}\boldsymbol{N}\boldsymbol{U} \in \mathcal{N}'$. Consequently, $\mathcal{N}' = \mathcal{P}'^{\perp_{\mathbb{S}'}}$. □

Corollary 2.6.1. *The set $\mathcal{P}' = \{\boldsymbol{P}' \mid \boldsymbol{P}' = \boldsymbol{U}^{\mathrm{H}}\boldsymbol{P}\boldsymbol{U},\ \boldsymbol{P} \in \mathcal{P}\}$ is a power shaping space if $\boldsymbol{U}$ is unitary.*

Proof. Since $\boldsymbol{U}\boldsymbol{U}^{\mathrm{H}} = \mathbf{I}_{M_{\mathbb{S}}} \in \mathcal{P}$ is fulfilled, Proposition 2.6.1 applies. □

Corollary 2.6.2. *Let* $[\boldsymbol{U},\ \boldsymbol{U}_0] \begin{bmatrix} \boldsymbol{\Lambda} & \\ & \mathbf{0} \end{bmatrix} [\boldsymbol{U},\ \boldsymbol{U}_0]^{\mathrm{H}} = \tilde{\boldsymbol{P}}$ *be the eigenvalue decomposition of* $\tilde{\boldsymbol{P}} \in \mathcal{P}$*. Then, the set* $\mathcal{P}' = \{\boldsymbol{P}' \mid \boldsymbol{P}' = \boldsymbol{U}^{\mathrm{H}}\boldsymbol{P}\boldsymbol{U},\ \boldsymbol{P} \in \mathcal{P}\} \subseteq \mathbb{S}'$ *is a power shaping space, and* $\boldsymbol{\Lambda} \in \mathcal{P}'$*. Moreover,* $\mathcal{P}'' = \{\boldsymbol{P}'' \mid \boldsymbol{P}'' = \boldsymbol{U}_0^{\mathrm{H}}\boldsymbol{P}\boldsymbol{U}_0,\ \boldsymbol{P} \in \mathcal{P}\} \subseteq \mathbb{S}''$ *is a power shaping space.*

Proof. As $\boldsymbol{U}\boldsymbol{U}^{\mathrm{H}} = [\boldsymbol{U},\ \boldsymbol{U}_0] \begin{bmatrix} \mathbf{I}_{M_{\mathbb{S}'}} & \\ & \mathbf{0} \end{bmatrix} [\boldsymbol{U},\ \boldsymbol{U}_0]^{\mathrm{H}} = \tilde{\boldsymbol{P}}^{+}\tilde{\boldsymbol{P}} \in \mathcal{P}$ (Corollary 2.4.3), $\mathcal{P}'$ is a power shaping space due to Proposition 2.6.1. As $\boldsymbol{U}^{\mathrm{H}}\boldsymbol{U} = \mathbf{I}_{M_{\mathbb{S}'}}$, we have $\boldsymbol{\Lambda} = \boldsymbol{U}^{\mathrm{H}}\boldsymbol{U}\boldsymbol{\Lambda}\boldsymbol{U}^{\mathrm{H}}\boldsymbol{U} = \boldsymbol{U}^{\mathrm{H}}\tilde{\boldsymbol{P}}\boldsymbol{U} \in \mathcal{P}'$. For $\mathcal{P}''$, note that $\boldsymbol{U}_0\boldsymbol{U}_0^{\mathrm{H}} = \mathbf{I}_{M_{\mathbb{S}}} - \tilde{\boldsymbol{P}}^{+}\tilde{\boldsymbol{P}} \in \mathcal{P}$ as well. □

Theorem 2.6.1. *Assume that* $\tilde{\boldsymbol{P}} \in \mathcal{P} \subseteq \mathbb{S}$ *has the highest number of distinct eigenvalues that is possible for a matrix from the power shaping space* $\mathcal{P}$*, and consider the eigenvalue decomposition* $\boldsymbol{U}\boldsymbol{\Lambda}\boldsymbol{U}^{\mathrm{H}} = \tilde{\boldsymbol{P}}$*. Then, the orthogonal projection* $\mathrm{proj}_{\mathcal{P}'}$ *to the power shaping space* $\mathcal{P}' = \{\boldsymbol{P}' \mid \boldsymbol{P}' = \boldsymbol{U}^{\mathrm{H}}\boldsymbol{P}\boldsymbol{U},\ \boldsymbol{P} \in \mathcal{P}\} \subseteq \mathbb{S}$ *commutes with the orthogonal projection* $\mathrm{proj}_{\mathrm{diag}}$ *to the space of diagonal matrices.*

Proof. Without loss of generality, we assume that the eigenvalues are sorted, so that we can use $\mathcal{I}_\ell,\ \ell = 1, \dots, L$ (the sets containing the indices of the eigenvectors $\boldsymbol{u}_i,\ \ i \in \mathcal{I}_\ell$ corresponding to the ℓth distinct eigenvalue) and $\boldsymbol{J}_\ell = \sum_{i\in\mathcal{I}_\ell} \boldsymbol{u}_i\boldsymbol{u}_i^{\mathrm{H}} \in \mathcal{P}$ as in the proof of Theorem 2.5.1. Let $\boldsymbol{J}'_\ell = \sum_{i\in\mathcal{I}_\ell} \mathbf{e}_i\mathbf{e}_i^{\mathrm{H}} = \boldsymbol{U}^{\mathrm{H}}\boldsymbol{J}_\ell\boldsymbol{U} \in \mathcal{P}'$, and let $\mathcal{P}'_\ell = \{\boldsymbol{P}' \in \mathcal{P}' \mid \exists \alpha_\ell \in \mathbb{R} : \boldsymbol{J}'_\ell\boldsymbol{P}'\boldsymbol{J}'_\ell = \alpha_\ell\boldsymbol{J}'_\ell\} \subseteq \mathcal{P}'$. This set contains $\boldsymbol{\Lambda}$ and all other matrices $\boldsymbol{P}' \in \mathcal{P}'$ that have a scaled identity as diagonal block at the position corresponding to the indices contained in $\mathcal{I}_\ell$. Note that for any $\boldsymbol{P}' \in \mathcal{P}'_\ell$ it holds that $\boldsymbol{J}'_\ell\boldsymbol{P}'\boldsymbol{J}'_\ell = \sum_{i\in\mathcal{I}_\ell} \mathbf{e}_i\mathbf{e}_i^{\mathrm{T}}\boldsymbol{P}'\mathbf{e}_i\mathbf{e}_i^{\mathrm{T}}$.

Now assume that there exists $\boldsymbol{P}' \in \mathcal{P}'$ such that $\boldsymbol{P}' \notin \mathcal{P}'_\ell$ for some ℓ. Then, there exists $\beta \in \mathbb{R}$ such that $\boldsymbol{X}' = \boldsymbol{\Lambda} + \beta\boldsymbol{J}'_\ell\boldsymbol{P}'\boldsymbol{J}'_\ell \in \mathcal{P}'$ has more distinct eigenvalues than $\boldsymbol{\Lambda}$. This is equivalent with $\boldsymbol{X} = \boldsymbol{U}\boldsymbol{X}'\boldsymbol{U}^{\mathrm{H}} \in \mathcal{P}$ having more distinct eigenvalues than $\tilde{\boldsymbol{P}}$ and contradicts the assumption. This proves that $\mathcal{P}'_\ell = \mathcal{P}'$ for all ℓ.

We thus have

$$\mathrm{proj}_{\mathrm{diag}}(\boldsymbol{P}') = \sum_{\ell=1}^{L} \sum_{i\in\mathcal{I}_\ell} \mathbf{e}_i\mathbf{e}_i^{\mathrm{T}}\boldsymbol{P}'\mathbf{e}_i\mathbf{e}_i^{\mathrm{T}} = \sum_{\ell=1}^{L} \boldsymbol{J}'_\ell\boldsymbol{P}'\boldsymbol{J}'_\ell \in \mathcal{P}' \tag{2.22}$$

for all $\boldsymbol{P}' \in \mathcal{P}'$ due to (2.12) since $\boldsymbol{J}'_\ell \in \mathcal{P}'$. For any $\boldsymbol{P}' \in \mathcal{P}'$ and $\boldsymbol{N}' \in \mathcal{N}'$, we have

$$\mathrm{tr}[\boldsymbol{P}'\,\mathrm{proj}_{\mathrm{diag}}(\boldsymbol{N}')] = \mathrm{tr}[\underbrace{\mathrm{proj}_{\mathrm{diag}}(\boldsymbol{P}')}_{\in\mathcal{P}'}\,\boldsymbol{N}'] = 0. \tag{2.23}$$

This shows that $\mathrm{proj}_{\mathrm{diag}}(\boldsymbol{N}') \in \mathcal{N}'$. As a result, we have

$$\begin{aligned}\mathrm{proj}_{\mathcal{P}'}(\mathrm{proj}_{\mathrm{diag}}(\boldsymbol{P}' + \boldsymbol{N}')) &= \mathrm{proj}_{\mathcal{P}'}(\mathrm{proj}_{\mathrm{diag}}(\boldsymbol{P}') + \mathrm{proj}_{\mathrm{diag}}(\boldsymbol{N}')) = \mathrm{proj}_{\mathrm{diag}}(\boldsymbol{P}') \\ &= \mathrm{proj}_{\mathrm{diag}}(\mathrm{proj}_{\mathcal{P}'}(\boldsymbol{P}' + \boldsymbol{N}')).\end{aligned} \tag{2.24}$$

□

If all eigenvalues of $\tilde{\boldsymbol{P}} \in \mathcal{P}$ have multiplicity one—we will see later that this is possible only in certain power shaping spaces—we have the following specialization.

Corollary 2.6.3. *If all eigenvalues of $\tilde{\boldsymbol{P}} \in \mathcal{P} \subseteq \mathbb{S}$ in Theorem 2.6.1 have multiplicity one, all diagonal matrices of appropriate dimension are contained in $\mathcal{P}'$.*

Proof. In this case, any matrix $\boldsymbol{J}'_\ell \in \mathcal{P}'$ in the proof of Theorem 2.6.1 can be expressed as $\boldsymbol{J}'_\ell = \mathbf{e}_i \mathbf{e}_i^{\mathrm{H}}$ for some i. Thus, any diagonal matrix can be written as a linear combination $\boldsymbol{D} = \sum_{\ell=1}^{L} d_\ell \boldsymbol{J}'_\ell,\ d_\ell \in \mathbb{R}$, which reveals that $\boldsymbol{D} \in \mathcal{P}'$. □

For the case that $\tilde{\boldsymbol{P}}$ does not have the maximal number of distinct eigenvalues, we have the following generalizations.

Corollary 2.6.4. *For any $\tilde{\boldsymbol{P}} \in \mathcal{P} \subseteq \mathbb{S}$, the modal matrix $\boldsymbol{U}$ in the eigenvalue decomposition $\boldsymbol{U}\boldsymbol{\Lambda}\boldsymbol{U}^{\mathrm{H}} = \tilde{\boldsymbol{P}}$ can be chosen in a way that the orthogonal projection $\mathrm{proj}_{\mathcal{P}'}$ to the space $\mathcal{P}' = \{\boldsymbol{P}' \mid \boldsymbol{P}' = \boldsymbol{U}^{\mathrm{H}}\boldsymbol{P}\boldsymbol{U},\ \boldsymbol{P} \in \mathcal{P}\} \subseteq \mathbb{S}$ commutes with the orthogonal projection $\mathrm{proj}_{\mathrm{diag}}$ to the space of diagonal matrices.*

Proof. In this case, the proof of Theorem 2.6.1 is adapted as follows. Finding a $\boldsymbol{P}' \in \mathcal{P}'$ such that $\boldsymbol{P}' \notin \mathcal{P}'_\ell$ for some ℓ, and constructing an $\boldsymbol{X}$ with a higher number of distinct eigenvalues than $\tilde{\boldsymbol{P}}$ no longer leads to a contradiction. Since $\boldsymbol{\Lambda} \in \mathcal{P}'_\ell$, i.e., $\boldsymbol{\Lambda}$ has a scaled identity as diagonal block at the position of interest, any modal matrix of $\boldsymbol{X}$ is also a modal matrix of $\boldsymbol{\Lambda}$. We can thus replace $\tilde{\boldsymbol{P}}$ by $\tilde{\boldsymbol{P}}_{\mathrm{new}} = \boldsymbol{X}$ and repeat the procedure until $\tilde{\boldsymbol{P}}_{\mathrm{new}}$ has the maximum number of distinct eigenvalues that is possible in $\mathcal{P}$. We then have $\mathcal{P}'_\ell = \mathcal{P}'$ for all ℓ and the proof continues as for Theorem 2.6.1. □

Corollary 2.6.5. *Consider the eigenvalue decomposition $\boldsymbol{U}\boldsymbol{\Lambda}\boldsymbol{U}^{\mathrm{H}} = \tilde{\boldsymbol{P}} \in \mathcal{P} \subseteq \mathbb{S}$. Then, all diagonal matrices of appropriate dimension which have repeated diagonal elements at the positions corresponding to the repeated eigenvalues are contained in $\mathcal{P}' = \{\boldsymbol{P}' \mid \boldsymbol{P}' = \boldsymbol{U}^{\mathrm{H}}\boldsymbol{P}\boldsymbol{U},\ \boldsymbol{P} \in \mathcal{P}\} \subseteq \mathbb{S}$.*

Proof. Any such matrix can be expressed as $\boldsymbol{D} = \sum_{\ell=1}^{L} d_\ell \boldsymbol{J}'_\ell,\ d_\ell \in \mathbb{R}$ with $\boldsymbol{J}'_\ell \in \mathcal{P}'$ as defined in the proof of Theorem 2.6.1. □

Remark 2.6.1. *If the underlying vector space $\mathbb{S}$ is chosen to be only a subspace of $\mathbb{H}^{M_{\mathbb{S}}}$ (see Remark 2.3.1), we do not necessarily have $\mathcal{P}' \subseteq \mathbb{S}$ in Theorem 2.6.1 and its corollaries. Instead, we need to define $\mathbb{S}' = \{\boldsymbol{P}' \mid \boldsymbol{P}' = \boldsymbol{U}^{\mathrm{H}}\boldsymbol{P}\boldsymbol{U},\ \boldsymbol{P} \in \mathbb{S}\}$. Then, the statements hold with $\mathcal{P}' \subseteq \mathbb{S}'$. The same phenomenon occurs for the unitary transformations in Proposition 2.7.3 in the next section.*

2.7 Compatible Matrices

The concept of a compatible matrix allows us to characterize transformations that map from a power shaping space $\mathcal{P}$ to a specified target power shaping space $\mathcal{P}'$.

Definition 2.7.1. *Let $\mathcal{P} \subseteq \mathbb{S}$ and $\mathcal{P}' \subseteq \mathbb{S}'$ be two power shaping spaces. A matrix $\boldsymbol{H} \in \mathbb{C}^{M_{\mathbb{S}'} \times M_{\mathbb{S}}}$ is called* compatible with the pair of power shaping spaces $(\mathcal{P}', \mathcal{P})$ *if $\boldsymbol{H}\boldsymbol{P}\boldsymbol{H}^{\mathrm{H}} \in \mathcal{P}'$ and $\boldsymbol{H}\boldsymbol{N}\boldsymbol{H}^{\mathrm{H}} \in \mathcal{N}' = \mathcal{P}'^{\perp_{\mathbb{S}'}}$ hold for all $\boldsymbol{P} \in \mathcal{P}$ and all $\boldsymbol{N} \in \mathcal{N} = \mathcal{P}^{\perp_{\mathbb{S}}}$.*

The following propositions summarize useful properties of compatible matrices.

Proposition 2.7.1. *Let $\mathcal{P} \subseteq \mathbb{S}$ and $\mathcal{P}' \subseteq \mathbb{S}'$ be two power shaping spaces, and let $\boldsymbol{H} \in \mathbb{C}^{M_{\mathbb{S}'} \times M_{\mathbb{S}}}$ such that $\boldsymbol{H}^{\mathrm{H}} \boldsymbol{S}' \boldsymbol{H} \in \mathbb{S}$, $\forall \boldsymbol{S}' \in \mathbb{S}'$. If $\boldsymbol{H}$ is compatible with $(\mathcal{P}', \mathcal{P})$, $\boldsymbol{H}^{\mathrm{H}}$ is compatible with $(\mathcal{P}, \mathcal{P}')$.*

Proof. For any $\boldsymbol{P}' \in \mathcal{P}'$ and $\boldsymbol{N} \in \mathcal{N}$, $\mathrm{tr}[(\boldsymbol{H}^{\mathrm{H}} \boldsymbol{P}' \boldsymbol{H}) \boldsymbol{N}] = \mathrm{tr}[\boldsymbol{P}' (\boldsymbol{H} \boldsymbol{N} \boldsymbol{H}^{\mathrm{H}})] = 0$ since $\boldsymbol{H} \boldsymbol{N} \boldsymbol{H}^{\mathrm{H}} \in \mathcal{N}'$. Thus, $\boldsymbol{H}^{\mathrm{H}} \boldsymbol{P}' \boldsymbol{H} \in \mathcal{P}$. The proof is completed by repeating the argument with $\boldsymbol{P}$ and $\boldsymbol{N}$ interchanged. □

Proposition 2.7.2. *Let $\mathcal{P} \subseteq \mathbb{S}$, $\mathcal{P}' \subseteq \mathbb{S}'$, and $\mathcal{P}'' \subseteq \mathbb{S}''$ be power shaping spaces. If $\boldsymbol{H} \in \mathbb{C}^{M_{\mathbb{S}'} \times M_{\mathbb{S}}}$ is compatible with $(\mathcal{P}', \mathcal{P})$ and $\boldsymbol{H}' \in \mathbb{C}^{M_{\mathbb{S}''} \times M_{\mathbb{S}'}}$ is compatible with $(\mathcal{P}'', \mathcal{P}')$, then the product $\boldsymbol{H}' \boldsymbol{H}$ is compatible with $(\mathcal{P}'', \mathcal{P})$.*

Proof. We have $\boldsymbol{P} \in \mathcal{P} \Rightarrow \boldsymbol{H} \boldsymbol{P} \boldsymbol{H}^{\mathrm{H}} \in \mathcal{P}' \Rightarrow \boldsymbol{P}'' = \boldsymbol{H}' (\boldsymbol{H} \boldsymbol{P} \boldsymbol{H}^{\mathrm{H}}) \boldsymbol{H}'^{\mathrm{H}} \in \mathcal{P}''$, and analogously for $\boldsymbol{N} \in \mathcal{N}$. □

As any $\boldsymbol{P} \in \mathcal{P}$ is compatible with $(\mathcal{P}, \mathcal{P})$ due to (2.12) and Proposition 2.4.2, a simple special case of the above proposition is that $\tilde{\boldsymbol{H}} = \boldsymbol{H} \boldsymbol{P}$ is compatible with $(\mathcal{P}', \mathcal{P})$ if $\boldsymbol{H}$ is compatible with $(\mathcal{P}', \mathcal{P})$ and $\boldsymbol{P} \in \mathcal{P}$.

Proposition 2.7.3. *Let $\mathcal{P} \subseteq \mathbb{S}$ and $\mathcal{P}' \subseteq \mathbb{S}'$ be two power shaping spaces, let $\boldsymbol{U} \in \mathbb{C}^{M_{\mathbb{S}} \times M_{\mathbb{S}}}$ and $\boldsymbol{U}' \in \mathbb{C}^{M_{\mathbb{S}'} \times M_{\mathbb{S}'}}$ be unitary, and let $\boldsymbol{H} \in \mathbb{C}^{M_{\mathbb{S}'} \times M_{\mathbb{S}}}$ be compatible with $(\mathcal{P}', \mathcal{P})$. Then, $\tilde{\boldsymbol{H}} = \boldsymbol{U}'^{\mathrm{H}} \boldsymbol{H} \boldsymbol{U}$ is compatible with $(\tilde{\mathcal{P}}', \tilde{\mathcal{P}})$ where $\tilde{\mathcal{P}} = \{\tilde{\boldsymbol{P}} \mid \tilde{\boldsymbol{P}} = \boldsymbol{U}^{\mathrm{H}} \boldsymbol{P} \boldsymbol{U},\ \boldsymbol{P} \in \mathcal{P}\} \subseteq \mathbb{S}$ and $\tilde{\mathcal{P}}' = \{\tilde{\boldsymbol{P}}' \mid \tilde{\boldsymbol{P}}' = \boldsymbol{U}'^{\mathrm{H}} \boldsymbol{P}' \boldsymbol{U}',\ \boldsymbol{P}' \in \mathcal{P}'\} \subseteq \mathbb{S}'$.*

Proof. $\tilde{\boldsymbol{H}} \tilde{\boldsymbol{P}} \tilde{\boldsymbol{H}}^{\mathrm{H}} = \boldsymbol{U}'^{\mathrm{H}} \boldsymbol{H} \boldsymbol{U} \boldsymbol{U}^{\mathrm{H}} \boldsymbol{P} \boldsymbol{U} \boldsymbol{U}^{\mathrm{H}} \boldsymbol{H}^{\mathrm{H}} \boldsymbol{U}' = \boldsymbol{U}'^{\mathrm{H}} \boldsymbol{H} \boldsymbol{P} \boldsymbol{H}^{\mathrm{H}} \boldsymbol{U}' = \boldsymbol{U}'^{\mathrm{H}} \boldsymbol{P}' \boldsymbol{U}' \in \tilde{\mathcal{P}}'$ with $\boldsymbol{P}' = \boldsymbol{H} \boldsymbol{P} \boldsymbol{H}^{\mathrm{H}} \in \mathcal{P}'$. Analogously, we can show that $\tilde{\boldsymbol{H}} \tilde{\boldsymbol{N}} \tilde{\boldsymbol{H}}^{\mathrm{H}} \in \tilde{\mathcal{N}}'$. □

Proposition 2.7.4. *Let $\mathcal{P} = \mathcal{A} \cap \mathcal{B} \subseteq \mathbb{S}$ as in Proposition 2.4.3, and let $\mathcal{P}' = \mathcal{A}' \cap \mathcal{B}' \subseteq \mathbb{S}'$ analogously. If $\boldsymbol{H} \in \mathbb{C}^{M_{\mathbb{S}'} \times M_{\mathbb{S}}}$ is compatible with $(\mathcal{A}', \mathcal{A})$ and at the same time compatible with $(\mathcal{B}', \mathcal{B})$, then it is compatible with $(\mathcal{P}', \mathcal{P})$ as well.*

Proof. Since $\boldsymbol{H} \boldsymbol{P} \boldsymbol{H}^{\mathrm{H}} \in \mathcal{A}'$ for all $\boldsymbol{P} \in \mathcal{A}$ and $\boldsymbol{H} \boldsymbol{P} \boldsymbol{H}^{\mathrm{H}} \in \mathcal{B}'$ for all $\boldsymbol{P} \in \mathcal{B}$, it holds that $\boldsymbol{H} \boldsymbol{P} \boldsymbol{H}^{\mathrm{H}} \in \mathcal{A}' \cap \mathcal{B}'$ for all $\boldsymbol{P} \in \mathcal{A} \cap \mathcal{B}$. We have $(\mathcal{A} \cap \mathcal{B})^{\perp_{\mathbb{S}}} = \mathcal{A}^{\perp_{\mathbb{S}}} + \mathcal{B}^{\perp_{\mathbb{S}}}$ [73, Th. 2.8], i.e., any $\boldsymbol{N} \in \mathcal{N} = (\mathcal{A} \cap \mathcal{B})^{\perp_{\mathbb{S}}}$ can be written as $\boldsymbol{N} = \boldsymbol{N}_{\mathcal{A}} + \boldsymbol{N}_{\mathcal{B}}$ with $\boldsymbol{N}_{\mathcal{A}} \in \mathcal{A}^{\perp_{\mathbb{S}}}, \boldsymbol{N}_{\mathcal{B}} \in \mathcal{B}^{\perp_{\mathbb{S}}}$. Thus, $\boldsymbol{H} \boldsymbol{N} \boldsymbol{H}^{\mathrm{H}} = \boldsymbol{H} \boldsymbol{N}_{\mathcal{A}} \boldsymbol{H}^{\mathrm{H}} + \boldsymbol{H} \boldsymbol{N}_{\mathcal{B}} \boldsymbol{H}^{\mathrm{H}} \in \mathcal{A}'^{\perp_{\mathbb{S}'}} + \mathcal{B}'^{\perp_{\mathbb{S}'}} = (\mathcal{A}' \cap \mathcal{B}')^{\perp_{\mathbb{S}'}} = \mathcal{N}'$. □

2.8 Examples

As the definition of a power shaping space given in Definition 2.3.1 is very general, let us now consider some examples of such spaces in order to get a better intuition about the concept.

Example 2.8.1. *The one-dimensional subspace $\mathcal{P} = \{\alpha \mathbf{I}_{M_{\mathbb{S}}} \mid \alpha \in \mathbb{R}\}$ is the smallest possible power shaping space in $\mathbb{S}$. The orthogonal complement $\mathcal{N}$ contains all matrices with trace zero.*

Example 2.8.2. *Let $\mathcal{P} \subseteq \mathbb{S}$ be the set of diagonal matrices of size $M_{\mathbb{S}} \times M_{\mathbb{S}}$. The orthogonal complement $\mathcal{N}$ is given by all matrices in $\mathbb{S}$ which have zeros on the diagonal and arbitrary off-diagonal elements.*

Example 2.8.3. *A set $\mathcal{P}' \in \mathbb{S}$ such that all matrices in $\mathcal{P}'$ have the same set of eigenvectors is a power shaping space. This can be seen by combining Corollary 2.6.1 with Example 2.8.2. The orthogonal complement is $\mathcal{N}' = \{\boldsymbol{N}' = \boldsymbol{U}\boldsymbol{N}\boldsymbol{U} \mid \boldsymbol{N} \in \mathcal{N}\}$ with $\mathcal{N}$ from Example 2.8.2, where $\boldsymbol{U}$ is a modal matrix of all $\boldsymbol{P}' \in \mathcal{P}'$.*

Example 2.8.4. *The real symmetric matrices form a power shaping space $\mathcal{P} = \mathbb{S}^M$ within the space of Hermitian matrices $\mathbb{S} = \mathbb{H}^M$. The orthogonal complement $\mathcal{N}$ is given by all purely imaginary Hermitian matrices of appropriate size.*

For the following examples, we use the notation for spaces of block-diagonal matrices introduced in Definition 2.1.1.

Example 2.8.5. *Any space of Hermitian (or real symmetric) block-diagonal matrices $\mathcal{P} = \mathbb{H}^{\mathcal{M}}$ (or $\mathcal{P} = \mathbb{S}^{\mathcal{M}}$) with $\mathcal{M} \in \mathbb{N}^J$ is a power shaping space. The orthogonal complement $\mathcal{N}$ is given by matrices where all diagonal blocks are zero (and the off-diagonal blocks may be nonzero).*

Example 2.8.6. *Let $\mathcal{M}, \mathcal{M}' \in \mathbb{N}^J$. Then, every block-diagonal matrix $\boldsymbol{H} \in \mathbb{C}^{\mathcal{M}' \times \mathcal{M}}$ (or $\boldsymbol{H} \in \mathbb{R}^{\mathcal{M}' \times \mathcal{M}}$) is compatible with $(\mathbb{H}^{\mathcal{M}'}, \mathbb{H}^{\mathcal{M}})$ (or with $(\mathbb{S}^{\mathcal{M}'}, \mathbb{S}^{\mathcal{M}})$, respectively).*

The spaces of block-diagonal matrices $\mathbb{C}^{\mathcal{M}' \times \mathcal{M}}$ and block-diagonal Hermitian matrices $\mathcal{P} = \mathbb{H}^{\mathcal{M}}$ were used in [22,25] to study multicarrier MIMO systems. In this work, we instead use the following slightly modified power shaping space, whose elements are matrices that consist of four block-diagonal submatrices. The reason for this will become clear in Section 3.4.3, when we discuss the mathematical model that we use for multicarrier MIMO systems.

Proposition 2.8.1. *Let $\mathcal{L}, \mathcal{M} \in \mathbb{N}^J$. Then,*

$$\mathcal{P} = \left\{ \boldsymbol{P} = \begin{bmatrix} \boldsymbol{A} & \boldsymbol{B} \\ \boldsymbol{B}^{\mathrm{H}} & \boldsymbol{C} \end{bmatrix} \;\middle|\; \boldsymbol{A} \in \mathbb{H}^{\mathcal{L}}, \boldsymbol{C} \in \mathbb{H}^{\mathcal{M}}, \boldsymbol{B} \in \mathbb{C}^{\mathcal{L} \times \mathcal{M}} \right\} \tag{2.25}$$

is a power shaping space. The same holds if $\mathbb{C}$ and $\mathbb{H}$ are replaced by $\mathbb{R}$ and $\mathbb{S}$, respectively.

Proof. There exists a permutation matrix $\boldsymbol{\Pi}$ such that $\boldsymbol{\Pi}\boldsymbol{P}\boldsymbol{\Pi}^{\mathrm{T}} \in \mathbb{H}^{\mathcal{L}+\mathcal{M}}$, $\forall \boldsymbol{P} \in \mathcal{P}$, where the addition of the tuples $\mathcal{L}$ and $\mathcal{M}$ is understood element-wise. The statement thus follows from Corollary 2.6.1 and Example 2.8.5. □

Proposition 2.8.2. *Let $\mathcal{L}, \mathcal{M}, \mathcal{L}', \mathcal{M}' \in \mathbb{N}^J$, let $\mathcal{P}$ be as in Proposition 2.8.1, and let $\mathcal{P}'$ be defined analogously based on $\mathcal{L}'$ and $\mathcal{M}'$. Then,*

$$\boldsymbol{H} = \begin{bmatrix} \boldsymbol{A} & \boldsymbol{B} \\ \boldsymbol{C} & \boldsymbol{D} \end{bmatrix}, \quad \boldsymbol{A} \in \mathbb{C}^{\mathcal{L}' \times \mathcal{L}}, \boldsymbol{B} \in \mathbb{C}^{\mathcal{L}' \times \mathcal{M}}, \boldsymbol{C} \in \mathbb{C}^{\mathcal{M}' \times \mathcal{L}}, \boldsymbol{D} \in \mathbb{C}^{\mathcal{M}' \times \mathcal{M}} \tag{2.26}$$

is compatible with $(\mathcal{P}', \mathcal{P})$.

Proof. Let $\boldsymbol{\Pi}$ be as in the proof of Proposition 2.8.1, and let $\boldsymbol{\Pi}'$ be defined analogously. Then, $\boldsymbol{\Pi}\boldsymbol{P}\boldsymbol{\Pi}^{\mathrm{T}} \in \mathbb{H}^{\mathcal{L}+\mathcal{M}}$, $\forall \boldsymbol{P} \in \mathcal{P}$, $\boldsymbol{\Pi}'\boldsymbol{P}'\boldsymbol{\Pi}'^{\mathrm{T}} \in \mathbb{H}^{\mathcal{L}'+\mathcal{M}'}$, $\forall \boldsymbol{P}' \in \mathcal{P}'$, and $\boldsymbol{\Pi}'\boldsymbol{H}\boldsymbol{\Pi}^{\mathrm{T}} \in \mathbb{C}^{(\mathcal{L}'+\mathcal{M}') \times (\mathcal{L}+\mathcal{M})}$. The statement then follows from Proposition 2.7.3 and Example 2.8.6. □

Note that the power shaping spaces given above are only examples, and infinitely many others exist. Another important example, which needs to be discussed in more detail, is presented in the following section.

Which particular power shaping space is useful finally depends on the question under investigation. Moreover, in a system where transformations of random vectors occur, such as due to the channel in a communication system, the choice for an appropriate power shaping space also depends on the properties of the possible channel matrices. For a sensible analysis, it may be preferable that the channel matrices are compatible with the power shaping spaces considered at the transmitter and at the receiver. This aspect is discussed in Section 3.4.4, which is devoted to power shaping spaces that are fundamental for the communication systems we consider, and in Section 4.5.4, where we consider examples that do not feature such a compatibility.

2.9 Improper Signals and Widely Linear Operations

When processing improper signals (see Section 1.4), it often makes sense to use so-called widely linear operations [74], which are linear functions of both the input signal and its complex conjugate. In this section, we summarize the formal definitions of improper signals and widely linear operations, and we discuss a real-valued representation of complex signals, which we then relate to the concept of power shaping spaces.

2.9.1 Fundamentals

We introduce the following definitions in accordance with the existing literature (e.g., [7, 63, 64, 74–78]).

Definition 2.9.1. *For a general complex random vector $\boldsymbol{x}$, the matrices*

$$\boldsymbol{C}_{\boldsymbol{x}} = \mathrm{E}[(\boldsymbol{x} - \mathrm{E}[\boldsymbol{x}])(\boldsymbol{x} - \mathrm{E}[\boldsymbol{x}])^{\mathrm{H}}] \quad \textit{and} \quad \tilde{\boldsymbol{C}}_{\boldsymbol{x}} = \mathrm{E}[(\boldsymbol{x} - \mathrm{E}[\boldsymbol{x}])(\boldsymbol{x} - \mathrm{E}[\boldsymbol{x}])^{\mathrm{T}}] \tag{2.27}$$

are called covariance matrix *and* pseudocovariance matrix*, respectively.*

In the special case that x is a scalar, we have a scalar variance C_x and a scalar pseudovariance $\tilde{C}_x$. Instead of the term pseudocovariance matrix, some authors prefer alternative names such as *complementary covariance matrix*, *conjugate covariance matrix*, or *relation matrix* (e.g., [75, 77]). If this matrix vanishes, there are no (strictly linear) correlations between the random vector and its complex conjugate. The following nomenclature is used.

Definition 2.9.2. *The complex random vector $\boldsymbol{x}$ is called* proper *if $\tilde{\boldsymbol{C}}_{\boldsymbol{x}} = \boldsymbol{0}$, and* improper *otherwise.*

Definition 2.9.3. *The complex random vectors $\boldsymbol{x}_1, \ldots, \boldsymbol{x}_N$ are called* jointly proper *if the vector $[\boldsymbol{x}_1^{\mathrm{T}}, \ldots, \boldsymbol{x}_N^{\mathrm{T}}]^{\mathrm{T}}$ is proper.*

Propriety shall not be confused with circular symmetry of the probability density function, which is a stricter requirement. However, in case of a zero-mean Gaussian distribution, the terms proper and circularly symmetric are equivalent [77] and can be used interchangeably.

Definition 2.9.4. *The complex random vectors* $\boldsymbol{x}$ *and* $\boldsymbol{y}$ *are called* uncorrelated *if*

$$\mathrm{E}[(\boldsymbol{x}-\mathrm{E}[\boldsymbol{x}])(\boldsymbol{y}-\mathrm{E}[\boldsymbol{y}])^{\mathrm{H}}]=\boldsymbol{0} \quad \textit{and} \quad \mathrm{E}[(\boldsymbol{x}-\mathrm{E}[\boldsymbol{x}])(\boldsymbol{y}-\mathrm{E}[\boldsymbol{y}])^{\mathrm{T}}]=\boldsymbol{0}. \tag{2.28}$$

This definition states that we use the term *uncorrelated* in the sense proposed, e.g., in [64, Sec. 2.2.1]. Such a clarification is necessary since competing definitions of uncorrelated complex random vectors exist in the literature (see [64, Sec. 2.2.1]).

Definition 2.9.5. *A complex mapping* $\boldsymbol{f}:\boldsymbol{x}\mapsto\boldsymbol{f}(\boldsymbol{x})$ *that can be expressed as [74]*

$$\boldsymbol{f}(\boldsymbol{x})=\boldsymbol{A}_{\mathrm{L}}\boldsymbol{x}+\boldsymbol{A}_{\mathrm{CL}}\boldsymbol{x}^{*} \tag{2.29}$$

with $\boldsymbol{A}_{\mathrm{L}},\boldsymbol{A}_{\mathrm{CL}}\in\mathbb{C}^{N\times M}$ *is called* widely linear.

Since a widely linear operation is the sum of a linear mapping (described by the matrix $\boldsymbol{A}_{\mathrm{L}}$) and a conjugate-linear one (described by $\boldsymbol{A}_{\mathrm{CL}}$), an alternative name is *linear-conjugate-linear* operation (e.g., [77]).

2.9.2 Composite Real Representation

The *composite real representation* $\check{\boldsymbol{x}}$ of a complex vector $\boldsymbol{x}$ is given by (e.g., [64])

$$\check{\boldsymbol{x}}=\check{\Re}(\boldsymbol{x})=\begin{bmatrix}\Re(\boldsymbol{x})\\ \Im(\boldsymbol{x})\end{bmatrix}. \tag{2.30}$$

For example in [64, Sec. 2.2], we find the equations

$$\boldsymbol{C}_{\boldsymbol{x}}=\boldsymbol{C}_{\Re\boldsymbol{x}}+\boldsymbol{C}_{\Im\boldsymbol{x}}+\mathrm{j}(\boldsymbol{C}_{\Re\boldsymbol{x}\Im\boldsymbol{x}}^{\mathrm{T}}-\boldsymbol{C}_{\Re\boldsymbol{x}\Im\boldsymbol{x}}) \tag{2.31}$$

$$\tilde{\boldsymbol{C}}_{\boldsymbol{x}}=\boldsymbol{C}_{\Re\boldsymbol{x}}-\boldsymbol{C}_{\Im\boldsymbol{x}}+\mathrm{j}(\boldsymbol{C}_{\Re\boldsymbol{x}\Im\boldsymbol{x}}^{\mathrm{T}}+\boldsymbol{C}_{\Re\boldsymbol{x}\Im\boldsymbol{x}}) \tag{2.32}$$

for the complex covariance matrix $\boldsymbol{C}_{\boldsymbol{x}}$ and the pseudocovariance matrix $\tilde{\boldsymbol{C}}_{\boldsymbol{x}}$. By comparing them with the blocks of the composite real covariance matrix

$$\boldsymbol{C}_{\check{\boldsymbol{x}}}=\begin{bmatrix}\boldsymbol{C}_{\Re\boldsymbol{x}} & \boldsymbol{C}_{\Re\boldsymbol{x}\Im\boldsymbol{x}}\\ \boldsymbol{C}_{\Re\boldsymbol{x}\Im\boldsymbol{x}}^{\mathrm{T}} & \boldsymbol{C}_{\Im\boldsymbol{x}}\end{bmatrix} \tag{2.33}$$

i.e., the covariance matrix of (2.30), we obtain [7, 26, 79]

$$\boldsymbol{C}_{\check{\boldsymbol{x}}}=\frac{1}{2}\begin{bmatrix}\Re(\boldsymbol{C}_{\boldsymbol{x}}) & -\Im(\boldsymbol{C}_{\boldsymbol{x}})\\ \Im(\boldsymbol{C}_{\boldsymbol{x}}) & \Re(\boldsymbol{C}_{\boldsymbol{x}})\end{bmatrix}+\frac{1}{2}\begin{bmatrix}\Re(\tilde{\boldsymbol{C}}_{\boldsymbol{x}}) & \Im(\tilde{\boldsymbol{C}}_{\boldsymbol{x}})\\ \Im(\tilde{\boldsymbol{C}}_{\boldsymbol{x}}) & -\Re(\tilde{\boldsymbol{C}}_{\boldsymbol{x}})\end{bmatrix}. \tag{2.34}$$

For a proper random vector $\boldsymbol{x}$, we have $\tilde{\boldsymbol{C}}_{\boldsymbol{x}}=\boldsymbol{0}$, and the second summand vanishes.

According to [64, Sec. 2.1], any real-valued linear mapping $\check{\boldsymbol{f}}(\check{\boldsymbol{x}})=\boldsymbol{A}_{\mathrm{WL}}\check{\boldsymbol{x}}$ with

$$\boldsymbol{A}_{\mathrm{WL}}=\begin{bmatrix}\boldsymbol{A}_{11} & \boldsymbol{A}_{12}\\ \boldsymbol{A}_{21} & \boldsymbol{A}_{22}\end{bmatrix} \tag{2.35}$$

and $\boldsymbol{A}_{ij}\in\mathbb{R}^{N\times M}$, $i,j\in\{1,2\}$, corresponds to a complex widely linear mapping (2.29) with

$$\boldsymbol{A}_{\mathrm{L}}=\frac{1}{2}(\boldsymbol{A}_{11}+\boldsymbol{A}_{22})+\mathrm{j}\frac{1}{2}(\boldsymbol{A}_{21}-\boldsymbol{A}_{12}) \tag{2.36}$$

$$\boldsymbol{A}_{\mathrm{CL}}=\frac{1}{2}(\boldsymbol{A}_{11}-\boldsymbol{A}_{22})+\mathrm{j}\frac{1}{2}(\boldsymbol{A}_{21}+\boldsymbol{A}_{12}) \tag{2.37}$$

i.e., $\check{\Re}(\boldsymbol{f}(\boldsymbol{x})) = \check{\boldsymbol{f}}(\check{\Re}(\boldsymbol{x}))$. Solving this for $\boldsymbol{A}_{\mathrm{WL}}$, we have [7]

$$\boldsymbol{A}_{\mathrm{WL}} = \begin{bmatrix} \Re(\boldsymbol{A}_{\mathrm{L}}) & -\Im(\boldsymbol{A}_{\mathrm{L}}) \\ \Im(\boldsymbol{A}_{\mathrm{L}}) & \Re(\boldsymbol{A}_{\mathrm{L}}) \end{bmatrix} + \begin{bmatrix} \Re(\boldsymbol{A}_{\mathrm{CL}}) & \Im(\boldsymbol{A}_{\mathrm{CL}}) \\ \Im(\boldsymbol{A}_{\mathrm{CL}}) & -\Re(\boldsymbol{A}_{\mathrm{CL}}) \end{bmatrix}. \tag{2.38}$$

The second summand in (2.38) vanishes if $\boldsymbol{A}_{\mathrm{CL}} = \boldsymbol{0}$, i.e., if (2.29) describes a conventional linear mapping in the complex domain.

2.9.3 Block-Skew-Circulant (BSC) Matrices

By looking at the first summands of (2.34) and (2.38), we note that there is a particular block structure that plays a role for the real-valued representation of both proper signals and linear operations. These matrices are block-Toeplitz matrices, where the second block row is a cyclically shifted copy of the first block row with a sign change for the block below the main diagonal. As proposed in [7], we thus call such a matrix *block-skew-circulant with* 2×2 *blocks* ($\mathcal{BSC}_2$), which is a generalization of the notion of skew-circulant matrices (e.g., [80]).[2] An alternative name can be found in [82–84], where real matrices of this form were said to have *complex structure*.

Another important block structure can be observed in the second summands of (2.34) and (2.38). These matrices have a block-Hankel structure instead, and we therefore call them *block-Hankel-skew-circulant with* 2×2 *blocks* ($\mathcal{BHSC}_2$) [7].

Definition 2.9.6. *The sets of real block-skew-circulant and real block-Hankel-skew-circulant matrices with* 2×2 *blocks of size* $N \times M$ *are defined as*

$$\mathcal{BSC}_2^{N\times M} = \left\{ \grave{\boldsymbol{A}} = \begin{bmatrix} \boldsymbol{A}_1 & -\boldsymbol{A}_2 \\ \boldsymbol{A}_2 & \boldsymbol{A}_1 \end{bmatrix} \,\middle|\, \boldsymbol{A}_1, \boldsymbol{A}_2 \in \mathbb{R}^{N\times M} \right\} \tag{2.39}$$

$$\mathcal{BHSC}_2^{N\times M} = \left\{ \acute{\boldsymbol{B}} = \begin{bmatrix} \boldsymbol{B}_1 & \boldsymbol{B}_2 \\ \boldsymbol{B}_2 & -\boldsymbol{B}_1 \end{bmatrix} \,\middle|\, \boldsymbol{B}_1, \boldsymbol{B}_2 \in \mathbb{R}^{N\times M} \right\}. \tag{2.40}$$

We denote the two matrix structures using grave $\grave{\bullet}$ and acute $\acute{\bullet}$ accents, which mimic the shape of the constant diagonals of Toeplitz matrices and of Hankel matrices, respectively.

The following Lemmas can be easily verified after inserting in the respective block structures.

Lemma 2.9.1 ([7, Lemma 1])**.** *$\mathcal{BSC}_2^{N\times M}$ and $\mathcal{BHSC}_2^{N\times M}$ are linear subspaces of $\mathbb{R}^{2N\times 2M}$.*

Lemma 2.9.2 ([7, Lemma 1])**.** *If $\grave{\boldsymbol{A}} \in \mathcal{BSC}_2^{N\times M}$ and $\acute{\boldsymbol{B}} \in \mathcal{BHSC}_2^{N\times M}$, we have $\grave{\boldsymbol{A}}^{\mathrm{T}} \in \mathcal{BSC}_2^{M\times N}$ and $\acute{\boldsymbol{B}}^{\mathrm{T}} \in \mathcal{BHSC}_2^{M\times N}$.*

Lemma 2.9.3 ([7, Lemma 3])**.** *Let $\grave{\boldsymbol{A}} \in \mathcal{BSC}_2^{N\times L}$, $\grave{\boldsymbol{A}}' \in \mathcal{BSC}_2^{L\times M}$, $\acute{\boldsymbol{B}} \in \mathcal{BHSC}_2^{N\times L}$, and $\acute{\boldsymbol{B}}' \in \mathcal{BHSC}_2^{L\times M}$. Then, $\grave{\boldsymbol{A}}\grave{\boldsymbol{A}}' \in \mathcal{BSC}_2^{N\times M}$, $\acute{\boldsymbol{B}}\acute{\boldsymbol{B}}' \in \mathcal{BSC}_2^{N\times M}$, $\grave{\boldsymbol{A}}\acute{\boldsymbol{B}}' \in \mathcal{BHSC}_2^{N\times M}$, $\acute{\boldsymbol{B}}\grave{\boldsymbol{A}}' \in \mathcal{BHSC}_2^{N\times M}$.*

Lemma 2.9.4 ([7, Lemma 4])**.** *If $\acute{\boldsymbol{B}} \in \mathcal{BHSC}_2^{M\times M}$, we have $\mathrm{tr}[\acute{\boldsymbol{B}}] = 0$.*

Combining these results, we obtain the following fundamental property of $\mathcal{BSC}_2$ and $\mathcal{BHSC}_2$ matrices.

[2] Note that [81] uses a different nomenclature where *skew-circulant* refers to a circulant Hankel matrix. Here, *skew* refers to the sign change instead.

Lemma 2.9.5 ([7, Lemma 5]). *$\mathcal{BSC}_2^{N\times M}$ and $\mathcal{BHSC}_2^{N\times M}$ are orthogonal complements in $\mathbb{R}^{2N\times 2M}$ with respect to the Frobenius inner product* (2.1)*.*

Proof. For $\grave{\boldsymbol{A}} \in \mathcal{BSC}_2^{N\times M}$ and $\acute{\boldsymbol{B}} \in \mathcal{BHSC}_2^{N\times M}$, we have $\grave{\boldsymbol{A}}^{\mathrm{T}}\acute{\boldsymbol{B}} \in \mathcal{BHSC}_2^{M\times M}$ due to Lemmas 2.9.2 and 2.9.3. Then, $\langle \grave{\boldsymbol{A}}, \acute{\boldsymbol{B}}\rangle = \mathrm{tr}[\grave{\boldsymbol{A}}^{\mathrm{T}}\acute{\boldsymbol{B}}] = 0$ due to Lemma 2.9.4. By counting that $\mathcal{BSC}_2^{N\times M}$ and $\mathcal{BHSC}_2^{N\times M}$ both have dimensionality $2MN$ while the dimensionality of $\mathbb{R}^{2N\times 2M}$ is $4MN$, we obtain $\mathcal{BSC}_2^{N\times M} \oplus \mathcal{BHSC}_2^{N\times M} = \mathbb{R}^{2N\times 2M}$. □

As a result, the decomposition of $\boldsymbol{A}_{\mathrm{WL}}$ into the two summands at the right hand side of (2.38) is unique. This means that we can easily identify the linear part and the conjugate linear part of a widely linear mapping in the composite real representation. To do so, we can use the following two projection operators.

Lemma 2.9.6 ([7, Lemma 6]). *The orthogonal projections to $\mathcal{BSC}_2^{N\times M}$ and $\mathcal{BHSC}_2^{N\times M}$ are given by*

$$\mathrm{proj}_{\mathcal{BSC}_2}\left(\begin{bmatrix}\boldsymbol{C}_{11} & \boldsymbol{C}_{12}\\ \boldsymbol{C}_{21} & \boldsymbol{C}_{22}\end{bmatrix}\right) = \frac{1}{2}\begin{bmatrix}\boldsymbol{C}_{11}+\boldsymbol{C}_{22} & \boldsymbol{C}_{12}-\boldsymbol{C}_{21}\\ \boldsymbol{C}_{21}-\boldsymbol{C}_{12} & \boldsymbol{C}_{11}+\boldsymbol{C}_{22}\end{bmatrix}, \tag{2.41}$$

$$\mathrm{proj}_{\mathcal{BHSC}_2}\left(\begin{bmatrix}\boldsymbol{C}_{11} & \boldsymbol{C}_{12}\\ \boldsymbol{C}_{21} & \boldsymbol{C}_{22}\end{bmatrix}\right) = \frac{1}{2}\begin{bmatrix}\boldsymbol{C}_{11}-\boldsymbol{C}_{22} & \boldsymbol{C}_{12}+\boldsymbol{C}_{21}\\ \boldsymbol{C}_{12}+\boldsymbol{C}_{21} & \boldsymbol{C}_{22}-\boldsymbol{C}_{11}\end{bmatrix} \tag{2.42}$$

where $\boldsymbol{C}_{ij} \in \mathbb{R}^{N\times M}$, $i,j \in \{1,2\}$.

Proof. By looking at the block structure, we can verify that $\mathrm{proj}_{\mathcal{BSC}_2}$ is idempotent and that $\boldsymbol{C} - \mathrm{proj}_{\mathcal{BSC}_2}(\boldsymbol{C}) \in \mathcal{BHSC}_2^{N\times M}$, i.e., it is orthogonal to all $\grave{\boldsymbol{A}} \in \mathcal{BSC}_2^{N\times M}$. In an analogous manner, $\mathrm{proj}_{\mathcal{BHSC}_2}$ is idempotent, and $\boldsymbol{C} - \mathrm{proj}_{\mathcal{BHSC}_2}(\boldsymbol{C}) \in \mathcal{BSC}_2^{N\times M}$, i.e., it is orthogonal to all $\acute{\boldsymbol{B}} \in \mathcal{BHSC}_2^{N\times M}$. □

2.9.4 The Power Shaping Space of BSC Matrices

We have seen above that $\mathcal{BSC}_2$ matrices do not only play a role for the composite real representations of widely linear transformations, but also when studying composite real covariance matrices (2.34). For this purpose, we need to consider the special case of symmetric $\mathcal{BSC}_2$ and $\mathcal{BHSC}_2$ matrices, for which we introduce the following definition.

Definition 2.9.7. *The sets of real symmetric block-skew-circulant and real symmetric block-Hankel-skew-circulant matrices with 2×2 blocks of size $M\times M$ are defined as*

$$\mathcal{SBSC}_2^M = \mathcal{BSC}_2^{M\times M} \cap \mathbb{S}^{2M} \tag{2.43}$$

$$\mathcal{SBHSC}_2^M = \mathcal{BHSC}_2^{M\times M} \cap \mathbb{S}^{2M}. \tag{2.44}$$

For the spaces $\mathcal{SBSC}_2^M$ and $\mathcal{SBHSC}_2^M$, we have the following orthogonality lemma.

Lemma 2.9.7. *$\mathcal{SBSC}_2^M$ and $\mathcal{SBHSC}_2^M$ are orthogonal complements in $\mathbb{S}^{2M}$ with respect to the Frobenius inner product* (2.1)*.*

Proof. Using Lemma 2.9.2, we can verify that the projection $\mathrm{proj}_{\mathbb{S}^{2M}}(\boldsymbol{C}) = \frac{1}{2}(\boldsymbol{C}+\boldsymbol{C}^{\mathrm{T}})$ commutes with the projection $\mathrm{proj}_{\mathcal{BSC}_2}$. The result thus follows from Lemma 2.9.5 combined with Lemma 2.9.8, which is given below. For an alternative proof, see [7, Lemma 9]. □

Lemma 2.9.8. *Let $\mathcal{A}$ and $\mathcal{B}$ be subspaces of a Hilbert space $\mathcal{V}$ such that the orthogonal projections* $\mathrm{proj}_{\mathcal{A}}$ *and* $\mathrm{proj}_{\mathcal{B}}$ *commute, i.e.,* $\mathrm{proj}_{\mathcal{A}} \circ \mathrm{proj}_{\mathcal{B}} = \mathrm{proj}_{\mathcal{B}} \circ \mathrm{proj}_{\mathcal{A}}$. *Then,* $(\mathcal{A} \cap \mathcal{B})^{\perp_{\mathcal{B}}} = \mathcal{A}^{\perp_{\mathcal{V}}} \cap \mathcal{B}$, *and* $\mathrm{proj}_{\mathcal{A}} \circ \mathrm{proj}_{\mathcal{B}} = \mathrm{proj}_{\mathcal{A}\cap\mathcal{B}}$.

Proof. If and only if the projections commute, we have the orthogonal decomposition

$$\mathcal{V} = (\mathcal{A} \cap \mathcal{B}) \oplus (\mathcal{A} \cap \mathcal{B}^{\perp_{\mathcal{V}}}) \oplus (\mathcal{A}^{\perp_{\mathcal{V}}} \cap \mathcal{B}) \oplus (\mathcal{A}^{\perp_{\mathcal{V}}} \cap \mathcal{B}^{\perp_{\mathcal{V}}}) \tag{2.45}$$

[85, Proposition 1.5], and we can identify that $\mathcal{B} = (\mathcal{A} \cap \mathcal{B}) \oplus (\mathcal{A}^{\perp_{\mathcal{V}}} \cap \mathcal{B})$. According to [85], this also implies that $\mathrm{proj}_{\mathcal{A}} \circ \mathrm{proj}_{\mathcal{B}} = \mathrm{proj}_{\mathcal{A}\cap\mathcal{B}}$. □

As a consequence of Lemma 2.9.7, the decomposition of the composite real covariance matrix $\boldsymbol{C}_{\check{\boldsymbol{x}}}$ into the two summands given at the right hand side of (2.34) is unique and can be performed using the projections from Lemma 2.9.6. By doing so, we can easily identify a power shaping component that corresponds to the complex covariance matrix $\boldsymbol{C}_{\boldsymbol{x}}$ and an impropriety component that corresponds to the pseudocovariance matrix $\tilde{\boldsymbol{C}}_{\boldsymbol{x}}$ (e.g., [6,7]). Indeed, this is in compliance with the notion of a power shaping space introduced in Definition 2.3.1.

Theorem 2.9.1. *The space $\mathcal{P} = \mathcal{SBSC}_2^M$ is a power shaping space. The corresponding entropy reduction space is $\mathcal{N} = \mathcal{SBHSC}_2^M$.*

Proof. The product condition (2.12) holds due to Lemma 2.9.3, and condition (2.13) is obvious. The orthogonal complement is $\mathcal{N} = \mathcal{SBHSC}_2^M$ due to Lemma 2.9.7. □

From this, we see that the second summand in (2.34), which has a one-to-one relation with the pseudocovariance matrix $\tilde{\boldsymbol{C}}_{\boldsymbol{x}}$, can be considered as the entropy reduction component of the composite real covariance matrix. If this component vanishes, the original complex random vector $\boldsymbol{x}$ is proper. This observation makes sense as it is well known that a proper Gaussian vector, whose pseudocovariance matrix is zero, has the highest differential entropy among all complex Gaussian vectors with a fixed covariance matrix $\boldsymbol{C}_{\boldsymbol{x}}$ (e.g., [29, 63, 64]). As $\boldsymbol{C}_{\boldsymbol{x}}$ has a one-to-one relation with the first summand in (2.34), this corresponds to fixing the power shaping component.

If the composite real representation $\check{\boldsymbol{x}}$ of a random vector $\boldsymbol{x}$ is transformed by a linear mapping $\check{\boldsymbol{x}} \mapsto \check{\boldsymbol{y}} = \grave{\boldsymbol{H}}\check{\boldsymbol{x}}$ with $\grave{\boldsymbol{H}} \in \mathcal{BSC}_2^{N\times M}$, the transformed random vector has the composite real covariance matrix $\boldsymbol{C}_{\check{\boldsymbol{y}}} = \grave{\boldsymbol{H}}\boldsymbol{C}_{\check{\boldsymbol{x}}}\grave{\boldsymbol{H}}^{\mathrm{T}}$. The following proposition enables us to study the properties of such a transformation.

Proposition 2.9.1. *Every matrix $\grave{\boldsymbol{H}} \in \mathcal{BSC}_2^{N\times M}$ is compatible with $(\mathcal{SBSC}_2^N, \mathcal{SBSC}_2^M)$.*

Proof. This can be verified using Lemma 2.9.3. □

As a result, $\boldsymbol{C}_{\check{\boldsymbol{y}}} = \grave{\boldsymbol{H}}\boldsymbol{C}_{\check{\boldsymbol{x}}}\grave{\boldsymbol{H}}^{\mathrm{T}}$ lies in the power shaping space $\mathcal{SBSC}_2^N$ if the original composite real covariance matrix $\boldsymbol{C}_{\check{\boldsymbol{x}}}$ lies in $\mathcal{SBSC}_2^M$, which means that the complex vector $\boldsymbol{y}$ corresponding to $\check{\boldsymbol{y}}$ is proper if $\boldsymbol{x}$ is proper. We know from (2.38) that linear transformations with $\mathcal{BSC}_2$ matrices are the composite real counterpart of complex linear transformations. Thus, Proposition 2.9.1 can be seen as the composite real formulation of the fact that propriety is preserved by complex linear transformations (e.g., [64, 77]).

In [7], a large variety of further properties of $\mathcal{BSC}_2$ and $\mathcal{BHSC}_2$ matrices were collected and derived. Noting that $\mathcal{P} = \mathcal{SBSC}_2^M$ is a power shaping space, many of them can be considered

as specializations of the results derived in this chapter to the particular power shaping space $\mathcal{P} = \mathcal{SBSC}_2^M$. Therefore, we do not reproduce those results from [7] here, but we instead use the more general properties of power shaping spaces. Nevertheless, the following observation from [7] is noteworthy and is reproduced here for later use.

Lemma 2.9.9 (consequence of [7, Lemma 11])**.** *All eigenvalues of a symmetric $\mathcal{BSC}_2$ matrix have even multiplicity.*

This implies that the power shaping space $\mathcal{SBSC}_2^M$ is an example where it is impossible that all eigenvalues of $\boldsymbol{P} \in \mathcal{SBSC}_2^M$ have multiplicity one (see the comment above Corollary 2.6.3).

2.9.5 Relations between BSC Matrices and Complex Matrices

In (2.38), the first summand can be interpreted as the equivalent real-valued $\mathcal{BSC}_2$ matrix of a complex matrix. In this section, we collect several properties of this equivalence for later reference. Let $\grave{\boldsymbol{A}} = \grave{\Re}(\boldsymbol{A}) \in \mathcal{BSC}_2^{N\times M}$ be the real-valued representation of $\boldsymbol{A} \in \mathbb{C}^{N\times M}$ defined as

$$\grave{\boldsymbol{A}} = \grave{\Re}(\boldsymbol{A}) = \begin{bmatrix} \Re(\boldsymbol{A}) & -\Im(\boldsymbol{A}) \\ \Im(\boldsymbol{A}) & \Re(\boldsymbol{A}) \end{bmatrix}. \tag{2.46}$$

We then have the following equivalences from [29].

$$\boldsymbol{A} = \boldsymbol{CD} \;\Leftrightarrow\; \grave{\Re}(\boldsymbol{A}) = \grave{\Re}(\boldsymbol{C})\,\grave{\Re}(\boldsymbol{D}) \tag{2.47}$$

$$\boldsymbol{A} = \boldsymbol{C}^{\mathrm{H}} \;\Leftrightarrow\; \grave{\Re}(\boldsymbol{A}) = \grave{\Re}(\boldsymbol{C})^{\mathrm{T}} \tag{2.48}$$

$$\boldsymbol{A} \text{ is Hermitian} \;\Leftrightarrow\; \grave{\Re}(\boldsymbol{A}) \text{ is symmetric} \tag{2.49}$$

$$\boldsymbol{A} \succeq \boldsymbol{0} \;\Leftrightarrow\; \grave{\Re}(\boldsymbol{A}) \succeq \boldsymbol{0} \tag{2.50}$$

$$\boldsymbol{A} = \boldsymbol{C}^{-1} \;\Leftrightarrow\; \grave{\Re}(\boldsymbol{A}) = \grave{\Re}(\boldsymbol{C})^{-1} \tag{2.51}$$

$$\boldsymbol{y} = \boldsymbol{A}\boldsymbol{x} \;\Leftrightarrow\; \check{\boldsymbol{y}} = \grave{\Re}(\boldsymbol{A})\,\check{\boldsymbol{x}} \tag{2.52}$$

with $\check{\boldsymbol{x}} = \check{\Re}(\boldsymbol{x})$ and $\check{\boldsymbol{y}} = \check{\Re}(\boldsymbol{y})$ as in (2.30). Moreover, we have [29]

$$\det(\grave{\Re}(\boldsymbol{A})) = |\det \boldsymbol{A}|^2. \tag{2.53}$$

From [7, Lemma 24], we have that the set of singular values of $\grave{\Re}(\boldsymbol{A})$ is the same as the set of singular values of $\boldsymbol{A}$, but the multiplicity of each singular value is doubled. This implies that [7, Lemma 25]

$$\operatorname{rank}\left[\grave{\Re}(\boldsymbol{A})\right] = 2\operatorname{rank}[\boldsymbol{A}]. \tag{2.54}$$

Finally, we have the relation that (e.g., [64, Sec. 2.2.3])

$$\mathrm{h}(\check{\boldsymbol{x}}) = \mathrm{h}(\boldsymbol{x}) \quad \text{and} \quad \mathrm{h}(\check{\boldsymbol{x}} \,|\, \check{\boldsymbol{y}}) = \mathrm{h}(\boldsymbol{x} \,|\, \boldsymbol{y}). \tag{2.55}$$

This provides us with a simple way of calculating the differential entropy of an improper Gaussian random vector by plugging in its composite real covariance matrix (2.34) into (2.7).

Chapter 3

Mathematical Description of MIMO Communication Systems

A brief introduction to MIMO communication systems was given in Section 1.2. The aims of this chapter are to provide further details on such systems, to present various mathematical representations that are used throughout the following chapters, and to link these descriptions to the concept of power shaping spaces from Chapter 2. In addition, we discuss the notion of a rate region and the concept of time-sharing, and we present an algorithmic framework that can be used to compute points on the Pareto boundary of a rate region.

3.1 RoP MIMO Systems

Before we turn our attention to multicarrier MIMO systems as described by (1.1), let us introduce a simple yet powerful model which we refer to as *RoP (real or proper) MIMO system*. Consider a transmission described by

$$\boldsymbol{y}_{\mathrm{D}} = \sum_{\mathrm{S} \in \mathcal{S}_{\mathrm{D}}} \boldsymbol{H}_{\mathrm{DS}} \boldsymbol{x}_{\mathrm{S}} + \boldsymbol{\eta}_{\mathrm{D}} \tag{3.1}$$

where $\mathcal{S}_{\mathrm{D}}$ is the set of transmitters whose signals $\boldsymbol{x}_{\mathrm{S}}$ are received by node D, and $\boldsymbol{\eta}_{\mathrm{D}}$ is additive noise, which is independent of the transmit signals. Unless otherwise stated, the signals $\boldsymbol{x}_{\mathrm{S}}$ are assumed to be mutually independent.

Definition 3.1.1. *We call the system model* (3.1) *a* RoP MIMO system *if one of the following two cases applies.*

1. *Real-valued Gaussian MIMO system: for all receiving nodes* $\mathrm{D} \in \mathcal{D}$*, the channel matrices* $\boldsymbol{H}_{\mathrm{DS}} \in \mathbb{R}^{M_{\mathrm{D}} \times M_{\mathrm{S}}}$, $\mathrm{S} \in \mathcal{S}_{\mathrm{D}}$ *are* real-valued*, the signals* $\boldsymbol{x}_{\mathrm{S}} \in \mathbb{R}^{M_{\mathrm{S}}}$, $\mathrm{S} \in \mathcal{S}_{\mathrm{D}}$ *are* real-valued*, and the noise* $\boldsymbol{\eta}_{\mathrm{D}} \in \mathbb{R}^{M_{\mathrm{D}}}$ *is* real-valued *Gaussian with mean zero.*

2. *Complex Gaussian MIMO system with proper signals and proper noise: for all receiving nodes* $\mathrm{D} \in \mathcal{D}$*, the channel matrices* $\boldsymbol{H}_{\mathrm{DS}} \in \mathbb{C}^{M_{\mathrm{D}} \times M_{\mathrm{S}}}$, $\mathrm{S} \in \mathcal{S}_{\mathrm{D}}$ *are* complex*, the signals* $\boldsymbol{x}_{\mathrm{S}} \in \mathbb{C}^{M_{\mathrm{S}}}$, $\mathrm{S} \in \mathcal{S}_{\mathrm{D}}$ *are* proper*, and the noise* $\boldsymbol{\eta}_{\mathrm{D}} \in \mathbb{C}^{M_{\mathrm{D}}}$ *is* proper *Gaussian with mean*

zero. If a transmit scheme is based on per-user input signals (see, e.g., Sections 6.1 and 7.1), these signals are assumed to be proper as well.

Note that this model consists of only one equation per receiving node, i.e., we do not describe a parallel transmission on C carriers. However, we will see later that this model can still be used to study multicarrier systems and even improper signaling.

The reason why we introduce the general term *RoP MIMO system*, which includes the two cases given above, is that these two cases behave very similar in many respects. For instance, if we have some algorithm or some analytical result for a complex Gaussian MIMO system with proper signals, we can in many cases easily obtain a counterpart for the real-valued case by reproducing the original derivation and verifying whether it includes any steps that need to be modified when working with real numbers. Usually, this transfer to the real-valued case does not pose any problems (see, e.g., [7]).

In particular, results that are based on differential entropies of Gaussian vectors can be easily transferred since (2.7) gives us a unified way of expressing differential entropies for the two cases under consideration. We only have to bear in mind that the factor μ in (2.7) has to be set to $\mu = \frac{1}{2}$ in the case of real-valued Gaussian vectors, and to $\mu = 1$ for proper Gaussian vectors. Thus, the constant μ as a placeholder for these two possible values occurs in many equations describing RoP MIMO systems, e.g., in mutual information expressions of the form

$$\mathrm{I}\left(\boldsymbol{x}_{\mathrm{S}'};\boldsymbol{y}_{\mathrm{D}}\right) = \mu \log_2 \frac{\det\left(\boldsymbol{C}_{\boldsymbol{\eta}_{\mathrm{D}}} + \sum_{\mathrm{S}\in\mathcal{S}_{\mathrm{D}}} \boldsymbol{H}_{\mathrm{DS}} \boldsymbol{C}_{\boldsymbol{x}_{\mathrm{S}}} \boldsymbol{H}_{\mathrm{DS}}^{\mathrm{H}}\right)}{\det\left(\boldsymbol{C}_{\boldsymbol{\eta}_{\mathrm{D}}} + \sum_{\mathrm{S}\in\mathcal{S}_{\mathrm{D}}\setminus\{\mathrm{S}'\}} \boldsymbol{H}_{\mathrm{DS}} \boldsymbol{C}_{\boldsymbol{x}_{\mathrm{S}}} \boldsymbol{H}_{\mathrm{DS}}^{\mathrm{H}}\right)} \tag{3.2}$$

with $\mathrm{S}' \in \mathcal{S}_{\mathrm{D}}$, which can be used if all transmit signals are Gaussian.

3.1.1 Constraints on the Transmit Covariance Matrices

In any sensible system, there are constraints that the transmit signals have to fulfill, e.g., in order to avoid an infinitely high transmit power. For all systems we consider, we assume constraints of the form

$$(\boldsymbol{C}_{\boldsymbol{x}_{\mathrm{S}}})_{\mathrm{S}\in\mathcal{S}} \in \mathcal{Q} \tag{3.3}$$

where $\mathcal{S} = (\mathrm{S}_1, \ldots, \mathrm{S}_{|\mathcal{S}|})$ are all transmitting nodes, and $\mathcal{Q}$ is a convex set of tuples of Hermitian matrices which is chosen in a way that we obtain a compact constraint set with nonempty interior if we in addition constrain the matrices $\boldsymbol{C}_{\boldsymbol{x}_{\mathrm{S}}}$ to be positive-semidefinite. Examples of constraints that can be modeled by means of (3.3) are a sum power constraint

$$\sum_{\mathrm{S}\in\mathcal{S}} \mathrm{tr}[\boldsymbol{C}_{\boldsymbol{x}_{\mathrm{S}}}] \leq Q \tag{3.4}$$

with a given maximum available transmit power Q, individual power constraints

$$\mathrm{tr}[\boldsymbol{C}_{\boldsymbol{x}_{\mathrm{S}}}] \leq Q_{\mathrm{S}},\ \forall \mathrm{S} \in \mathcal{S} \tag{3.5}$$

with given constants Q_{S}, and individual shaping constraints $\boldsymbol{C}_{\boldsymbol{x}_{\mathrm{S}}} \preceq \boldsymbol{Q}_{\mathrm{S}},\ \forall \mathrm{S} \in \mathcal{S}$ with given constant matrices $\boldsymbol{Q}_{\mathrm{S}} \succeq \boldsymbol{0}$ (e.g., [21, 25, 72, 86]).

3.1.2 Compatibility with Power Shaping Spaces

A special case that is particularly important for our further studies is when the constraint set $\mathcal{Q}$ acts only on the power shaping components of the transmit covariance matrices. We formalize this as follows.

Definition 3.1.2. *Let $\mathcal{P}_{\mathrm{S}} \subseteq \mathbb{H}^{M_{\mathrm{S}}}$ (or $\mathcal{P}_{\mathrm{S}} \subseteq \mathbb{S}^{M_{\mathrm{S}}}$ in a real-valued MIMO system) for $\mathrm{S} \in \mathcal{S}$ be power shaping spaces, and let $\mathcal{N}_{\mathrm{S}}$ be the corresponding entropy reduction spaces. Then, a constraint of the form* (3.3) *for which*

$$(\boldsymbol{C}_{\boldsymbol{x}_{\mathrm{S}}})_{\mathrm{S}\in\mathcal{S}} \in \mathcal{Q} \;\Leftrightarrow\; (\boldsymbol{C}_{\boldsymbol{x}_{\mathrm{S}}} + \boldsymbol{N}_{\mathrm{S}})_{\mathrm{S}\in\mathcal{S}} \in \mathcal{Q} \tag{3.6}$$

for arbitrary $\boldsymbol{N}_{\mathrm{S}} \in \mathcal{N}_{\mathrm{S}}$, $\mathrm{S} \in \mathcal{S}$ is called compatible *with $\bigotimes_{i=1}^{|\mathcal{S}|} \mathcal{P}_{\mathrm{S}_i}$.*

Due to Proposition 2.4.1, a sum power constraint (3.4) is compatible with any combination of power shaping spaces, and the same is true for individual power constraints at each transmitter (3.5). However, for other constraint sets, the compatibility defined above is a property that can depend on the particular choice of power shaping spaces $\bigotimes_{i=1}^{|\mathcal{S}|} \mathcal{P}_{\mathrm{S}_i}$, i.e., a given constraint set $\mathcal{Q}$ might be compatible with some choice $\bigotimes_{i=1}^{|\mathcal{S}|} \mathcal{P}_{\mathrm{S}_i}$, but not with some other choice $\bigotimes_{i=1}^{|\mathcal{S}|} \mathcal{P}'_{\mathrm{S}_i}$.

For later reference, we introduce the following *compatibility assumption* for RoP MIMO systems.

Definition 3.1.3. *Given power shaping spaces $\mathcal{P}_{\mathrm{T}} \subseteq \mathbb{H}^{M_{\mathrm{T}}}$ (or $\mathcal{P}_{\mathrm{T}} \subseteq \mathbb{S}^{M_{\mathrm{T}}}$ in a real-valued MIMO system) for all transmitting and receiving nodes $\mathrm{T} \in \mathcal{T} = \mathcal{S} \cup \mathcal{D}$, we say that the* compatibility assumption *is fulfilled for a RoP MIMO system if the constraint set* (3.3) *is compatible with $\bigotimes_{i=1}^{|\mathcal{S}|} \mathcal{P}_{\mathrm{S}_i}$, and it holds $\forall \mathrm{D} \in \mathcal{D}$, $\forall \mathrm{S} \in \mathcal{S}_{\mathrm{D}}$ that the channel matrix $\boldsymbol{H}_{\mathrm{DS}}$ is compatible with $(\mathcal{P}_{\mathrm{D}}, \mathcal{P}_{\mathrm{S}})$.*

3.2 Rate Regions

In [59], the channel capacity of a point-to-point link was defined as the maximum of all data rates achievable with a vanishing probability of error. However, in multiuser systems, the K individual achievable rates ρ_k of the users $k \in \mathcal{K} = \{1, \ldots, K\}$ might be of interest. This can be accounted for by defining the *capacity region* $\mathcal{C} \subset \mathbb{R}_{0,+}^{K}$ as the set of vectors $\boldsymbol{\rho} = [\rho_1, \ldots, \rho_K]^{\mathrm{T}}$ that are simultaneously achievable with vanishing error probability (e.g., [62]). If we consider only rate vectors that are achievable with a certain class of suboptimal transmit strategies, we obtain a subset $\mathcal{R} \subseteq \mathcal{C}$ of the capacity region, which we call *rate region* instead.

The rate region of a MIMO communication system depends on the set of feasible transmit signals (determined by the constraint set $\mathcal{Q}$) as can be seen in

$$\mathcal{R}(\mathcal{Q}) = \left\{ \boldsymbol{\rho} \in \mathbb{R}_{0,+}^{K} \;\middle|\; \exists \mathcal{X} \in \mathbb{X} : \boldsymbol{\rho} \leq \boldsymbol{r}(\mathcal{X}) \text{ and } (\boldsymbol{C}_{\boldsymbol{x}_{\mathrm{S}}}(\mathcal{X}))_{\mathrm{S}\in\mathcal{S}} \in \mathcal{Q} \right\}. \tag{3.7}$$

In (3.7), the abstract variable $\mathcal{X}$ represents the chosen transmit strategy, and the abstract constraint set $\mathbb{X}$ accounts for the set of allowed strategies as well as for fundamental restrictions such as the fact that all covariance matrices have to be positive-semidefinite. The vector $\boldsymbol{r}(\mathcal{X}) = [r_1(\mathcal{X}), \ldots, r_K(\mathcal{X})]^{\mathrm{T}}$ contains the per-user rates achieved by strategy $\mathcal{X}$, and any rates $\rho_k \leq r_k(\mathcal{X})$ are achievable. We use $\boldsymbol{C}_{\boldsymbol{x}_{\mathrm{S}}}(\mathcal{X})$ to denote the covariance matrix of the transmit

signal $\boldsymbol{x}_{\mathrm{S}}$ when strategy $\mathcal{X}$ is applied. The explicit dependence of $\mathcal{R}$ on $\mathcal{Q}$ may be omitted if the choice of $\mathcal{Q}$ is clear from the context. If we consider the special case of a sum power constraint (3.4), the rate region depends only on the maximum available transmit power Q, in which case we may use the alternative notation $\mathcal{R}(Q)$.

For the points $\boldsymbol{\rho}$ on the upper right boundary of a rate region, it is not possible to increase any individual rate ρ_k without decreasing some rate ρ_j with $j \neq k$. These points are called Pareto-optimal points, and the boundary is called Pareto boundary (e.g., [61]).

3.2.1 Rate-Time-Sharing and Time-Sharing

The rate region (3.7) can sometimes be enlarged if we apply multiple transmit strategies $\mathcal{X}_\ell$, $\ell = 1, 2, \ldots$ and average over the rate vectors achieved by these various strategies. The resulting rate region is

$$\overline{\mathcal{R}} = \left\{ \boldsymbol{\rho} \in \mathbb{R}_{0,+}^{K} \;\middle|\; \exists \tau_\ell \geq 0, \exists \mathcal{X}_\ell \in \mathbb{X},\ \ell = 1, 2, \ldots : \right. \\ \left. \boldsymbol{\rho} \leq \sum_\ell \tau_\ell \boldsymbol{r}(\mathcal{X}_\ell) \text{ and } \left(\boldsymbol{C}_{\boldsymbol{x}_{\mathrm{S}}}(\mathcal{X}_\ell)\right)_{\mathrm{S}\in\mathcal{S}} \in \mathcal{Q},\ \forall \ell \text{ and } \sum_\ell \tau_\ell = 1 \right\} \quad (3.8)$$

where the factor τ_ℓ specifies during which fraction of the total time the strategy $\mathcal{X}_\ell$ is applied. By comparing (3.8) to (3.7), we see that this averaging corresponds to forming convex combinations of rate vectors $\boldsymbol{\rho} \in \mathcal{R}$, i.e., we obtain $\overline{\mathcal{R}} = \operatorname{conv} \mathcal{R}$ by taking the convex hull of the original rate region $\mathcal{R}$.

Such an averaging over the rates of various transmit strategies is often called time-sharing in the literature (e.g., [31, 33, 34, 38]). In [87], it was referred to as the convex-hull formulation, and in [1, 8], it was called time-sharing under short-term average power constraints. In order to distinguish it from a second type of time-sharing discussed below, we refer to this approach as *rate-time-sharing (RTS)*.

As pointed out, e.g., in [87], a further enlargement of the rate region can be possible if we average not only the rates over the various strategies, but also the transmit covariance matrices. The resulting rate region is

$$\overline{\overline{\mathcal{R}}} = \left\{ \boldsymbol{\rho} \in \mathbb{R}_{0,+}^{K} \;\middle|\; \exists \tau_\ell \geq 0, \exists \mathcal{X}_\ell \in \mathbb{X},\ \ell = 1, 2, \ldots : \right. \\ \left. \boldsymbol{\rho} \leq \sum_\ell \tau_\ell \boldsymbol{r}(\mathcal{X}_\ell) \text{ and } \left(\sum_\ell \tau_\ell \boldsymbol{C}_{\boldsymbol{x}_{\mathrm{S}}}(\mathcal{X}_\ell) \right)_{\mathrm{S}\in\mathcal{S}} \in \mathcal{Q} \text{ and } \sum_\ell \tau_\ell = 1 \right\}. \quad (3.9)$$

This more flexible kind of time-sharing was called the formulation with a time-sharing parameter in [87], time-sharing under long-term average power constraints in [1, 8], and simply time-sharing, e.g., in [3, 88–90]. Following the nomenclature of the latter references, we refer to this technique as *time-sharing (TS)*, and we write (R)TS if a statement holds for both RTS and TS.

Note that this operation cannot be easily expressed by means of a convex hull operator, but we can find a description based on a convex hull if we introduce the set of operation points

$$\mathcal{O} = \left\{ \left(\boldsymbol{\rho}, \left(\boldsymbol{C}'_{\boldsymbol{x}_{\mathrm{S}}}\right)_{\mathrm{S}\in\mathcal{S}} \right) \;\middle|\; \exists \mathcal{X} \in \mathbb{X} : \boldsymbol{0} \leq \boldsymbol{\rho} \leq \boldsymbol{r}(\mathcal{X}) \text{ and } \left(\boldsymbol{C}'_{\boldsymbol{x}_{\mathrm{S}}} = \boldsymbol{C}_{\boldsymbol{x}_{\mathrm{S}}}(\mathcal{X})\right)_{\mathrm{S}\in\mathcal{S}} \right\} \quad (3.10)$$

and define

$$\mathcal{R}_{\mathcal{O}}(\mathcal{Q}) = \left\{ \boldsymbol{\rho} \in \mathbb{R}_{0,+}^{K} \;\middle|\; \exists \left(\boldsymbol{C}'_{\boldsymbol{x}_{\mathrm{S}}}\right)_{\mathrm{S}\in\mathcal{S}} \in \mathcal{Q} : \left(\boldsymbol{\rho}, \left(\boldsymbol{C}'_{\boldsymbol{x}_{\mathrm{S}}}\right)_{\mathrm{S}\in\mathcal{S}}\right) \in \mathcal{O} \right\}. \tag{3.11}$$

The rate region (3.7) is then equivalent to $\mathcal{R} = \mathcal{R}_{\mathcal{O}}(\mathcal{Q})$ while the rate region with RTS (3.8) can be written as $\overline{\mathcal{R}} = \operatorname{conv} \mathcal{R}_{\mathcal{O}}(\mathcal{Q})$. To obtain the rate region with TS (3.9), we have to allow an averaging of both the rates and the covariance matrices, which corresponds to taking the convex hull of the higher-dimensional set $\mathcal{O}$. Thus, we have $\overline{\overline{\mathcal{R}}} = \mathcal{R}_{\operatorname{conv}\mathcal{O}}(\mathcal{Q})$.

Note that there are cases in which the possibility of (R)TS does not bring any gains. In particular, this happens if we can find a parametrization in terms of optimization variables $\mathcal{X} \in \mathbb{X}$ from a convex set $\mathbb{X}$, such that $\boldsymbol{r}(\mathcal{X})$ is concave and $\boldsymbol{C}_{\boldsymbol{x}_{\mathrm{S}}}(\mathcal{X})$ are affine functions for all $\mathrm{S} \in \mathcal{S}$. In this case, $\mathcal{O}$ is a convex set, so that $\operatorname{conv}\mathcal{O} = \mathcal{O}$. As we have assumed $\mathcal{Q}$ to be convex as well, this implies that $\overline{\overline{\mathcal{R}}} = \overline{\mathcal{R}} = \mathcal{R}$. An example where such an effect occurs is the MIMO multiple access channel with joint decoding (see [57]), which we consider in Chapter 5. On the other hand, a rate region plot for a system where $\mathcal{R}$, $\overline{\mathcal{R}}$, and $\overline{\overline{\mathcal{R}}}$ are all different can be found in Section 8.3.4, where we consider a one-sided interference channel.

Implementing rate-time-sharing or time-sharing in a practical system may lead, e.g., to signaling overhead and to undesirable fluctuations of the data rates and transmit powers. Therefore, transmission without (R)TS (using neither RTS nor TS, i.e., transmission with one fixed transmit strategy for each given channel realization) has a high practical relevance and is assumed in many publications (e.g., [32, 65, 91–96]). For this reason, some of the investigations in the following chapters are performed separately for the case without (R)TS and for the cases with (R)TS. Whenever we do so, we make the differences clear either by distinguishing between $\mathcal{R}$, $\overline{\mathcal{R}}$, and $\overline{\overline{\mathcal{R}}}$ in the equations or by explanations in the text.

When considering the capacity region $\mathcal{C}$, the underlying assumption is that arbitrary transmit strategies are allowed, which includes the possibility of (R)TS (e.g., [87]). Therefore, $\mathcal{C}$ is always a convex set. Nevertheless, if we know that (R)TS cannot bring any gains (e.g., in the MIMO multiple access channel, see above), we can exploit this knowledge to obtain a simpler formulation for $\mathcal{C}$, where the possibility of (R)TS does not need to be included.

3.2.2 Weighted Sum Rate Maximization

A weighted sum rate maximization is an optimization of the form

$$\max_{\boldsymbol{\rho}\in\mathcal{R}} \sum_{k=1}^{K} w_k \rho_k \tag{3.12}$$

with nonnegative weighting factors $(w_k)_{\forall k}$. If the rate region $\mathcal{R}$ under consideration is convex (or if we consider $\overline{\mathcal{R}}$, $\overline{\overline{\mathcal{R}}}$, or $\mathcal{C}$ instead of $\mathcal{R}$), all Pareto-optimal points of $\mathcal{R}$ are solutions to the weighted sum rate maximization problem (3.12) for different choices of the weighting factors $(w_k)_{\forall k}$ (see, e.g., [57], [97, Proposition A5.6]). Thus, the properties of Pareto-optimal points can be studied by studying the solutions of a weighted sum rate maximization.

On the other hand, when applied to a nonconvex rate region $\mathcal{R}$, (3.12) cannot be used to find all Pareto-optimal points since only those points which are also Pareto-optimal in $\overline{\mathcal{R}} = \operatorname{conv}\mathcal{R}$ can be solutions of a weighted sum rate maximization [97, Corollary A5.9]. Moreover, replacing $\mathcal{R}$ by $\overline{\mathcal{R}}$ in (3.12) cannot increase the optimal value [97, Corollary A5.9], i.e., applying RTS can

never bring an improvement if our aim is to maximize a weighted sum rate. However, replacing $\mathcal{R}$ by $\overline{\overline{\mathcal{R}}}$, i.e., applying the more flexible TS, can indeed improve the outcome of a weighted sum rate maximization (see, e.g., [8] and Section 8.3.4).

3.2.3 Rate Balancing

A second method to compute Pareto-optimal points of a rate region is based on the so-called rate balancing problem (e.g., [50, 98])

$$\max_{R\in\mathbb{R},\mathcal{X}\in\mathbb{X}} R \quad \text{s.t.} \quad \boldsymbol{r}(\mathcal{X}) \geq R\boldsymbol{\varrho} \quad \text{and} \quad (\boldsymbol{C}_{\boldsymbol{x}_\mathrm{S}}(\mathcal{X}))_{\mathrm{S}\in\mathcal{S}} \in \mathcal{Q} \tag{3.13}$$

where the nonnegative relative rate targets $\boldsymbol{\varrho} = [\varrho_1, \ldots, \varrho_K] \geq \mathbf{0}$ decide which point on the Pareto boundary we obtain. This approach, which is called rate-profile method (e.g., [34,49,99]), is applicable to arbitrary (convex or nonconvex) rate regions.

A modified rate balancing problem that allows for RTS is given by

$$\max_{\substack{R\in\mathbb{R},L\in\mathbb{N},(\mathcal{X}_\ell\in\mathbb{X})_{\forall\ell}\\(\tau_\ell\geq 0)_{\forall\ell}:\sum_{\ell=1}^{L}\tau_\ell=1}} R \;\; \text{s.t.} \;\; \sum_{\ell=1}^{L}\tau_\ell\boldsymbol{r}(\mathcal{X}_\ell) \geq R\boldsymbol{\varrho} \;\; \text{and} \;\; (\boldsymbol{C}_{\boldsymbol{x}_\mathrm{S}}(\mathcal{X}_\ell))_{\mathrm{S}\in\mathcal{S}} \in \mathcal{Q} \;\; \forall\ell \tag{3.14}$$

and to allow for TS, we have to solve

$$\max_{\substack{R\in\mathbb{R},L\in\mathbb{N},(\mathcal{X}_\ell\in\mathbb{X})_{\forall\ell}\\(\tau_\ell\geq 0)_{\forall\ell}:\sum_{\ell=1}^{L}\tau_\ell=1}} R \;\; \text{s.t.} \;\; \sum_{\ell=1}^{L}\tau_\ell\boldsymbol{r}(\mathcal{X}_\ell) \geq R\boldsymbol{\varrho} \;\; \text{and} \;\; \left(\sum_{\ell=1}^{L}\tau_\ell\boldsymbol{C}_{\boldsymbol{x}_\mathrm{S}}(\mathcal{X}_\ell)\right)_{\mathrm{S}\in\mathcal{S}} \in \mathcal{Q}. \tag{3.15}$$

3.2.3.1 Dual Approach for Time-Sharing

Since there does not seem to be a simple way to directly solve the rate balancing problem for the cases of (R)TS, we resort to the following algorithmic framework, which is based on Lagrangian duality (e.g., [100, 101]). Similar approaches can be found, e.g., in [3, 8, 13, 49, 50, 90].

For the sake of brevity, we restrict the derivation to covariance constraints that can be expressed in the form $\boldsymbol{p}(\mathcal{X}) \leq \boldsymbol{q}$, where $\boldsymbol{q}$ is a constant vector, and $\boldsymbol{p}(\mathcal{X}) = \tilde{\boldsymbol{p}}\left((\boldsymbol{C}_{\boldsymbol{x}_\mathrm{S}}(\mathcal{X}))_{\mathrm{S}\in\mathcal{S}}\right)$ with a linear function $\tilde{\boldsymbol{p}}$. This is, e.g., the case for individual power constraints, for a sum power constraint (where $\boldsymbol{p}(\mathcal{X})$ and $\boldsymbol{q}$ are scalars), and for many other types of constraints. An extension to further constraints that cannot be expressed in this form (e.g., shaping constraints [21, 25, 72, 86]) is possible.

We consider the rate balancing problem with TS

$$\max_{\substack{R\in\mathbb{R},L\in\mathbb{N},(\mathcal{X}_\ell\in\mathbb{X})_{\forall\ell}\\(\tau_\ell\geq 0)_{\forall\ell}:\sum_{\ell=1}^{L}\tau_\ell=1}} R \quad \text{s.t.} \quad \sum_{\ell=1}^{L}\tau_\ell\boldsymbol{r}(\mathcal{X}_\ell) \geq R\boldsymbol{\varrho} \quad \text{and} \quad \sum_{\ell=1}^{L}\tau_\ell\boldsymbol{p}(\mathcal{X}_\ell) \leq \boldsymbol{q} \tag{3.16}$$

and construct its Lagrangian dual problem (see, e.g., [100, 101]). By introducing the vector of dual variables $\boldsymbol{\nu} = [\boldsymbol{\nu}_1^\mathrm{T}, \boldsymbol{\nu}_2^\mathrm{T}]^\mathrm{T}$, we obtain

$$\min_{\boldsymbol{\nu}\geq 0} \max_{\substack{R\in\mathbb{R},L\in\mathbb{N},(\mathcal{X}_\ell\in\mathbb{X})_{\forall\ell}\\(\tau_\ell\geq 0)_{\forall\ell}:\sum_{\ell=1}^{L}\tau_\ell=1}} R(1-\boldsymbol{\nu}_1^\mathrm{T}\boldsymbol{\varrho}) + \boldsymbol{\nu}_2^\mathrm{T}\boldsymbol{q} + \sum_{\ell=1}^{L}\tau_\ell\left(\boldsymbol{\nu}_1^\mathrm{T}\boldsymbol{r}(\mathcal{X}_\ell) - \boldsymbol{\nu}_2^\mathrm{T}\boldsymbol{p}(\mathcal{X}_\ell)\right). \tag{3.17}$$

The optimal value of (3.17) is an upper bound to the solution of the primal maximization (3.16), but there might be a so-called duality gap between these two values (weak duality). Later on, we will see that this gap vanishes so that both problems have the same optimal value (strong duality).

To avoid that the inner problem in (3.17) is unbounded, the vector $\boldsymbol{\nu}_1$ must fulfill $\boldsymbol{\varrho}^{\mathrm{T}}\boldsymbol{\nu}_1 = 1$. We can rewrite the optimization as

$$\min_{\substack{\boldsymbol{\nu}\geq 0 \\ \boldsymbol{\varrho}^{\mathrm{T}}\boldsymbol{\nu}_1=1}} \max_{\substack{L\in\mathbb{N} \\ (\tau_\ell\geq 0)_{\forall\ell}:\sum_{\ell=1}^{L}\tau_\ell=1}} \boldsymbol{\nu}_2^{\mathrm{T}}\boldsymbol{q} + \sum_{\ell=1}^{L}\tau_\ell\left(\max_{\mathcal{X}_\ell\in\mathbb{X}} \boldsymbol{\nu}_1^{\mathrm{T}}\boldsymbol{r}(\mathcal{X}_\ell) - \boldsymbol{\nu}_2^{\mathrm{T}}\boldsymbol{p}(\mathcal{X}_\ell)\right). \tag{3.18}$$

As the optimization over $\mathcal{X}_\ell$ has the same objective function and the same constraints for all ℓ, the solution does not depend on the value of ℓ. Using

$$\mathcal{X}^\star(\boldsymbol{\nu}) = \left(\operatorname*{argmax}_{\mathcal{X}\in\mathbb{X}} \boldsymbol{\nu}_1^{\mathrm{T}}\boldsymbol{r}(\mathcal{X}) - \boldsymbol{\nu}_2^{\mathrm{T}}\boldsymbol{p}(\mathcal{X})\right) \tag{3.19}$$

we thus obtain

$$\min_{\substack{\boldsymbol{\nu}\geq 0 \\ \boldsymbol{\varrho}^{\mathrm{T}}\boldsymbol{\nu}_1=1}} \max_{\substack{L\in\mathbb{N} \\ (\tau_\ell\geq 0)_{\forall\ell}:\sum_{\ell=1}^{L}\tau_\ell=1}} \boldsymbol{\nu}_2^{\mathrm{T}}\boldsymbol{q} + \boldsymbol{\nu}^{\mathrm{T}}\begin{bmatrix}\boldsymbol{r}(\mathcal{X}^\star(\boldsymbol{\nu})) \\ -\boldsymbol{p}(\mathcal{X}^\star(\boldsymbol{\nu}))\end{bmatrix}\sum_{\ell=1}^{L}\tau_\ell \tag{3.20}$$

where we always have $\sum_{\ell=1}^{L}\tau_\ell = 1$ so that we can drop the maximization over L and $(\tau_\ell)_{\forall\ell}$. Note that it depends on the system under consideration how the inner problem (3.19) can be solved (see, e.g., Section 7.3).

The outer minimization can be solved using the cutting plane method [101, 102], which introduces an auxiliary variable z and successively refines an approximation based on the linear program

$$\min_{\substack{z\in\mathbb{R},\boldsymbol{\nu}\geq 0 \\ \boldsymbol{\varrho}^{\mathrm{T}}\boldsymbol{\nu}_1=1}} z + \boldsymbol{\nu}_2^{\mathrm{T}}\boldsymbol{q} \quad \text{s. t.} \quad z \geq \boldsymbol{\nu}^{\mathrm{T}}\begin{bmatrix}\boldsymbol{r}(\mathcal{X}^\star(\boldsymbol{\nu}^{(\ell)})) \\ -\boldsymbol{p}(\mathcal{X}^\star(\boldsymbol{\nu}^{(\ell)}))\end{bmatrix} \quad \forall\boldsymbol{\nu}^{(\ell)}\in\mathcal{U}. \tag{3.21}$$

In this formulation, $\mathcal{U}$ is a set containing constant vectors $\boldsymbol{\nu}^{(\ell)}$, so that the corresponding transmit strategies $\mathcal{X}^\star(\boldsymbol{\nu}^{(\ell)})$ are constants as well. The so-called master problem (3.21) is a relaxation of (3.20), which becomes tight if the optimizer of (3.20) is contained in the set $\mathcal{U}$. In each iteration, the cutting plane method computes an optimizer $\tilde{\boldsymbol{\nu}}^\star$ of the approximated problem (3.21) and adds this vector $\tilde{\boldsymbol{\nu}}^\star$ to the set $\mathcal{U}$. Then, (3.21) is solved again in the subsequent iteration. This procedure can be shown to converge to the optimum of (3.20) [101, 102]. For the first iteration, the initial set $\mathcal{U}$ has to be chosen such that (3.21) is bounded.

What remains to be done is to recover a solution of the primal problem (3.16). As described, e.g., in [3, 101], let us now dualize the cutting plane master problem (3.21) by introducing the dual variables $\boldsymbol{\tau} = [\tau_1, \ldots, \tau_{|\mathcal{U}|}]^{\mathrm{T}}$ for the constraints on z, and the dual variable R for the constraint $\boldsymbol{\varrho}^{\mathrm{T}}\boldsymbol{\nu}_1 = 1$. We obtain the optimization

$$\max_{R\in\mathbb{R},\boldsymbol{\tau}\geq\mathbf{0}} \min_{z\in\mathbb{R},\boldsymbol{\nu}\geq 0} R + z(1-\mathbf{1}^{\mathrm{T}}\boldsymbol{\tau}) + \boldsymbol{\nu}^{\mathrm{T}}\left(\begin{bmatrix}-R\boldsymbol{\varrho} \\ \boldsymbol{q}\end{bmatrix} + \sum_{\ell=1}^{|\mathcal{U}|}\tau_\ell\begin{bmatrix}\boldsymbol{r}(\mathcal{X}^\star(\boldsymbol{\nu}^{(\ell)})) \\ -\boldsymbol{p}(\mathcal{X}^\star(\boldsymbol{\nu}^{(\ell)}))\end{bmatrix}\right). \tag{3.22}$$

As we again have to choose the variables of the outer optimization such that the inner problem is bounded, R and $\boldsymbol{\tau}$ need to fulfill three conditions, which we incorporate as constraints in the reformulation of the primal recovery

$$\max_{\substack{R\in\mathbb{R},\boldsymbol{\tau}\geq\mathbf{0}\\ \mathbf{1}^{\mathrm{T}}\boldsymbol{\tau}=1}} R \quad \text{s.t.} \quad \sum_{\ell=1}^{|\mathcal{U}|}\tau_\ell \boldsymbol{r}(\mathcal{X}^\star(\boldsymbol{\nu}^{(\ell)})) \geq R\boldsymbol{\varrho}$$
$$\sum_{\ell=1}^{|\mathcal{U}|}\tau_\ell \boldsymbol{p}(\mathcal{X}^\star(\boldsymbol{\nu}^{(\ell)})) \leq \boldsymbol{q}. \tag{3.23}$$

Due to these conditions, $\boldsymbol{\nu}=\mathbf{0}$ minimizes the objective function of (3.22), so that all summands except R vanish. For this reason, the inner minimization is no longer written down in (3.23).

Since the duality gap of linear programs is zero [100, 101], the optimum of (3.23) equals the optimum of (3.21), which converges to the optimal value of (3.20), and we recall that this value is an upper bound to the solution of (3.16). On the other hand, it is easy to verify that any solution of (3.23) delivers a feasible TS strategy for the primal problem (3.16), and thus a lower bound to the solution of (3.16). This shows that the duality gap of (3.16) is zero and that (3.23) converges to an optimum of (3.16). The fact that the duality gap vanishes in systems with TS was also reported in [90].

A special situation occurs if we can find a parametrization of the problem such that the components of $\boldsymbol{r}(\mathcal{X})$ are concave functions of the optimization variables and the components of $\boldsymbol{p}(\mathcal{X})$ are convex functions of the optimization variables, where these optimization variables $\mathcal{X}$ come from a convex set $\mathbb{X}$. In this case, the strategy $\mathcal{X}=\sum_{\ell=1}^{|\mathcal{U}|}\tau_\ell\mathcal{X}^\star(\boldsymbol{\nu}^{(\ell)})\in\mathbb{X}$ achieves $\boldsymbol{r}(\mathcal{X})\geq\sum_{\ell=1}^{|\mathcal{U}|}\tau_\ell\boldsymbol{r}(\mathcal{X}^\star(\boldsymbol{\nu}^{(\ell)}))$ and $\boldsymbol{p}(\mathcal{X})\leq\sum_{\ell=1}^{|\mathcal{U}|}\tau_\ell\boldsymbol{r}(\mathcal{X}^\star(\boldsymbol{\nu}^{(\ell)}))$, i.e., the same performance as in the optimal solution of (3.23) can be achieved without the use of TS.

If we know a method to solve the inner maximization (3.19) in a MIMO system, the framework derived in this section can be applied to solve the rate balancing problem with TS numerically. Note that several alternative approaches for solving the outer problem (3.20) exist, e.g., the ellipsoid method used in [49].

The above framework also enables us to obtain analytical results about Pareto-optimal transmit strategies with TS. Since all strategies $\mathcal{X}^\star(\boldsymbol{\nu}^{(\ell)})$ applied in the TS solution (3.23) are obtained from (3.19), it is sufficient to study the properties of (3.19) in order to obtain insights about Pareto-optimal strategies.

3.2.3.2 Dual Approach for Rate-Time-Sharing

In a similar manner, we can derive a framework for the case of RTS. The only difference is that we have to dualize only the rate constraints, but not the covariance constraints. The inner problem then reads as

$$\mathcal{X}^\star(\boldsymbol{\nu})=\left(\operatorname*{argmax}_{\mathcal{X}\in\mathbb{X}} \boldsymbol{\nu}^{\mathrm{T}}\boldsymbol{r}(\mathcal{X}) \;\text{ s.t. }\; \boldsymbol{p}(\mathcal{X})\leq\boldsymbol{q}\right) \tag{3.24}$$

the cutting plane master problem is given by

$$\min_{\substack{z\in\mathbb{R},\boldsymbol{\nu}\geq 0\\ \boldsymbol{\varrho}^{\mathrm{T}}\boldsymbol{\nu}=1}} z \quad \text{s.t.} \quad z\geq\boldsymbol{\nu}^{\mathrm{T}}\boldsymbol{r}(\mathcal{X}^\star(\boldsymbol{\nu}^{(\ell)}))\;\;\forall\boldsymbol{\nu}^{(\ell)}\in\mathcal{U} \tag{3.25}$$

and the primal recovery is performed by solving

$$\max_{\substack{R\in\mathbb{R},\boldsymbol{\tau}\geq\mathbf{0}\\ \mathbf{1}^{\mathrm{T}}\boldsymbol{\tau}=1}} R \quad \text{s.t.} \quad \sum_{\ell=1}^{|\mathcal{U}|}\tau_\ell \boldsymbol{r}(\mathcal{X}^\star(\boldsymbol{\nu}^{(\ell)})) \geq R\boldsymbol{\varrho}. \tag{3.26}$$

3.3 RoP CN MIMO Systems

For some derivations, we need to extend the notion of a RoP MIMO system (Definition 3.1.1) to the case of multiple carriers, i.e.,

$$\boldsymbol{y}_{\mathrm{D}}^{(c)} = \sum_{\mathrm{S}\in\mathcal{S}_{\mathrm{D}}} \boldsymbol{H}_{\mathrm{DS}}^{(c)}\boldsymbol{x}_{\mathrm{S}}^{(c)} + \boldsymbol{\eta}_{\mathrm{D}}^{(c)}, \;\; c = 1,\ldots,C \tag{3.27}$$

where we assume separate coding on each carrier.

Definition 3.3.1. *We call the system described by* (3.27) *a* RoP CN MIMO system *if the noise is CN, the transmit signals are CN, and the transmission on each carrier c complies to the definition of a RoP MIMO system (Definition 3.1.1).*

The notion of a CN signal is introduced in Section 1.4.2 and is formally defined as follows.

Definition 3.3.2. *We call a signal $\boldsymbol{x}$ consisting of the per-carrier signals $\boldsymbol{x}^{(c)}$* CN *(carriers not correlated) if $\boldsymbol{x}^{(c)}$ and $\boldsymbol{x}^{(c')}$ are uncorrelated for all c and all $c' \neq c$. Otherwise, the signal is called* CC *(carriers correlated). For complex signals, the term uncorrelated is understood in the sense of Definition 2.9.4.*

The model of a RoP CN MIMO system is adequate to describe CN transmission in a real-valued multicarrier MIMO system or in a complex multicarrier MIMO system with proper noise and proper signals. Due to the assumption of separate coding on each carrier, we can express each achievable rate vector as a sum $\boldsymbol{r} = \sum_{c=1}^{C}\boldsymbol{r}^{(c)}$, where the vector $\boldsymbol{r}^{(c)}$ contains the rates achieved on carrier c.

3.3.1 Constraints on the Transmit Covariance Matrices

We assume that the constraints on the transmit covariance matrices have the form

$$\left(\boldsymbol{C}_{\boldsymbol{x}_{\mathrm{S}}^{(1)}},\ldots,\boldsymbol{C}_{\boldsymbol{x}_{\mathrm{S}}^{(C)}}\right)_{\mathrm{S}\in\mathcal{S}} \in \bar{\mathcal{Q}} \tag{3.28}$$

where $\bar{\mathcal{Q}}$ is a convex set of tuples of Hermitian matrices which is chosen in a way that we obtain a compact constraint set with nonempty interior if we in addition constrain the matrices $\boldsymbol{C}_{\boldsymbol{x}_{\mathrm{S}}^{(c)}}$ to be positive-semidefinite.

Even though we consider CN transmission, this constraint might—depending on which particular set $\bar{\mathcal{Q}}$ is considered—introduce a coupling between the carriers that complicates the optimization of the transmit strategy. For example, a constraint on the total transmit power

$$\sum_{c=1}^{C}\sum_{\mathrm{S}\in\mathcal{S}} \mathrm{tr}\left[\boldsymbol{C}_{\boldsymbol{x}_{\mathrm{S}}^{(c)}}\right] \leq Q \tag{3.29}$$

introduces a coupling between all carriers. If TS is allowed, we can still decouple the optimization into per-carrier problems by applying the dual approach from Section 3.2.3.1 as shown below.

3.3.2 Rate Balancing with Dual Decomposition

To formulate the rate balancing problem with TS, we introduce the abstract variables $\mathcal{X}^{(c)}$ to represent the chosen transmit strategy on carrier c, so that the overall transmit strategy is $\mathcal{X} = \left(\mathcal{X}^{(c)}\right)_{\forall c}$. Let us focus on the special case that the covariance constraints can be expressed in the form $\sum_{c=1}^{C} \boldsymbol{p}^{(c)}\left(\mathcal{X}^{(c)}\right) \leq \boldsymbol{q}$ where $\boldsymbol{q}$ is a constant vector, and

$$\boldsymbol{p}^{(c)}\left(\mathcal{X}^{(c)}\right) = \tilde{\boldsymbol{p}}^{(c)}\left(\left(\boldsymbol{C}_{\boldsymbol{x}_{\mathrm{S}}^{(c)}}\left(\mathcal{X}^{(c)}\right)\right)_{\mathrm{S}\in\mathcal{S}}\right) \tag{3.30}$$

with linear functions $\tilde{\boldsymbol{p}}^{(c)}$. This is, e.g., possible for a sum power constraint (3.29). We obtain

$$\begin{aligned} \max_{\substack{R\in\mathbb{R},L\in\mathbb{N},(\mathcal{X}_\ell\in\mathbb{X})_{\forall\ell} \\ (\tau_\ell\geq 0)_{\forall\ell}:\sum_{\ell=1}^{L}\tau_\ell=1}} R \quad \text{s.t.} \quad & \sum_{\ell=1}^{L}\tau_\ell\sum_{c=1}^{C}\boldsymbol{r}^{(c)}\left(\mathcal{X}_\ell^{(c)}\right) \geq R\boldsymbol{\varrho} \\ & \sum_{\ell=1}^{L}\tau_\ell\sum_{c=1}^{C}\boldsymbol{p}^{(c)}\left(\mathcal{X}_\ell^{(c)}\right) \leq \boldsymbol{q}. \end{aligned} \tag{3.31}$$

When applying the dual approach from Section 3.2.3.1 to this problem, we can rewrite (3.19) as

$$\mathcal{X}^\star(\boldsymbol{\nu}) = \left(\operatorname*{argmax}_{(\mathcal{X}^{(c)})_{\forall c}\in\mathbb{X}} \boldsymbol{\nu}_1^{\mathrm{T}}\sum_{c=1}^{C}\boldsymbol{r}^{(c)}\left(\mathcal{X}^{(c)}\right) - \boldsymbol{\nu}_2^{\mathrm{T}}\sum_{c=1}^{C}\boldsymbol{p}^{(c)}\left(\mathcal{X}^{(c)}\right)\right). \tag{3.32}$$

This can be decomposed into $\mathcal{X}^\star(\boldsymbol{\nu}) = (\mathcal{X}^{(c),\star}(\boldsymbol{\nu}))_{\forall c}$ with

$$\mathcal{X}^{(c),\star}(\boldsymbol{\nu}) = \left(\operatorname*{argmax}_{\mathcal{X}^{(c)}\in\mathbb{X}^{(c)}} \boldsymbol{\nu}_1^{\mathrm{T}}\boldsymbol{r}^{(c)}\left(\mathcal{X}^{(c)}\right) - \boldsymbol{\nu}_2^{\mathrm{T}}\boldsymbol{p}^{(c)}\left(\mathcal{X}^{(c)}\right)\right) \tag{3.33}$$

where the abstract set $\mathbb{X}^{(c)}$ contains the possible strategies on carrier c. This means that we can solve the inner problem separately on each carrier while the master problem (3.21) acts as a connecting element between the carriers. Note that this decomposition is not possible for RTS, where only the rate constraints are dualized (see Section 3.2.3.2).

3.4 Description of Complex Multicarrier MIMO Systems

Let us now turn our attention to complex multicarrier MIMO systems as already introduced in Section 1.2. For the sake of a simple and unified treatment, we aim at performing all derivations by means of the RoP MIMO model from Definition 3.1.1 or, when necessary, the RoP CN MIMO model from Definition 3.3.1. To make this possible, it is necessary to introduce the following equivalent representations of complex multicarrier MIMO systems.

3.4.1 Four Equivalent Representations of Complex Multicarrier MIMO Systems

In Table 3.1, we formulate four equivalent representations of the data transmission in a complex multicarrier MIMO system. To do so, we use block-diagonal matrices $\boldsymbol{A} = \mathrm{blkdiag}(\boldsymbol{A}^{(c)})$ and stacked vectors $\boldsymbol{a} = \mathrm{stack}(\boldsymbol{a}^{(c)})$ on the one hand and real-valued representations $\grave{\boldsymbol{A}} = \grave{\Re}(\boldsymbol{A})$ and $\check{\boldsymbol{a}} = \check{\Re}(\boldsymbol{a})$ of complex matrices and vectors (see Section 2.9.5) on the other hand.

	multicarrier formulation	combined representation
complex	For $c = 1, \ldots, C$: $\boldsymbol{y}_{\mathrm{D}}^{(c)} = \sum_{\mathrm{S} \in \mathcal{S}_{\mathrm{D}}} \boldsymbol{H}_{\mathrm{DS}}^{(c)} \boldsymbol{x}_{\mathrm{S}}^{(c)} + \boldsymbol{\eta}_{\mathrm{D}}^{(c)}$ (3.34) $\boldsymbol{H}_{\mathrm{DS}}^{(c)} \in \mathbb{C}^{m_{\mathrm{D}} \times m_{\mathrm{S}}}$ $\boldsymbol{x}_{\mathrm{S}}^{(c)} \in \mathbb{C}^{m_{\mathrm{S}}}$ $\boldsymbol{\eta}_{\mathrm{D}}^{(c)} \in \mathbb{C}^{m_{\mathrm{D}}}$ $\boldsymbol{y}_{\mathrm{D}}^{(c)} \in \mathbb{C}^{m_{\mathrm{D}}}$	$\boldsymbol{y}_{\mathrm{D}} = \sum_{\mathrm{S} \in \mathcal{S}_{\mathrm{D}}} \boldsymbol{H}_{\mathrm{DS}} \boldsymbol{x}_{\mathrm{S}} + \boldsymbol{\eta}_{\mathrm{D}}$ (3.35) $\boldsymbol{H}_{\mathrm{DS}} = \mathrm{blkdiag}(\boldsymbol{H}_{\mathrm{DS}}^{(c)}) \in \mathbb{C}^{Cm_{\mathrm{D}} \times Cm_{\mathrm{S}}}$ $\boldsymbol{x}_{\mathrm{S}} = \mathrm{stack}(\boldsymbol{x}_{\mathrm{S}}^{(c)}) \in \mathbb{C}^{Cm_{\mathrm{S}}}$ $\boldsymbol{\eta}_{\mathrm{D}} = \mathrm{stack}(\boldsymbol{\eta}_{\mathrm{D}}^{(c)}) \in \mathbb{C}^{Cm_{\mathrm{D}}}$ $\boldsymbol{y}_{\mathrm{D}} = \mathrm{stack}(\boldsymbol{y}_{\mathrm{D}}^{(c)}) \in \mathbb{C}^{Cm_{\mathrm{D}}}$
real-valued	For $c = 1, \ldots, C$: $\check{\boldsymbol{y}}_{\mathrm{D}}^{(c)} = \sum_{\mathrm{S} \in \mathcal{S}_{\mathrm{D}}} \grave{\boldsymbol{H}}_{\mathrm{DS}}^{(c)} \check{\boldsymbol{x}}_{\mathrm{S}}^{(c)} + \check{\boldsymbol{\eta}}_{\mathrm{D}}^{(c)}$ (3.36) $\grave{\boldsymbol{H}}_{\mathrm{DS}}^{(c)} = \grave{\Re}(\boldsymbol{H}_{\mathrm{DS}}^{(c)}) \in \mathbb{R}^{2m_{\mathrm{D}} \times 2m_{\mathrm{S}}}$ $\check{\boldsymbol{x}}_{\mathrm{S}}^{(c)} = \check{\Re}(\boldsymbol{x}_{\mathrm{S}}^{(c)}) \in \mathbb{R}^{2m_{\mathrm{S}}}$ $\check{\boldsymbol{\eta}}_{\mathrm{D}}^{(c)} = \check{\Re}(\boldsymbol{\eta}_{\mathrm{D}}^{(c)}) \in \mathbb{R}^{2m_{\mathrm{D}}}$ $\check{\boldsymbol{y}}_{\mathrm{D}}^{(c)} = \check{\Re}(\boldsymbol{y}_{\mathrm{D}}^{(c)}) \in \mathbb{R}^{2m_{\mathrm{D}}}$	$\check{\boldsymbol{y}}_{\mathrm{D}} = \sum_{\mathrm{S} \in \mathcal{S}_{\mathrm{D}}} \grave{\boldsymbol{H}}_{\mathrm{DS}} \check{\boldsymbol{x}}_{\mathrm{S}} + \check{\boldsymbol{\eta}}_{\mathrm{D}}$ (3.37) $\grave{\boldsymbol{H}}_{\mathrm{DS}} = \grave{\Re}(\boldsymbol{H}_{\mathrm{DS}}) \in \mathbb{R}^{2Cm_{\mathrm{D}} \times 2Cm_{\mathrm{S}}}$ $\check{\boldsymbol{x}}_{\mathrm{S}} = \check{\Re}(\boldsymbol{x}_{\mathrm{S}}) \in \mathbb{R}^{2Cm_{\mathrm{S}}}$ $\check{\boldsymbol{\eta}}_{\mathrm{D}} = \check{\Re}(\boldsymbol{\eta}_{\mathrm{D}}) \in \mathbb{R}^{2Cm_{\mathrm{D}}}$ $\check{\boldsymbol{y}}_{\mathrm{D}} = \check{\Re}(\boldsymbol{y}_{\mathrm{D}}) \in \mathbb{R}^{2Cm_{\mathrm{D}}}$

Table 3.1: Four equivalent representations of complex multicarrier MIMO systems with m_{T} antennas at terminal T.

Remark 3.4.1. *To define the combined real representation* (3.37)*, we have used the composite real representation of the combined complex vectors from* (3.35)*. Note that it would also be possible to establish a different definition by instead stacking the composite real per-carrier vectors from* (3.36)*. This would not make a conceptual difference, but it would permute the rows and columns of the resulting matrices and vectors and would, thus, lead to different block structures in our further investigations. In all our derivations, we stick to the definition of the combined real representation given in Table 3.1.*

Among the four formulations given in Table 3.1, the combined real representation (3.37) is the only one that always complies to the definition of a RoP MIMO system (Definition 3.1.1). Thus, this model is used for most of our derivations and is discussed in detail in Sections 3.4.3 and 3.4.4. If all signals and noise vectors are proper, the combined complex representation (3.35) is a RoP MIMO system as well. In case of CN signals and noise (in the sense of Definition 3.3.2), the real-valued multicarrier formulation (3.36) is a RoP CN MIMO system as defined in Definition 3.3.1. Finally, if the signals and the noise are proper and CN, the complex multicarrier formulation (3.34) complies to the definition of a RoP CN MIMO system.

3.4.2 Constraints on the Transmit Signals

Throughout this work, we assume constraints on the per-carrier covariance matrices of all transmitting nodes $\mathrm{S} \in \mathcal{S} = (\mathrm{S}_1, \ldots, \mathrm{S}_{|\mathcal{S}|})$ in the form

$$\left(\boldsymbol{C}_{\boldsymbol{x}_{\mathrm{S}}^{(1)}}, \ldots, \boldsymbol{C}_{\boldsymbol{x}_{\mathrm{S}}^{(C)}}\right)_{\mathrm{S}\in\mathcal{S}} \in \bar{\mathcal{Q}} \tag{3.38}$$

where $\bar{\mathcal{Q}}$ is a convex set of tuples of Hermitian matrices which is chosen in a way that we obtain a compact constraint set with nonempty interior if we in addition demand that $\boldsymbol{C}_{\boldsymbol{x}_{\mathrm{S}}^{(c)}} \succeq \boldsymbol{0}$ for all carriers c and all transmitting nodes S.

Special cases of constraints of this kind include per-transmitter power constraints

$$\sum_{c=1}^{C} \mathrm{tr}\left[\boldsymbol{C}_{\boldsymbol{x}_{\mathrm{S}}^{(c)}}\right] \leq Q_{\mathrm{S}} \quad \forall \mathrm{S} \in \mathcal{S} \tag{3.39}$$

for given constants Q_{S}, individual per-carrier power constraints of all transmitters

$$\mathrm{tr}\left[\boldsymbol{C}_{\boldsymbol{x}_{\mathrm{S}}^{(c)}}\right] \leq Q_{\mathrm{S}}^{(c)} \quad \forall c,\ \forall \mathrm{S} \in \mathcal{S} \tag{3.40}$$

for given constants $Q_{\mathrm{S}}^{(c)}$, and individual per-carrier shaping constraints of all transmitters

$$\boldsymbol{C}_{\boldsymbol{x}_{\mathrm{S}}^{(c)}} \preceq \boldsymbol{Q}_{\mathrm{S}}^{(c)} \quad \forall c,\ \forall \mathrm{S} \in \mathcal{S} \tag{3.41}$$

for given positive-semidefinite matrices $\boldsymbol{Q}_{\mathrm{S}}^{(c)}$. Moreover, we can consider global constraints, such as a sum power constraint

$$\sum_{\mathrm{S}\in\mathcal{S}} \sum_{c=1}^{C} \mathrm{tr}\left[\boldsymbol{C}_{\boldsymbol{x}_{\mathrm{S}}^{(c)}}\right] \leq Q \tag{3.42}$$

for a given maximum available transmit power Q, or, e.g., overall per-carrier shaping constraints

$$\sum_{\mathrm{S}\in\mathcal{S}} \boldsymbol{C}_{\boldsymbol{x}_{\mathrm{S}}^{(c)}} \preceq \boldsymbol{Q}^{(c)} \quad \forall c \tag{3.43}$$

for given positive-semidefinite matrices $\boldsymbol{Q}^{(c)}$.

If we work with one of the alternative representations given in Table 3.1, the constraint set (3.38) has to be translated to constraints on $\left(\boldsymbol{C}_{\check{\boldsymbol{x}}_{\mathrm{S}}^{(1)}}, \ldots, \boldsymbol{C}_{\check{\boldsymbol{x}}_{\mathrm{S}}^{(C)}}\right)_{\mathrm{S}\in\mathcal{S}}$, $(\boldsymbol{C}_{\boldsymbol{x}_{\mathrm{S}}})_{\mathrm{S}\in\mathcal{S}}$, or $(\boldsymbol{C}_{\check{\boldsymbol{x}}_{\mathrm{S}}})_{\mathrm{S}\in\mathcal{S}}$, respectively.

3.4.3 Combined Real Representation of Proper Signals and CN Signals

In order to be able to study proper signals and CN signals in the combined real representation (3.37), we define the following three spaces.

Definition 3.4.1. *For a terminal $\mathrm{T} \in \mathcal{T}$ with $m_{\mathrm{T}} \in \mathbb{N}$ antennas in a complex multicarrier MIMO system with C carriers, we define*

- *the space of symmetric $\mathcal{BSC}_2$ matrices $\grave{\mathcal{P}}_{\mathrm{T}} = \mathcal{SBSC}_2^{Cm_{\mathrm{T}}}$,*

- *the space of symmetric matrices with block-diagonal submatrices*
$$\mathcal{P}_{\mathrm{T}}^{\mathrm{CN}} = \left\{ \boldsymbol{P} = \begin{bmatrix} \boldsymbol{A} & \boldsymbol{B} \\ \boldsymbol{B}^{\mathrm{T}} & \boldsymbol{C} \end{bmatrix} \;\middle|\; \boldsymbol{A}, \boldsymbol{C} \in \mathbb{S}^{\mathcal{M}}, \boldsymbol{B} \in \mathbb{R}^{\mathcal{M} \times \mathcal{M}} \right\} \text{ with } \mathcal{M} = (m_{\mathrm{T}})_{\forall c},$$

- *the space of symmetric $\mathcal{BSC}_2$ matrices with block-diagonal submatrices* $\grave{\mathcal{P}}_{\mathrm{T}}^{\mathrm{CN}} = \grave{\mathcal{P}}_{\mathrm{T}} \cap \mathcal{P}_{\mathrm{T}}^{\mathrm{CN}}$.

Proposition 3.4.1. *The spaces $\grave{\mathcal{P}}_{\mathrm{T}}$, $\mathcal{P}_{\mathrm{T}}^{\mathrm{CN}}$, and $\grave{\mathcal{P}}_{\mathrm{T}}^{\mathrm{CN}}$ from Definition 3.4.1 are power shaping spaces.*

Proof. The space $\grave{\mathcal{P}}_{\mathrm{T}}$ is a power shaping space due to Theorem 2.9.1, and $\mathcal{P}_{\mathrm{T}}^{\mathrm{CN}}$ is a power shaping space due to Proposition 2.8.1. As a consequence, $\grave{\mathcal{P}}_{\mathrm{T}}^{\mathrm{CN}}$ is a power shaping space due to Proposition 2.4.3. □

The following proposition states that proper signals (Definition 2.9.2), CN signals (Definition 3.3.2), and signals that are both proper and CN can be considered as maximum-entropy signals with respect to these three power shaping spaces, respectively. The signal $\boldsymbol{z}_{\mathrm{T}}$ is used as a placeholder for any signal at node T, i.e., the transmit signal $\boldsymbol{x}_{\mathrm{T}}$, the received signal $\boldsymbol{y}_{\mathrm{T}}$, or the noise $\boldsymbol{\eta}_{\mathrm{T}}$. Recall that we call a multicarrier signal proper if the per-carrier signals are jointly proper (see Section 1.4.1), i.e., if the combined complex vector is proper.

Proposition 3.4.2. *For a signal $\boldsymbol{z}_{\mathrm{T}} = \mathrm{stack}(\boldsymbol{z}_{\mathrm{T}}^{(c)})$ and its combined real covariance matrix $\boldsymbol{C}_{\check{\boldsymbol{z}}_{\mathrm{T}}} \in \mathbb{S}^{2Cm_{\mathrm{T}}}$, we have the following equivalences using the power shaping spaces from Definition 3.4.1.*

- $\boldsymbol{C}_{\check{\boldsymbol{z}}_{\mathrm{T}}} \in \grave{\mathcal{P}}_{\mathrm{T}} \Leftrightarrow \boldsymbol{z}_{\mathrm{T}}$ *is proper (but possibly CC)* $\Leftrightarrow \boldsymbol{z}_{\mathrm{T}}^{(1)}, \ldots, \boldsymbol{z}_{\mathrm{T}}^{(C)}$ *are jointly proper,*

- $\boldsymbol{C}_{\check{\boldsymbol{z}}_{\mathrm{T}}} \in \mathcal{P}_{\mathrm{T}}^{\mathrm{CN}} \Leftrightarrow \boldsymbol{z}_{\mathrm{T}}$ *is CN (but possibly improper)* $\Leftrightarrow \boldsymbol{z}_{\mathrm{T}}^{(1)}, \ldots, \boldsymbol{z}_{\mathrm{T}}^{(C)}$ *are uncorrelated across carriers,*

- $\boldsymbol{C}_{\check{\boldsymbol{z}}_{\mathrm{T}}} \in \grave{\mathcal{P}}_{\mathrm{T}}^{\mathrm{CN}} \Leftrightarrow \boldsymbol{z}_{\mathrm{T}}$ *is proper and CN* $\Leftrightarrow \boldsymbol{z}_{\mathrm{T}}^{(1)}, \ldots, \boldsymbol{z}_{\mathrm{T}}^{(C)}$ *are proper and uncorrelated across carriers.*

Proof. If and only if $\boldsymbol{z}_{\mathrm{T}}$ is proper, the pseudocovariance matrix $\tilde{\boldsymbol{C}}_{\boldsymbol{z}_{\mathrm{T}}}$ is zero, so that the second summand in (2.34) vanishes, i.e., $\boldsymbol{C}_{\check{\boldsymbol{z}}_{\mathrm{T}}}$ is a $\mathcal{BSC}_2$ matrix. If and only if $\boldsymbol{z}_{\mathrm{T}}^{(1)}, \ldots, \boldsymbol{z}_{\mathrm{T}}^{(C)}$ are uncorrelated across carriers, the covariance matrix $\boldsymbol{C}_{\boldsymbol{z}_{\mathrm{T}}}$ and the pseudocovariance matrix $\tilde{\boldsymbol{C}}_{\boldsymbol{z}_{\mathrm{T}}}$ are block-diagonal. We then obtain from (2.34) that $\boldsymbol{C}_{\check{\boldsymbol{z}}_{\mathrm{T}}}$ consists of block-diagonal submatrices. If and only if $\boldsymbol{z}_{\mathrm{T}}$ is proper and CN, $\boldsymbol{C}_{\boldsymbol{z}_{\mathrm{T}}}$ is block-diagonal and $\tilde{\boldsymbol{C}}_{\boldsymbol{z}_{\mathrm{T}}} = \boldsymbol{0}$, i.e., $\boldsymbol{C}_{\check{\boldsymbol{z}}_{\mathrm{T}}}$ is $\mathcal{BSC}_2$ with block-diagonal submatrices. □

To see how the power shaping spaces defined above can be used in mathematical derivations, let us consider the following example.

Example 3.4.1. *If a signal $\boldsymbol{z}_{\mathrm{T}}$ is proper, the combined real representation $\check{\boldsymbol{z}}_{\mathrm{T}}$ is a maximum-entropy signal with respect to $\mathcal{P}_{\mathrm{T}} = \grave{\mathcal{P}}_{\mathrm{T}}$, so that we have $\boldsymbol{C}_{\check{\boldsymbol{z}}_{\mathrm{T}}} = \boldsymbol{P}_{\check{\boldsymbol{z}}_{\mathrm{T}}} \in \mathcal{P}_{\mathrm{T}}$. Impropriety of $\boldsymbol{z}_{\mathrm{T}}$ can be described by adding a component from the orthogonal complement, i.e., $\boldsymbol{N}_{\check{\boldsymbol{z}}_{\mathrm{T}}} \in \mathcal{N}_{\mathrm{T}}$, so that $\boldsymbol{C}_{\check{\boldsymbol{z}}_{\mathrm{T}}} = \boldsymbol{P}_{\check{\boldsymbol{z}}_{\mathrm{T}}} + \boldsymbol{N}_{\check{\boldsymbol{z}}_{\mathrm{T}}} \notin \mathcal{P}_{\mathrm{T}}$. Thus, we can check if $\boldsymbol{z}_{\mathrm{T}}$ is proper by verifying whether the projection $\mathrm{proj}_{\mathcal{N}_{\mathrm{T}}}(\boldsymbol{C}_{\check{\boldsymbol{z}}_{\mathrm{T}}})$ is zero, which is equivalent to checking whether $\mathrm{proj}_{\mathcal{P}_{\mathrm{T}}}(\boldsymbol{C}_{\check{\boldsymbol{z}}_{\mathrm{T}}}) = \boldsymbol{C}_{\check{\boldsymbol{z}}_{\mathrm{T}}}$.*

If all signals in a system are proper, we may decide to study the system in the combined complex representation, which then complies to the definition of a RoP MIMO system. The following example shows that the framework of power shaping spaces can be applied in this case as well.

Example 3.4.2. *If a proper signal* $\boldsymbol{z}_{\mathrm{T}} = \mathrm{stack}(\boldsymbol{z}_{\mathrm{T}}^{(c)})$ *is CN, the covariance matrix* $\boldsymbol{C}_{\boldsymbol{z}_{\mathrm{T}}}$ *is block-diagonal, i.e., the combined complex representation* $\boldsymbol{z}_{\mathrm{T}}$ *is a maximum-entropy signal with respect to the power shaping space* $\mathcal{P}_{\mathrm{T}} = \mathbb{H}^{(m_{\mathrm{T}})\forall c}$ *(the space of block-diagonal matrices with appropriate block sizes, see Example 2.8.5). A CC signal with correlations across carriers can be described by adding a component from the orthogonal complement, i.e.,* $\boldsymbol{N}_{\boldsymbol{z}_{\mathrm{T}}} \in \mathcal{N}_{\mathrm{T}}$*, so that* $\boldsymbol{C}_{\boldsymbol{z}_{\mathrm{T}}} = \boldsymbol{P}_{\boldsymbol{z}_{\mathrm{T}}} + \boldsymbol{N}_{\boldsymbol{z}_{\mathrm{T}}} \notin \mathcal{P}_{\mathrm{T}}$.

3.4.4 Compatibility with Power Shaping Spaces

For our further analysis, it is important to study how the compatibility assumption given in Definition 3.1.3 translates to the combined real representation (3.37) of a complex multicarrier MIMO system.

The combined real channel matrix $\grave{\boldsymbol{H}}_{\mathrm{DS}}$ is a $\mathcal{BSC}_2$ matrix since the corresponding complex channel is assumed to be linear, i.e., there is no conjugate linear component in (2.38). Due to the assumption of orthogonal carriers, it holds in addition that $\grave{\boldsymbol{H}}_{\mathrm{DS}}$ consists of block-diagonal submatrices with dimensions $\mathcal{M}_{\mathrm{D}} \times \mathcal{M}_{\mathrm{S}}$, where $\mathcal{M}_{\mathrm{D}} = (m_{\mathrm{D}})_{\forall c}$, and $\mathcal{M}_{\mathrm{S}} = (m_{\mathrm{S}})_{\forall c}$. This leads to the following Proposition.

Proposition 3.4.3. *For the following choices of* $\mathcal{P}_{\mathrm{S}}$ *and* $\mathcal{P}_{\mathrm{D}}$*, the channel matrix* $\grave{\boldsymbol{H}}_{\mathrm{DS}}$ *in* (3.37) *is compatible with* $(\mathcal{P}_{\mathrm{D}}, \mathcal{P}_{\mathrm{S}})$*:*

- $\mathcal{P}_{\mathrm{S}} = \grave{\mathcal{P}}_{\mathrm{S}}$ *and* $\mathcal{P}_{\mathrm{D}} = \grave{\mathcal{P}}_{\mathrm{D}}$*,*
- $\mathcal{P}_{\mathrm{S}} = \mathcal{P}_{\mathrm{S}}^{\mathrm{CN}}$ *and* $\mathcal{P}_{\mathrm{D}} = \mathcal{P}_{\mathrm{D}}^{\mathrm{CN}}$*,*
- $\mathcal{P}_{\mathrm{S}} = \grave{\mathcal{P}}_{\mathrm{S}}^{\mathrm{CN}}$ *and* $\mathcal{P}_{\mathrm{D}} = \grave{\mathcal{P}}_{\mathrm{D}}^{\mathrm{CN}}$*.*

Proof. The first bullet follows from Proposition 2.9.1, the second from Proposition 2.8.2, and the last from Proposition 2.7.4. □

Therefore, the following statement holds no matter which of the three possible choices in Proposition 3.4.3 we make: the signal portion $\grave{\boldsymbol{H}}_{\mathrm{DS}}\check{\boldsymbol{x}}_{\mathrm{S}}$ in the combined real received signal at node D is a maximum-entropy signal with respect to $\mathcal{P}_{\mathrm{D}}$ if the respective transmit signal $\check{\boldsymbol{x}}_{\mathrm{S}}$ is a maximum-entropy signal with respect to $\mathcal{P}_{\mathrm{S}}$.

The fact that the constraints act only on the complex per-carrier covariance matrices $\left(\boldsymbol{C}_{\boldsymbol{x}_{\mathrm{S}}^{(1)}}, \ldots, \boldsymbol{C}_{\boldsymbol{x}_{\mathrm{S}}^{(C)}}\right)_{\mathrm{S}\in\mathcal{S}}$ (but not on the pseudocovariance matrices or on cross-covariance matrices between per-carrier signals) translates to the combined real representation as follows.

Proposition 3.4.4. *Let* $\mathcal{P}_{\mathrm{S}}$ *for each transmitter* $\mathrm{S} \in \mathcal{S}$ *be chosen according to one of the possibilities in Definition 3.4.1. Then, the combined real representation* $(\boldsymbol{C}_{\check{\boldsymbol{x}}_{\mathrm{S}}})_{\mathrm{S}\in\mathcal{S}} \in \mathcal{Q}$ *of the constraint* (3.38) *is compatible with* $\bigotimes_{i=1}^{|\mathcal{S}|} \mathcal{P}_{\mathrm{S}_i}$ *(in the sense of Definition 3.1.2).*

Proof. The matrices $\boldsymbol{C}_{\boldsymbol{x}_{\mathrm{S}}^{(c)}},\ c=1,\ldots,C$ are the diagonal blocks of the covariance matrix $\boldsymbol{C}_{\boldsymbol{x}_{\mathrm{S}}}$ of $\boldsymbol{x}_{\mathrm{S}}$ in (3.35). Thus, when calculating the covariance matrix of $\check{\boldsymbol{x}}_{\mathrm{S}}$ in (3.37), we see from (2.34) that the elements of the combined real covariance matrix $\boldsymbol{C}_{\check{\boldsymbol{x}}_{\mathrm{S}}}$ that correspond to $\boldsymbol{C}_{\boldsymbol{x}_{\mathrm{S}}^{(c)}},\ c=1,\ldots,C$ are the diagonal blocks of the submatrices in the $\mathcal{BSC}_2$ component. Thus, adding arbitrary off-diagonal blocks to the submatrices or adding an arbitrary $\mathcal{BHSC}_2$ component does not affect the feasibility of $\boldsymbol{C}_{\check{\boldsymbol{x}}_{\mathrm{S}}}$ in terms of the considered constraint. □

If all signals in a system are proper and we decide to switch to the combined complex representation (3.35), we can exploit that the block-diagonal channel matrix $\boldsymbol{H}_{\mathrm{DS}}$ in (3.35) is compatible with $(\mathcal{P}_{\mathrm{D}},\mathcal{P}_{\mathrm{S}})$ if $\mathcal{P}_{\mathrm{S}}=\mathbb{H}^{(m_{\mathrm{S}})_{\forall c}}$ and $\mathcal{P}_{\mathrm{D}}=\mathbb{H}^{(m_{\mathrm{D}})_{\forall c}}$. The signal portion $\boldsymbol{H}_{\mathrm{DS}}\boldsymbol{x}_{\mathrm{S}}$ in the received signal at node D is a maximum-entropy signal with respect to $\mathcal{P}_{\mathrm{D}}$ if the respective transmit signal $\boldsymbol{x}_{\mathrm{S}}$ is a maximum-entropy signal with respect to $\mathcal{P}_{\mathrm{S}}$, i.e., a CN signal. When choosing $\mathcal{P}_{\mathrm{S}}$ in this manner at all transmitting nodes $\mathrm{S}\in\mathcal{S}$, it is easy to verify that the combined complex version $(\boldsymbol{C}_{\boldsymbol{x}_{\mathrm{S}}})_{\mathrm{S}\in\mathcal{S}}\in\mathcal{Q}$ of the constraint (3.38) is compatible with $\bigotimes_{i=1}^{|\mathcal{S}|}\mathcal{P}_{\mathrm{S}_i}$.

3.4.5 Mutual Information Expressions

When studying MIMO systems, we often have to evaluate mutual information expressions of the form given in (3.2). When applied to the combined real representation (3.37) of a complex multicarrier MIMO system, this expression reads as

$$\mathrm{I}\left(\check{\boldsymbol{x}}_{\mathrm{S}'};\check{\boldsymbol{y}}_{\mathrm{D}}\right)=\frac{1}{2}\log_2\frac{\det\left(\boldsymbol{C}_{\check{\boldsymbol{\eta}}_{\mathrm{D}}}+\sum_{\mathrm{S}\in\mathcal{S}_{\mathrm{D}}}\grave{\boldsymbol{H}}_{\mathrm{DS}}\boldsymbol{C}_{\check{\boldsymbol{x}}_{\mathrm{S}}}\grave{\boldsymbol{H}}_{\mathrm{DS}}^{\mathrm{T}}\right)}{\det\left(\boldsymbol{C}_{\check{\boldsymbol{\eta}}_{\mathrm{D}}}+\sum_{\mathrm{S}\in\mathcal{S}_{\mathrm{D}}\setminus\{\mathrm{S}'\}}\grave{\boldsymbol{H}}_{\mathrm{DS}}\boldsymbol{C}_{\check{\boldsymbol{x}}_{\mathrm{S}}}\grave{\boldsymbol{H}}_{\mathrm{DS}}^{\mathrm{T}}\right)} \tag{3.44}$$

with $\mathrm{S}'\in\mathcal{S}_{\mathrm{D}}$. If all transmit signals are maximum-entropy signals with respect to one of the power shaping spaces defined above, this expression can be simplified as follows.

Proposition 3.4.5. *The mutual information between* $\check{\boldsymbol{x}}_{\mathrm{S}'},\ \mathrm{S}'\in\mathcal{S}_{\mathrm{D}}$ *and* $\check{\boldsymbol{y}}_{\mathrm{D}}$ *in* (3.44) *equals*

$$\mathrm{I}\left(\check{\boldsymbol{x}}_{\mathrm{S}'};\check{\boldsymbol{y}}_{\mathrm{D}}\right)=\log_2\frac{\det\left(\boldsymbol{C}_{\boldsymbol{\eta}_{\mathrm{D}}}+\sum_{\mathrm{S}\in\mathcal{S}_{\mathrm{D}}}\boldsymbol{H}_{\mathrm{DS}}\boldsymbol{C}_{\boldsymbol{x}_{\mathrm{S}}}\boldsymbol{H}_{\mathrm{DS}}^{\mathrm{H}}\right)}{\det\left(\boldsymbol{C}_{\boldsymbol{\eta}_{\mathrm{D}}}+\sum_{\mathrm{S}\in\mathcal{S}_{\mathrm{D}}\setminus\{\mathrm{S}'\}}\boldsymbol{H}_{\mathrm{DS}}\boldsymbol{C}_{\boldsymbol{x}_{\mathrm{S}}}\boldsymbol{H}_{\mathrm{DS}}^{\mathrm{H}}\right)} \tag{3.45}$$

if $\boldsymbol{C}_{\check{\boldsymbol{x}}_{\mathrm{S}}}\in\grave{\mathcal{P}}_{\mathrm{S}}$ *for all* $\mathrm{S}\in\mathcal{S}_{\mathrm{D}}$ *and* $\boldsymbol{C}_{\check{\boldsymbol{\eta}}_{\mathrm{D}}}\in\grave{\mathcal{P}}_{\mathrm{D}}$. *It equals*

$$\mathrm{I}\left(\check{\boldsymbol{x}}_{\mathrm{S}'};\check{\boldsymbol{y}}_{\mathrm{D}}\right)=\sum_{c=1}^{C}\frac{1}{2}\log_2\frac{\det\left(\boldsymbol{C}_{\check{\boldsymbol{\eta}}_{\mathrm{D}}^{(c)}}+\sum_{\mathrm{S}\in\mathcal{S}_{\mathrm{D}}}\grave{\boldsymbol{H}}_{\mathrm{DS}}^{(c)}\boldsymbol{C}_{\check{\boldsymbol{x}}_{\mathrm{S}}^{(c)}}\grave{\boldsymbol{H}}_{\mathrm{DS}}^{(c),\mathrm{T}}\right)}{\det\left(\boldsymbol{C}_{\check{\boldsymbol{\eta}}_{\mathrm{D}}^{(c)}}+\sum_{\mathrm{S}\in\mathcal{S}_{\mathrm{D}}\setminus\{\mathrm{S}'\}}\grave{\boldsymbol{H}}_{\mathrm{DS}}^{(c)}\boldsymbol{C}_{\check{\boldsymbol{x}}_{\mathrm{S}}^{(c)}}\grave{\boldsymbol{H}}_{\mathrm{DS}}^{(c),\mathrm{T}}\right)} \tag{3.46}$$

if $\boldsymbol{C}_{\check{\boldsymbol{x}}_{\mathrm{S}}}\in\mathcal{P}_{\mathrm{S}}^{\mathrm{CN}}$ *for all* $\mathrm{S}\in\mathcal{S}_{\mathrm{D}}$ *and* $\boldsymbol{C}_{\check{\boldsymbol{\eta}}_{\mathrm{D}}}\in\mathcal{P}_{\mathrm{D}}^{\mathrm{CN}}$. *Finally, it equals*

$$\mathrm{I}\left(\check{\boldsymbol{x}}_{\mathrm{S}'};\check{\boldsymbol{y}}_{\mathrm{D}}\right)=\sum_{c=1}^{C}\log_2\frac{\det\left(\boldsymbol{C}_{\boldsymbol{\eta}_{\mathrm{D}}^{(c)}}+\sum_{\mathrm{S}\in\mathcal{S}_{\mathrm{D}}}\boldsymbol{H}_{\mathrm{DS}}^{(c)}\boldsymbol{C}_{\boldsymbol{x}_{\mathrm{S}}^{(c)}}\boldsymbol{H}_{\mathrm{DS}}^{(c),\mathrm{H}}\right)}{\det\left(\boldsymbol{C}_{\boldsymbol{\eta}_{\mathrm{D}}^{(c)}}+\sum_{\mathrm{S}\in\mathcal{S}_{\mathrm{D}}\setminus\{\mathrm{S}'\}}\boldsymbol{H}_{\mathrm{DS}}^{(c)}\boldsymbol{C}_{\boldsymbol{x}_{\mathrm{S}}^{(c)}}\boldsymbol{H}_{\mathrm{DS}}^{(c),\mathrm{H}}\right)} \tag{3.47}$$

if $\boldsymbol{C}_{\check{\boldsymbol{x}}_{\mathrm{S}}}\in\grave{\mathcal{P}}_{\mathrm{S}}^{\mathrm{CN}}$ *for all* $\mathrm{S}\in\mathcal{S}_{\mathrm{D}}$ *and* $\boldsymbol{C}_{\check{\boldsymbol{\eta}}_{\mathrm{D}}}\in\grave{\mathcal{P}}_{\mathrm{D}}^{\mathrm{CN}}$.

Proof. If $\boldsymbol{C}_{\check{\boldsymbol{x}}_{\mathrm{S}}} \in \grave{\mathcal{P}}_{\mathrm{S}}\ \forall \mathrm{S} \in \mathcal{S}_{\mathrm{D}}$ and $\boldsymbol{C}_{\check{\boldsymbol{\eta}}_{\mathrm{D}}} \in \grave{\mathcal{P}}_{\mathrm{D}}$, all matrices in (3.44) are $\mathcal{BSC}_2$. Therefore, we can use the equivalences from Section 2.9.5 to get (3.45). If $\boldsymbol{C}_{\check{\boldsymbol{x}}_{\mathrm{S}}} \in \mathcal{P}_{\mathrm{S}}^{\mathrm{CN}}$ for all $\mathrm{S} \in \mathcal{S}_{\mathrm{D}}$ and $\boldsymbol{C}_{\check{\boldsymbol{\eta}}_{\mathrm{D}}} \in \mathcal{P}_{\mathrm{D}}^{\mathrm{CN}}$, all matrices in (3.44) consist of block-diagonal submatrices. Thus, we can use a permutation matrix (as in the proof of Proposition 2.8.1) to bring the matrices whose determinants are to be calculated to block-diagonal form without changing the values of the determinants. We then obtain (3.46) by exploiting the fact that the determinant of a block-diagonal matrix equals the product of the individual determinants of the blocks. This fact is also used to obtain (3.47). □

Chapter 4

Point-to-Point Transmission: the Gaussian MIMO Channel

In this chapter, we consider a single-user MIMO transmission as in [29], which we refer to as a (Gaussian) MIMO channel. For the complex multicarrier MIMO channel, the optimal transmit strategy under the assumption of proper and/or CN noise can be concluded from [29]. It turns out that the transmit signal should be proper and/or CN as well. We rederive and generalize these results using the framework of power shaping spaces in order to see the functioning of this framework in a rather simple scenario before turning our attention to the more complicated multiuser systems, and in order to obtain some fundamental insights that can be reused at several points later on. It turns out that the abovementioned existing results can be obtained as simple special cases of a more general theorem based on the notion of maximum-entropy signals.

In addition, we study optimal transmit strategies for cases with reduced-entropy noise, such as improper noise or CC noise. By adapting the transmit strategy to the properties of the noise, performance gains can be obtained in these cases. However, even if the transmitter is oblivious of the noise properties and sticks to a maximum-entropy transmit signal, the achievable rate in case of reduced-entropy noise is still higher than for maximum-entropy noise. This remarkable aspect is shown at the end of this chapter, where we prove that maximum-entropy noise is the worst-case noise in the Gaussian MIMO channel.

All results in this chapter are first derived in a general manner for a RoP MIMO system without specifying which particular kind of reduced-entropy signals we consider. Then, they are specialized to the complex multicarrier MIMO channel, where we are interested in particular in improper signaling and CC transmission.

4.1 System Model and Channel Capacity

As we have only one transmitter S and one receiver D, we can introduce the abbreviations $\boldsymbol{y} = \boldsymbol{y}_{\mathrm{D}}$, $\boldsymbol{H} = \boldsymbol{H}_{\mathrm{DS}}$, $\boldsymbol{x} = \boldsymbol{x}_{\mathrm{S}}$, $\boldsymbol{\eta} = \boldsymbol{\eta}_{\mathrm{D}}$, and $M = M_{\mathrm{D}}$. The general model for RoP MIMO systems in (3.1) then simplifies to the description of the RoP MIMO channel

$$\boldsymbol{y} = \boldsymbol{H}\boldsymbol{x} + \boldsymbol{\eta}. \tag{4.1}$$

The case of the complex MIMO channel with proper noise was studied in detail in [29], and the derivations given therein analogously hold in the real-valued MIMO channel.

A rate r is achievable in the RoP MIMO channel if it does not exceed the mutual information (2.9) between the transmitted signal $\boldsymbol{x}$ and the received signal $\boldsymbol{y}$ [29], i.e., we can achieve

$$r = \mathrm{I}(\boldsymbol{x};\boldsymbol{y}) = \mathrm{h}(\boldsymbol{y}) - \mathrm{h}(\boldsymbol{y}\,|\,\boldsymbol{x}) = \mathrm{h}(\boldsymbol{y}) - \mathrm{h}(\boldsymbol{\eta}). \tag{4.2}$$

Since $\mathrm{h}(\boldsymbol{\eta})$ does not depend on the transmit strategy, r can be maximized by maximizing $\mathrm{h}(\boldsymbol{y})$. For any fixed $\boldsymbol{C}_{\boldsymbol{x}}$, which leads to a fixed

$$\boldsymbol{C}_{\boldsymbol{y}} = \boldsymbol{H}\boldsymbol{C}_{\boldsymbol{x}}\boldsymbol{H}^{\mathrm{H}} + \boldsymbol{C}_{\boldsymbol{\eta}} \tag{4.3}$$

$\mathrm{h}(\boldsymbol{y})$ is maximal if $\boldsymbol{y}$ follows a Gaussian distribution (see [59, 62] for a real-valued system and [29, 63] for a complex system). Under the assumption of Gaussian noise that is independent of $\boldsymbol{x}$, we can choose $\boldsymbol{x}$ to be Gaussian in order to achieve this. The constraints on the transmit strategy affect only $\boldsymbol{C}_{\boldsymbol{x}}$, and the above reasoning applies for any $\boldsymbol{C}_{\boldsymbol{x}}$ including the optimal one. Thus, a Gaussian $\boldsymbol{x}$ maximizes (4.2).

Remark 4.1.1. *For complex signals, [29, 63] show that the entropy-maximizing $\boldsymbol{y}$ is not only Gaussian, but also proper. In [29], it was concluded from this that proper transmit signals are optimal in a complex MIMO channel with proper noise. When we study the complex multicarrier MIMO channel later on, we obtain the same result as a simple special case of a more general theorem, which we prove based on the framework of power shaping spaces. As long as we consider the RoP MIMO channel, we are not interested in the question of (im)proper signals since we consider either a setting where all signals are proper by assumption (see Definition 3.1.1) or a real-valued setting.*

As the optimal $\boldsymbol{x}$ is Gaussian, we can use the mutual information expression for Gaussian signals given in (3.2), and we obtain

$$r = \mathrm{I}(\boldsymbol{x};\boldsymbol{y}) = \mu \log_2 \frac{\det\left(\boldsymbol{C}_{\boldsymbol{\eta}} + \boldsymbol{H}\boldsymbol{C}_{\boldsymbol{x}}\boldsymbol{H}^{\mathrm{H}}\right)}{\det \boldsymbol{C}_{\boldsymbol{\eta}}}. \tag{4.4}$$

The aim is then to find the optimal transmit covariance matrix

$$\max_{\boldsymbol{C}_{\boldsymbol{x}} \succeq \boldsymbol{0}} \; r \quad \text{s.t.} \quad \boldsymbol{C}_{\boldsymbol{x}} \in \mathcal{Q} \tag{4.5}$$

where $\mathcal{Q}$ is defined as in (3.3). The solution to (4.5) is the channel capacity of the RoP MIMO channel.

4.2 Optimality of Maximum-Entropy Transmission

Our aim is now to study how knowledge about noise properties can enable us to draw direct conclusions about the optimal transmit signal without even carrying out the optimization (4.5). In particular, we assume that the noise is a maximum-entropy signal with respect to some power shaping space. According to the following theorem, the optimal transmit signal then is a maximum-entropy signal, too.

Theorem 4.2.1. *Let $\mathcal{P}_{\mathrm{S}}$ and $\mathcal{P}_{\mathrm{D}}$ be power shaping spaces fulfilling the compatibility assumption (Definition 3.1.3). If the noise is a maximum-entropy signal with respect to $\mathcal{P}_{\mathrm{D}}$, the capacity of the RoP MIMO channel* (4.1) *is achieved by a maximum-entropy transmit signal with respect to $\mathcal{P}_{\mathrm{S}}$.*

Proof. Let $\boldsymbol{P}_{\boldsymbol{x}} = \mathrm{proj}_{\mathcal{P}_{\mathrm{S}}}(\boldsymbol{C}_{\boldsymbol{x}})$ and $\boldsymbol{N}_{\boldsymbol{x}} = \mathrm{proj}_{\mathcal{N}_{\mathrm{S}}}(\boldsymbol{C}_{\boldsymbol{x}})$, so that $\boldsymbol{C}_{\boldsymbol{x}} = \boldsymbol{P}_{\boldsymbol{x}} + \boldsymbol{N}_{\boldsymbol{x}}$. Since $\boldsymbol{x}$ and $\boldsymbol{\eta}$ are independent, and $\boldsymbol{H}$ is compatible with $(\mathcal{P}_{\mathrm{D}}, \mathcal{P}_{\mathrm{S}})$, we have $\boldsymbol{C}_{\boldsymbol{y}} = \boldsymbol{P}_{\boldsymbol{y}} + \boldsymbol{N}_{\boldsymbol{y}}$ with

$$\boldsymbol{P}_{\boldsymbol{y}} = \boldsymbol{H}\boldsymbol{P}_{\boldsymbol{x}}\boldsymbol{H}^{\mathrm{H}} + \boldsymbol{P}_{\boldsymbol{\eta}} \in \mathcal{P}_{\mathrm{D}} \qquad \boldsymbol{N}_{\boldsymbol{y}} = \boldsymbol{H}\boldsymbol{N}_{\boldsymbol{x}}\boldsymbol{H}^{\mathrm{H}} + \boldsymbol{N}_{\boldsymbol{\eta}} \in \mathcal{N}_{\mathrm{D}} \tag{4.6}$$

where $\boldsymbol{N}_{\boldsymbol{\eta}} = \mathrm{proj}_{\mathcal{N}_{\mathrm{D}}}(\boldsymbol{C}_{\boldsymbol{\eta}}) = \boldsymbol{0}$ and $\boldsymbol{P}_{\boldsymbol{\eta}} = \mathrm{proj}_{\mathcal{P}_{\mathrm{D}}}(\boldsymbol{C}_{\boldsymbol{\eta}}) = \boldsymbol{C}_{\boldsymbol{\eta}}$ by assumption. We can assume $\boldsymbol{P}_{\boldsymbol{x}} \succeq \boldsymbol{0}$ due to Proposition 2.5.1. For any given $\boldsymbol{P}_{\boldsymbol{x}}$, the power shaping matrix $\boldsymbol{P}_{\boldsymbol{y}}$ is fixed, and the entropy of $\boldsymbol{y}$ is maximized by $\boldsymbol{N}_{\boldsymbol{y}} = \boldsymbol{0}$ (Theorem 2.5.2), which can be achieved by choosing $\boldsymbol{N}_{\boldsymbol{x}} = \boldsymbol{0}$. To see that this choice is feasible, note that $\boldsymbol{C}_{\boldsymbol{x}} = \boldsymbol{P}_{\boldsymbol{x}} + \boldsymbol{N}_{\boldsymbol{x}} \succeq \boldsymbol{0}$ holds for $\boldsymbol{N}_{\boldsymbol{x}} = \boldsymbol{0}$ and that the compatibility assumption makes the covariance constraint equivalent to $\boldsymbol{P}_{\boldsymbol{x}} \in \mathcal{Q}$, which does not depend on $\boldsymbol{N}_{\boldsymbol{x}}$. This reasoning holds for any $\boldsymbol{P}_{\boldsymbol{x}} \succeq \boldsymbol{0}$ including the optimal one. Thus, we can always choose $\boldsymbol{N}_{\boldsymbol{x}} = \boldsymbol{0}$, i.e., $\boldsymbol{C}_{\boldsymbol{x}} \in \mathcal{P}_{\mathrm{S}}$. □

4.3 Optimal Transmit Covariance Matrix under a Sum Power Constraint

While the statement of Theorem 4.2.1 could be shown regardless of the choice of $\mathcal{Q}$ as long as the compatibility assumption is fulfilled, we need to know the constraint set if we want to carry out the covariance optimization (4.5). In this section, we consider the optimization for the special case of a sum power constraint (3.4). For more complicated constraints, where an analytic solution may not be easy to obtain, the optimization could be solved by a convex programming solver since the objective function is concave in $\boldsymbol{C}_{\boldsymbol{x}}$ and the constraint set is convex by assumption (see Section 3.1.1).

In [29], the optimal transmit covariance matrix $\boldsymbol{C}_{\boldsymbol{x}}$ under a sum power constraint was derived for the complex MIMO channel with proper noise, and the derivation can be transferred to the real-valued MIMO channel. We can express the achievable rate (4.4) as

$$r = \mu \log_2 \det\left(\mathbf{I}_{M_{\mathrm{S}}} + \boldsymbol{H}^{\mathrm{H}}\boldsymbol{C}_{\boldsymbol{\eta}}^{-1}\boldsymbol{H}\boldsymbol{C}_{\boldsymbol{x}}\right) \tag{4.7}$$

where we have used that

$$\det(\mathbf{I}_m + \boldsymbol{A}\boldsymbol{B}^{\mathrm{H}}) = \det(\mathbf{I}_n + \boldsymbol{B}^{\mathrm{H}}\boldsymbol{A}) \tag{4.8}$$

for $\boldsymbol{A}, \boldsymbol{B} \in \mathbb{C}^{m\times n}$ (e.g., [29]).

Based on the eigenvalue decomposition

$$\boldsymbol{U}\,\mathrm{diag}(\lambda_i)\boldsymbol{U}^{\mathrm{H}} = \boldsymbol{H}^{\mathrm{H}}\boldsymbol{C}_{\boldsymbol{\eta}}^{-1}\boldsymbol{H} \tag{4.9}$$

the optimal transmit covariance matrix can be expressed as [29]

$$\boldsymbol{C}_{\boldsymbol{x}} = \boldsymbol{U}\,\mathrm{diag}(p_i)\boldsymbol{U}^{\mathrm{H}} \tag{4.10}$$

with the power allocation

$$p_i = \max\left\{\omega - \frac{1}{\lambda_i},\ 0\right\}. \tag{4.11}$$

In this so-called waterfilling solution (see, e.g., [62]), the water level ω must be chosen such that the sum power constraint (3.4) is fulfilled with equality. The fact that $\boldsymbol{C_x}$ must have the modal matrix $\boldsymbol{U}$ can be shown using the Hadamard inequality [68, Sec. 7.8].

Unlike in the previous section, we have not made any assumptions on the noise covariance matrix $\boldsymbol{C_\eta}$. Therefore, this solution is generally valid no matter whether we are facing maximum-entropy noise or reduced-entropy noise.

4.3.1 Maximum-Entropy Noise

As a plausibility check, we can plug in the assumption of maximum-entropy noise into the solution for $\boldsymbol{C_x}$ from above. Due to Theorem 4.2.1, the resulting $\boldsymbol{C_x}$ must then correspond to maximum-entropy transmission. This can be verified as follows.

If $\boldsymbol{C_\eta} \in \mathcal{P}_\mathrm{D}$, we have $\boldsymbol{C_\eta}^{-1} \in \mathcal{P}_\mathrm{D}$ by Corollary 2.4.2 and $\boldsymbol{P} = \boldsymbol{H}^\mathrm{H}\boldsymbol{C_\eta}^{-1}\boldsymbol{H} \in \mathcal{P}_\mathrm{S}$ by Proposition 2.7.1. For any given value of ω, (4.10) describes a mapping $\boldsymbol{P} \mapsto \boldsymbol{C_x}$ with a structure as in Theorem 2.4.1 with f defined in (4.11). Thus, $\boldsymbol{C_x} \in \mathcal{P}_\mathrm{S}$.

Note that we have used other properties of power shaping spaces than in the proof of Theorem 4.2.1, i.e., we have found an alternative way of showing the statement of Theorem 4.2.1 for the special case of a sum power constraint.

4.3.2 Reduced-Entropy Noise

If the noise covariance matrix does not lie in a power shaping space fulfilling the compatibility assumption, the conclusion that the optimal transmit signal should be a maximum-entropy signal is not possible. In the following, we see that the optimal transmit signal is then a reduced-entropy signal in general.

As in the proof of Theorem 4.2.1, the aim is still to maximize the entropy of $\boldsymbol{y}$, i.e., it would still be desirable to choose $\boldsymbol{C_x}$ such that $\boldsymbol{N_y} = \boldsymbol{0}$. However, due to the assumption of reduced-entropy noise, we have $\boldsymbol{N_\eta} \neq \boldsymbol{0}$ in (4.6), which changes the situation significantly.

To make $\boldsymbol{N_y}$ vanish, we would have to choose $\boldsymbol{N_x}$ such that $\boldsymbol{H}\boldsymbol{N_x}\boldsymbol{H}^\mathrm{H} = -\boldsymbol{N_\eta}$, but this is not always possible. On the one hand, the range space of $\boldsymbol{H}$ might be a strict subspace of $\mathbb{C}^M$ (or $\mathbb{R}^M$ for a real-valued system). In this case, it can happen that the equation does not have a solution. On the other hand, when choosing $\boldsymbol{N_x} \neq \boldsymbol{0}$, the positive-semidefiniteness constraint $\boldsymbol{C_x} = \boldsymbol{P_x} + \boldsymbol{N_x} \succeq \boldsymbol{0}$ introduces a coupling between $\boldsymbol{P_x}$ and $\boldsymbol{N_x}$, so that focusing solely on achieving $\boldsymbol{N_y} = \boldsymbol{0}$ might no longer be the best strategy. It can even be impossible to find a feasible combination of $\boldsymbol{P_x}$ and $\boldsymbol{N_x}$ that makes $\boldsymbol{N_y}$ vanish, even though the covariance constraint $\boldsymbol{C_x} \in \mathcal{Q}$ does not act on $\boldsymbol{N_x}$ directly. To get a better intuition about this, let us consider the following minimal example.

Example 4.3.1. *Let $\mathcal{P}_\mathrm{S} = \mathcal{P}_\mathrm{D} = \{\boldsymbol{P} \mid \boldsymbol{P} = \alpha\mathbf{I}_2,\ \alpha \in \mathbb{R}\}$, and consider the RoP MIMO channel with channel matrix $\boldsymbol{H} = \mathbf{I}_2$ and reduced-entropy noise with covariance matrix*

$$\boldsymbol{C_\eta} = \begin{bmatrix} 3 & 0 \\ 0 & 1 \end{bmatrix} = \underbrace{\begin{bmatrix} 2 & 0 \\ 0 & 2 \end{bmatrix}}_{\boldsymbol{P_\eta}} + \underbrace{\begin{bmatrix} 1 & 0 \\ 0 & -1 \end{bmatrix}}_{\boldsymbol{N_\eta}}. \tag{4.12}$$

Let us assume a power constraint $\mathrm{tr}[\boldsymbol{C_x}] \leq 1$, which is equivalent to $\mathrm{tr}[\boldsymbol{P_x}] \leq 1$ since $\mathrm{tr}[\boldsymbol{N_x}] = 0$ for all $\boldsymbol{N_x} \in \mathcal{N}_\mathrm{S}$ (Proposition 2.4.1). To make $\boldsymbol{N_y}$ vanish, we would need

$\boldsymbol{N_x} = -\boldsymbol{N_\eta}$, which would require $\boldsymbol{P_x} \succeq \mathbf{I}_2$ in order to fulfill the positive-semidefiniteness constraint $\boldsymbol{P_x} + \boldsymbol{N_x} \succeq \mathbf{0}$ (since $\boldsymbol{P_x}$ is a scaled identity and must fulfill $\boldsymbol{P_x} \succeq -\boldsymbol{N_x}$). However, this is not possible due to the power constraint. The best that can be done in terms of compensating the reduced-entropy noise is to choose $\boldsymbol{N_x} = -\frac{1}{2}\boldsymbol{N_\eta}$ and $\boldsymbol{P_x} = \frac{1}{2}\mathbf{I}_2$. It can be verified using (4.10) *that this best-effort approach is indeed the optimal transmit strategy in the considered scenario. If the power constraint is relaxed to $\mathrm{tr}[\boldsymbol{C_x}] \leq 2$, the optimal solution is $\boldsymbol{N_x} = -\boldsymbol{N_\eta}$ and $\boldsymbol{P_x} = \mathbf{I}_2$, and we obtain $\boldsymbol{N_y} = \mathbf{0}$.*

If the system is larger or if we consider more general channel matrices and more complicated power shaping spaces, the optimal solution can of course not be identified so easily, but the qualitative result will be the same. The optimal transmit covariance (4.10) will in general have a nonzero entropy reduction component $\boldsymbol{N_x}$ that is chosen in a way that it compensates the entropy reduction component $\boldsymbol{N_\eta}$ of the noise covariance matrix at least partially.

4.4 Worst-Case Noise

It is well known that Gaussian noise is the worst-case noise in a single-antenna point-to-point channel with additive noise (see, e.g., [103], [62, Prob. 9.21]). In [66, 67], this result was extended to more general wireless networks, and it was remarked in [67] that the results can be easily transferred to MIMO systems. The intuition behind these results is that the worst possible disturbance (with fixed second-order properties) is the one which has the highest entropy, i.e., the Gaussian distribution.

It therefore is to be expected that the worst possible noise among all Gaussian noise distributions, i.e., the one with the worst-case choice of the second-order properties, has to be a maximum-entropy signal in the sense of Definition 2.5.1. Even though this seems to be intuitively clear, we have to be aware that (4.2) is a difference of two differential entropies that both get smaller if the entropy of the noise is reduced. For a formal proof, we have to study which of the two terms is affected more strongly.

We still consider the RoP MIMO channel (4.1), i.e., we assume the noise to be proper in case of a complex MIMO channel. Later on, we will present a result stating that proper noise is the worst-case when compared to improper noise (see Corollary 4.5.5), but at the current point, the noise is proper Gaussian by assumption, and we are only interested in the worst-case noise covariance matrix. For the real-valued MIMO channel, the real-valued Gaussian distribution is known to be the worst-case noise distribution (see above), and we ask for the worst-case noise covariance matrix as well.

We are interested in two types of worst-case noise optimization. In the first one, we assume the transmit covariance matrix to be fixed and ask for the noise covariance matrix that minimizes the achievable rate, i.e., we need to solve

$$\min_{\boldsymbol{C_\eta} \succeq \mathbf{0}} \; r \quad \text{s.t.} \qquad \boldsymbol{C_\eta} \in \mathcal{Q}_{\text{noise}} \tag{4.13}$$

with r from (4.4) for a fixed $\boldsymbol{C_x} \in \mathcal{Q}$. As a second question, we ask for the worst-case noise in the case that the transmit strategy is adapted to the noise properties in an optimal manner, i.e.,

$$\min_{\boldsymbol{C_\eta} \succeq \mathbf{0}} \max_{\boldsymbol{C_x} \succeq \mathbf{0}} \; r \quad \text{s.t.} \quad \boldsymbol{C_x} \in \mathcal{Q} \quad \text{and} \quad \boldsymbol{C_\eta} \in \mathcal{Q}_{\text{noise}}. \tag{4.14}$$

In both formulations, $\mathcal{Q}_{\text{noise}}$ is a convex set of Hermitian matrices such that we obtain a compact constraint set with nonempty interior if we in addition demand that $\boldsymbol{C}_{\boldsymbol{\eta}} \succeq \mathbf{0}$.

Unlike previous publications, such as [86, 104–106], we are not interested in solving worst-case noise optimizations for particular choices of the constraint sets and the channel matrices. Instead, we aim at deriving structural properties of the worst-case noise in terms of the concept of power shaping spaces. The result is stated in the following worst-case noise theorem, whose proof uses similar arguments as [28], but in a more general framework.

Theorem 4.4.1. *Let $\mathcal{P}_{\text{S}}$ and $\mathcal{P}_{\text{D}}$ be power shaping spaces fulfilling the compatibility assumption (Definition 3.1.3), and let the constraint $\boldsymbol{C}_{\boldsymbol{\eta}} \in \mathcal{Q}_{\text{noise}}$ be compatible with $\mathcal{P}_{\text{D}}$ (in the sense of Definition 3.1.2). If $\boldsymbol{x}$ is an arbitrary maximum-entropy signal with respect to $\mathcal{P}_{\text{S}}$,* (4.13) *is minimized by maximum-entropy noise with respect to $\mathcal{P}_{\text{D}}$.*

Proof. Let $\boldsymbol{P}_{\varepsilon} = \boldsymbol{H}\boldsymbol{C}_{\boldsymbol{x}}\boldsymbol{H}^{\text{H}} + \varepsilon\mathbf{I}_M$. Using the compatibility assumption, we have $\boldsymbol{P}_{\varepsilon} \in \mathcal{P}_{\text{D}}$ since $\boldsymbol{C}_{\boldsymbol{x}} \in \mathcal{P}_{\text{S}}$ and since $\mathbf{I}_M \in \mathcal{P}_{\text{D}}$. As determinant and logarithm are continuous functions, we can calculate the achievable rate from $r(\boldsymbol{C}_{\boldsymbol{\eta}}) = \lim_{\varepsilon\to 0}\ r_{\varepsilon}(\boldsymbol{C}_{\boldsymbol{\eta}})$ with

$$r_{\varepsilon}(\boldsymbol{C}_{\boldsymbol{\eta}}) = \mu \log_2 \frac{\det\left(\boldsymbol{P}_{\varepsilon} + \boldsymbol{C}_{\boldsymbol{\eta}}\right)}{\det \boldsymbol{C}_{\boldsymbol{\eta}}} = \mu \log_2 \frac{\det\left(\mathbf{I}_M + \boldsymbol{C}_{\boldsymbol{\eta}_{\varepsilon}}\right)}{\det \boldsymbol{C}_{\boldsymbol{\eta}_{\varepsilon}}} \tag{4.15}$$

where $\boldsymbol{C}_{\boldsymbol{\eta}_{\varepsilon}} = \boldsymbol{P}_{\varepsilon}^{-\frac{1}{2}}\boldsymbol{C}_{\boldsymbol{\eta}}\boldsymbol{P}_{\varepsilon}^{-\frac{1}{2}}$ with the positive-semidefinite square root $\boldsymbol{P}_{\varepsilon}^{\frac{1}{2}} \succeq \mathbf{0}$. Due to Corollaries 2.4.1 and 2.4.2, we have $\boldsymbol{P}_{\varepsilon}^{-\frac{1}{2}} \in \mathcal{P}_{\text{D}}$, and

$$\boldsymbol{C}_{\boldsymbol{\eta}_{\varepsilon}} = \underbrace{\boldsymbol{P}_{\varepsilon}^{-\frac{1}{2}}\boldsymbol{P}_{\boldsymbol{\eta}}\boldsymbol{P}_{\varepsilon}^{-\frac{1}{2}}}_{=\boldsymbol{P}_{\boldsymbol{\eta}_{\varepsilon}} \in \mathcal{P}_{\text{D}}} + \underbrace{\boldsymbol{P}_{\varepsilon}^{-\frac{1}{2}}\boldsymbol{N}_{\boldsymbol{\eta}}\boldsymbol{P}_{\varepsilon}^{-\frac{1}{2}}}_{=\boldsymbol{N}_{\boldsymbol{\eta}_{\varepsilon}} \in \mathcal{N}_{\text{D}}} \tag{4.16}$$

where $\boldsymbol{P}_{\boldsymbol{\eta}} = \text{proj}_{\mathcal{P}_{\text{D}}}(\boldsymbol{C}_{\boldsymbol{\eta}})$ and $\boldsymbol{N}_{\boldsymbol{\eta}} = \text{proj}_{\mathcal{N}_{\text{D}}}(\boldsymbol{C}_{\boldsymbol{\eta}})$. For any $\boldsymbol{P}_{\boldsymbol{\eta}} \in \mathcal{P}_{\text{D}}$, $\boldsymbol{N}_{\boldsymbol{\eta}} \in \mathcal{N}_{\text{D}}$, it thus holds that

$$\begin{aligned} r_{\varepsilon}(\boldsymbol{P}_{\boldsymbol{\eta}} + \boldsymbol{N}_{\boldsymbol{\eta}}) &= \mu \log_2 \det\left(\mathbf{I}_M + (\boldsymbol{P}_{\boldsymbol{\eta}_{\varepsilon}} + \boldsymbol{N}_{\boldsymbol{\eta}_{\varepsilon}})^{-1}\right) \\ &\geq \mu \log_2 \det\left(\mathbf{I}_M + \boldsymbol{P}_{\boldsymbol{\eta}_{\varepsilon}}^{-1}\right) = r_{\varepsilon}(\boldsymbol{P}_{\boldsymbol{\eta}}). \end{aligned} \tag{4.17}$$

where the inequality is due to Proposition 2.5.2. Since this inequality holds for arbitrary $\varepsilon > 0$, we have

$$r(\boldsymbol{P}_{\boldsymbol{\eta}} + \boldsymbol{N}_{\boldsymbol{\eta}}) = \lim_{\varepsilon\to 0}\ r_{\varepsilon}(\boldsymbol{P}_{\boldsymbol{\eta}} + \boldsymbol{N}_{\boldsymbol{\eta}}) \geq \lim_{\varepsilon\to 0}\ r_{\varepsilon}(\boldsymbol{P}_{\boldsymbol{\eta}}) = r(\boldsymbol{P}_{\boldsymbol{\eta}}). \tag{4.18}$$

As this is true for any $\boldsymbol{P}_{\boldsymbol{\eta}} \in \mathcal{P}_{\text{D}}$, there is a solution of (4.13) with $\boldsymbol{N}_{\boldsymbol{\eta}} = \mathbf{0}$. □

The formulation of the theorem includes, amongst others, a worst-case noise optimization with limited total noise power, i.e., $\mathcal{Q}_{\text{noise}} = \{\boldsymbol{C} \in \mathbb{H}^M \mid \text{tr}[\boldsymbol{C}] \leq Q_{\text{noise}}\} \Leftrightarrow \text{tr}[\boldsymbol{P}_{\boldsymbol{\eta}}] \leq Q_{\text{noise}}$, as well as a worst-case noise optimization with a fixed noise power shaping matrix, i.e., $\mathcal{Q}_{\text{noise}} = \{\boldsymbol{C} \in \mathbb{H}^M \mid \text{proj}_{\mathcal{P}_{\text{D}}}(\boldsymbol{C}) = \boldsymbol{P}\} \Leftrightarrow \boldsymbol{P}_{\boldsymbol{\eta}} = \boldsymbol{P}$ for some given $\boldsymbol{P} \in \mathcal{P}_{\text{D}}$ (with $\mathbb{S}^M$ instead of $\mathbb{H}^M$ in a real-valued system).

Even though the result is not entirely surprising, it is remarkable that the only assumption on the transmit strategy was that a maximum-entropy signal is used. From a technical point of view, this means that reduced-entropy noise brings an advantage even if the transmitter is oblivious of the noise properties and still uses a maximum-entropy transmit signal. Another

interpretation is that designing a maximum-entropy transmit signal based on the assumption of maximum-entropy noise is robust in the sense that the achievable rate is not reduced if the actual noise turns out to be a reduced-entropy signal (with the same power shaping component as assumed).

Let us now turn our attention to the second optimization (4.14), where the transmitter adapts its strategy to the properties of the noise. We can easily extend the worst-case noise theorem to this case.

Corollary 4.4.1. *Let $\mathcal{P}_{\mathrm{S}}$, $\mathcal{P}_{\mathrm{D}}$, and $\mathcal{Q}_{\mathrm{noise}}$ be as in Theorem 4.4.1. Then,* (4.14) *is minimized by maximum-entropy noise with respect to $\mathcal{P}_{\mathrm{D}}$.*

Proof. The optimal transmit strategy for maximum-entropy noise employs a maximum-entropy transmit signal (Theorem 4.2.1). The achievable rate is nondecreasing when replacing the noise by reduced-entropy noise while keeping the transmit strategy unchanged (Theorem 4.4.1). Further, the achievable rate is obviously nondecreasing when optimizing the transmit strategy for the new situation while keeping the reduced-entropy noise unchanged. □

4.5 Complex Multicarrier MIMO Channel

To study the complex multicarrier MIMO channel with transmitter S and receiver D, we introduce the abbreviations $\boldsymbol{y}^{(c)} = \boldsymbol{y}_{\mathrm{D}}^{(c)}$, $\boldsymbol{H}^{(c)} = \boldsymbol{H}_{\mathrm{DS}}^{(c)}$, $\boldsymbol{x}^{(c)} = \boldsymbol{x}_{\mathrm{S}}^{(c)}$, and $\boldsymbol{\eta}^{(c)} = \boldsymbol{\eta}_{\mathrm{D}}^{(c)}$, so that the general model in (3.34) can be written as

$$\boldsymbol{y}^{(c)} = \boldsymbol{H}^{(c)}\boldsymbol{x}^{(c)} + \boldsymbol{\eta}^{(c)}, \quad c = 1, \ldots, C. \tag{4.19}$$

with a constraint on the per-carrier covariance matrices as in (3.38), i.e.,

$$\left(\boldsymbol{C}_{\boldsymbol{x}^{(1)}}, \ldots, \boldsymbol{C}_{\boldsymbol{x}^{(C)}}\right) \in \bar{\mathcal{Q}}. \tag{4.20}$$

Since the combined real representation (3.37) of a complex multicarrier MIMO system fulfills the assumptions for a RoP MIMO system, we can apply the results of the previous sections to the combined real representation of (4.19). To this end, we set $\boldsymbol{H}$ in (4.1) to $\boldsymbol{H} = \grave{\boldsymbol{H}} = \grave{\boldsymbol{H}}_{\mathrm{DS}}$ as defined in (3.37), and we replace $\boldsymbol{x}$, $\boldsymbol{\eta}$, and $\boldsymbol{y}$ by $\check{\boldsymbol{x}}$, $\check{\boldsymbol{\eta}}$, and $\check{\boldsymbol{y}}$, respectively.

4.5.1 Optimality of Maximum-Entropy Transmission

In the literature, we can find several statements about the optimal transmit signal in the complex multicarrier MIMO channel under various assumptions on the statistical properties of the noise. For instance, it was shown in [29] that a proper Gaussian transmit signal is optimal in the complex single-carrier MIMO channel if the noise is proper Gaussian. Another example is that it is accepted as common knowledge (e.g., [40]) that separate transmission on each carrier is optimal in the complex multicarrier MIMO channel as long as the noise is CN. This result can be found, e.g., in [39, Sec. 5.3] for a single-antenna system with proper noise, and can be generalized to the complex multicarrier MIMO channel.

A connection between these two examples might not be obvious at first glance. However, in both of them, the noise is a maximum-entropy signal: in the case of proper noise with respect to the power shaping space $\grave{\mathcal{P}}_{\mathrm{D}}$, and in the case of CN noise with respect to $\mathcal{P}_{\mathrm{D}}^{\mathrm{CN}}$ (see

Proposition 3.4.2). Therefore, both statements can be considered as specializations of the more general result obtained in Theorem 4.2.1.

Using the various power shaping spaces from Definition 3.4.1, we obtain the following corollaries of Theorem 4.2.1. Note that Propositions 3.4.2, 3.4.3, and 3.4.4 can be used to verify that the assumptions of Theorem 4.2.1 are fulfilled.

Corollary 4.5.1 ($\mathcal{P}_{\mathrm{S}} = \grave{\mathcal{P}}_{\mathrm{S}}^{\mathrm{CN}}$ and $\mathcal{P}_{\mathrm{D}} = \grave{\mathcal{P}}_{\mathrm{D}}^{\mathrm{CN}}$)**.** *The capacity of the complex multicarrier MIMO channel* (4.19) *with a covariance constraint* (4.20) *is achieved by a transmit signal that is proper and CN if the noise is proper and CN.*

Theorem 4.2.1 is general enough to cover scenarios in which the noise is a maximum-entropy signal in some respect, but a reduced-entropy signal in another. This includes the following two cases where the noise is either proper or CN, but not both.

Corollary 4.5.2 ($\mathcal{P}_{\mathrm{S}} = \grave{\mathcal{P}}_{\mathrm{S}}$ and $\mathcal{P}_{\mathrm{D}} = \grave{\mathcal{P}}_{\mathrm{D}}$)**.** *The capacity of the complex (multicarrier) MIMO channel* (4.19) *with a covariance constraint* (4.20) *is achieved by a transmit signal that is proper (but possibly CC) if the noise is proper (but possibly CC).*

Corollary 4.5.3 ($\mathcal{P}_{\mathrm{S}} = \mathcal{P}_{\mathrm{S}}^{\mathrm{CN}}$ and $\mathcal{P}_{\mathrm{D}} = \mathcal{P}_{\mathrm{D}}^{\mathrm{CN}}$)**.** *The capacity of the complex multicarrier MIMO channel* (4.19) *with a covariance constraint* (4.20) *is achieved by a transmit signal that is CN (but possibly improper) if the noise is CN (but possibly improper).*

Note that the above results on optimality of CN transmission differ from a statement in [65] about benefits of CC transmission in a MIMO point-to-point system. The difference is that the authors of [65] assumed rate requirements for individual data streams while only the total data rate counts for the formulation in (4.4), i.e., it does not matter how the data can be split into streams. In fact, the formulation used in this chapter does not even make use of the notion of a data stream. We use this notion later on in a different context when studying the MIMO broadcast channel with interference treated as noise (Chapter 7).

4.5.2 Optimal Transmit Covariance Matrix for the Case of Proper CN Noise

The corollaries given above make general statements about the optimal transmit strategy, but they do not deliver an optimal solution in terms of an optimal transmit covariance matrix. To obtain such a solution in the case of a sum power constraint, we could apply (4.10) to the combined real representation of the complex multicarrier MIMO channel. As an alternative, we can exploit the above statements on the optimality of maximum-entropy transmission in order to derive a simplified reformulation, which can be easily extended to some further types of constraints.

We consider the complex multicarrier MIMO channel (4.19) under the assumption that the noise is proper and CN as in Corollary 4.5.1. As we know that the optimal transmit signal is proper and CN, we have $\boldsymbol{C}_{\check{\boldsymbol{x}}} \in \grave{\mathcal{P}}_{\mathrm{S}}^{\mathrm{CN}}$ and $\boldsymbol{C}_{\check{\boldsymbol{\eta}}} \in \grave{\mathcal{P}}_{\mathrm{D}}^{\mathrm{CN}}$, and we can apply Proposition 3.4.5 to rewrite the achievable rate (4.4) with $\mu = \frac{1}{2}$ as

$$\begin{aligned} r &= \log_2 \frac{\det\left(\boldsymbol{C}_{\boldsymbol{\eta}} + \boldsymbol{H}\boldsymbol{C}_{\boldsymbol{x}}\boldsymbol{H}^{\mathrm{H}}\right)}{\det \boldsymbol{C}_{\boldsymbol{\eta}}} = \sum_{c=1}^{C} \log_2 \frac{\det\left(\boldsymbol{C}_{\boldsymbol{\eta}^{(c)}} + \boldsymbol{H}^{(c)}\boldsymbol{C}_{\boldsymbol{x}^{(c)}}\boldsymbol{H}^{(c),\mathrm{H}}\right)}{\det \boldsymbol{C}_{\boldsymbol{\eta}^{(c)}}} \\ &= \sum_{c=1}^{C} \log_2 \det\left(\mathbf{I}_{m_{\mathrm{S}}} + \boldsymbol{H}^{(c),\mathrm{H}}\boldsymbol{C}_{\boldsymbol{\eta}^{(c)}}^{-1}\boldsymbol{H}^{(c)}\boldsymbol{C}_{\boldsymbol{x}^{(c)}}\right) = \sum_{c=1}^{C} r^{(c)} \end{aligned} \tag{4.21}$$

where we have used (4.8) in the second line. Obviously, we can express the total achievable rate as a sum of per-carrier rates $r^{(c)}$, which are calculated using the differential entropy of the proper complex Gaussian distribution (2.7) with $\mu = 1$. This complies to the observation that we obtain a RoP CN MIMO system if the transmit signal and the noise are proper and CN (see Section 3.4.1). What remains to be done is to find optimal complex per-carrier covariance matrices $\boldsymbol{C}_{\boldsymbol{x}^{(c)}}$ under various types of constraints.

Let us first consider per-carrier power constraints (3.40). In this case, the various carriers are not coupled by the constraint, and we can apply the solution for the RoP MIMO channel (4.9)–(4.11) individually on each carrier, i.e., we compute the eigenvalue decomposition

$$\boldsymbol{U}^{(c)} \operatorname{diag}(\lambda_i^{(c)}) \boldsymbol{U}^{(c),\mathrm{H}} = \boldsymbol{H}^{(c),\mathrm{H}} \boldsymbol{C}_{\boldsymbol{\eta}^{(c)}}^{-1} \boldsymbol{H}^{(c)} \tag{4.22}$$

and we set

$$\boldsymbol{C}_{\boldsymbol{x}^{(c)}} = \boldsymbol{U}^{(c)} \operatorname{diag}(p_i^{(c)}) \boldsymbol{U}^{(c),\mathrm{H}} \tag{4.23}$$

where

$$p_i^{(c)} = \max\left\{ \omega^{(c)} - \frac{1}{\lambda_i^{(c)}},\, 0 \right\}. \tag{4.24}$$

For the sum power constraint (3.39), we can keep the modal matrix $\boldsymbol{U}^{(c)}$ in (4.23), but we have to optimize the powers $p_i^{(c)}$ jointly over all carriers. To do so, we replace $\omega^{(c)}$ in (4.24) by a common water level ω, which we choose such that the sum power constraint (3.39) is fulfilled with equality.

Finally, if we assume per-carrier shaping constraints (3.41), we can use that $\boldsymbol{H}^{(c)} \boldsymbol{X} \boldsymbol{H}^{(c),\mathrm{H}} \succeq \boldsymbol{H}^{(c)} \boldsymbol{X}' \boldsymbol{H}^{(c),\mathrm{H}}$ for $\boldsymbol{X} \succeq \boldsymbol{X}'$ and that $\det \boldsymbol{X}$ is nondecreasing in $\boldsymbol{X} \succeq \boldsymbol{0}$ [68, Sec. 7.7]. Thus, $r^{(c)}$ is nondecreasing in $\boldsymbol{C}_{\boldsymbol{x}^{(c)}}$, and the optimal solution is $\boldsymbol{C}_{\boldsymbol{x}^{(c)}} = \boldsymbol{Q}^{(c)}\ \forall c$, i.e., the shaping constraints are active.

Especially for per-carrier power constraints or per-carrier shaping constraints, solving the problem via the combined real representation would be more effort than the above derivations based on the corollaries from Section 4.5.1.

4.5.3 Optimal Transmit Covariance Matrix for the Case of Improper or CC Noise

The situation is different if the noise is improper (as considered, e.g., in [7, 36] for the MIMO channel and in [107] for the continuous-time SISO channel) or CC or both. As Corollary 4.5.1 is no longer applicable in that case, the optimal transmit signal is a reduced-entropy signal in general. More precisely, the type of entropy reduction that we need for the optimal transmit signal is the same as the type of entropy reduction of the noise. That is, improper noise can require improper signaling, CC noise can require CC transmission, and noise that is both improper and CC can require a transmit signal that is both improper and CC.

In all these cases, at least one of the equalities in (4.21) is no longer valid. When using the complex multicarrier model, it would thus be necessary to derive a solution that accounts for the impropriety and/or the correlations between carriers when evaluating the mutual information $\mathrm{I}\left((\boldsymbol{x}^{(1)}, \ldots, \boldsymbol{x}^{(C)}); (\boldsymbol{y}^{(1)}, \ldots, \boldsymbol{y}^{(C)})\right)$.

It seems to be much simpler to instead perform the optimization directly in the combined real representation in the form given in (4.5). As pointed out in Section 4.3, the solution can be

computed by a convex programming solver, and it can be obtained analytically from (4.10) in case of a sum power constraint. This approach was pursued, e.g., in [7, 36].

To get a better intuition about the optimal transmit strategy in case of improper noise, we reconsider the minimal example from Section 4.3.2.

Example 4.5.1. *Consider a complex single-carrier single-antenna channel, i.e., $C = m_{\mathrm{S}} = m_{\mathrm{D}} = 1$, with the channel $h = 1$, and improper noise with variance $C_{\eta} = 4$ and pseudovariance $\tilde{C}_{\eta} = 2$. The combined real representation of this system corresponds exactly to the RoP MIMO channel considered in Example 4.3.1. We can identify the power shaping spaces considered therein as $\mathcal{P}_{\mathrm{S}} = \grave{\mathcal{P}}_{\mathrm{S}}$ and $\mathcal{P}_{\mathrm{D}} = \grave{\mathcal{P}}_{\mathrm{D}}$ since any 2×2 symmetric $\mathcal{BSC}_2$ matrix is a scaled identity. The results obtained in Example 4.3.1 translate to $\tilde{C}_x = -\frac{1}{2}\tilde{C}_{\eta} = -1$ (obtained from $\boldsymbol{N}_{\boldsymbol{x}} = -\frac{1}{2}\boldsymbol{N}_{\boldsymbol{\eta}}$ for the constraint $\mathrm{tr}[\boldsymbol{C}_{\check{\boldsymbol{x}}}] \leq 1 \Leftrightarrow C_x \leq 1$) and $\tilde{C}_x = -\tilde{C}_{\eta} = -2$ (from $\boldsymbol{N}_{\boldsymbol{x}} = -\boldsymbol{N}_{\boldsymbol{\eta}}$ for $\mathrm{tr}[\boldsymbol{C}_{\check{\boldsymbol{x}}}] \leq 2 \Leftrightarrow C_x \leq 2$). By parameterizing the pseudovariance as $\tilde{C}_x = |\tilde{C}_x| \mathrm{e}^{\mathrm{j}\varphi}$, these results can be interpreted as follows. In the considered scenario, the impropriety of the intended signal should try to compensate the impropriety of the noise in the following sense. The direction of impropriety of the intended signal (parametrized by φ) should be the exact opposite of the direction of impropriety of the noise, and the strength of impropriety of the intended signal (parametrized by $|\tilde{C}_x|$) should be the same as the strength of impropriety of the noise as long as this does not violate the constraints.*

4.5.4 Scenarios that Violate the Compatibility Assumption

It shall be noted that there are situations that lead to a reduced-entropy signal as optimal input even if we have maximum-entropy noise. This can happen if the compatibility assumption from Definition 3.1.3 is violated for the power shaping spaces of interest, so that Theorem 4.2.1 is no longer applicable.

An important part of the compatibility assumption is that the channel matrix has to be compatible with the power shaping spaces $(\mathcal{P}_{\mathrm{D}}, \mathcal{P}_{\mathrm{S}})$. For the study of proper signaling, i.e., for the power shaping spaces $(\grave{\mathcal{P}}_{\mathrm{D}}, \grave{\mathcal{P}}_{\mathrm{S}})$, this assumption is violated if the original complex channel is widely linear (Definition 2.9.5) instead of linear, so that its real-valued representation (2.38) is no longer a $\mathcal{BSC}_2$ matrix. In particular, this is the case if I/Q imbalance occurs (e.g., [108, 109]) and is modeled as part of the channel (cf., e.g., [110] and the references therein). In a similar manner, if the assumption of orthogonal carriers is not fulfilled, the combined real channel matrix no longer consists of block-diagonal submatrices and is no longer compatible with $(\mathcal{P}_{\mathrm{D}}^{\mathrm{CN}}, \mathcal{P}_{\mathrm{S}}^{\mathrm{CN}})$, i.e., with the power shaping spaces that we use to study CN transmission.

We do not consider such scenarios in detail, but the solution that we obtain when applying (4.10) to the combined real representation is general enough to cover these cases as well. By plugging in a combined real channel matrix that is not compatible with $(\mathcal{P}_{\mathrm{D}}, \mathcal{P}_{\mathrm{S}})$, we obtain a solution $\boldsymbol{C}_{\check{\boldsymbol{x}}}$ that can have a nonzero entropy reduction component $\mathrm{proj}_{\mathcal{N}_{\mathrm{S}}}(\boldsymbol{C}_{\check{\boldsymbol{x}}})$ even in the case of maximum-entropy noise with $\boldsymbol{C}_{\check{\boldsymbol{\eta}}} \in \mathcal{P}_{\mathrm{D}}$.

The second part of the compatibility assumption requires that the constraint $\boldsymbol{C}_{\check{\boldsymbol{x}}} \in \mathcal{Q}$ acts only on the power shaping component $\mathrm{proj}_{\mathcal{P}_{\mathrm{S}}}(\boldsymbol{C}_{\check{\boldsymbol{x}}})$ of the transmit covariance matrix. If this is violated, we can again obtain a reduced-entropy transmit signal as optimal solution even in the case of a compatible combined real channel matrix and maximum-entropy noise. However, we do not further discuss this case since the assumption is fulfilled by the most common transmit

covariance constraints (see Section 3.4.2 and Proposition 3.4.4).

The aspects discussed above apply in a similar manner to the multiuser systems treated in the following chapters, but they will not be considered in detail any further.

4.5.5 Worst-Case Noise

By applying Theorem 4.4.1 and Corollary 4.4.1 to the combined real representation, we can obtain several specialized worst-case noise results for the complex multicarrier MIMO channel. In all three corollaries, the term *optimized* has to be understood as a rate maximization under a transmit covariance constraint (4.20). The various power shaping spaces from Proposition 3.4.2 that we use in the corollaries allow for different kinds of constraints on the statistical properties of the noise.

Corollary 4.5.4 ($\mathcal{P}_{\mathrm{S}} = \grave{\mathcal{P}}_{\mathrm{S}}^{\mathrm{CN}}$ and $\mathcal{P}_{\mathrm{D}} = \grave{\mathcal{P}}_{\mathrm{D}}^{\mathrm{CN}}$)**.** *In the complex multicarrier MIMO channel* (4.19) *with constraints on the complex per-carrier noise covariance matrices, the worst-case noise is proper and CN if the transmit signal is either fixed to be proper and CN or optimized based on the noise properties.*

Corollary 4.5.5 ($\mathcal{P}_{\mathrm{S}} = \grave{\mathcal{P}}_{\mathrm{S}}$ and $\mathcal{P}_{\mathrm{D}} = \grave{\mathcal{P}}_{\mathrm{D}}$)**.** *In the complex (multicarrier) MIMO channel* (4.19) *with constraints on the combined complex noise covariance matrix, the worst-case noise is proper if the transmit signal is either fixed to be proper or optimized based on the noise properties.*

Corollary 4.5.6 ($\mathcal{P}_{\mathrm{S}} = \mathcal{P}_{\mathrm{S}}^{\mathrm{CN}}$ and $\mathcal{P}_{\mathrm{D}} = \mathcal{P}_{\mathrm{D}}^{\mathrm{CN}}$)**.** *In the complex multicarrier MIMO channel* (4.19) *with constraints on the per-carrier noise properties, the worst-case noise is CN if the transmit signal is either fixed to be CN or optimized based on the noise properties.*

A theorem stating that proper noise is the worst-case noise was shown in [36] under the assumption that the transmit covariance matrix is either chosen optimally or at least with optimal modal matrix and a uniform power allocation. This result was generalized in [28] by showing that it holds even if the transmitter does not adapt its signal to the potential impropriety of the noise. Moreover, some restrictive assumptions that were made in [36] (e.g., on the rank of the channels) can be avoided by means of the proof technique used in [28] and for Theorem 4.4.1. The result from [28], which includes the one from [36] as a special case, corresponds to Corollary 4.5.5, i.e., it can be considerd as a corollary of the more general Theorem 4.4.1. Note that this result holds under arbitrary constraints on the combined complex noise covariance matrix $\boldsymbol{C}_{\boldsymbol{\eta}}$, including a limited total noise power and the case of a fixed $\boldsymbol{C}_{\boldsymbol{\eta}}$ (see discussion below Theorem 4.4.1).

Chapter 5

The Gaussian MIMO Multiple Access Channel

From now on, we turn our attention to systems with multiple users that are served in the same spectrum, so that inter-user interference occurs. The first example we consider is a MIMO uplink scenario, where K user terminals U_k transmit independent signals $\boldsymbol{x}_{\mathrm{U}_k}$ to a base station B (see Figure 5.1). In the information theoretic literature, this scenario is referred to as a (Gaussian) MIMO multiple access channel (MIMO MAC, e.g., [46]) or Gaussian vector MAC (e.g., [57]).

Even though inter-user interference is present in this scenario, the MIMO MAC turns out to behave in many regards similar to an interference-free single-user MIMO channel as long as we eliminate part of the interference by means of coding. This can be done either by a joint decoding of all received signals or by a successive interference cancellation scheme (see Section 5.1.1). If we instead treat all interference as noise, we obtain a different situation, which is described at a later point in Section 7.2.

Just like in Chapter 4, we first consider a RoP MIMO system, for which we show that maximum-entropy transmission is optimal in case of maximum-entropy noise. The obtained result can then be used to study the complex multicarrier MIMO MAC afterwards, and it also forms the basis for our later derivations on the MIMO broadcast channel in Chapter 6 and on the MIMO relay channel in Chapter 9. In addition to the theoretical findings, we review several numerical algorithms from the existing literature and discuss how they can be applied in the cases of maximum-entropy noise and reduced-entropy noise.

5.1 System Model and Capacity Region

We introduce the abbreviations $\boldsymbol{y} = \boldsymbol{y}_{\mathrm{B}}$, $\boldsymbol{H}_k = \boldsymbol{H}_{\mathrm{BU}_k}$, $\boldsymbol{x}_k = \boldsymbol{x}_{\mathrm{U}_k}$, and $\boldsymbol{\eta} = \boldsymbol{\eta}_{\mathrm{B}}$. From the general model in (3.1), we obtain the description of the RoP MIMO MAC as

$$\boldsymbol{y} = \sum_{k=1}^{K} \boldsymbol{H}_k \boldsymbol{x}_k + \boldsymbol{\eta}. \tag{5.1}$$

As we have multiple data rates of interest, namely the achievable rates ρ_k of all users k, we

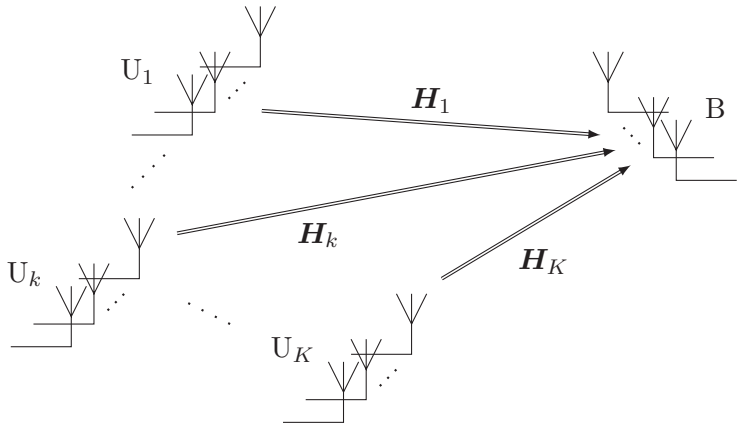

Figure 5.1: Illustration of the MIMO multiple access channel.

consider a rate region as introduced in Section 3.2. The following derivation can be obtained by applying a result for general memoryless multiple access channels (from [58, 111] as cited in [48]) to the RoP MIMO MAC. Instead of focusing on power constraints $\mathrm{tr}[\boldsymbol{C}_{\boldsymbol{x}_k}] \leq Q_k,\ \forall k$ as, e.g., in [57, 112, 113], we consider general covariance constraints of the form (3.3).

By decoding the signals of all users jointly, the rates $\boldsymbol{\rho} = [\rho_1, \ldots, \rho_K]^{\mathrm{T}}$ are achievable if $\sum_{k\in\mathcal{K}} \rho_k$ for any group of users $\mathcal{K} \subseteq \{1, \ldots, K\}$ fulfills [48]

$$\sum_{k\in\mathcal{K}} \rho_k \leq \mathrm{I}\left(\{\boldsymbol{x}_k\}_{k\in\mathcal{K}}; \boldsymbol{y} \,|\, (\boldsymbol{x}_k)_{k\notin\mathcal{K}}\right) = \mathrm{h}\left(\boldsymbol{y}_{\mathcal{K}}\right) - \mathrm{h}\left(\boldsymbol{y}_{\mathcal{K}} \,|\, \{\boldsymbol{x}_k\}_{k\in\mathcal{K}}\right) = \mathrm{h}\left(\boldsymbol{y}_{\mathcal{K}}\right) - \mathrm{h}\left(\boldsymbol{\eta}\right) \quad (5.2)$$

where

$$\boldsymbol{y}_{\mathcal{K}} = \sum_{k\in\mathcal{K}} \boldsymbol{H}_k \boldsymbol{x}_k + \boldsymbol{\eta}. \quad (5.3)$$

Note that $\mathrm{h}\left(\boldsymbol{\eta}\right)$ in (5.2) does not depend on the transmit strategy, and assume some fixed $(\boldsymbol{C}_{\boldsymbol{x}_k})_{\forall k}$ so that

$$\boldsymbol{C}_{\boldsymbol{y}_{\mathcal{K}}} = \boldsymbol{C}_{\boldsymbol{\eta}} + \sum_{k\in\mathcal{K}} \boldsymbol{H}_k \boldsymbol{C}_{\boldsymbol{x}_k} \boldsymbol{H}_k^{\mathrm{H}}. \quad (5.4)$$

is fixed. Then, $\mathrm{h}\left(\boldsymbol{y}_{\mathcal{K}}\right)$ is maximized if $\boldsymbol{y}_{\mathcal{K}}$ follows a Gaussian distribution (see [59, 62] for a real-valued system and [29, 63] for a complex system). As the noise $\boldsymbol{\eta}$ is assumed to be Gaussian, and as $\boldsymbol{\eta}, \boldsymbol{x}_1, \ldots, \boldsymbol{x}_K$ are independent, we can make all $\boldsymbol{y}_{\mathcal{K}}$ Gaussian by choosing all $\boldsymbol{x}_k$ to be Gaussian. The constraints on the transmit strategy affect only $(\boldsymbol{C}_{\boldsymbol{x}_k})_{\forall k}$, and the above reasoning holds for any $(\boldsymbol{C}_{\boldsymbol{x}_k})_{\forall k}$. Thus, Gaussian transmit signals are optimal for all inequalities in (5.2). For a complex setting, note that Remark 4.1.1 applies accordingly to the current chapter.

As the optimal transmit signals are Gaussian, we can plug in the differential entropy from (2.7) to obtain the rate region

$$\mathcal{R} = \bigcup_{\substack{(\boldsymbol{C}_{\boldsymbol{x}_k} \succeq \boldsymbol{0})_{\forall k} \\ (\boldsymbol{C}_{\boldsymbol{x}_k})_{\forall k} \in \mathcal{Q}}} \left\{ \boldsymbol{\rho} \in \mathbb{R}_{0,+}^{K} \;\middle|\; \sum_{k\in\mathcal{K}} \rho_k \leq \mu \log_2 \frac{\det \boldsymbol{C}_{\boldsymbol{y}_{\mathcal{K}}}}{\det \boldsymbol{C}_{\boldsymbol{\eta}}},\ \ \forall \mathcal{K} \subseteq \{1, \ldots, K\} \right\} \quad (5.5)$$

where the constraint set $\mathcal{Q}$ is defined as in (3.3).

As pointed out in [57], this rate region is convex, i.e., it cannot be enlarged by taking its convex hull, meaning that RTS does not bring any gains. To see that this is true and that more flexible TS does not help either, we express the rate region in (5.5) by means of (3.11) using

$$\mathcal{O} = \left\{ \left(\boldsymbol{\rho}, (\boldsymbol{C}_{\boldsymbol{x}_k})_{\forall k}\right) \;\middle|\; (\boldsymbol{C}_{\boldsymbol{x}_k} \succeq \mathbf{0})_{\forall k} \;\text{ and } \right. \\ \left. 0 \leq \sum_{k\in\mathcal{K}} \rho_k \leq \mu \log_2 \frac{\det \boldsymbol{C}_{\boldsymbol{y}_\mathcal{K}}}{\det \boldsymbol{C}_{\boldsymbol{\eta}}},\;\; \forall \mathcal{K} \subseteq \{1,\ldots,K\} \right\}. \quad (5.6)$$

As the expressions on the right hand side of the rate inequalities are concave functions of $(\boldsymbol{C}_{\boldsymbol{x}_k})_{\forall k}$, the set $\mathcal{O}$ is convex and cannot be enlarged by taking its convex hull. As the constraint set $\mathcal{Q}$ is convex, this implies that $\overline{\overline{\mathcal{R}}} = \overline{\mathcal{R}} = \mathcal{R}$ (see Section 3.2.1).

An alternative proof of $\overline{\overline{\mathcal{R}}} = \overline{\mathcal{R}}$ can be obtained, e.g., for the case of a sum power constraint (3.4) by showing that the solution of the rate balancing problem (3.13) in the RoP MIMO MAC is a concave function of the available sum transmit power Q (see [17, Prop. 1]). This can be extended to other constraints, e.g., to a sum shaping constraint by following the lines of [114, Th. 1].

As Gaussian transmit signals are optimal and (R)TS is not necessary, the rate region given in (5.4) is the capacity region of the RoP MIMO MAC, i.e., $\mathcal{C} = \mathcal{R}$.

5.1.1 Successive Interference Cancellation

As an alternative to decoding the signals of all users jointly, we can adopt the following successive interference cancellation (SIC) strategy (see, e.g., [112, 113, 115]). Let $\pi : k \mapsto \pi(k)$ be a permutation of the user indices $k \in \{1,\ldots,K\}$, which determines the so-called decoding order. When decoding the signal of the first user $k : \pi(k) = 1$, all other signals $\boldsymbol{x}_j$, $j \neq k$ are treated as additional noise. Afterwards, the signal $\boldsymbol{x}_k$ is known to the receiver, and the signal portion $\boldsymbol{H}_k\boldsymbol{x}_k$ can be subtracted from $\boldsymbol{y}$, so that it no longer acts as interference when decoding the signal of user $k' : \pi(k') = 2$. By continuing this scheme until all users are decoded, we can achieve the per-user rates

$$r_k = \mu \log_2 \frac{\det \boldsymbol{C}_{\boldsymbol{v}_k}}{\det \boldsymbol{C}_{\boldsymbol{\zeta}_k}} \quad (5.7)$$

in analogy to (3.2), where

$$\boldsymbol{C}_{\boldsymbol{v}_k} = \boldsymbol{C}_{\boldsymbol{\eta}} + \sum_{j:\pi(j)\geq\pi(k)} \boldsymbol{H}_j \boldsymbol{C}_{\boldsymbol{x}_j} \boldsymbol{H}_j^{\mathrm{H}} \qquad \text{and} \qquad \boldsymbol{C}_{\boldsymbol{\zeta}_k} = \boldsymbol{C}_{\boldsymbol{v}_k} - \boldsymbol{H}_k \boldsymbol{C}_{\boldsymbol{x}_k} \boldsymbol{H}_k^{\mathrm{H}}. \quad (5.8)$$

The corresponding rate region is

$$\overline{\mathcal{R}}' = \mathrm{conv} \bigcup_{\pi} \bigcup_{\substack{(\boldsymbol{C}_{\boldsymbol{x}_k}\succeq\mathbf{0})_{\forall k} \\ (\boldsymbol{C}_{\boldsymbol{x}_k})_{\forall k}\in\mathcal{Q}}} \left\{ \boldsymbol{\rho} \in \mathbb{R}_{0,+}^K \;\middle|\; \rho_k \leq r_k,\; \forall k \right\} \quad (5.9)$$

with r_k from (5.7).

It can be shown that any rate vector achievable with joint decoding is achievable with SIC as well, but unlike for joint decoding, it can then be necessary to perform RTS, namely over strategies with different decoding orders π (see, e.g., [113, 115]). Therefore, the convex hull is needed in (5.9) to obtain $\overline{\mathcal{R}}' = \mathcal{R}$ with $\mathcal{R}$ from (5.5).

5.2 Optimality of Maximum-Entropy Transmission

Just like for the single-user system considered in the previous chapter, we are interested in studying which conclusions we can draw about the optimal transmit signal if we know that the noise is a maximum-entropy signal with respect to some power shaping space. Based on $\boldsymbol{y}_{\mathcal{K}}$ defined in (5.3), we obtain the following theorem as an extension of Theorem 4.2.1.

Theorem 5.2.1. *Let $(\mathcal{P}_k = \mathcal{P}_{\mathrm{U}_k})_{\forall k}$ and $\mathcal{P}_{\mathrm{B}}$ be power shaping spaces fulfilling the compatibility assumption (Definition 3.1.3). If the noise is a maximum-entropy signal with respect to $\mathcal{P}_{\mathrm{B}}$, the whole capacity region of the RoP MIMO MAC is achieved by maximum-entropy transmit signals with respect to $(\mathcal{P}_k)_{\forall k}$.*

Proof. For all k, let $\boldsymbol{P}_{\boldsymbol{x}_k} = \mathrm{proj}_{\mathcal{P}_k}(\boldsymbol{C}_{\boldsymbol{x}_k})$ and $\boldsymbol{N}_{\boldsymbol{x}_k} = \mathrm{proj}_{\mathcal{N}_k}(\boldsymbol{C}_{\boldsymbol{x}_k})$ so that $\boldsymbol{C}_{\boldsymbol{x}_k} = \boldsymbol{P}_{\boldsymbol{x}_k} + \boldsymbol{N}_{\boldsymbol{x}_k}$. Since $\boldsymbol{\eta}, \boldsymbol{x}_1, \ldots, \boldsymbol{x}_K$ are independent, the assumption of compatible channel matrices leads to $\boldsymbol{C}_{\boldsymbol{y}_{\mathcal{K}}} = \boldsymbol{P}_{\boldsymbol{y}_{\mathcal{K}}} + \boldsymbol{N}_{\boldsymbol{y}_{\mathcal{K}}}$ with

$$\boldsymbol{P}_{\boldsymbol{y}_{\mathcal{K}}} = \sum_{k \in \mathcal{K}} \boldsymbol{H}_k \boldsymbol{P}_{\boldsymbol{x}_k} \boldsymbol{H}_k^{\mathrm{H}} + \boldsymbol{P}_{\boldsymbol{\eta}} \in \mathcal{P}_{\mathrm{B}} \qquad \boldsymbol{N}_{\boldsymbol{y}_{\mathcal{K}}} = \sum_{k \in \mathcal{K}} \boldsymbol{H}_k \boldsymbol{N}_{\boldsymbol{x}_k} \boldsymbol{H}_k^{\mathrm{H}} + \boldsymbol{N}_{\boldsymbol{\eta}} \in \mathcal{N}_{\mathrm{B}} \tag{5.10}$$

where $\boldsymbol{N}_{\boldsymbol{\eta}} = \mathrm{proj}_{\mathcal{N}_{\mathrm{B}}}(\boldsymbol{C}_{\boldsymbol{\eta}}) = \boldsymbol{0}$ and $\boldsymbol{P}_{\boldsymbol{\eta}} = \mathrm{proj}_{\mathcal{P}_{\mathrm{B}}}(\boldsymbol{C}_{\boldsymbol{\eta}}) = \boldsymbol{C}_{\boldsymbol{\eta}}$ by assumption. We can assume $\boldsymbol{P}_{\boldsymbol{x}_k} \succeq \boldsymbol{0},\ \forall k$ due to Proposition 2.5.1. For any given $(\boldsymbol{P}_{\boldsymbol{x}_k})_{\forall k}$, the power shaping matrices $\boldsymbol{P}_{\boldsymbol{y}_{\mathcal{K}}}$ are fixed, and $\det \boldsymbol{C}_{\boldsymbol{y}_{\mathcal{K}}}$ is maximized by $\boldsymbol{N}_{\boldsymbol{y}_{\mathcal{K}}} = \boldsymbol{0}$ (Theorem 2.5.2), which can be achieved simultaneously for all sets $\mathcal{K}$ by choosing $\boldsymbol{N}_{\boldsymbol{x}_k} = \boldsymbol{0},\ \forall k$. To see that this choice is feasible, note that $\boldsymbol{C}_{\boldsymbol{x}_k} = \boldsymbol{P}_{\boldsymbol{x}_k} + \boldsymbol{N}_{\boldsymbol{x}_k} \succeq \boldsymbol{0}$ for $\boldsymbol{N}_{\boldsymbol{x}_k} = \boldsymbol{0}$ and that the compatibility assumption makes the covariance constraint equivalent to $(\boldsymbol{P}_{\boldsymbol{x}_k})_{\forall k} \in \mathcal{Q}$, which does not depend on $\boldsymbol{N}_{\boldsymbol{x}_k} = \boldsymbol{0}$. This reasoning holds for any given $(\boldsymbol{P}_{\boldsymbol{x}_k} \succeq \boldsymbol{0})_{\forall k}$ including the optimal ones. Thus, we can always choose $\boldsymbol{N}_{\boldsymbol{x}_k} = \boldsymbol{0},\ \forall k$, i.e., $\boldsymbol{C}_{\boldsymbol{x}_k} \in \mathcal{P}_k,\ \forall k$. □

5.3 Optimal Transmit Covariance Matrices

In the MIMO MAC, the Pareto-optimal covariance matrices cannot be simply characterized by waterfilling [113, Sec. 2.4.2], i.e., we do not obtain a quasi-closed-form solution as for the single-user MIMO channel in Section 4.3. Instead, we need to apply numerical algorithms to find Pareto-optimal solutions as described below.

Since the rate region (5.9) is convex, any point on the Pareto boundary corresponds to a solution of a weighted sum rate maximization (see [57] and Section 3.2.2).[1] For given weights $(w_k)_{\forall k}$, the weighted sum rate $\sum_{k=1}^{K} w_k r_k$ with r_k from (5.7) is optimized by choosing π such that users with the higher weights w_k are decoded later [57]. The weighted sum rate is then a concave function of $(\boldsymbol{C}_{\boldsymbol{x}_k})_{\forall k}$ [57]. Considering the example $w_1 \leq \cdots \leq w_K$ without loss of generality, we obtain

$$\sum_{k=1}^{K} w_k r_k = -w_K \mu \log_2 \det \boldsymbol{C}_{\boldsymbol{\eta}} + \sum_{k=1}^{K} (w_k - w_{k-1}) \mu \log_2 \det \left(\boldsymbol{C}_{\boldsymbol{\eta}} + \sum_{j \geq k} \boldsymbol{H}_j \boldsymbol{C}_{\boldsymbol{x}_j} \boldsymbol{H}_j^{\mathrm{H}} \right) \tag{5.11}$$

[1] When using the SIC formulation from Section 5.1.1, RTS between several solutions of weighted sum rate problems can be necessary to achieve a particular point of the capacity region.

with $w_0 = 0$, which is concave since the factors in front of the logarithms that depend on the transmit covariance matrices are nonnegative. Therefore, iterative methods for convex programming (e.g., [100, 101]) can be applied to compute Pareto-optimal transmit strategies.

Under per-user power constraints (3.39), a specialized algorithm called iterative waterfilling [57] can solve the sum rate maximization (with equal weights) extremely efficiently [113, Sec. 2.4.2]. This is done by iteratively applying the waterfilling solution (4.9)–(4.11) with $\boldsymbol{C}_{\boldsymbol{\eta}}$ replaced by

$$\boldsymbol{X}_k = \boldsymbol{C}_{\boldsymbol{\eta}} + \sum_{j \neq k} \boldsymbol{H}_j \boldsymbol{C}_{\boldsymbol{x}_j} \boldsymbol{H}_j^{\mathrm{H}} \tag{5.12}$$

for one user after another and by repeating this procedure until convergence. Several extensions of this algorithm have been proposed, e.g., to a sum power constraint [116] and to weighted sum rate maximization under per-user power constraints [117] or under a sum power constraint [118].

Another efficient method for weighted sum rate maximization under a sum power constraint, which is based on gradient-projection steps for the transmit covariance matrices, was proposed in [119]. In [120], this method was generalized to allow for more general constraints and to incorporate a worst-case noise optimization.

5.3.1 Maximum-Entropy Noise

As a plausibility check, we can study how the iterative waterfilling algorithm from [57] behaves in the case of maximum-entropy noise with $\boldsymbol{N}_{\boldsymbol{\eta}} = \boldsymbol{0}$. Since the initial transmit covariance matrices $\boldsymbol{C}_{\boldsymbol{x}_k}$ may be chosen arbitrarily [57], let us use scaled identities that fulfill the power constraints. This initialization fulfills $\boldsymbol{C}_{\boldsymbol{x}_k} \in \mathcal{P}_k$ for all k.

From $\boldsymbol{C}_{\boldsymbol{x}_j} \in \mathcal{P}_j$ for all $j \neq k$ and $\boldsymbol{C}_{\boldsymbol{\eta}} \in \mathcal{P}_{\mathrm{B}}$, it follows that $\boldsymbol{X}_k \in \mathcal{P}_{\mathrm{B}}$ due to the assumption of compatible channel matrices. Using the reasoning from Section 4.3.2, we then obtain that the waterfilling solution fulfills $\boldsymbol{C}_{\boldsymbol{x}_k} \in \mathcal{P}_k$. This argument can be applied iteratively, which shows that we have $(\boldsymbol{C}_{\boldsymbol{x}_k} \in \mathcal{P}_k)_{\forall k}$ in the optimal solution obtained by the iterative waterfilling algorithm from [57].

The same line of argumentation can be applied to other algorithms that employ waterfilling in every iteration. In particular, we obtain the same result for the weighted sum rate maximization algorithms from [117, 118], which can be used to compute Pareto-optimal points of the capacity region under a sum power constraint or under per-user power constraints, respectively. This confirms that Pareto-optimal points can be achieved using maximum-entropy transmission with respect to $(\mathcal{P}_k)_{\forall k}$, which was shown in Theorem 5.2.1.

5.3.2 Reduced-Entropy Noise

If we do not make any assumptions on the covariance matrix of the noise, we might have $\boldsymbol{N}_{\boldsymbol{\eta}} \neq \boldsymbol{0}$, and the conclusion that all entropy reduction matrices $\boldsymbol{N}_{\boldsymbol{x}_k}$ need to vanish (as in Theorem 5.2.1) is no longer true. The same applies if the compatibility assumption in Theorem 5.2.1 is violated. An optimization algorithm such as iterative waterfilling can still be used to find the optimal covariance matrices in these cases, but the solution will no longer behave as described in Section 5.3.1. A more detailed description of this is given in Sections 4.3.2 and 4.5.4 for a single-user system.

5.4 Worst-Case Noise

The worst-case noise result from Section 4.4 can be extended to the MIMO MAC as well. Again, we make the assumption of real-valued or proper Gaussian noise whose covariance matrix is restricted by a constraint that acts only on the power shaping component. We obtain the following generalization of Theorem 4.4.1. The proof technique is similar to the one in [28], but we consider a more general framework.

Theorem 5.4.1. *Let $(\mathcal{P}_k = \mathcal{P}_{\mathrm{U}_k})_{\forall k}$ and $\mathcal{P}_{\mathrm{B}}$ be power shaping spaces fulfilling the compatibility assumption (Definition 3.1.3), and let the constraint $\boldsymbol{C}_{\boldsymbol{\eta}} \in \mathcal{Q}_{\mathrm{noise}}$ be compatible with $\mathcal{P}_{\mathrm{B}}$ (in the sense of Definition 3.1.2). If it holds for all users k in the RoP MIMO MAC that $\boldsymbol{x}_k$ is an arbitrary maximum-entropy signal with respect to $\mathcal{P}_k$, maximum-entropy noise with respect to $\mathcal{P}_{\mathrm{B}}$ minimizes the achievable rates of all users simultaneously.*

Proof. For any $\mathcal{K} \subseteq \{1, \ldots, K\}$, let $\boldsymbol{P}_{\mathcal{K},\varepsilon} = \sum_{k\in\mathcal{K}} \boldsymbol{H}_k \boldsymbol{C}_{\boldsymbol{x}_k} \boldsymbol{H}_k^{\mathrm{H}} + \varepsilon \mathbf{I}_{M_{\mathrm{B}}}$. As $\boldsymbol{C}_{\boldsymbol{x}_k} \in \mathcal{P}_k$, $\forall k$ implies that $\boldsymbol{P}_{\mathcal{K},\varepsilon} \in \mathcal{P}_{\mathrm{B}}$ (due to compatible channel matrices), we can use the same reasoning as in the proof of Theorem 4.4.1 to show that maximum-entropy noise $\boldsymbol{\eta}$ minimizes

$$r_{\mathcal{K},\varepsilon}(\boldsymbol{C}_{\boldsymbol{\eta}}) = \mu \log_2 \frac{\det\left(\boldsymbol{P}_{\mathcal{K},\varepsilon} + \boldsymbol{C}_{\boldsymbol{\eta}}\right)}{\det \boldsymbol{C}_{\boldsymbol{\eta}}}. \tag{5.13}$$

By again taking $\varepsilon \to 0$, we obtain that maximum-entropy noise is the worst-case noise for each of the inequalities in (5.5). □

Similar as in the single-user case (Section 4.4), reduced-entropy noise relaxes the rate inequalities in (5.5) even if the transmitters are oblivious of the noise properties and use maximum-entropy transmit signals. For optimal strategies, which adapt the transmit signals to the noise properties, we have the following extension.

Corollary 5.4.1. *Let $(\mathcal{P}_k)_{\forall k}$, $\mathcal{P}_{\mathrm{B}}$, and $\mathcal{Q}_{\mathrm{noise}}$ be as in Theorem 5.4.1, but assume that the transmit covariance matrices $\boldsymbol{C}_{\boldsymbol{x}_k}$ are optimized (for given $\boldsymbol{C}_{\boldsymbol{\eta}}$) to achieve a Pareto-optimal point of the capacity region under a constraint* (3.3) *that is compatible with $\bigotimes_{k=1}^{K} \mathcal{P}_k$. Then, maximum-entropy noise with respect to $\mathcal{P}_{\mathrm{B}}$ minimizes the achievable rates of all users simultaneously.*

Proof. This is a consequence of Theorem 5.2.1 combined with Theorem 5.4.1 following the same line of argumentation as Corollary 4.4.1. □

5.5 Complex Multicarrier MIMO MAC

For the complex multicarrier MIMO MAC, we introduce the abbreviations $\boldsymbol{y}^{(c)} = \boldsymbol{y}_{\mathrm{B}}^{(c)}$, $\boldsymbol{H}_k^{(c)} = \boldsymbol{H}_{\mathrm{BU}_k}^{(c)}$, $\boldsymbol{x}_k^{(c)} = \boldsymbol{x}_{\mathrm{U}_k}^{(c)}$, and $\boldsymbol{\eta}^{(c)} = \boldsymbol{\eta}_{\mathrm{B}}^{(c)}$. From the general model in (3.34), we obtain the description

$$\boldsymbol{y}^{(c)} = \sum_{k=1}^{K} \boldsymbol{H}_k^{(c)} \boldsymbol{x}_k^{(c)} + \boldsymbol{\eta}^{(c)}, \quad c = 1, \ldots, C. \tag{5.14}$$

We assume a constraint on the per-carrier covariance matrices of all transmitting users as in (3.38). The above results on the RoP MIMO MAC can be applied to the combined real representation of (5.14) by setting $\boldsymbol{H}_k$ in (5.1) to $\boldsymbol{H}_k = \grave{\boldsymbol{H}}_k = \grave{\boldsymbol{H}}_{\mathrm{BU}_k}$ as defined in (3.37).

5.5.1 Optimality of Maximum-Entropy Transmission

Similar as for the single-user case considered in Chapter 4, we can find several statements about the optimal transmit signals for the complex multicarrier MIMO MAC in the literature. Under the assumption of proper CN noise, it is accepted as common knowledge that the optimal transmit signals are proper (e.g., [30]) and CN (e.g., [40]). Formal proofs can be found for various special cases, e.g., for the optimality of CN signals in [49, 50] under the assumption of proper transmit signals and a sum power constraint (3.42). For more general covariance constraints (3.38), the optimality of proper transmit signals was shown in [21] (for the special case of a single-carrier system with $C = 1$), and the optimality of CN transmit signals was shown in [25] (under the assumption of proper transmit signals).

All these results can be considered as special cases of Theorem 5.2.1 for the various power shaping spaces from Proposition 3.4.2.

Corollary 5.5.1 ($\mathcal{P}_k = \grave{\mathcal{P}}_{\mathrm{U}_k}^{\mathrm{CN}},\ \forall k$ and $\mathcal{P}_{\mathrm{B}} = \grave{\mathcal{P}}_{\mathrm{B}}^{\mathrm{CN}}$)**.** *The whole capacity region of the complex multicarrier MIMO MAC* (5.14) *with covariance constraint* (3.38) *is achieved by transmit signals that are proper and CN if the noise is proper and CN.*

Corollary 5.5.2 ($\mathcal{P}_k = \grave{\mathcal{P}}_{\mathrm{U}_k},\ \forall k$ and $\mathcal{P}_{\mathrm{B}} = \grave{\mathcal{P}}_{\mathrm{B}}$)**.** *The whole capacity region of the complex (multicarrier) MIMO MAC* (5.14) *with covariance constraint* (3.38) *is achieved by transmit signals that are proper (but possibly CC) if the noise is proper (but possibly CC).*

Corollary 5.5.3 ($\mathcal{P}_k = \mathcal{P}_{\mathrm{U}_k}^{\mathrm{CN}},\ \forall k$ and $\mathcal{P}_{\mathrm{B}} = \mathcal{P}_{\mathrm{B}}^{\mathrm{CN}}$)**.** *The whole capacity region of the complex multicarrier MIMO MAC* (5.14) *with covariance constraint* (3.38) *is achieved by transmit signals that are CN (but possibly improper) if the noise is CN (but possibly improper).*

5.5.2 Optimal Transmit Covariance Matrices for the Case of Proper CN Noise

When studying the capacity region of the complex multicarrier MIMO MAC (5.14) under the assumption that the noise is proper and CN as in Corollary 5.5.1, the combined real noise covariance matrix $\boldsymbol{C}_{\check{\boldsymbol{\eta}}}$ lies in the power shaping space $\grave{\mathcal{P}}_{\mathrm{B}}^{\mathrm{CN}}$, and the optimal combined real transmit covariance matrices $\boldsymbol{C}_{\check{\boldsymbol{x}}_k}$ lie in the power shaping spaces $\grave{\mathcal{P}}_{\mathrm{U}_k}^{\mathrm{CN}}$ for all k (see Proposition 3.4.2). This means that all these matrices are symmetric $\mathcal{BSC}_2$ matrices with block-diagonal submatrices (see Definition 3.4.1). In addition, the combined real channel matrices $\grave{\boldsymbol{H}}_k$ are $\mathcal{BSC}_2$ with block-diagonal submatrices as discussed in Section 3.4.4.

For the inequalities in (5.5), we thus obtain

$$\sum_{k\in\mathcal{K}} \rho_k \leq \frac{1}{2}\log_2 \frac{\det \boldsymbol{C}_{\check{\boldsymbol{y}}_{\mathcal{K}}}}{\det \boldsymbol{C}_{\check{\boldsymbol{\eta}}}} = \log_2 \frac{\det \boldsymbol{C}_{\boldsymbol{y}_{\mathcal{K}}}}{\det \boldsymbol{C}_{\boldsymbol{\eta}}} = \sum_{c=1}^{C} \log_2 \frac{\det \boldsymbol{C}_{\boldsymbol{y}_{\mathcal{K}}^{(c)}}}{\det \boldsymbol{C}_{\boldsymbol{\eta}^{(c)}}} \tag{5.15}$$

in analogy to Proposition 3.4.5, where $\boldsymbol{C}_{\boldsymbol{y}_{\mathcal{K}}} = \boldsymbol{C}_{\boldsymbol{\eta}} + \sum_{k\in\mathcal{K}} \boldsymbol{H}_k \boldsymbol{C}_{\boldsymbol{x}_k} \boldsymbol{H}_k^{\mathrm{H}}$ and $\boldsymbol{C}_{\boldsymbol{y}_{\mathcal{K}}^{(c)}} = \boldsymbol{C}_{\boldsymbol{\eta}^{(c)}} + \sum_{k\in\mathcal{K}} \boldsymbol{H}_k^{(c)} \boldsymbol{C}_{\boldsymbol{x}_k^{(c)}} \boldsymbol{H}_k^{(c),\mathrm{H}}$.

Thus, a rate vector $\boldsymbol{\rho} = [\rho_1, \ldots, \rho_K]^{\mathrm{T}}$ is achievable if we can find $\rho_k^{(c)},\ \forall c, \forall k$ such that

$$\rho_k = \sum_{c=1}^{C} \rho_k^{(c)} \quad \text{and} \quad \sum_{k\in\mathcal{K}} \rho_k^{(c)} \leq \log_2 \frac{\det \boldsymbol{C}_{\boldsymbol{y}_{\mathcal{K}}^{(c)}}}{\det \boldsymbol{C}_{\boldsymbol{\eta}^{(c)}}}. \tag{5.16}$$

This means that we can decompose the problem of finding optimal covariance matrices into separate problems for each carrier which are only coupled by the first sum of (5.16) and by the covariance constraint. Indeed, the complex multicarrier MIMO MAC is a RoP CN MIMO system (see Definition 3.3.1) if the signals and the noise are proper and CN. Therefore, the dual decomposition framework presented in Section 3.3.2 can be applied to decouple the per-carrier problems.

For the case of per-user power constraints (3.39) and the case of a sum power constraint (3.42), such a dual decomposition was performed in [49]. The remaining task is then to solve the inner problem (3.33), i.e., to find optimal complex covariance matrices $\boldsymbol{C}_{\boldsymbol{x}_k^{(c)}}$ on each carrier. As we have a RoP MIMO MAC on each carrier, any weighted sum rate can be expressed as a concave function of these covariance matrices (see Section 5.3), so that (3.33) has a concave objective function and can be solved by convex programming methods.

An alternative decomposition was used in [50] by instead introducing per-carrier sum powers $Q^{(c)}$ as auxiliary variables. The proposed method then alternates between an optimization of $Q^{(c)}$ for fixed covariance matrices and a covariance optimization under per-carrier power constraints $\sum_{k=1}^{K} \mathrm{tr}[\boldsymbol{C}_{\boldsymbol{x}_k^{(c)}}] \leq Q^{(c)}$.

5.5.3 Optimal Transmit Covariance Matrices for the Case of Improper or CC Noise

If the noise is improper or CC or both, we can no longer apply Corollary 5.5.1, and at least one of the equalities in (5.15) becomes invalid. In particular, if the noise is both improper and CC, we need to apply the methods presented in Section 5.3 directly to the combined real representation in order to obtain an optimal transmit strategy.

In the case of improper CN noise, we can make use of the real-valued multicarrier formulation (3.36) in order to again be able to perform a decomposition into per-carrier problems. As pointed out in Section 3.4.1, the real-valued multicarrier formulation is a RoP CN MIMO system in this case.

On the other hand, if the noise is CC, but proper, the combined complex representation (3.35) can be used. In this case, it is no longer possible to perform a dual decomposition, but we can at least obtain a slight reduction of the computational complexity compared to the combined real representation (cf., e.g., the statements about computational complexity of complex formulations compared to composite real representations in [24]).

If we are interested in a universal method whose applicability does not depend on the noise properties, we can always apply a numerical solver directly to the combined real representation. From the considerations in Section 5.3.1, we know that a special structure of the noise (e.g., CN or proper) automatically leads to a numerical solution where the transmit signals have the corresponding structure.

5.5.4 Worst-Case Noise

The following corollaries of Theorem 5.4.1 are obtained for the complex multicarrier MIMO MAC (5.14) with various choices of the considered power shaping spaces (see Proposition 3.4.2). The term *optimized* is always understood in the sense of finding Pareto-optimal solutions under a transmit covariance constraint (3.38). Note that the statement of Corollary 5.5.5 was also shown in [28].

Corollary 5.5.4 ($\mathcal{P}_k = \grave{\mathcal{P}}^{\mathrm{CN}}_{\mathrm{U}_k},\ \forall k$ and $\mathcal{P}_{\mathrm{B}} = \grave{\mathcal{P}}^{\mathrm{CN}}_{\mathrm{B}}$)**.** *In the complex multicarrier MIMO MAC* (5.14) *with constraints on the complex per-carrier noise covariance matrices, the worst-case noise is proper and CN if the transmit signals are either fixed to be proper and CN or optimized based on the noise properties.*

Corollary 5.5.5 ($\mathcal{P}_k = \grave{\mathcal{P}}_{\mathrm{U}_k},\ \forall k$ and $\mathcal{P}_{\mathrm{B}} = \grave{\mathcal{P}}_{\mathrm{B}}$)**.** *In the complex (multicarrier) MIMO MAC* (5.14) *with constraints on the combined complex noise covariance matrix, the worst-case noise is proper if the transmit signals are either fixed to be proper or optimized based on the noise properties.*

Corollary 5.5.6 ($\mathcal{P}_k = \mathcal{P}^{\mathrm{CN}}_{\mathrm{U}_k},\ \forall k$ and $\mathcal{P}_{\mathrm{B}} = \mathcal{P}^{\mathrm{CN}}_{\mathrm{B}}$)**.** *In the complex multicarrier MIMO MAC* (5.14) *with constraints on the per-carrier noise properties, the worst-case noise is CN if the transmit signals are either fixed to be CN or optimized based on the noise properties.*

Chapter 6

The Gaussian MIMO Broadcast Channel

If we still consider a base station B with K user terminals U_k, but consider the downlink operation where information is transmitted from the base station to the users (see Figure 6.1), we have a so-called (Gaussian) MIMO broadcast channel (BC) [46, 121]. After introducing the system model and summarizing the capacity-achieving coding scheme, we revisit the uplink-downlink duality from [106], which enables us to study the MIMO BC via the dual MIMO MAC. By exploiting this duality, we can extend the results from Chapter 5 to the RoP MIMO BC and finally to the complex multicarrier MIMO BC.

6.1 System Model and Capacity Region

We introduce the abbreviations $\boldsymbol{y}_k = \boldsymbol{y}_{\mathrm{U}_k}$, $\boldsymbol{H}_k^{\mathrm{H}} = \boldsymbol{H}_{\mathrm{U}_k\mathrm{B}}$, $\boldsymbol{x} = \boldsymbol{x}_{\mathrm{B}}$, $\boldsymbol{\eta}_k = \boldsymbol{\eta}_{\mathrm{U}_k}$, $M = M_{\mathrm{B}}$, and $M_k = M_{\mathrm{U}_k}$. The description of the RoP MIMO BC is obtained from the general model (3.1) as

$$\boldsymbol{y}_k = \boldsymbol{H}_k^{\mathrm{H}}\boldsymbol{x} + \boldsymbol{\eta}_k, \ \forall k \tag{6.1}$$

with a covariance constraint $\boldsymbol{C}_{\boldsymbol{x}} \in \mathcal{Q}$ as given by (3.3).

It was shown in [121] that the complete capacity region of the real-valued MIMO BC can be achieved by so-called dirty paper coding (DPC) with real-valued Gaussian input signals. As the proof is quite lengthy, we do not reproduce it here. For the complex MIMO BC, we can apply this result to the composite real representation to show that complex Gaussian signals are optimal in this case [121]. However, as pointed out in [21], this does not give a response to the question whether proper or improper signals should be used. Since the definition of a RoP MIMO system (Definition 3.1.1) anyway assumes that all signals in a complex system are proper, we come back to this question later when we study the complex multicarrier MIMO BC.

DPC exploits a result from [122] stating that interference that is noncausally known to the transmitter (but not to the receiver) can be pre-eliminated by means of coding without influencing the transmit covariance matrix. In the MIMO BC, this can be applied in a successive manner so that the interference from all users encoded earlier than user k is removed from the signal intended for user k (e.g., [46]). The interference caused by users encoded after user k cannot be removed in this manner and is treated as additional noise. Any point in the capacity region can be achieved by RTS between DPC strategies with different encoding orders [121].

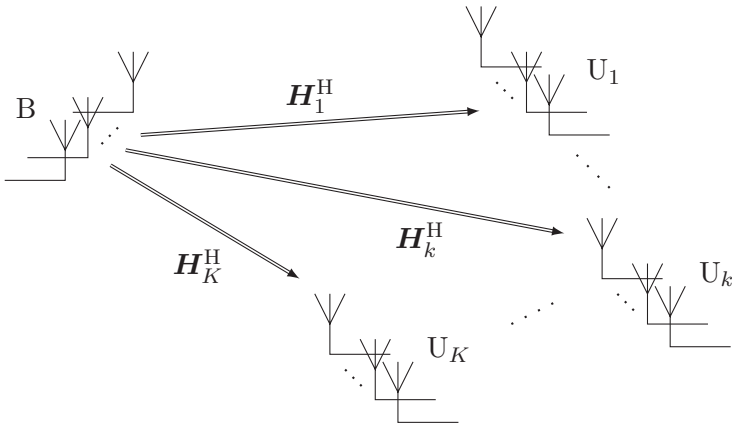

Figure 6.1: Illustration of the MIMO broadcast channel.

To describe this mathematically, we introduce auxiliary signals called per-user input signals $\boldsymbol{\xi}_k$, which correspond to the messages intended for the various users. The transmit signal $\boldsymbol{x}$ that is constructed by means of DPC then has the covariance matrix $\boldsymbol{C}_{\boldsymbol{x}} = \sum_{k=1}^{K} \boldsymbol{C}_{\boldsymbol{\xi}_k}$.

With the encoding order specified by the permutation $\bar{\pi} : k \mapsto \bar{\pi}(k)$, so that user $k : \bar{\pi}(k) = 1$ is encoded first, we can achieve the per-user rates [46, 121]

$$r_k^{\mathrm{BC}} = \mu \log_2 \frac{\det \boldsymbol{C}_{\boldsymbol{y}_k}}{\det \boldsymbol{C}_{\boldsymbol{z}_k}} \tag{6.2}$$

where

$$\boldsymbol{C}_{\boldsymbol{y}_k} = \boldsymbol{C}_{\boldsymbol{\eta}_k} + \sum_{j:\bar{\pi}(j)\geq\bar{\pi}(k)} \boldsymbol{H}_k^{\mathrm{H}} \boldsymbol{C}_{\boldsymbol{\xi}_j} \boldsymbol{H}_k \qquad \text{and} \qquad \boldsymbol{C}_{\boldsymbol{z}_k} = \boldsymbol{C}_{\boldsymbol{y}_k} - \boldsymbol{H}_k^{\mathrm{H}} \boldsymbol{C}_{\boldsymbol{\xi}_k} \boldsymbol{H}_k. \tag{6.3}$$

The resulting rate region

$$\overline{\mathcal{R}} = \operatorname{conv} \bigcup_{\bar{\pi}} \bigcup_{\substack{(\boldsymbol{C}_{\boldsymbol{\xi}_k} \succeq \boldsymbol{0})_{\forall k} \\ \sum_{k=1}^{K} \boldsymbol{C}_{\boldsymbol{\xi}_k} \in \mathcal{Q}}} \left\{ \boldsymbol{\rho} \in \mathbb{R}_{0,+}^{K} \;\middle|\; \rho_k \leq r_k^{\mathrm{BC}},\ \forall k \right\} \tag{6.4}$$

with r_k^{BC} from (6.2) is the capacity region of the RoP MIMO channel [112, 113, 121]. Note that the transmit strategy that was shown to be capacity-achieving in [121] only makes use of RTS, i.e., applying the more flexible TS would lead to the same rate region $\overline{\overline{\mathcal{R}}} = \overline{\mathcal{R}}$.

Just like in the MIMO MAC, we can find Pareto-optimal points of the capacity region $\mathcal{C} = \overline{\mathcal{R}}$ by solving weighted sum rate maximizations (3.12). However, due to the different structure of the involved matrices in the rate equations (6.2) and (5.7), the MIMO BC does not feature the favorable property of the MIMO MAC that weighted sum rates can be written as concave functions of the covariance matrices of the per-user signals (e.g., [46]). A common approach to overcome this problem is the so-called uplink-downlink duality which allows us to solve optimization problems for the MIMO BC via a transformation to the dual MIMO MAC.

6.2 Uplink-Downlink Duality

In the literature, we can find various duality theorems stating conditions under which two considered networks have the same rate regions, the same regions of achievable signal-to-

interference-and-noise ratios (SINRs), or the same regions of achievable mean square errors (MSEs) (see [45, 46, 51, 106] and the references therein). For our derivations, we make use of a rate duality between the MIMO BC and the MIMO MAC, which is often called uplink-downlink duality (e.g., [45]). Since classical results on uplink-downlink duality, such as the ones in [46, 51], are restricted to a sum power constraint, we instead apply the recently established minimax duality with linear conic constraints [106].

Lemma 6.2.1. *Given $\boldsymbol{E} \succ \mathbf{0}$ and $(\boldsymbol{F}_k \succ \mathbf{0})_{\forall k}$ such that $\sum_{k=1}^{K} \mathrm{tr}[\boldsymbol{F}_k \boldsymbol{F}_k] = \mathrm{tr}[\boldsymbol{E}\boldsymbol{E}]$, define $\mathcal{E} = \{\alpha \boldsymbol{E} \mid \alpha \in \mathbb{R}\}$ and $\mathcal{F} = \{(\alpha \boldsymbol{F}_k)_{\forall k} \mid \alpha \in \mathbb{R}\}$. Let $\mathbb{H}^{M_\mathrm{B}} = \mathcal{E} \oplus \mathcal{Z} \oplus \mathcal{Z}'$ and $\bigotimes_{k=1}^{K} \mathbb{H}^{M_{\mathrm{U}_k}} = \mathcal{F} \oplus \mathcal{Y} \oplus \mathcal{Y}'$ (with $\mathbb{S}$ instead of $\mathbb{H}$ in case of real-valued systems) be divisions into three mutually orthogonal subspaces with respect to the Frobenius inner product* (2.1)*. For given channel matrices $(\boldsymbol{H}_k^{\mathrm{H}})_{\forall k}$, non-negative weights $(w_k)_{\forall k}$, and a permutation $\bar{\pi} : k \mapsto \bar{\pi}(k)$, the downlink minimax problem*

$$\min_{\substack{(\boldsymbol{C}_{\boldsymbol{\eta}_k} \succeq \mathbf{0})_{\forall k} \\ (\boldsymbol{Y}'_k)_{\forall k} \in \mathcal{Y}'}} \left(\max_{\substack{(\boldsymbol{C}_{\boldsymbol{\xi}_k} \succeq \mathbf{0})_{\forall k} \\ \boldsymbol{Z} \in \mathcal{Z}}} \sum_{k=1}^{K} w_k r_k^{\mathrm{BC}} \ \text{s.t.} \ \sum_{k=1}^{K} \boldsymbol{C}_{\boldsymbol{\xi}_k} \preceq \boldsymbol{E} + \boldsymbol{Z} \right) \ \text{s.t.} \ \boldsymbol{C}_{\boldsymbol{\eta}_k} \preceq \boldsymbol{F}_k + \boldsymbol{Y}'_k, \ \forall k \tag{6.5}$$

with r_k^{BC} from (6.2) *using $\bar{\pi}$ as encoding order has the same optimal value as the uplink minimax problem*

$$\min_{\substack{\boldsymbol{C}_{\boldsymbol{\eta}} \succeq \mathbf{0} \\ \boldsymbol{Z}' \in \mathcal{Z}'}} \left(\max_{\substack{(\boldsymbol{C}_{\boldsymbol{x}_k} \succeq \mathbf{0})_{\forall k} \\ (\boldsymbol{Y}_k)_{\forall k} \in \mathcal{Y}}} \sum_{k=1}^{K} w_k r_k \ \text{s.t.} \ \boldsymbol{C}_{\boldsymbol{x}_k} \preceq \boldsymbol{F}_k + \boldsymbol{Y}_k, \ \forall k \right) \ \text{s.t.} \ \boldsymbol{C}_{\boldsymbol{\eta}} \preceq \boldsymbol{E} + \boldsymbol{Z}' \tag{6.6}$$

with r_k from (5.7) *using the reverse order $\pi(k) = K + 1 - \bar{\pi}(k)$ as decoding order.*

Sketch of Proof. The proof of [106, Th. 1] for complex systems with proper signals and noise can be transferred to real-valued systems. The lemma is obtained by applying [106, Th. 1] to the RoP MIMO BC following the description in [106, Sec. 4.1.5]. The assumptions $\boldsymbol{E} \succ \mathbf{0}$ and $(\boldsymbol{F}_k \succ \mathbf{0})_{\forall k}$ are sufficient for the conditions in [106, Th. 1]. □

The linear subspaces $\mathcal{Z}$ and $\mathcal{Y}$ can be used to model various constraints on the transmit covariance matrices such as sum power constraints or shaping constraints (see [86, 106]). The orthogonal spaces $\mathcal{Y}'$ and $\mathcal{Z}'$ determine which noise covariance matrices are allowed for the worst-case noise minimizations in (6.5) and (6.6).

6.3 Optimality of Maximum-Entropy Transmission

We are now ready to study the optimal per-user input signals under the assumption of maximum-entropy noise. To avoid an analysis of the complicated nonconcave rate equations of the MIMO BC, the proof of the following theorem is performed by exploiting the uplink-downlink duality introduced in Lemma 6.2.1.

Theorem 6.3.1. *Let $(\mathcal{P}_k = \mathcal{P}_{\mathrm{U}_k})_{\forall k}$ and $\mathcal{P}_\mathrm{B}$ be power shaping spaces fulfilling the compatibility assumption (Definition 3.1.3). If the noise vectors are maximum-entropy signals with respect to $(\mathcal{P}_k)_{\forall k}$, the whole capacity region of the RoP MIMO BC is achieved by maximum-entropy per-user input signals with respect to $\mathcal{P}_\mathrm{B}$.*

Proof. Due to [121, Lemma 1], a rate vector $\boldsymbol{\rho}$ is achievable under the constraint $\boldsymbol{C_x} \in \mathcal{Q}$ if and only if there exists an $\boldsymbol{S} \in \mathcal{Q}$, $\boldsymbol{S} \succeq \boldsymbol{0}$ such that the rate vector is achievable under the constraint $\boldsymbol{C_x} \preceq \boldsymbol{S}$. Equivalently, $\boldsymbol{\rho}$ is achievable if and only if there exists $\boldsymbol{P} \in \mathcal{P}_{\mathrm{B}}$ and $\boldsymbol{N} \in \mathcal{N}_{\mathrm{B}}$ such that $\boldsymbol{P}+\boldsymbol{N} \in \mathcal{Q}$, $\boldsymbol{P}+\boldsymbol{N} \succeq \boldsymbol{0}$, and $\boldsymbol{\rho}$ is achievable with $\boldsymbol{C_x} \preceq \boldsymbol{P}+\boldsymbol{N}$.

Due to the compatibility assumption, we have from (3.6) that $\boldsymbol{P} \in \mathcal{Q} \Leftrightarrow \boldsymbol{P}+\boldsymbol{N} \in \mathcal{Q}$, $\forall \boldsymbol{N} \in \mathcal{N}_{\mathrm{B}}$. Thus, $\boldsymbol{\rho}$ is achievable if and only if there exists a $\boldsymbol{P} \in \mathcal{P}_{\mathrm{B}} \cap \mathcal{Q}$ with $\boldsymbol{P} \succeq \boldsymbol{0}$ (see Proposition 2.5.1) such that $\boldsymbol{\rho}$ is achievable under the constraint $\boldsymbol{C_x} \preceq \boldsymbol{P}+\boldsymbol{N}$ where $\boldsymbol{N} \in \mathcal{N}_{\mathrm{B}}$ is considered as an additional optimization variable.

As all Pareto-optimal points in $\overline{\mathcal{R}}$ correspond to solutions of weighted sum rate maximizations or to RTS between such solutions (see Sections 3.2.2 and 6.1), it is sufficient to show that maximum-entropy signals optimize

$$\max_{\substack{(\boldsymbol{C_{\xi_k}} \succeq \boldsymbol{0})_{\forall k} \\ \boldsymbol{N} \in \mathcal{N}_{\mathrm{B}}}} \sum_{k=1}^{K} w_k r_k^{\mathrm{BC}} \quad \text{s.t.} \quad \sum_{k=1}^{K} \boldsymbol{C_{\xi_k}} \preceq \boldsymbol{P}+\boldsymbol{N} \tag{6.7}$$

for any positive-semidefinite $\boldsymbol{P} \in \mathcal{P}_{\mathrm{B}}$ and arbitrary $(w_k \geq 0)_{\forall k}$. We can assume $\boldsymbol{P} \succ \boldsymbol{0}$ since any zero eigenvalue in $\boldsymbol{P}$ can be interpreted as a forbidden transmit direction, which can be eliminated by a transformation to an equivalent system [114].

This optimization is equivalent to (6.5) with $\boldsymbol{E} = \boldsymbol{P} \succ \boldsymbol{0}$, $\mathcal{Z} = \mathcal{N}_{\mathrm{B}}$, $\boldsymbol{F}_k = \boldsymbol{C_{\eta_k}} \succ \boldsymbol{0}$, $\forall k$, and $\mathcal{Y}' = \{(\boldsymbol{0})_{\forall k}\}$. Let $\beta^2 = \frac{\sum_{k=1}^{K} \mathrm{tr}[\boldsymbol{F}_k \boldsymbol{F}_k]}{\mathrm{tr}[\boldsymbol{E}\boldsymbol{E}]}$. In order to apply Lemma 6.2.1, we need that $\beta^2 = 1$. If $\beta^2 \neq 1$, we can replace all channel matrices $\boldsymbol{H}_k^{\mathrm{H}}$ by $\frac{1}{\sqrt{\beta}}\boldsymbol{H}_k^{\mathrm{H}}$ and all noise covariance matrices $\boldsymbol{C_{\eta_k}}$ by $\frac{1}{\beta}\boldsymbol{C_{\eta_k}}$ without changing the rates in (6.2). Then, $\sum_{k=1}^{K} \mathrm{tr}[\frac{1}{\beta}\boldsymbol{C_{\eta_k}} \frac{1}{\beta}\boldsymbol{C_{\eta_k}}] = \mathrm{tr}[\boldsymbol{E}\boldsymbol{E}]$. We can thus assume without loss of generality that $\sum_{k=1}^{K} \mathrm{tr}[\boldsymbol{F}_k \boldsymbol{F}_k] = \mathrm{tr}[\boldsymbol{E}\boldsymbol{E}]$ holds.

We have $\mathcal{F} \oplus \mathcal{Y}' = \mathcal{F} \subseteq \bigotimes_{k=1}^{K} \mathcal{P}_k$ since $\boldsymbol{F}_k = \boldsymbol{C_{\eta_k}} \in \mathcal{P}_k$, $\forall k$. Thus, $\bigotimes_{k=1}^{K} \mathcal{N}_k \subseteq \mathcal{Y}$, which shows that the uplink transmit covariance constraints $\boldsymbol{C_{x_k}} \preceq \boldsymbol{F}_k + \boldsymbol{Y}_k$, $\forall k$, $(\boldsymbol{Y}_k)_{\forall k} \in \mathcal{Y}$ are compatible with $\bigotimes_{k=1}^{K} \mathcal{P}_k$. Moreover, we have $\mathcal{E} \oplus \mathcal{Z}' = \mathcal{P}_{\mathrm{B}}$ since $\mathcal{Z} = \mathcal{N}_{\mathrm{B}}$. As we can always assume that the noise covariance constraint $\boldsymbol{C_\eta} \preceq \boldsymbol{E} + \boldsymbol{Z}'$ in (6.6) is fulfilled with equality [106, Remark 2], we have $\boldsymbol{C_\eta} \in \mathcal{P}_{\mathrm{B}}$, i.e., maximum-entropy noise in the dual uplink. Therefore, maximum-entropy signals are optimal in the uplink problem (6.6) due to Theorem 5.2.1, i.e., we have $\boldsymbol{C_{x_k}} \in \mathcal{P}_k$.

From [106], we get the uplink-to-downlink transformation

$$\boldsymbol{C_{\xi_k}} = \alpha w_k \left(\boldsymbol{C_{\zeta_k}}^{-1} - \boldsymbol{C_{\upsilon_k}}^{-1} \right) \quad \forall k \tag{6.8}$$

with $\boldsymbol{C_{\zeta_k}}$ and $\boldsymbol{C_{\upsilon_k}}$ from (5.8). The common scaling factor $\alpha > 0$ can be obtained as described in [106]. Due to the compatible channel matrices $\boldsymbol{H}_k^{\mathrm{H}}$, we have $\boldsymbol{C_{\zeta_k}} \in \mathcal{P}_{\mathrm{B}}$, $\boldsymbol{C_{\upsilon_k}} \in \mathcal{P}_{\mathrm{B}}$, $\forall k$ (using Proposition 2.7.1), and we obtain $\boldsymbol{C_{\xi_k}} \in \mathcal{P}_{\mathrm{B}}$, $\forall k$ by Corollary 2.4.2. □

6.4 Optimal Input Covariance Matrices

To optimize the transmit strategy in the MIMO BC, it is common practice to exploit uplink-downlink duality and to solve a convex optimization problem in the dual MAC (e.g., [116, 119, 123] for a sum power constraint and [86, 114, 120] for other covariance constraints). Therefore, the behavior of numerical methods discussed in Section 5.3 carries over to optimization problems in the MIMO BC.

If the assumptions of Theorem 6.3.1 are fulfilled in the downlink, the dual uplink complies to the assumptions made in Theorem 5.2.1 (see proof of Theorem 6.3.1). Then, the methods described in Section 5.3 converge to solutions that apply maximum-entropy transmission in the uplink (see Section 5.3.1), and the uplink-to-downlink transformation (6.8) translates this to maximum-entropy transmission in the downlink.

On the other hand, if we have reduced-entropy noise in the downlink, the conclusion that the constraints in the dual uplink are compatible with $\bigotimes_{k=1}^{K} \mathcal{P}_k$ (see the proof of Theorem 6.3.1) is no longer valid. In this case, Theorem 5.2.1 is not applicable, and we can obtain strategies that employ reduced-entropy transmission (see Section 5.3.2).

6.5 Worst-Case Noise

Finally, we can again consider the question of worst-case noise. Assuming Gaussian noise with constraints that act only on the power shaping components of the noise covariance matrices, we obtain the following theorem, whose proof is similar to a proof in [28], but in a more general framework.

Theorem 6.5.1. *Let $(\mathcal{P}_k = \mathcal{P}_{\mathrm{U}_k})_{\forall k}$ and $\mathcal{P}_{\mathrm{B}}$ be power shaping spaces fulfilling the compatibility assumption (Definition 3.1.3), and let the constraint $(\boldsymbol{C}_{\boldsymbol{\eta}_k})_{\forall k} \in \mathcal{Q}_{\mathrm{noise}}$ be compatible with $\bigotimes_{k=1}^{K} \mathcal{P}_k$ (in the sense of Definition 3.1.2). If it holds for all per-user input signals in the RoP MIMO BC that $\boldsymbol{\xi}_k$ is an arbitrary maximum-entropy signal with respect to $\mathcal{P}_{\mathrm{B}}$, maximum-entropy noise with respect to $(\mathcal{P}_k)_{\forall k}$ minimizes the achievable rates of all users simultaneously.*

Proof. We can consider $\boldsymbol{C}_{\boldsymbol{z}_k}$ from (6.3) as effective noise covariance matrix and apply Theorem 4.4.1 for each receiver U_k separately to obtain that $\boldsymbol{C}_{\boldsymbol{z}_k} \in \mathcal{P}_k,\ \forall k$ is the worst-case. As $\boldsymbol{C}_{\boldsymbol{\xi}_k} \in \mathcal{P}_{\mathrm{B}},\ \forall k$ implies $\boldsymbol{C}_{\boldsymbol{z}_k} - \boldsymbol{C}_{\boldsymbol{\eta}_k} \in \mathcal{P}_k$ (due to compatible channel matrices), we need $\boldsymbol{C}_{\boldsymbol{\eta}_k} \in \mathcal{P}_k$ in order to obtain $\boldsymbol{C}_{\boldsymbol{z}_k} \in \mathcal{P}_k$. □

This result, which applies to the case of a base station that is oblivious of the noise properties and always uses maximum-entropy input signals, can again be extended to optimized transmit strategies.

Corollary 6.5.1. *Let $(\mathcal{P}_k)_{\forall k}$, $\mathcal{P}_{\mathrm{B}}$, and $\mathcal{Q}_{\mathrm{noise}}$ be as in Theorem 6.5.1, but assume that the per-user input covariance matrices $\boldsymbol{C}_{\boldsymbol{\xi}_k}$ are optimized (for given $(\boldsymbol{C}_{\boldsymbol{\eta}_k})_{\forall k}$) to achieve a Pareto-optimal point of the capacity region under a constraint* (3.3) *that is compatible with $\mathcal{P}_{\mathrm{B}}$. Then, maximum-entropy noise with respect to $(\mathcal{P}_k)_{\forall k}$ minimizes the achievable rates of all users simultaneously.*

Proof. This is a consequence of Theorem 6.3.1 combined with Theorem 6.5.1 following the same line of argumentation as Corollary 4.4.1. □

6.6 Complex Multicarrier MIMO BC

From the general model in (3.34), we obtain the description of the complex multicarrier MIMO BC as

$$\boldsymbol{y}_k^{(c)} = \boldsymbol{H}_k^{(c),\mathrm{H}} \boldsymbol{x}^{(c)} + \boldsymbol{\eta}_k^{(c)}, \quad c = 1, \ldots, C \tag{6.9}$$

where we have introduced the abbreviations $\boldsymbol{y}_k^{(c)} = \boldsymbol{y}_{\mathrm{U}_k}^{(c)}$, $\boldsymbol{H}_k^{(c),\mathrm{H}} = \boldsymbol{H}_{\mathrm{U}_k\mathrm{B}}^{(c)}$, $\boldsymbol{x}^{(c)} = \boldsymbol{x}_{\mathrm{B}}^{(c)}$, $\boldsymbol{\eta}_k^{(c)} = \boldsymbol{\eta}_{\mathrm{U}_k}^{(c)}$, $m = m_{\mathrm{B}}$, and $m_k = m_{\mathrm{U}_k}$. We assume a constraint of the form (3.38) for the per-carrier transmit covariance matrices $\boldsymbol{C}_{\boldsymbol{x}^{(c)}}$. To obtain a RoP MIMO system, we make use of the combined real representation of (6.9), which corresponds to setting $\boldsymbol{H}_k^{\mathrm{H}}$ in (6.1) to $\boldsymbol{H}_k^{\mathrm{H}} = \grave{\boldsymbol{H}}_k^{\mathrm{T}} = \grave{\boldsymbol{H}}_{\mathrm{U}_k\mathrm{B}}$ as defined in (3.37).

6.6.1 Optimality of Maximum-Entropy Transmission

In the derivation of the sum rate capacity of the complex MIMO BC with proper noise under a sum power constraint in [46], proper Gaussian signals were used as optimal input distribution, and this result was extended to the whole capacity region under more general covariance constraints in [21]. For the complex multicarrier MIMO BC with CN noise, CN signals were shown to be optimal under a sum power constraint in [49, 50] and for general constraints on the per-carrier covariance matrices in [25].

These results can be obtained as corollaries of Theorem 6.3.1 using the various power shaping spaces from Proposition 3.4.2.

Corollary 6.6.1 ($\mathcal{P}_k = \grave{\mathcal{P}}_{\mathrm{U}_k}^{\mathrm{CN}}$, $\forall k$ and $\mathcal{P}_{\mathrm{B}} = \grave{\mathcal{P}}_{\mathrm{B}}^{\mathrm{CN}}$)**.** *The whole capacity region of the complex multicarrier MIMO BC* (6.9) *with a covariance constraint* (3.38) *is achieved by per-user input signals that are proper and CN if the noise is proper and CN.*

Corollary 6.6.2 ($\mathcal{P}_k = \grave{\mathcal{P}}_{\mathrm{U}_k}$, $\forall k$ and $\mathcal{P}_{\mathrm{B}} = \grave{\mathcal{P}}_{\mathrm{B}}$)**.** *The whole capacity region of the complex (multicarrier) MIMO BC* (6.9) *with a covariance constraint* (3.38) *is achieved by per-user input signals that are proper (but possibly CC) if the noise is proper (but possibly CC).*

Corollary 6.6.3 ($\mathcal{P}_k = \mathcal{P}_{\mathrm{U}_k}^{\mathrm{CN}}$, $\forall k$ and $\mathcal{P}_{\mathrm{B}} = \mathcal{P}_{\mathrm{B}}^{\mathrm{CN}}$)**.** *The whole capacity region of the complex multicarrier MIMO BC* (6.9) *with a covariance constraint* (3.38) *is achieved by per-user input signals that are CN (but possibly improper) if the noise is CN (but possibly improper).*

6.6.2 Optimal Input Covariance Matrices

If the noise is proper and CN as in Corollary 6.6.1, the achievable rates (6.2) with $\mu = \frac{1}{2}$ can be rewritten using Proposition 3.4.5. We obtain

$$r_k^{\mathrm{BC}} = \frac{1}{2}\log_2 \frac{\det \boldsymbol{C}_{\check{\boldsymbol{y}}_k}}{\det \boldsymbol{C}_{\check{\boldsymbol{z}}_k}} = \log_2 \frac{\det \boldsymbol{C}_{\boldsymbol{y}_k}}{\det \boldsymbol{C}_{\boldsymbol{z}_k}} = \sum_{c=1}^{C} \log_2 \frac{\det \boldsymbol{C}_{\boldsymbol{y}_k^{(c)}}}{\det \boldsymbol{C}_{\boldsymbol{z}_k^{(c)}}} = \sum_{c=1}^{C} r_k^{(c)} \tag{6.10}$$

with

$$\boldsymbol{C}_{\boldsymbol{y}_k} = \boldsymbol{C}_{\boldsymbol{\eta}_k} + \sum_{j:\bar{\pi}(j)\geq\bar{\pi}(k)} \boldsymbol{H}_k^{\mathrm{H}} \boldsymbol{C}_{\boldsymbol{\xi}_j} \boldsymbol{H}_k \qquad \text{and} \qquad \boldsymbol{C}_{\boldsymbol{z}_k} = \boldsymbol{C}_{\boldsymbol{y}_k} - \boldsymbol{H}_k^{\mathrm{H}} \boldsymbol{C}_{\boldsymbol{\xi}_k} \boldsymbol{H}_k \tag{6.11}$$

as well as

$$\boldsymbol{C}_{\boldsymbol{y}_k^{(c)}} = \boldsymbol{C}_{\boldsymbol{\eta}_k^{(c)}} + \sum_{j:\bar{\pi}(j)\geq\bar{\pi}(k)} \boldsymbol{H}_k^{(c),\mathrm{H}} \boldsymbol{C}_{\boldsymbol{\xi}_j^{(c)}} \boldsymbol{H}_k^{(c)} \quad \text{and} \quad \boldsymbol{C}_{\boldsymbol{z}_k^{(c)}} = \boldsymbol{C}_{\boldsymbol{y}_k^{(c)}} - \boldsymbol{H}_k^{(c),\mathrm{H}} \boldsymbol{C}_{\boldsymbol{\xi}_k^{(c)}} \boldsymbol{H}_k^{(c)}. \tag{6.12}$$

This means that the achievable rate r_k^{BC} of each user can be expressed as a sum of per-carrier rates $r_k^{(c)}$, and that we can apply the dual decomposition from Section 3.3.2. When optimizing a transmit strategy for the complex multicarrier MIMO BC via the dual MAC, we have the following two possibilities. We can either apply Lagrange duality directly in the BC and make use of uplink-downlink duality on each carrier separately, or we can make use of uplink-downlink duality for the overall system (using the combined real representation) and apply Lagrange duality afterwards in the MAC.

If we drop the assumption of proper CN noise, we can still use uplink-downlink duality in the combined real representation. Then, the comments in Section 5.5.3 apply for the optimization in the dual MAC.

6.6.3 Worst-Case Noise

In [25], it was shown that the worst-case noise in the complex multicarrier MIMO BC under a sum noise power constraint is CN if the input signals of the users are optimized according to the noise properties. Under similar assumptions, proper noise was shown to be the worst-case noise in [21]. The latter result was generalized in [28] to include the case where the per-user input signals are fixed to an arbitrary proper signaling strategy.

These results can be obtained as corollaries of Theorem 6.5.1 using the power shaping spaces from Proposition 3.4.2. The term *optimized* has to be understood in the sense of finding Pareto-optimal solutions under a transmit covariance constraint (3.38).

Corollary 6.6.4 ($\mathcal{P}_k = \grave{\mathcal{P}}_{\mathrm{U}_k}^{\mathrm{CN}},\ \forall k$ and $\mathcal{P}_{\mathrm{B}} = \grave{\mathcal{P}}_{\mathrm{B}}^{\mathrm{CN}}$)**.** *In the complex multicarrier MIMO BC* (6.9) *with constraints on the complex per-carrier noise covariance matrices, the worst-case noise is proper and CN if the per-user input signals are either fixed to be proper and CN or optimized based on the noise properties.*

Corollary 6.6.5 ($\mathcal{P}_k = \grave{\mathcal{P}}_{\mathrm{U}_k},\ \forall k$ and $\mathcal{P}_{\mathrm{B}} = \grave{\mathcal{P}}_{\mathrm{B}}$)**.** *In the complex (multicarrier) MIMO BC* (6.9) *with constraints on the combined complex noise covariance matrices, the worst-case noise is proper if the per-user input signals are either fixed to be proper or optimized based on the noise properties.*

Corollary 6.6.6 ($\mathcal{P}_k = \mathcal{P}_{\mathrm{U}_k}^{\mathrm{CN}},\ \forall k$ and $\mathcal{P}_{\mathrm{B}} = \mathcal{P}_{\mathrm{B}}^{\mathrm{CN}}$)**.** *In the complex multicarrier MIMO BC* (6.9) *with constraints on the per-carrier noise properties, the worst-case noise is CN if the per-user input signals are either fixed to be CN or optimized based on the noise properties.*

6.7 Different Behavior in Case of Suboptimal DPC Schemes

In addition to numerical methods that optimize transmit strategies in the MIMO BC via a transformation to the dual uplink, various suboptimal low-complexity alternatives have been proposed in the literature. An example for this are algorithms that are based on zero-forcing constraints, which demand that the inter-user interference must be completely suppressed by a combination of coding and filtering (for details on transmit and receive filters, see Section 7.1.1).

In [50, 91, 124, 125], we find examples of algorithms that keep the assumption of optimal coding by means of DPC, but design suboptimal per-user input covariance matrices by introducing zero-forcing constraints. In addition, these publications assume that (R)TS is

not applied. A typical approach (e.g,. [50, 91, 125]) is to successively allocate data streams to users based on some heuristic criterion, and to use analytic expressions for choosing the corresponding transmit and receive filters instead of performing a joint iterative optimization of the input covariance matrices.

To investigate how such suboptimal DPC schemes behave, we can consider their characteristic restrictions as system assumptions which restrict the possible solutions to a smaller feasible set. For instance, we can study the rate region of the MIMO BC without (R)TS under zero-forcing constraints. When doing so, the following result is obtained.

Theorem 6.7.1. *Consider the RoP MIMO BC with maximum-entropy noise as in Theorem 6.3.1, but restrict the allowed transmit strategies to a subset of the feasible DPC strategies. Then, the resulting rate region can contain points that are achievable only with reduced-entropy per-user input signals.*

Proof. The proof is postponed to Section 7.5.4 since we can then give a very brief argumentation based on other results from Chapter 7. □

In Chapter 7, we consider the MIMO BC with a restriction to non-DPC strategies which instead treat interference as noise (TIN). It turns out that this restriction leads to the same effect, namely that reduced-entropy transmission can become beneficial. Without Theorem 6.7.1, one might get the idea that this suboptimality of maximum-entropy transmission is specific to TIN strategies. The significance of Theorem 6.7.1 is that it disproves this interpretation. The optimality of maximum-entropy signals is apparently a special property of the capacity-achieving strategy, and it seems that any deviation from this strategy has the potential to render maximum-entropy transmission suboptimal.

Following this train of thought, we could consider TIN strategies as just one example of a class of strategies that are not capacity-achieving. However, as TIN strategies are studied intensely in the literature and are widely applied in practice, they represent a special case of particular importance. Therefore, the whole Chapter 7 is devoted to them.

Chapter 7

The Gaussian MIMO BC with Interference Treated as Noise

We now turn our attention to the MIMO broadcast channel (BC) with the constraint that no nonlinear interference cancellation is employed, i.e., all interference is treated as noise. In the literature, such transmit strategies are also referred to as *linear transceivers* (e.g., [61, 126]) since nonlinear operations (such as encoding, detection, and decoding) are only applied to single data streams while all operations that involve more than one data stream are linear.

In order to be able to adequately treat improper signals, we can apply linear transceivers in the combined real representation, which corresponds to so-called *widely linear* operations in the complex domain (see Definition 2.9.5 and [74]). Widely linear processing has been applied to a large variety of communication systems that employ improper signal constellations (e.g., [31, 35, 127–137]), perform linear-dispersion space-time coding, e.g., [138–141], or encounter improper noise (e.g., [107, 142]) or I/Q imbalance (e.g., [108–110]).

Accordingly, the term MIMO BC with *widely linear transceivers* (e.g., [5]) instead of *linear transceivers* is appropriate to describe that interference is treated as noise in a system with improper signaling. To avoid confusion with this subtle difference, we use the term *treat-interference-as-noise strategies* (TIN strategies), which is meant to include both linear and widely linear transceivers. More details on the concept of widely linear transceivers are given in Section 7.1.3.

Even though they lead to a reduced system performance, i.e., a smaller achievable rate region, TIN strategies are interesting for practical implementation due to the fact that (widely) linear transceivers can be implemented with significantly less complexity than the optimal nonlinear strategy. In the MIMO BC, even approximate implementations of DPC as in [143, 144] require complicated concatenated coding schemes with high complexity [145], and additional problems arise, e.g., due to imperfect channel state information at the transmitter [146]. Also an approximate implementation based on *Tomlinson-Harashima precoding (THP)* has drawbacks such as the shaping, power, and modulo loss [147–149]. Therefore, TIN strategies seem to be an attractive low-complexity alternative and have been intensely studied by researchers and widely applied in practical systems (e.g., [61] and the references therein).

However, while the actual data transmission is simplified by TIN strategies, the process of optimizing the transmit strategy becomes more complicated. Unlike in the case of DPC, we can no longer reformulate the arising optimization problems as convex programs in the dual MAC. Moreover, we see in this chapter that paradigms that are known from the MIMO BC with DPC no longer need to hold when a restriction to TIN strategies is imposed. In particular, it turns out that maximum-entropy transmission is no longer optimal in the MIMO BC with TIN strategies (BC-TIN).

To obtain this result, we need a significantly different proof technique than before. In the system models studied so far, we have shown that maximum-entropy transmission is optimal for arbitrary system dimensions, any channel realization, and under a wide class of transmit constraints. To disprove the optimality of maximum-entropy transmission in the case of TIN strategies, it is sufficient to provide a counterexample, i.e., we only need to find a single combination of system dimensions, channel realization, and transmit constraint for which reduced-entropy transmission can bring a performance gain. We therefore assume a sum power constraint (3.4) throughout this chapter for the sake of simplicity. For the same reason, the systems we consider for proofs of this kind can be very simple cases, e.g., with only one or two carriers or with terminals that have only a single antenna. Constructing examples of larger systems with more carriers and with multiple antennas at all terminals is possible, but not necessarily more insightful.

We first introduce the details of the system model including a filter-based approach that allows for stream-wise decoding. Using this approach, uplink-downlink duality theorems for the MIMO BC-TIN can be established with and without a restriction to maximum-entropy signals. The main part of this chapter is then devoted to showing the possible benefits of reduced-entropy transmission and to study additional aspects that arise in systems without (R)TS, such as the question of so-called quality of service (QoS) feasibility. Finally, we discuss how transmit strategies with reduced-entropy transmission can be optimized using existing algorithms for transceiver design, and we discuss the worst-case noise.

7.1 System Model and Achievable Rates

The system model of the RoP MIMO BC (6.1) is still valid if a restriction to TIN strategies is imposed. However, since an interference cancellation by means of coding (as in DPC) is no longer possible, the transmit signal $\boldsymbol{x}$ is instead constructed by simply summing up the per-user input signals, i.e., $\boldsymbol{x} = \sum_{k=1}^{K} \boldsymbol{\xi}_k$. Consequently, all other users have to be treated as interferers when calculating the achievable rate of a user k.

Even though we cannot show this to be optimal in the RoP MIMO BC-TIN (see also Chapter 10), we keep the assumption that all input signals are Gaussian. This means that all results that are proven for the MIMO BC-TIN in this chapter hold for the case that the input signals are restricted to be Gaussian by assumption. In the RoP MIMO BC-TIN, we can then achieve the per-user rates

$$r_k = \mu \log_2 \frac{\det \boldsymbol{C}_{\boldsymbol{y}_k}}{\det \boldsymbol{C}_{\boldsymbol{z}_k}} = \mu \log_2 \det \left(\mathbf{I}_{M_k} + \boldsymbol{H}_k^{\mathrm{H}} \boldsymbol{C}_{\boldsymbol{\xi}_k} \boldsymbol{H}_k \boldsymbol{C}_{\boldsymbol{z}_k}^{-1} \right) \tag{7.1}$$

with

$$\boldsymbol{C}_{\boldsymbol{y}_k} = \boldsymbol{C}_{\boldsymbol{\eta}_k} + \sum_{j=1}^{K} \boldsymbol{H}_k^{\mathrm{H}} \boldsymbol{C}_{\boldsymbol{\xi}_j} \boldsymbol{H}_k \qquad \text{and} \qquad \boldsymbol{C}_{\boldsymbol{z}_k} = \boldsymbol{C}_{\boldsymbol{y}_k} - \boldsymbol{H}_k^{\mathrm{H}} \boldsymbol{C}_{\boldsymbol{\xi}_k} \boldsymbol{H}_k. \tag{7.2}$$

Accordingly, we can only achieve the rate region

$$\mathcal{R}_{\mathrm{TIN}}(Q) = \bigcup_{\substack{(\boldsymbol{C}_{\boldsymbol{\xi}_k} \succeq \boldsymbol{0})_{\forall k} \\ \mathrm{tr}[\sum_{k=1}^{K} \boldsymbol{C}_{\boldsymbol{\xi}_k}] \leq Q}} \left\{ \boldsymbol{\rho} \in \mathbb{R}_{0,+}^{K} \;\middle|\; \rho_k \leq r_k, \;\; \forall k \right\} \tag{7.3}$$

with r_k from (7.1) instead of the whole capacity region. This rate region is a nonconvex set in general (see, e.g., the plots in [34, 150]), so that allowing (R)TS as described in Section 3.2.1 can lead to enlarged rate regions $\overline{\mathcal{R}}_{\mathrm{TIN}}(Q)$ (with RTS) and $\overline{\overline{\mathcal{R}}}_{\mathrm{TIN}}(Q)$ (with TS).

The difference between $\overline{\overline{\mathcal{R}}}_{\mathrm{TIN}}(Q)$ and the capacity region is that the sum in (7.2) is over all other users while the sum in (6.3) is only over the users encoded after user k. Moreover, we have plugged in the assumption of a sum power constraint. An extension to other types of constraints could of course be considered as well.

7.1.1 Transmit and Receive Filters

To optimize or study TIN strategies, it is convenient to introduce full-rank transmit filter matrices $\boldsymbol{B}_k$ of size $M \times S_k$ (also known as beamforming matrices) with $S_k \leq M$ such that $\boldsymbol{B}_k \boldsymbol{B}_k^{\mathrm{H}} = \boldsymbol{C}_{\boldsymbol{\xi}_k}$. The interpretation is that the input signal $\boldsymbol{\xi}_k$ of user k is constructed as $\boldsymbol{\xi}_k = \boldsymbol{B}_k \boldsymbol{\chi}_k$, where $\boldsymbol{\chi}_k$ is Gaussian with covariance matrix $\boldsymbol{C}_{\boldsymbol{\chi}_k} = \mathbf{I}_{S_k}$, which corresponds to S_k independent data streams. In the complex MIMO BC-TIN, we can assume $\boldsymbol{\xi_k}$ and $\boldsymbol{\chi}_k$ to be proper in case of a RoP MIMO system (Definition 3.1.1). The case of improper input signals is discussed later on in the complex multicarrier MIMO BC-TIN (Section 7.1.3).

Note that the choice of the transmit filter $\boldsymbol{B}_k$ for a given per-user input covariance matrix $\boldsymbol{C}_{\boldsymbol{\xi}_k}$ is not unique. Any transmit filter $\boldsymbol{B}_k' = \boldsymbol{B}_k \boldsymbol{W}_k$ with a unitary matrix $\boldsymbol{W}_k$ leads to the same covariance matrix $\boldsymbol{C}_{\boldsymbol{\xi}_k}$, and thus to the same per-user rates and the same sum transmit power.

In addition, it is often assumed that the received signal at each user terminal is processed by a linear receive filter $\boldsymbol{R}_k^{\mathrm{H}}$ of size $s_k \times M_k$ with $s_k \leq M_k$ in order to obtain an estimate

$$\hat{\boldsymbol{\chi}}_k = \boldsymbol{R}_k^{\mathrm{H}} \boldsymbol{H}_k^{\mathrm{H}} \sum_{j=1}^{K} \boldsymbol{B}_j \boldsymbol{\chi}_j + \boldsymbol{R}_k^{\mathrm{H}} \boldsymbol{\eta}_k. \tag{7.4}$$

The achievable rate of user k is then given by

$$r_k' = \mu \log_2 \frac{\det\left(\boldsymbol{R}_k^{\mathrm{H}} \left(\boldsymbol{C}_{\boldsymbol{\eta}_k} + \sum_{j=1}^{K} \boldsymbol{H}_k^{\mathrm{H}} \boldsymbol{B}_j \boldsymbol{B}_j^{\mathrm{H}} \boldsymbol{H}_k\right) \boldsymbol{R}_k\right)}{\det\left(\boldsymbol{R}_k^{\mathrm{H}} \left(\boldsymbol{C}_{\boldsymbol{\eta}_k} + \sum_{j \neq k} \boldsymbol{H}_k^{\mathrm{H}} \boldsymbol{B}_j \boldsymbol{B}_j^{\mathrm{H}} \boldsymbol{H}_k\right) \boldsymbol{R}_k\right)}. \tag{7.5}$$

If $s_k = S_k$ and each of the receive filter outputs $\hat{\chi}_{k,s} = \mathbf{e}_s^{\mathrm{T}} \hat{\boldsymbol{\chi}}_k$ is decoded separately to recover the information contained in the data stream $\chi_{k,s} = \mathbf{e}_s^{\mathrm{T}} \boldsymbol{\chi}_k$, we obtain

$$r_k'' = \sum_{s=1}^{S_k} \mu \log_2 \left(1 + \frac{\left|\mathbf{e}_s^{\mathrm{T}} \boldsymbol{R}_k^{\mathrm{H}} \boldsymbol{H}_k^{\mathrm{H}} \boldsymbol{B}_k \mathbf{e}_s\right|^2}{\mathbf{e}_s^{\mathrm{T}} \boldsymbol{R}_k^{\mathrm{H}} \left(\boldsymbol{C}_{\boldsymbol{\eta}_k} + \sum_{(j,t) \neq (k,s)} \boldsymbol{H}_k^{\mathrm{H}} \boldsymbol{B}_j \mathbf{e}_t \mathbf{e}_t^{\mathrm{T}} \boldsymbol{B}_j^{\mathrm{H}} \boldsymbol{H}_k\right) \boldsymbol{R}_k \mathbf{e}_s}\right) \tag{7.6}$$

where the other streams of the same user are considered as interference as well (intra-user interference). We have obtained r_k'' in analogy to (7.1) by replacing user k by S_k virtual single-antenna users with channels $\mathbf{e}_s^{\mathrm{T}}\boldsymbol{R}_k^{\mathrm{H}}\boldsymbol{H}_k^{\mathrm{H}}$, noise variances $\mathbf{e}_s^{\mathrm{T}}\boldsymbol{R}_k^{\mathrm{H}}\boldsymbol{C}_{\boldsymbol{\eta}_k}\boldsymbol{R}_k\mathbf{e}_s$, and input covariance matrices $\boldsymbol{B}_k\mathbf{e}_s\mathbf{e}_s^{\mathrm{T}}\boldsymbol{B}_k^{\mathrm{H}}$. The rate r_k'' is in general smaller than (7.1) and (7.5). However, if minimum mean square error (MMSE) receive filters (e.g., [126, Sec. 3.3])

$$\boldsymbol{R}_{k,\mathrm{MMSE}}^{\mathrm{H}} = \boldsymbol{B}_k^{\mathrm{H}}\boldsymbol{H}_k\boldsymbol{C}_{\boldsymbol{y}_k}^{-1} \tag{7.7}$$

are used, we have the following lemma.

Lemma 7.1.1. *For any $\boldsymbol{C}_{\boldsymbol{\xi}_k}$, the transmit filter $\boldsymbol{B}_k$ fulfilling $\boldsymbol{B}_k\boldsymbol{B}_k^{\mathrm{H}} = \boldsymbol{C}_{\boldsymbol{\xi}_k}$ can be chosen such that $\boldsymbol{R}_{k,\mathrm{MMSE}}^{\mathrm{H}}\boldsymbol{H}_k^{\mathrm{H}}\boldsymbol{B}_k$ is diagonal. For this choice of $\boldsymbol{B}_k$, the rate r_k in* (7.1) *is achievable with stream-wise decoding* (7.6) *using the MMSE receiver filter $\boldsymbol{R}_k^{\mathrm{H}} = \boldsymbol{R}_{k,\mathrm{MMSE}}^{\mathrm{H}}$ (i.e., $r_k'' = r_k$).*

Sketch of Proof. A proof for complex systems with proper signals was given in [126, Sec. 3.3] and can be transferred to real-valued systems. Let $\boldsymbol{W}_k$ be a modal matrix of $\boldsymbol{R}_k^{\mathrm{H}}\boldsymbol{H}_k^{\mathrm{H}}\boldsymbol{B}_k$, where $\boldsymbol{R}_k^{\mathrm{H}} = \boldsymbol{R}_{k,\mathrm{MMSE}}^{\mathrm{H}}$. If we then replace $\boldsymbol{B}_k$ and $\boldsymbol{R}_k^{\mathrm{H}}$ by

$$\boldsymbol{B}_k' = \boldsymbol{B}_k\boldsymbol{W}_k \quad \text{and} \quad \boldsymbol{R}_k'^{\mathrm{H}} = \boldsymbol{W}_k^{\mathrm{H}}\boldsymbol{R}_k^{\mathrm{H}} \tag{7.8}$$

$\boldsymbol{R}_k'^{\mathrm{H}}\boldsymbol{H}_k^{\mathrm{H}}\boldsymbol{B}_k'$ is diagonal. In this case, the terms corresponding to intra-user interference in the denominator of (7.6) cancel out, i.e.,

$$r_k'' = \sum_{s=1}^{S_k} \mu \log_2\left(1 + \frac{\left(\mathbf{e}_s^{\mathrm{T}}\boldsymbol{R}_k'^{\mathrm{H}}\boldsymbol{H}_k^{\mathrm{H}}\boldsymbol{B}_k'\mathbf{e}_s\right)^2}{\mathbf{e}_s^{\mathrm{T}}\boldsymbol{R}_k'^{\mathrm{H}}\boldsymbol{C}_{\boldsymbol{z}_k}\boldsymbol{R}_k'\mathbf{e}_s}\right). \tag{7.9}$$

Using the matrix inversion lemma (e.g., [68, Sec. 0.7.4])

$$(\boldsymbol{A}+\boldsymbol{B}\boldsymbol{C}\boldsymbol{D})^{-1} = \boldsymbol{A}^{-1} - \boldsymbol{A}^{-1}\boldsymbol{B}(\boldsymbol{C}^{-1}+\boldsymbol{D}\boldsymbol{A}^{-1}\boldsymbol{B})^{-1}\boldsymbol{D}\boldsymbol{A}^{-1} \tag{7.10}$$

it can then be shown that r_k'' from (7.9) equals r_k from (7.1). For details, see [126, Sec. 3.3]. □

7.1.2 Zero-Forcing

As mentioned for the case of DPC in Section 6.7, a common approach for suboptimal transceiver design is to introduce zero-forcing constraints. If we assume TIN strategies instead of DPC, a partial interference suppression by means of coding is no longer possible. Therefore, the complete inter-user interference has to be eliminated by means of filtering if zero-forcing constraints are imposed in the MIMO BC-TIN.

Zero-forcing has become a key ingredient in many publications on transceiver design for the MIMO BC-TIN (e.g., [91, 124, 125, 145, 151–156]) as it simplifies the arising optimization problems and allows, e.g., for developing simple successive allocation schemes (see also Section 6.7). To study the behavior of such algorithms, we can consider zero-forcing constraints

$$\boldsymbol{R}_k^{\mathrm{H}}\boldsymbol{H}_k^{\mathrm{H}}\boldsymbol{B}_j = \mathbf{0},\ \forall k, \forall j \neq k \quad \Leftrightarrow \quad \boldsymbol{R}_k^{\mathrm{H}}\boldsymbol{H}_k^{\mathrm{H}}\boldsymbol{C}_{\boldsymbol{\xi}_j}\boldsymbol{H}_k\boldsymbol{R}_k = \mathbf{0},\ \forall k, \forall j \neq k \tag{7.11}$$

as a system assumption that reduces the set of feasible transmit strategies and thus leads to a smaller rate region $\mathcal{R}_{\mathrm{TIN-ZF}}(Q) \subseteq \mathcal{R}_{\mathrm{TIN}}(Q)$. By studying reduced-entropy transmission in

the MIMO BC-TIN with zero-forcing constraints, we can derive results that can be used to draw conclusions about the solutions obtained by zero-forcing-based algorithms.

To eliminate all inter-user interference at receiver k, we apply a zero-forcing filter $\boldsymbol{R}_k^{\mathrm{H}} = \boldsymbol{R}_{k,\mathrm{ZF}}^{\mathrm{H}}$ of size $d_k \times M_k$, whose rows are an orthonormal basis of the null space of $\sum_{j \neq k} \boldsymbol{H}_k^{\mathrm{H}} \boldsymbol{C}_{\boldsymbol{\xi}_j} \boldsymbol{H}_k$, where d_k is the dimensionality of this null space. We obtain

$$r_{\mathrm{ZF},k} = \begin{cases} \mu \log_2 \frac{\det\left(\boldsymbol{R}_k^{\mathrm{H}}\left(\boldsymbol{C}_{\boldsymbol{\eta}_k} + \boldsymbol{H}_k^{\mathrm{H}} \boldsymbol{C}_{\boldsymbol{\xi}_k} \boldsymbol{H}_k\right) \boldsymbol{R}_k\right)}{\det\left(\boldsymbol{R}_k^{\mathrm{H}} \boldsymbol{C}_{\boldsymbol{\eta}_k} \boldsymbol{R}_k\right)} & \text{if } d_k > 0 \\ 0 & \text{otherwise} \end{cases} \tag{7.12}$$

with $\boldsymbol{C}_{\boldsymbol{\xi}_k} = \boldsymbol{B}_k \boldsymbol{B}_k^{\mathrm{H}}$. If the number of transmitted streams S_k is smaller than the dimensionality of the null space d_k, we can apply a second filter stage $\tilde{\boldsymbol{R}}_k^{\mathrm{H}}$ of size $S_k \times d_k$, so that $\boldsymbol{R}_k^{\mathrm{H}} = \tilde{\boldsymbol{R}}_k^{\mathrm{H}} \boldsymbol{R}_{k,\mathrm{ZF}}^{\mathrm{H}}$ has size $S_k \times M_k$.

As a stricter version of zero-forcing, we could impose the requirement that all inter-stream interference needs to be suppressed even between streams belonging to the same user (intra-user interference). However, this requirement can always be fulfilled by applying a transformation as in Lemma 7.1.1 (for an example, see the proof of Lemma 7.2.3). It is therefore sufficient to study zero-forcing filters that cancel the inter-user interference.

7.1.3 The Complex Multicarrier MIMO BC-TIN

If we consider the complex multicarrier MIMO BC as given in (6.9) and impose a restriction to TIN strategies, we can still use the four representations from Table 3.1, and the transition between the combined representations and the multicarrier formulations can be done in an analogous manner to the previous chapters. However, when switching between real-valued and complex representations, the following needs to be considered.

In real-valued systems with TIN strategies, we can only apply linear transceivers, i.e., linear transmit and receive filters as introduced above. By contrast, the concept can be extended to widely linear transceivers in a complex system. This is depicted for the combined complex representation in Figure 7.1. Note that the data symbols $\boldsymbol{\chi}_k$ can be chosen to be proper without loss of generality since any desired impropriety can be introduced by the widely linear transmit filters (e.g., [5]).

When switching to the combined real representation (and analogously for the real-valued multicarrier formulation), any widely linear filter is expressed by a real linear filter using (2.38). If the aim is that the data symbols $\boldsymbol{\chi}_k$ are normalized to unit variance both in the complex representation and in the real-valued representation, an additional scaling factor has to be introduced in the transformation since the real-valued symbol vectors $\boldsymbol{\chi}_k$ then need to be a scaled version of the composite real representation of $\boldsymbol{\chi}_k$ due to the factor of $\frac{1}{2}$ in (2.34). As we perform all derivations for which the scaling of the filters matters in the combined real representation, this issue does not arise in the course of this chapter.

The special case of linear transceivers is obtained in Figure 7.1 by setting the conjugate linear filters $\boldsymbol{B}_{\mathrm{CL},k}$ and $\boldsymbol{R}_{\mathrm{CL},k}^{\mathrm{H}}$ of all users k to zero. This is appropriate especially in the case of proper signals, as stated in the following result, which is an extension of [16, Lemma 2].

Proposition 7.1.1. *When using proper Gaussian input signals in the complex (multicarrier) MIMO BC with proper Gaussian noise and a sum power constraint, a rate vector is achievable*

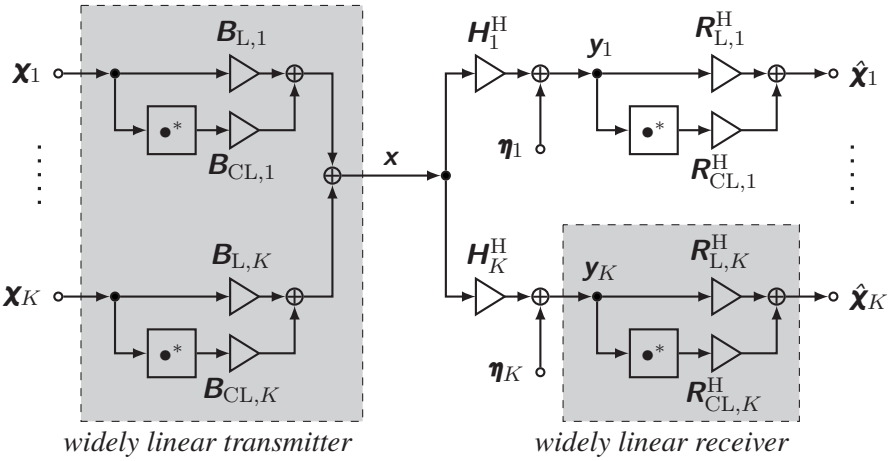

Figure 7.1: The complex MIMO BC-TIN with widely linear transceivers. If the conjugate linear filters $\boldsymbol{B}_{\mathrm{CL},k}$ and $\boldsymbol{R}_{\mathrm{CL},k}^{\mathrm{H}}$ are zero for all users k, we obtain linear transceivers.

with widely linear transceivers if and only if it is also achievable with (strictly) linear transceivers. The same is true in case of zero-forcing constraints.

Sketch of Proof. Since every strictly linear filter is also widely linear, the "if" part is obvious. In the combined real representation (3.37), any desired $\mathcal{SBSC}_2$ input covariance matrix (corresponding to proper signaling) can be created using a $\mathcal{BSC}_2$ transmit filter matrix (corresponding to a complex linear filter), which shows the "only if" part for the transmitter side. The widely linear MMSE filter used at the receiver side becomes a linear filter if all signals in the system are proper (due to [74]). The same is true for a widely linear zero-forcing filter, which can be seen using a similar reasoning as in the proof of Theorem 7.2.2 given later in this chapter. □

Due to this proposition, we can reuse results from the existing literature on linear transceivers whenever we want to study proper signaling. This is sometimes easier than plugging in the special case of proper signaling (i.e., maximum-entropy transmission with respect to the power shaping spaces $\mathcal{P}_k = \grave{\mathcal{P}}_{\mathrm{U}_k}$, $\forall k$ and $\mathcal{P}_{\mathrm{B}} = \grave{\mathcal{P}}_{\mathrm{B}}$) into the combined real representation. On the other hand, by using the combined real representation, we can derive results that not only hold for proper signaling, but for any kind of maximum-entropy transmission.

7.2 Uplink-Downlink Duality

Performing SIC in the uplink seems to be much more realistic than performing DPC in the downlink—in terms of the computational complexity as well as in terms of requirements on the availability of channel state information (e.g., [146]). Therefore, we do not provide a detailed study of the MIMO MAC with TIN strategies (MAC-TIN) as a low-complexity alternative of the MIMO MAC with SIC. Nevertheless, when studying the MIMO BC-TIN, uplink-downlink duality again turns out to be a very useful mathematical tool. We therefore introduce the MIMO MAC-TIN in this section in a way that it serves as the dual uplink of the MIMO BC-TIN.

Although other formulations are possible, e.g., based on [106], the most convenient description for our purposes seems to be the one from [51, 126], which is based on a dual uplink

with flipped whitened channels. That is, we consider the RoP MIMO MAC (5.1) with the noise covariance matrix $\boldsymbol{C}_{\boldsymbol{\eta}} = \mu \mathbf{I}_M$ and the channel matrices

$$\boldsymbol{H}_{\mathrm{UL},k} = \left(\left(\frac{1}{\mu} \boldsymbol{C}_{\boldsymbol{\eta}_k} \right)^{-\frac{1}{2}} \boldsymbol{H}_k^{\mathrm{H}} \right)^{\mathrm{H}} = \sqrt{\mu} \boldsymbol{H}_k \boldsymbol{C}_{\boldsymbol{\eta}_k}^{-\frac{1}{2}} \tag{7.13}$$

where $\boldsymbol{C}_{\boldsymbol{\eta}_k}^{\frac{1}{2}}$ is the positive-semidefinite square root of $\boldsymbol{C}_{\boldsymbol{\eta}_k}$. Note that it would also be possible to instead define the dual uplink with an identity matrix as noise covariance matrix without a dependence on μ. This dependence is just a convention that simplifies switching between different representations because it accounts for the factor of $\frac{1}{2}$ in (2.34).

Due to the restriction to TIN strategies, we must account for the interference from all other users in the rate equation

$$r_k = \mu \log_2 \frac{\det \boldsymbol{X}}{\det \boldsymbol{X}_k} = \mu \log_2 \det \left(\mathbf{I}_M + \boldsymbol{H}_{\mathrm{UL},k} \boldsymbol{C}_{\boldsymbol{x}_k} \boldsymbol{H}_{\mathrm{UL},k}^{\mathrm{H}} \boldsymbol{X}_k^{-1} \right) \tag{7.14}$$

where the covariance matrix $\boldsymbol{X}$ of the received signal and the covariance matrix $\boldsymbol{X}_k$ of the noise-plus-interference for user k are given by[1]

$$\boldsymbol{X} = \mu \mathbf{I}_M + \sum_{j=1}^{K} \boldsymbol{H}_{\mathrm{UL},j} \boldsymbol{C}_{\boldsymbol{x}_j} \boldsymbol{H}_{\mathrm{UL},j}^{\mathrm{H}} \qquad \text{and} \qquad \boldsymbol{X}_k = \boldsymbol{X} - \boldsymbol{H}_{\mathrm{UL},k} \boldsymbol{C}_{\boldsymbol{x}_k} \boldsymbol{H}_{\mathrm{UL},k}^{\mathrm{H}}. \tag{7.15}$$

The corresponding rate region under a sum power constraint without (R)TS is

$$\mathcal{R}_{\mathrm{UL,TIN}}(Q) = \bigcup_{\substack{(\boldsymbol{C}_{\boldsymbol{x}_k} \succeq \mathbf{0})_{\forall k} \\ \mathrm{tr}[\sum_{k=1}^{K} \boldsymbol{C}_{\boldsymbol{x}_k}] \leq Q}} \left\{ \boldsymbol{\rho} \in \mathbb{R}_{0,+}^{K} \;\middle|\; \rho_k \leq r_k, \;\; \forall k \right\} \tag{7.16}$$

with r_k from (7.14). With (R)TS, the enlarged rate regions $\overline{\mathcal{R}}_{\mathrm{UL,TIN}}(Q)$ (with RTS) and $\overline{\overline{\mathcal{R}}}_{\mathrm{UL,TIN}}(Q)$ (with TS) are achievable (see Section 3.2.1).

7.2.1 Transmit and Receive Filters in the Uplink

Similar as in the downlink, we can introduce uplink transmit filters $\boldsymbol{T}_k$ of size $M_k \times s_k$ such that $\boldsymbol{T}_k \boldsymbol{T}_k^{\mathrm{H}} = \boldsymbol{C}_{\boldsymbol{x}_k}$, and uplink receive filters $\boldsymbol{G}_k^{\mathrm{H}}$ of size $S_k \times M$. We obtain the rate equation

$$r_k' = \mu \log_2 \frac{\det \left(\boldsymbol{G}_k^{\mathrm{H}} \left(\mu \mathbf{I}_M + \sum_{j=1}^{K} \boldsymbol{H}_{\mathrm{UL},j} \boldsymbol{T}_j \boldsymbol{T}_j^{\mathrm{H}} \boldsymbol{H}_{\mathrm{UL},j}^{\mathrm{H}} \right) \boldsymbol{G}_k \right)}{\det \left(\boldsymbol{G}_k^{\mathrm{H}} \left(\mu \mathbf{I}_M + \sum_{j \neq k} \boldsymbol{H}_{\mathrm{UL},j} \boldsymbol{T}_j \boldsymbol{T}_j^{\mathrm{H}} \boldsymbol{H}_{\mathrm{UL},j}^{\mathrm{H}} \right) \boldsymbol{G}_k \right)}. \tag{7.17}$$

In the case of stream-wise decoding with $S_k = s_k$, we have

$$r_k'' = \sum_{s=1}^{S_k} \mu \log_2 \left(1 + \frac{\left| \mathbf{e}_s^{\mathrm{T}} \boldsymbol{G}_k^{\mathrm{H}} \boldsymbol{H}_{\mathrm{UL},k} \boldsymbol{T}_k \mathbf{e}_s \right|^2}{\mathbf{e}_s^{\mathrm{T}} \boldsymbol{G}_k^{\mathrm{H}} \left(\mu \mathbf{I}_M + \sum_{(j,t) \neq (k,s)} \boldsymbol{H}_{\mathrm{UL},j} \boldsymbol{T}_j \mathbf{e}_t \mathbf{e}_t^{\mathrm{T}} \boldsymbol{T}_j^{\mathrm{H}} \boldsymbol{H}_{\mathrm{UL},j}^{\mathrm{H}} \right) \boldsymbol{G}_k \mathbf{e}_s} \right). \tag{7.18}$$

Using MMSE receive filters (e.g., [126, Sec. 3.3])

$$\boldsymbol{G}_{k,\mathrm{MMSE}}^{\mathrm{H}} = \boldsymbol{T}_k^{\mathrm{H}} \boldsymbol{H}_{\mathrm{UL},k}^{\mathrm{H}} \boldsymbol{X}^{-1} \tag{7.19}$$

the following lemma holds.

[1] Since these two covariance matrices occur in many derivations, we deviate from our usual notation for covariance matrices and instead use the shorthand notations $\boldsymbol{X}$ and $\boldsymbol{X}_k$ for the sake of notational brevity.

Lemma 7.2.1. *For any $\boldsymbol{C}_{\boldsymbol{x}_k}$, the transmit filter $\boldsymbol{T}_k$ fulfilling $\boldsymbol{T}_k\boldsymbol{T}_k^{\mathrm{H}} = \boldsymbol{C}_{\boldsymbol{x}_k}$ can be chosen such that $\boldsymbol{G}_{k,\mathrm{MMSE}}^{\mathrm{H}}\boldsymbol{H}_{\mathrm{UL},k}\boldsymbol{T}_k$ is diagonal. For this choice of $\boldsymbol{T}_k$, the rate r_k in* (7.14) *is achievable with stream-wise decoding* (7.18) *using the MMSE receiver filter $\boldsymbol{G}_k^{\mathrm{H}} = \boldsymbol{G}_{k,\mathrm{MMSE}}^{\mathrm{H}}$.*

Sketch of Proof. The proof follows the same lines as the proof of Lemma 7.1.1, see also [126, Sec. 3.3]. Using a modal matrix $\boldsymbol{W}_k$ of $\boldsymbol{G}_k^{\mathrm{H}}\boldsymbol{H}_{\mathrm{UL},k}\boldsymbol{T}_k$, where $\boldsymbol{G}_k^{\mathrm{H}} = \boldsymbol{G}_{k,\mathrm{MMSE}}^{\mathrm{H}}$, we set

$$\boldsymbol{T}_k' = \boldsymbol{T}_k\boldsymbol{W}_k \quad \text{and} \quad \boldsymbol{G}_k'^{\mathrm{H}} = \boldsymbol{W}_k^{\mathrm{H}}\boldsymbol{G}_k^{\mathrm{H}} \tag{7.20}$$

and obtain

$$r_k'' = \sum_{s=1}^{S_k} \mu \log_2 \left(1 + \frac{\left(\mathbf{e}_s^{\mathrm{T}}\boldsymbol{G}_k'^{\mathrm{H}}\boldsymbol{H}_{\mathrm{UL},k}\boldsymbol{T}_k'\mathbf{e}_s\right)^2}{\mathbf{e}_s^{\mathrm{T}}\boldsymbol{G}_k'^{\mathrm{H}}\boldsymbol{X}_k\boldsymbol{G}_k'\mathbf{e}_s}\right) \tag{7.21}$$

which can be shown to be equal to (7.14). □

7.2.2 Zero-Forcing in the Uplink

If zero-forcing constraints

$$\boldsymbol{G}_k^{\mathrm{H}}\boldsymbol{H}_{\mathrm{UL},j}\boldsymbol{T}_j = \mathbf{0},\ \forall k, \forall j \neq k \quad \Leftrightarrow \quad \boldsymbol{G}_k^{\mathrm{H}}\boldsymbol{H}_{\mathrm{UL},j}\boldsymbol{C}_{\boldsymbol{x}_j}\boldsymbol{H}_{\mathrm{UL},j}^{\mathrm{H}}\boldsymbol{G}_k = \mathbf{0},\ \forall k, \forall j \neq k \tag{7.22}$$

are imposed, we can use a receive filter $\boldsymbol{G}_k^{\mathrm{H}} = \boldsymbol{G}_{k,\mathrm{ZF}}^{\mathrm{H}}$ of size $M \times D_k$, whose rows are an orthonormal basis of the null space of $\sum_{j\neq k} \boldsymbol{H}_{\mathrm{UL},j}\boldsymbol{C}_{\boldsymbol{x}_j}\boldsymbol{H}_{\mathrm{UL},j}^{\mathrm{H}}$, where D_k is the dimensionality of this null space. We obtain

$$r_{\mathrm{ZF},k} = \begin{cases} \mu \log_2 \det\left(\mathbf{I}_{D_k} + \frac{1}{\mu}\boldsymbol{G}_k^{\mathrm{H}}\boldsymbol{H}_{\mathrm{UL},k}\boldsymbol{C}_{\boldsymbol{x}_k}\boldsymbol{H}_{\mathrm{UL},k}^{\mathrm{H}}\boldsymbol{G}_k\right) & \text{if } D_k > 0 \\ 0 & \text{otherwise} \end{cases} \tag{7.23}$$

with $\boldsymbol{C}_{\boldsymbol{x}_k} = \boldsymbol{T}_k\boldsymbol{T}_k^{\mathrm{H}}$, where we have used $\boldsymbol{G}_k^{\mathrm{H}}\boldsymbol{G}_k = \mathbf{I}_{D_k}$ and the fact that the uplink noise covariance matrix is a scaled identity. The resulting reduced rate region is $\mathcal{R}_{\mathrm{UL,TIN-ZF}}(Q) \subseteq \mathcal{R}_{\mathrm{UL,TIN}}(Q)$. If a smaller number of streams $s_k < D_k$ is transmitted, we can again combine a zero-forcing filter with a second filter stage $\tilde{\boldsymbol{G}}_k^{\mathrm{H}}$ of size $s_k \times D_k$, so that $\boldsymbol{G}_k^{\mathrm{H}} = \tilde{\boldsymbol{G}}_k^{\mathrm{H}}\boldsymbol{G}_{k,\mathrm{ZF}}^{\mathrm{H}}$ has size $s_k \times M$.

7.2.3 Duality Theorem

It was shown in [51], [126, Sec. 3.3] that the complex MIMO BC and MIMO MAC share the same achievable rate region under a sum power constraint if linear transceivers and proper complex signals are employed in both systems. Since the same derivation can also be applied to real-valued systems, we have the following duality lemma for the RoP MIMO BC-TIN.

Lemma 7.2.2. *For any given channel matrices $\boldsymbol{H}_k^{\mathrm{H}}$ and noise covariance matrices $\boldsymbol{C}_{\boldsymbol{\eta}_k}$, the rate region of the RoP MIMO BC-TIN* (7.3) *and the rate region of the dual RoP MIMO MAC-TIN* (7.16) *under a sum power constraint are the same, i.e., $\mathcal{R}_{\mathrm{TIN}}(Q) = \mathcal{R}_{\mathrm{UL,TIN}}(Q)$.*

Sketch of Proof. A proof for complex systems with proper signals was given in [51, Th. IV.1] and can be transferred to real-valued systems. We summarize the main steps in the following.

To study the uplink-to-downlink conversion, let $\boldsymbol{G}_k^{\mathrm{H}} = \boldsymbol{G}_{k,\mathrm{MMSE}}^{\mathrm{H}}$ be the uplink MMSE receive filters (7.19), and use a modal matrix $\boldsymbol{W}_k$ of $\boldsymbol{G}_k^{\mathrm{H}}\boldsymbol{H}_{\mathrm{UL},k}\boldsymbol{T}_k$ to decorrelate the streams by

means of the filters from (7.20). Note that we can assume $\mathbf{e}_s^{\mathrm{T}}\boldsymbol{T}_k'\boldsymbol{T}_k'^{\mathrm{H}}\mathbf{e}_s > 0$ for all streams s of all users k, which can be ensured by removing zero columns from $\boldsymbol{T}_k'$ (and the corresponding rows from $\boldsymbol{G}_k'^{\mathrm{H}}$) [51], i.e., we assume $\boldsymbol{T}_k'$ to be a full-rank tall (or square) matrix.

From (7.21), the rate of the sth stream of user k is then given by $r_{k,s}^{\mathrm{UL}} = \mu \log_2(1+\gamma_{k,s}^{\mathrm{UL}})$ with the signal-to-interference-and-noise ratio (SINR)

$$\gamma_{k,s}^{\mathrm{UL}} = \frac{(\mathbf{e}_s^{\mathrm{T}}\boldsymbol{G}_k'^{\mathrm{H}}\boldsymbol{H}_{\mathrm{UL},k}\boldsymbol{T}_k'\mathbf{e}_s)^2}{\mathbf{e}_s^{\mathrm{T}}\boldsymbol{G}_k'^{\mathrm{H}}\boldsymbol{X}_k\boldsymbol{G}_k'\mathbf{e}_s} \tag{7.24}$$

in the uplink. Assuming stream-wise decoding in the downlink using the filters

$$\boldsymbol{B}_k = \boldsymbol{G}_k'\boldsymbol{A}_k \qquad\qquad \boldsymbol{R}_k^{\mathrm{H}} = \boldsymbol{A}_k^{-1}\boldsymbol{T}_k'^{\mathrm{H}}\left(\frac{1}{\mu}\boldsymbol{C}_{\boldsymbol{\eta}_k}\right)^{-\frac{1}{2}} \tag{7.25}$$

where $\boldsymbol{A}_k = \mathrm{diag}(\alpha_{k,s}),\ \alpha_{k,s} \in \mathbb{R}$, the intra-user interference in the denominator of (7.6) cancels out, and we obtain the per-stream rate $r_{k,s}^{\mathrm{DL}} = \mu \log_2(1+\gamma_{k,s}^{\mathrm{DL}})$ with the SINR

$$\gamma_{k,s}^{\mathrm{DL}} = \frac{(\mathbf{e}_s^{\mathrm{T}}\boldsymbol{R}_k^{\mathrm{H}}\boldsymbol{H}_k^{\mathrm{H}}\boldsymbol{B}_k\mathbf{e}_s)^2}{\mathbf{e}_s^{\mathrm{T}}\boldsymbol{R}_k^{\mathrm{H}}\boldsymbol{C}_{\boldsymbol{z}_k}\boldsymbol{R}_k\mathbf{e}_s} = \frac{\alpha_{k,s}^2(\mathbf{e}_s^{\mathrm{T}}\boldsymbol{T}_k'^{\mathrm{H}}\boldsymbol{H}_{\mathrm{UL},k}^{\mathrm{H}}\boldsymbol{G}_k'\mathbf{e}_s)^2}{\mathbf{e}_s^{\mathrm{T}}\boldsymbol{T}_k'^{\mathrm{H}}\boldsymbol{C}_{\boldsymbol{z}_k'}\boldsymbol{T}_k'\mathbf{e}_s} \tag{7.26}$$

where

$$\boldsymbol{C}_{\boldsymbol{z}_k'} = \left(\frac{1}{\mu}\boldsymbol{C}_{\boldsymbol{\eta}_k}\right)^{-\frac{1}{2}}\boldsymbol{C}_{\boldsymbol{z}_k}\left(\frac{1}{\mu}\boldsymbol{C}_{\boldsymbol{\eta}_k}\right)^{-\frac{1}{2}} = \mu\mathbf{I}_{M_k} + \sum_{j\neq k}\boldsymbol{H}_{\mathrm{UL},k}^{\mathrm{H}}\boldsymbol{G}_j'\boldsymbol{A}_j^2\boldsymbol{G}_j'^{\mathrm{H}}\boldsymbol{H}_{\mathrm{UL},k}. \tag{7.27}$$

We have used (7.2), (7.13), and (7.25) to obtain this reformulation.

To achieve $\gamma_{k,s}^{\mathrm{UL}} = \gamma_{k,s}^{\mathrm{DL}}$ (and thus $r_{k,s}^{\mathrm{UL}} = r_{k,s}^{\mathrm{DL}}$), we need

$$\mathbf{e}_s^{\mathrm{T}}\left(\boldsymbol{A}_k\boldsymbol{G}_k'^{\mathrm{H}}\boldsymbol{X}_k\boldsymbol{G}_k'\boldsymbol{A}_k - \boldsymbol{T}_k'^{\mathrm{H}}\boldsymbol{C}_{\boldsymbol{z}_k'}\boldsymbol{T}_k'\right)\mathbf{e}_s = 0 \tag{7.28}$$

for all streams s of all users k. As shown in detail in the proof of [51, Th. IV.1], this condition can be rewritten as a system of linear equations in the variables $\alpha_{k,s}^2$. Based on results on nonnegative matrices from [157], it can then be shown that there exists a unique set of positive scalars $\alpha_{k,s}^2$ solving this system of equations. Moreover, it can be shown that plugging in this solution into (7.25) leads to downlink transmit filters that require the same sum transmit power as the original uplink transmit filters.

The proof is completed by repeating the same reasoning for the downlink-to-uplink transformation, where the transformation rule is given by

$$\boldsymbol{T}_k = \left(\frac{1}{\mu}\boldsymbol{C}_{\boldsymbol{\eta}_k}\right)^{\frac{1}{2}}\boldsymbol{R}_k'\bar{\boldsymbol{A}}_k \qquad\qquad \boldsymbol{G}_k^{\mathrm{H}} = \bar{\boldsymbol{A}}_k^{-1}\boldsymbol{B}_k'^{\mathrm{H}} \tag{7.29}$$

with $\boldsymbol{R}_k'$ and $\boldsymbol{B}_k'$ from (7.8). The scaling factors contained in the diagonal matrix $\bar{\boldsymbol{A}}_k$ are obtained from solving

$$\mathbf{e}_s^{\mathrm{T}}\left(\bar{\boldsymbol{A}}_k\boldsymbol{R}_k'^{\mathrm{H}}\boldsymbol{C}_{\boldsymbol{z}_k}\boldsymbol{R}_k'\bar{\boldsymbol{A}}_k - \boldsymbol{B}_k'^{\mathrm{H}}\boldsymbol{X}_k'\boldsymbol{B}_k'\right)\mathbf{e}_s = 0 \tag{7.30}$$

where

$$\boldsymbol{X}_k' = \mu\mathbf{I}_M + \sum_{j\neq k}\boldsymbol{H}_j\boldsymbol{R}_j'\bar{\boldsymbol{A}}_j^2\boldsymbol{R}_j'^{\mathrm{H}}\boldsymbol{H}_j^{\mathrm{H}}. \tag{7.31}$$

and $\boldsymbol{C}_{\boldsymbol{z}_k}$ is obtained by setting $\boldsymbol{C}_{\boldsymbol{\xi}_k} = \boldsymbol{B}_k'\boldsymbol{B}_k'^{\mathrm{H}},\ \forall k$ in (7.2). □

As a basis for the further derivations in this chapter, we need to analyze the relation between maximum-entropy transmission in the downlink and in the dual uplink. The result is stated in the following theorem.

Theorem 7.2.1. *Let $(\mathcal{P}_k = \mathcal{P}_{\mathrm{U}_k})_{\forall k}$ and $\mathcal{P}_{\mathrm{B}}$ be power shaping spaces fulfilling the compatibility assumption (Definition 3.1.3). If the noise vectors $\boldsymbol{\eta}_k$ are maximum-entropy signals with respect to $\mathcal{P}_k$, respectively, a rate vector is achievable with sum power Q in the RoP MIMO BC-TIN with maximum-entropy per-user input signals (with respect to the power shaping space $\mathcal{P}_{\mathrm{B}}$) if and only if it is achievable with the same sum power Q in the dual RoP MIMO MAC-TIN with maximum-entropy transmit signals (with respect to the power shaping spaces $(\mathcal{P}_k)_{\forall k}$).*

Proof. We need to show that the transformation derived in the proof of Lemma 7.2.2 leads to maximum-entropy transmission in the downlink if maximum-entropy transmission is used in the uplink and vice versa. For later use, note that $\boldsymbol{C}_{\boldsymbol{\eta}_k}^{-\frac{1}{2}} \in \mathcal{P}_k$ by Corollaries 2.4.1 and 2.4.2, and $\boldsymbol{H}_{\mathrm{UL},k}$ is compatible with $(\mathcal{P}_{\mathrm{B}}, \mathcal{P}_k)$ (see Proposition 2.7.2).

For the uplink-to-downlink transformation, we have to show that all $\boldsymbol{B}_k$ from (7.25) correspond to maximum-entropy transmission with respect to $\mathcal{P}_{\mathrm{B}}$ if all $\boldsymbol{T}_k$ correspond to maximum-entropy transmission with respect to $\mathcal{P}_k$. To this end, we need to study the transformations between several involved power shaping spaces (amongst others due to the transformation with $\boldsymbol{W}_k$) and the properties of the matrix $\boldsymbol{A}_k$ obtained from solving (7.28).

Consider the singular value decomposition $\boldsymbol{T}_k = \boldsymbol{U}_k \boldsymbol{\Sigma}_k \boldsymbol{V}_k^{\mathrm{H}}$ with a tall matrix $\boldsymbol{U}_k$ and square matrices $\boldsymbol{\Sigma}_k$ and $\boldsymbol{V}_k$. If maximum-entropy transmission is employed by user k, we have $\boldsymbol{U}_k \boldsymbol{\Sigma}_k^2 \boldsymbol{U}_k^{\mathrm{H}} = \boldsymbol{T}_k \boldsymbol{T}_k^{\mathrm{H}} \in \mathcal{P}_k$. Then, $\bar{\mathcal{P}}_k = \{\bar{\boldsymbol{P}} \mid \bar{\boldsymbol{P}} = \boldsymbol{V}_k \boldsymbol{U}_k^{\mathrm{H}} \boldsymbol{P} \boldsymbol{U}_k \boldsymbol{V}_k^{\mathrm{H}},\ \boldsymbol{P} \in \mathcal{P}_k\}$ is a power shaping space due to Proposition 2.6.1, and $\boldsymbol{T}_k$ is compatible with $(\mathcal{P}_k, \bar{\mathcal{P}}_k)$. The latter can be seen by noting that $\boldsymbol{\Sigma}_k \in \tilde{\mathcal{P}}_k = \{\tilde{\boldsymbol{P}} \mid \tilde{\boldsymbol{P}} = \boldsymbol{U}_k^{\mathrm{H}} \boldsymbol{P} \boldsymbol{U}_k,\ \boldsymbol{P} \in \mathcal{P}_k\}$ (Corollary 2.6.2 and Corollary 2.4.1) and that $\bar{\mathcal{P}}$ is obtained from $\tilde{\mathcal{P}}$ by applying a transformation with the unitary matrix $\boldsymbol{V}_k$. Moreover, if maximum-entropy transmission is employed by all users, $\boldsymbol{X}^{-1} \in \mathcal{P}_{\mathrm{B}}$ by Corollary 2.4.2, and $\boldsymbol{G}_k^{\mathrm{H}} \boldsymbol{H}_{\mathrm{UL},k} \boldsymbol{T}_k = \boldsymbol{T}_k^{\mathrm{H}} \boldsymbol{H}_{\mathrm{UL},k}^{\mathrm{H}} \boldsymbol{X}^{-1} \boldsymbol{H}_{\mathrm{UL},k} \boldsymbol{T}_k \in \bar{\mathcal{P}}_k$.

Decorrelating the streams by means of (7.20) leads to another power shaping space $\mathcal{P}'_k = \{\boldsymbol{P}' \mid \boldsymbol{P}' = \boldsymbol{W}_k^{\mathrm{H}} \bar{\boldsymbol{P}} \boldsymbol{W}_k,\ \bar{\boldsymbol{P}} \in \bar{\mathcal{P}}_k\}$. In case of maximum-entropy transmission with $\boldsymbol{T}'_k \boldsymbol{T}'^{\mathrm{H}}_k = \boldsymbol{T}_k \boldsymbol{T}_k^{\mathrm{H}} \in \mathcal{P}_k$, the matrix $\boldsymbol{T}'_k$ is compatible with $(\mathcal{P}_k, \mathcal{P}'_k)$. Moreover, if maximum-entropy transmission is employed by all users, $\boldsymbol{G}'^{\mathrm{H}}_k = \boldsymbol{T}'^{\mathrm{H}}_k \boldsymbol{H}_{\mathrm{UL},k}^{\mathrm{H}} \boldsymbol{X}^{-1}$ is compatible with $(\mathcal{P}'_k, \mathcal{P}_{\mathrm{B}})$ (see Proposition 2.7.2). For later use, note that we can choose $\boldsymbol{W}_k$ such that the projection $\mathrm{proj}_{\mathcal{P}'_k}$ to $\mathcal{P}'_k$ commutes with the projection $\mathrm{proj}_{\mathrm{diag}}$ to the space of diagonal matrices (see Corollary 2.6.4).

Let $\boldsymbol{\Xi}_k = \boldsymbol{T}'^{\mathrm{H}}_k \boldsymbol{H}_{\mathrm{UL},k}^{\mathrm{H}} \boldsymbol{X}_k^{-1} \boldsymbol{H}_{\mathrm{UL},k} \boldsymbol{T}'_k$. Applying the matrix inversion lemma (7.10) to $\boldsymbol{X}^{-1} = (\boldsymbol{X}_k + \boldsymbol{H}_{\mathrm{UL},k} \boldsymbol{T}'_k \boldsymbol{T}'^{\mathrm{H}}_k \boldsymbol{H}_{\mathrm{UL},k}^{\mathrm{H}})^{-1}$, we have

$$\boldsymbol{X}^{-1} = \boldsymbol{X}_k^{-1} - \boldsymbol{X}_k^{-1} \boldsymbol{H}_{\mathrm{UL},k} \boldsymbol{T}'_k \left(\mathbf{I}_M + \boldsymbol{T}'^{\mathrm{H}}_k \boldsymbol{H}_{\mathrm{UL},k}^{\mathrm{H}} \boldsymbol{X}_k^{-1} \boldsymbol{H}_{\mathrm{UL},k} \boldsymbol{T}'_k\right)^{-1} \boldsymbol{T}'^{\mathrm{H}}_k \boldsymbol{H}_{\mathrm{UL},k}^{\mathrm{H}} \boldsymbol{X}_k^{-1} \quad (7.32)$$

and we can show that $\boldsymbol{\Xi}_k$ is diagonal (e.g., [51]) since

$$\boldsymbol{\Xi}_k - \boldsymbol{\Xi}_k \left(\mathbf{I}_M + \boldsymbol{\Xi}_k\right)^{-1} \boldsymbol{\Xi}_k = \boldsymbol{G}'^{\mathrm{H}}_k \boldsymbol{H}_{\mathrm{UL},k} \boldsymbol{T}'_k \quad (7.33)$$

is diagonal. Moreover, we have that

$$\begin{aligned} \boldsymbol{\Phi}_k &= \boldsymbol{G}'^{\mathrm{H}}_k \boldsymbol{X}_k \boldsymbol{G}'_k = \boldsymbol{T}'^{\mathrm{H}}_k \boldsymbol{H}_{\mathrm{UL},k}^{\mathrm{H}} \boldsymbol{X}^{-1} \boldsymbol{X}_k \boldsymbol{X}^{-1} \boldsymbol{H}_{\mathrm{UL},k} \boldsymbol{T}'_k \\ &= \boldsymbol{\Xi}_k - 2\boldsymbol{\Xi}_k \left(\mathbf{I}_M + \boldsymbol{\Xi}_k\right)^{-1} \boldsymbol{\Xi}_k + \boldsymbol{\Xi}_k \left(\mathbf{I}_M + \boldsymbol{\Xi}_k\right)^{-1} \boldsymbol{\Xi}_k \left(\mathbf{I}_M + \boldsymbol{\Xi}_k\right)^{-1} \boldsymbol{\Xi}_k \end{aligned} \quad (7.34)$$

is a nonnegative diagonal matrix. From the first line of (7.34), we can see that $\boldsymbol{\Phi}_k \in \mathcal{P}'_k$ if all users employ maximum-entropy transmission since $\boldsymbol{G}'^{\mathrm{H}}_k$ is compatible with $(\mathcal{P}'_k, \mathcal{P}_{\mathrm{B}})$ in that case. We can rewrite (7.28) as

$$0 = \mathbf{e}_s^{\mathrm{T}} \left(\boldsymbol{\Phi}_k^{\frac{1}{2}} \boldsymbol{A}_k^2 \boldsymbol{\Phi}_k^{\frac{1}{2}} - \sum_{j \neq k} \boldsymbol{T}'^{\mathrm{H}}_k \boldsymbol{H}^{\mathrm{H}}_{\mathrm{UL},k} \boldsymbol{G}'_j \boldsymbol{A}_j^2 \boldsymbol{G}'^{\mathrm{H}}_j \boldsymbol{H}_{\mathrm{UL},k} \boldsymbol{T}'_k - \mu \boldsymbol{T}'^{\mathrm{H}}_k \boldsymbol{T}'_k \right) \mathbf{e}_s \tag{7.35}$$

$$= \mathbf{e}_s^{\mathrm{T}} \left(\boldsymbol{L}_{kk} \boldsymbol{A}_k^2 \boldsymbol{L}^{\mathrm{H}}_{kk} - \sum_{j \neq k} \boldsymbol{L}_{kj} \boldsymbol{A}_j^2 \boldsymbol{L}^{\mathrm{H}}_{kj} - \boldsymbol{\Theta}_k \right) \mathbf{e}_s \tag{7.36}$$

where $\boldsymbol{L}_{kj} = \boldsymbol{T}'^{\mathrm{H}}_k \boldsymbol{H}^{\mathrm{H}}_{\mathrm{UL},k} \boldsymbol{G}'_j$, $j \neq k$ is compatible with $(\mathcal{P}'_k, \mathcal{P}'_j)$, $\boldsymbol{L}_{kk} = \boldsymbol{\Phi}_k^{\frac{1}{2}} \in \mathcal{P}'_k$, and $\boldsymbol{\Theta}_k = \mu \boldsymbol{T}'^{\mathrm{H}}_k \boldsymbol{T}'_k \in \mathcal{P}'_k$.

Let $\boldsymbol{A}_k^2 = \boldsymbol{P}'_k + \boldsymbol{N}'_k$ with diagonal matrices $\boldsymbol{P}'_k \in \mathcal{P}'_k$ and $\boldsymbol{N}'_k \in \mathcal{N}'_k$. Since the projections $\mathrm{proj}_{\mathcal{P}'_k}$ and $\mathrm{proj}_{\mathrm{diag}}$ commute, the unique solution for the set of scalars $\alpha^2_{k,s}$ must solve the two systems of equations

$$0 = \mathbf{e}_s^{\mathrm{T}} \left(\boldsymbol{L}_{kk} \boldsymbol{P}'_k \boldsymbol{L}^{\mathrm{H}}_{kk} - \sum_{j \neq k} \boldsymbol{L}_{kj} \boldsymbol{P}'_j \boldsymbol{L}^{\mathrm{H}}_{kj} - \boldsymbol{\Theta}_k \right) \mathbf{e}_s, \quad \forall k, \forall s, \tag{7.37}$$

$$0 = \mathbf{e}_s^{\mathrm{T}} \left(\boldsymbol{L}_{kk} \boldsymbol{N}'_k \boldsymbol{L}^{\mathrm{H}}_{kk} - \sum_{j \neq k} \boldsymbol{L}_{kj} \boldsymbol{N}'_j \boldsymbol{L}^{\mathrm{H}}_{kj} \right) \mathbf{e}_s, \quad \forall k, \forall s. \tag{7.38}$$

The homogeneous system of equations (7.38) is solved by setting $\boldsymbol{N}'_k = \mathbf{0}$ for all k. From this, we see that the solution to (7.36) fulfills $\boldsymbol{A}_k^2 = \boldsymbol{P}'_k \in \mathcal{P}'$ for all users k. As a result, $\boldsymbol{B}_k \boldsymbol{B}_k^{\mathrm{H}} = \boldsymbol{G}'_k \boldsymbol{A}_k^2 \boldsymbol{G}'^{\mathrm{H}}_k \in \mathcal{P}_{\mathrm{B}}$, i.e., the solution corresponds to maximum-entropy transmission in the downlink.

The proof is completed by repeating the same reasoning for the downlink-to-uplink transformation. □

Due to this Theorem, we can prove all further statements in this chapter via the dual uplink whenever this is more convenient. If we do so, no further justification for switching to the uplink is given.

7.2.4 Duality Theorem with Zero-Forcing

For the case with zero-forcing constraints, we can establish an analogous uplink-downlink duality.

Lemma 7.2.3. *For any given channel matrices $\boldsymbol{H}_k^{\mathrm{H}}$ and noise covariance matrices $\boldsymbol{C}_{\boldsymbol{\eta}_k}$, the rate region of the RoP MIMO BC-TIN with zero-forcing constraints (Section 7.1.2) and the rate region of the dual RoP MIMO MAC-TIN with zero-forcing constraints (Section 7.2.2) under a sum power constraint are the same, i.e., $\mathcal{R}_{\mathrm{TIN-ZF}}(Q) = \mathcal{R}_{\mathrm{UL,TIN-ZF}}(Q)$.*

Proof. Given uplink transmit filters $\boldsymbol{T}_k$, we can obtain $\boldsymbol{G}^{\mathrm{H}}_{k,\mathrm{ZF}}$ (see Section 7.2.2) from the eigenvalue decomposition of the interference covariance matrix

$$\sum_{j \neq k} \boldsymbol{H}_{\mathrm{UL},j} \boldsymbol{T}_j \boldsymbol{T}_j^{\mathrm{H}} \boldsymbol{H}^{\mathrm{H}}_{\mathrm{UL},j} = [\boldsymbol{G}_{k,0},\ \boldsymbol{G}_{k,\mathrm{ZF}}] \begin{bmatrix} \boldsymbol{\Lambda} & \\ & \mathbf{0} \end{bmatrix} [\boldsymbol{G}_{k,0},\ \boldsymbol{G}_{k,\mathrm{ZF}}]^{\mathrm{H}} \tag{7.39}$$

with $\boldsymbol{\Lambda} \succ \mathbf{0}$. Letting $\boldsymbol{H}_{\mathrm{eff},k} = \boldsymbol{G}_{k,\mathrm{ZF}}^{\mathrm{H}} \boldsymbol{H}_{\mathrm{UL},k}$, we can apply the proof of Lemma 7.2.2 individually to K separate single-user systems, where the uplink channels $\boldsymbol{H}_{\mathrm{UL},k}$ are replaced by the effective channels $\boldsymbol{H}_{\mathrm{eff},k}$, and no interference is present. Note that the MMSE filter $\boldsymbol{G}_k^{\mathrm{H}}$ from (7.19) with $\boldsymbol{H}_{\mathrm{UL},k}$ replaced by $\boldsymbol{H}_{\mathrm{eff},k}$ then acts as a second filter stage. This delivers a downlink solution that achieves the same rates with the same per-user powers in the equivalent single-user systems, but it remains to be shown that this solution fulfills the zero-forcing constraints and the power constraint in the original system where $\boldsymbol{G}_{k,\mathrm{ZF}}$ is no longer considered as a part of an effective channel. The transmit filters in the original downlink system are given by $\boldsymbol{B}_k'' = \boldsymbol{G}_{k,\mathrm{ZF}} \boldsymbol{B}_k$. Using $\boldsymbol{R}_k^{\mathrm{H}}$ from (7.25), we have

$$\boldsymbol{R}_k^{\mathrm{H}} \boldsymbol{H}_k^{\mathrm{H}} \boldsymbol{B}_j'' = \boldsymbol{A}_k^{-1} \boldsymbol{W}_k^{\mathrm{H}} \boldsymbol{T}_k^{\mathrm{H}} \left(\frac{1}{\mu} \boldsymbol{C}_{\boldsymbol{\eta}_k} \right)^{-\frac{1}{2}} \boldsymbol{H}_k^{\mathrm{H}} \boldsymbol{G}_{j,\mathrm{ZF}} \boldsymbol{B}_j = \mathbf{0} \tag{7.40}$$

for all k and $j \neq k$ since $\boldsymbol{G}_{j,\mathrm{ZF}}^{\mathrm{H}} \boldsymbol{H}_{\mathrm{UL},k} \boldsymbol{T}_k = \mathbf{0}$ holds due to the zero-forcing in the uplink. Thus, the zero-forcing constraints in the downlink are fulfilled. Moreover,

$$\mathrm{tr}[\boldsymbol{B}_k'' \boldsymbol{B}_k''^{\mathrm{H}}] = \mathrm{tr}[\boldsymbol{G}_{k,\mathrm{ZF}} \boldsymbol{B}_k \boldsymbol{B}_k^{\mathrm{H}} \boldsymbol{G}_{k,\mathrm{ZF}}^{\mathrm{H}}] = \mathrm{tr}[\boldsymbol{B}_k \boldsymbol{B}_k^{\mathrm{H}}] \tag{7.41}$$

since $\boldsymbol{G}_{k,\mathrm{ZF}}$ has orthonormal columns, which shows that using $\boldsymbol{G}_{k,\mathrm{ZF}}$ as a second transmit filter stage in the downlink does not change the transmit power. The proof is completed by repeating the same reasoning for the downlink-to-uplink transformation, where we perform the eigenvalue decomposition

$$\sum_{j \neq k} \boldsymbol{H}_k^{\mathrm{H}} \boldsymbol{B}_j \boldsymbol{B}_j^{\mathrm{H}} \boldsymbol{H}_k = [\boldsymbol{R}_{k,0},\ \boldsymbol{R}_{k,\mathrm{ZF}}] \begin{bmatrix} \boldsymbol{\Lambda} & \\ & \mathbf{0} \end{bmatrix} [\boldsymbol{R}_{k,0},\ \boldsymbol{R}_{k,\mathrm{ZF}}]^{\mathrm{H}} \tag{7.42}$$

and use the effective channels $\boldsymbol{H}_{\mathrm{eff},k}^{\mathrm{H}} = \boldsymbol{R}_{k,\mathrm{ZF}}^{\mathrm{H}} \boldsymbol{H}_k^{\mathrm{H}}$. □

Theorem 7.2.2. *The statement of Theorem 7.2.1 holds analogously if zero-forcing constraints are imposed both in the uplink and in the downlink.*

Proof. Note that $\boldsymbol{H}_{\mathrm{UL},k}$ is compatible with $(\mathcal{P}_{\mathrm{B}}, \mathcal{P}_k)$ (see the proof of Theorem 7.2.1). If all users apply maximum-entropy transmission in the uplink, we have $\sum_{j \neq k} \boldsymbol{H}_{\mathrm{UL},j} \boldsymbol{T}_k \boldsymbol{T}_k^{\mathrm{H}} \boldsymbol{H}_{\mathrm{UL},j}^{\mathrm{H}} \in \mathcal{P}_{\mathrm{B}}$, and we can apply Corollary 2.6.2 to (7.39). This introduces new power shaping spaces $\tilde{\mathcal{P}}_k = \{\tilde{\boldsymbol{P}} \mid \tilde{\boldsymbol{P}} = \boldsymbol{G}_{k,\mathrm{ZF}}^{\mathrm{H}} \boldsymbol{P} \boldsymbol{G}_{k,\mathrm{ZF}},\ \boldsymbol{P} \in \mathcal{P}_{\mathrm{B}}\}$, where $\boldsymbol{G}_{k,\mathrm{ZF}}^{\mathrm{H}}$ is compatible with $(\tilde{\mathcal{P}}_k, \mathcal{P}_{\mathrm{B}})$, and $\boldsymbol{H}_{\mathrm{eff},k}$ is compatible with $(\tilde{\mathcal{P}}_k, \mathcal{P}_k)$ due to Proposition 2.7.2. As the further proof of Lemma 7.2.3 is based on the duality from Lemma 7.2.2, we can apply the steps from the proof of Theorem 7.2.1 to see that $\boldsymbol{B}_k \boldsymbol{B}_k^{\mathrm{H}} \in \tilde{\mathcal{P}}_k$. Consequently, we have $\boldsymbol{B}_k'' \boldsymbol{B}_k''^{\mathrm{H}} = \boldsymbol{G}_{k,\mathrm{ZF}} \boldsymbol{B}_k \boldsymbol{B}_k^{\mathrm{H}} \boldsymbol{G}_{k,\mathrm{ZF}}^{\mathrm{H}} \in \mathcal{P}_{\mathrm{B}}$ for the input covariance matrix in the original downlink system. The proof is completed by repeating the same reasoning for the downlink-to-uplink transformation. □

7.2.5 Uplink-Downlink Duality for the Complex Multicarrier MIMO BC-TIN

Let us now summarize the implications of the above duality results for the complex multicarrier MIMO BC (6.9) with a restriction to TIN strategies. The combined real uplink channel matrices are then defined via

$$\boldsymbol{H}_{\mathrm{UL},k} = \grave{\boldsymbol{H}}_k \left(2 \boldsymbol{C}_{\tilde{\boldsymbol{\eta}}_k} \right)^{-\frac{1}{2}} \tag{7.43}$$

which is obtained from (7.13) with $\mu = \frac{1}{2}$. If the noise is proper and CN, $\boldsymbol{H}_{\mathrm{UL},k}$ has the structure that we expect from a combined real channel matrix, i.e., $\boldsymbol{H}_{\mathrm{UL},k} = \grave{\boldsymbol{H}}_{\mathrm{UL},k}$ is a $\mathcal{BSC}_2$ matrix with block-diagonal submatrices. The corresponding complex channel matrix on carrier c can then be expressed as

$$\boldsymbol{H}_{\mathrm{UL},k}^{(c)} = \boldsymbol{H}_{k}^{(c)} \boldsymbol{C}_{\boldsymbol{\eta}_k^{(c)}}^{-\frac{1}{2}} \tag{7.44}$$

where we have used that $\boldsymbol{C}_{\grave{\boldsymbol{\eta}}_k} = \frac{1}{2}\Re(\boldsymbol{C}_{\boldsymbol{\eta}_k})$ due to (2.34).

If the downlink noise is CC, the transmission on the various carriers of the dual uplink is no longer orthogonal. Analogously, the uplink is a widely linear system instead of a linear one if the downlink noise is improper. In these cases, we cannot describe the dual uplink by matrices $\boldsymbol{H}_{\mathrm{UL},k}^{(c)}$. However, this does not lead to any problems as long as we perform our derivations in the combined real representation. The only thing that has to be kept in mind is that $\boldsymbol{H}_{\mathrm{UL},k}$ is then not necessarily compatible with the power shaping spaces under consideration.

From the two duality theorems shown above, we obtain the following corollaries for various types of entropy reduction. The first of them was used implicitly in [1], and the second one was proven and exploited in [16].

Corollary 7.2.1 ($\mathcal{P}_k = \grave{\mathcal{P}}_{\mathrm{U}_k}^{\mathrm{CN}}$, $\forall k$ and $\mathcal{P}_{\mathrm{B}} = \grave{\mathcal{P}}_{\mathrm{B}}^{\mathrm{CN}}$)**.** *In the complex multicarrier MIMO BC-TIN with proper CN noise, a rate vector is achievable with sum power Q using proper CN input signals if and only if it is achievable with the same sum power Q in the dual MIMO MAC-TIN using proper CN transmit signals. The same is true in case of zero-forcing constraints.*

Corollary 7.2.2 ($\mathcal{P}_k = \grave{\mathcal{P}}_{\mathrm{U}_k}$, $\forall k$ and $\mathcal{P}_{\mathrm{B}} = \grave{\mathcal{P}}_{\mathrm{B}}$)**.** *In the complex (multicarrier) MIMO BC-TIN with proper noise, a rate vector is achievable with sum power Q using proper input signals if and only if it is achievable with the same sum power Q in the dual MIMO MAC-TIN using proper transmit signals. The same is true in case of zero-forcing constraints.*

Corollary 7.2.3 ($\mathcal{P}_k = \mathcal{P}_{\mathrm{U}_k}^{\mathrm{CN}}$, $\forall k$ and $\mathcal{P}_{\mathrm{B}} = \mathcal{P}_{\mathrm{B}}^{\mathrm{CN}}$)**.** *In the complex multicarrier MIMO BC-TIN with CN noise, a rate vector is achievable with sum power Q using CN input signals if and only if it is achievable with the same sum power Q in the dual MIMO MAC-TIN using CN transmit signals. The same is true in case of zero-forcing constraints.*

7.3 Optimization of the Transmit Covariance Matrices

When trying to find Pareto-optimal transmit strategies for the MIMO BC-TIN, we are facing the problem that the rate equations (7.1) are not concave in the input covariance matrices. Unfortunately, going via the dual uplink, as we did in Chapter 6 for the MIMO BC with DPC, does not help either since the uplink rates (7.14) are nonconcave functions as well if all interference is treated as noise. Filter-based formulations as in (7.5) and (7.17) do not lead to more tractable expressions either. Therefore, we cannot express transceiver optimizations for the MIMO BC-TIN as convex programs, meaning that there is no simple way to find globally optimal solutions to such optimizations.

Several suboptimal approaches can be found in the literature, e.g., for weighted sum rate maximization (3.12) in [145, 151, 153–155, 158–160], for weighted sum rate maximization with additional constraints on the per-user rates in [91, 93, 96], for rate balancing (3.13) in [9, 93, 161], and for minimization of the total transmit power under constraints on the per-user

rates in [2, 88, 89, 91–93, 156, 161, 162]. We discuss some of these suboptimal algorithms in Section 7.6, but as an ingredient for the proofs in the following sections, we need a method that is able to find globally optimal transmit strategies instead.

7.3.1 Globally Optimal Rate Balancing in the RoP MISO BC-TIN

To simplify the problem, we restrict ourselves to the special case of single-antenna users, i.e., to the RoP multiple-input single-output (MISO) BC. While the weighted sum rate maximization is still a difficult nonconvex problem in this setting (see, e.g., [163]), the abovementioned power minimization and the so-called SINR balancing problem can be solved efficiently in this case [94, 162, 164] as long as we do not allow (R)TS. These approaches can be easily extended to the rate balancing problem (3.13) as shown, e.g., in [9], [97, Sec. 4.1.3].

However, when applying the dual approach from Sections 3.2.3.1 and 3.2.3.2 in order to solve the rate balancing problem with TS or RTS, we need to find a solution to the inner problem (3.19) or (3.24), respectively, which is difficult due to the nonconcave weighted sum rate in the objective functions of these problems. In this section, we propose an algorithm for the rate balancing problem with TS based on the branch-and-bound method (e.g., [165, Sec. 6.2]). We briefly comment on the case with RTS afterwards.

7.3.1.1 Branch-And-Bound Method

The branch-and-bound method is summarized below in Algorithm 7.3.1. It needs to be initialized with a collection $\mathbb{B}$ of disjoint sets $\mathcal{B}$ such that the optimizer is contained in one of the sets $\mathcal{B} \in \mathbb{B}$. To implement the method, we have to decide for a subdivision rule that divides a set $\mathcal{B}$ into disjoint sets $\mathcal{B}_1$ and $\mathcal{B}_2$ such that $\mathcal{B} = \mathcal{B}_1 \cup \mathcal{B}_2$. Moreover, we need a method to calculate an upper bound $U(\mathcal{B}) \geq f(\boldsymbol{p}),\ \forall \boldsymbol{p} \in \mathcal{B}$ and an achievable value $L(\mathcal{B}) = f(\boldsymbol{p})$ for some $\boldsymbol{p} \in \mathcal{B}$, where f is the function to be maximized.

Algorithm 7.3.1 Branch-and-Bound Method

1. Find the set with the highest upper bound, i.e., $\hat{\mathcal{B}} = \operatorname{argmax}_{\mathcal{B}\in\mathbb{B}} U(\mathcal{B})$.
2. Replace $\mathbb{B}$ by $(\mathbb{B} \setminus \{\hat{\mathcal{B}}\}) \cup \{\mathcal{B}_1, \mathcal{B}_2\}$ where $\mathcal{B}_1$ and $\mathcal{B}_2$ form a subdivision of $\hat{\mathcal{B}}$.
3. Repeat Steps 1. and 2. until $\max_{\mathcal{B}\in\mathbb{B}} U(\mathcal{B}) - \max_{\mathcal{B}\in\mathbb{B}} L(\mathcal{B}) \leq \epsilon$.
4. Return the vector $\boldsymbol{p}$ that achieves $\max_{\mathcal{B}\in\mathbb{B}} L(\mathcal{B})$.

Convergence of the method can be shown (see [165, Sec. 6.2]) if the subdivision rule is exhaustive, i.e., the sets $\mathcal{B}$ finally converge to singletons, and if the utopian bound $U(\mathcal{B})$ is consistent, i.e., it converges to an achievable value when the set $\mathcal{B}$ converges to a singleton. The stopping criterion in Step 3 leads to an ϵ-optimal solution, i.e., the obtained value $f(\boldsymbol{p})$ is at most ϵ away from the global optimum.

7.3.1.2 Application to the Rate Balancing Problem with TS

To solve the rate balancing problem with TS in the RoP MISO BC-TIN, we can apply the dual approach from Section 3.2.3.1 if we have a solver for the inner problem (3.19). Accordingly, with a solver for (3.33), the dual decomposition from Section 3.3.2 can be applied in the RoP CN MISO BC-TIN. Therefore, we now discuss how the branch-and-bound method can be applied to solve problem (3.19) or (3.33).

To this end, we exploit that the transmit covariance matrices degenerate to scalar variances C_{x_k} in the dual uplink of the RoP MISO BC-TIN, i.e., the transmit strategy is completely determined by the per-user transmit powers $(p_k = C_{x_k})_{\forall k}$. As the analogous statement holds in a carrier-wise manner for each carrier of the RoP CN MISO BC-TIN, the following derivation can be easily extended to solve (3.33).

We let $f(\boldsymbol{p})$ denote the objective function of (3.19) with r_k from (7.14), and we introduce the function

$$F(\boldsymbol{p}, \bar{\boldsymbol{p}}) = \sum_{k=1}^{K} \mathbf{e}_k^{\mathrm{T}} \boldsymbol{\nu}_1 \, \mu \log_2 \left(1 + p_k \boldsymbol{h}_{\mathrm{UL},k}^{\mathrm{H}} \left(\mu \mathbf{I}_M + \sum_{j \neq k} \bar{p}_j \boldsymbol{h}_{\mathrm{UL},j} \boldsymbol{h}_{\mathrm{UL},j}^{\mathrm{H}} \right)^{-1} \boldsymbol{h}_{\mathrm{UL},k} \right) - \boldsymbol{\nu}_2^{\mathrm{T}} \bar{\boldsymbol{p}} \quad (7.45)$$

so that $F(\boldsymbol{p}, \boldsymbol{p}) = f(\boldsymbol{p})$.

It can be easily verified (e.g., by calculating the partial derivatives) that the function F is nondecreasing in $\boldsymbol{p}$ and nonincreasing in $\bar{\boldsymbol{p}}$. Consequently, if the considered sets are boxes $\mathcal{B} = [\boldsymbol{a},\ \boldsymbol{b}] = \{\boldsymbol{p} \mid \boldsymbol{a} \leq \boldsymbol{p} \leq \boldsymbol{b}\}$, it holds that

$$f(\boldsymbol{p}) = F(\boldsymbol{p}, \boldsymbol{p}) \leq \underbrace{F(\boldsymbol{b}, \boldsymbol{a})}_{U([\boldsymbol{a},\ \boldsymbol{b}])}, \ \forall \boldsymbol{p} \in [\boldsymbol{a},\ \boldsymbol{b}]\,. \quad (7.46)$$

Even though there is usually no $\boldsymbol{p} \in [\boldsymbol{a},\ \boldsymbol{b}]$ fulfilling (7.46) with equality, this bound becomes tight as $\boldsymbol{b} - \boldsymbol{a} \to \mathbf{0}$, i.e., this utopian bound is consistent. On the other hand, an achievable value of $f(\boldsymbol{p})$ inside a box $[\boldsymbol{a},\ \boldsymbol{b}]$ is, e.g., given by $L([\boldsymbol{a},\ \boldsymbol{b}]) = F(\boldsymbol{a}, \boldsymbol{a}) = f(\boldsymbol{a})$.

An exhaustive subdivision rule that is appropriate for boxes $\mathcal{B} = [\boldsymbol{a},\ \boldsymbol{b}]$ is the adaptive bisection [165, Sec. 6.2]

$$\mathcal{B}_1 = \left[\boldsymbol{a},\ \boldsymbol{b} - \frac{b_{k^\star} - a_{k^\star}}{2} \boldsymbol{e}_{k^\star} \right] \quad \text{and} \quad \mathcal{B}_2 = \left[\boldsymbol{a} + \frac{b_{k^\star} - a_{k^\star}}{2} \boldsymbol{e}_{k^\star},\ \boldsymbol{b} \right] \quad (7.47)$$

where

$$k^\star = \underset{k \in \{1,\ldots,K\}}{\operatorname{argmax}} \ b_k - a_k. \quad (7.48)$$

This can be interpreted as cutting the $\mathcal{B}$ box along its longest edge into two subboxes.

To obtain an initial set $\mathbb{B}$, we introduce the functions

$$\hat{f}_k(p_k) = \mathbf{e}_k^{\mathrm{T}} \boldsymbol{\nu}_1 \, \mu \log_2 \left(1 + \frac{1}{\mu} p_k \boldsymbol{h}_{\mathrm{UL},k}^{\mathrm{H}} \boldsymbol{h}_{\mathrm{UL},k} \right) - \mathbf{e}_k^{\mathrm{T}} \boldsymbol{\nu}_2 p_k \quad (7.49)$$

so that $\hat{f}(\boldsymbol{p}) = \sum_{k=1}^{K} \hat{f}_k(p_k)$ is an upper bound to $f(\boldsymbol{p})$. As $\hat{f}_k(p_k)$ is concave and tends to $-\infty$ for $p_k \to \infty$ (due to the sublinear growth of the logarithm), we can find $\hat{f}_{\max,k} =$

$\max_{p_k \geq 0} \hat{f}_k(p_k)$ for all k. Moreover, we can apply simple root finding to find a value $p_{0,k}$ such that $\hat{f}_k(p_k) + \sum_{j \neq k} \hat{f}_{\max,j} \leq 0, \ \forall p_k \geq p_{0,k}$. As choosing $p_k \geq p_{0,k}$ for any k then implies that $\hat{f}(\boldsymbol{p}) \leq 0$, all positive values of $\hat{f}(\boldsymbol{p})$ lie in $[\mathbf{0}, \ \boldsymbol{p}_0]$, where $\boldsymbol{p}_0 = [p_{0,1}, \ldots, p_{0,K}]^{\mathrm{T}}$. Since $f(\mathbf{0}) = 0$ is an achievable value and $f(\boldsymbol{p}) \leq \hat{f}(\boldsymbol{p})$, the maximum of f is surely contained in $[\mathbf{0}, \ \boldsymbol{p}_0]$, and we can use the initialization $\mathbb{B} = \{[\mathbf{0}, \ \boldsymbol{p}_0]\}$.

These choices for the initialization, the upper bound, and the subdivision rule fulfill the requirements stated in Section 7.3.1.1. It is thus guaranteed that the proposed application of the branch-and-bound method converges to an ϵ-optimal solution of (3.19). By choosing ϵ small enough, an arbitrarily precise solution to the overall problem (3.15) can be obtained if enough computation time is invested (see Section 7.3.1.5).

7.3.1.3 Application to the Rate Balancing Problem with RTS

When applying the method to solve problem (3.24) for the case of RTS in the dual uplink of the RoP MISO BC-TIN, the difference is that we have a compact constraint set in (3.24). The initialization can then be done by finding a box $\mathcal{B}$ such that all feasible power vectors $\boldsymbol{p}$ are contained in $\mathcal{B}$. As the rectangular shape of the boxes does not fit to the shape of the upper boundary of the constraint set, e.g., in case of a sum power constraint $\sum_{k=1}^{K} p_k \leq Q$, a so-called reduction step as described in [166] should be incorporated into the algorithm. As an alternative, we can add a step that drops boxes which do not contain any feasible point.

7.3.1.4 Related Approaches

A problem equivalent to (3.19) arises as a subproblem of the power minimization with TS performed in [3]. To solve this problem, a similar monotonic optimization method as above was applied, but with the per-user rates as optimization variables instead of the per-user powers. The advantage of the above formulation is that the rates as a function of the powers can be calculated explicitly while it is necessary to apply an iterative numerical algorithm to calculate the powers as a function of the rates. This means that an inner loop is executed whenever $U(\mathcal{B})$ and $L(\mathcal{B})$ are calculated in the method used in [3].

Other examples of monotonic optimization approaches for solving nonconvex transceiver optimization problems using the branch-and-bound method can be found, e.g., in [10, 14, 167]. In [97, 163, 168–171], the so-called polyblock method (e.g., [165, Sec. 11.2]) was used, which can be considered as a modified branch-and-bound method.

7.3.1.5 Computational Complexity

The striking disadvantage of all these methods including the one proposed above is that their worst-case complexity order is $\left(\frac{c_1}{\epsilon}\right)^{\frac{N}{c_2}}$, where c_1 and c_2 are constants that depend on properties of the objective function, and N is the number of optimization variables. This can be concluded from [172, Theorem 4], and it means that the complexity of the above method is exponential in the number of users K. However, for the considered nonconvex problem, no globally optimal solution with lower complexity order is known. Therefore, suboptimal methods for transceiver design as discussed in Section 7.6 are more appropriate for practical implementations, but whenever we need a globally optimal solution as a benchmark in offline simulations or as an

ingredient of a proof, it can make sense to resort to algorithms based on the branch-and-bound method.

7.4 Benefits of Reduced-Entropy Transmission

In Chapter 6, we considered the MIMO BC with nonlinear interference cancellation using DPC, and we showed that maximum-entropy per-user input signals are optimal if maximum-entropy noise is assumed. If we instead consider TIN strategies, this result changes completely. Even if we keep all other assumptions unchanged—in particular, we still allow for (R)TS—it can happen that maximum-entropy transmission no longer achieves the whole rate region if the MIMO BC-TIN is considered.

Due to the different nature of this result, it also requires a different proof technique. So far, we have proven theorems stating that reduced-entropy transmission can never bring a gain in certain scenarios. Now, we want to show that there exist situations, in which reduced-entropy transmission can be beneficial in a certain scenario. As a proof, it is thus sufficient to provide a single example where this happens.

Therefore, we do not state and prove a general theorem for the RoP MIMO BC-TIN, which is specialized to several detailed results in the complex multicarrier MIMO BC-TIN subsequently. Instead, we directly study the complex multicarrier MIMO BC-TIN, and we provide examples where a gain can be obtained either by improper signaling or by CC transmission. As both are special cases of reduced-entropy transmission, each of these detailed results is sufficient as a proof of the following general theorem.

Theorem 7.4.1. *Let $(\mathcal{P}_k = \mathcal{P}_{\mathrm{U}_k})_{\forall k}$ and $\mathcal{P}_{\mathrm{B}}$ be power shaping spaces fulfilling the compatibility assumption (Definition 3.1.3). Even if the noise vectors $\boldsymbol{\eta}_k$ are maximum-entropy signals with respect to $(\mathcal{P}_k)_{\forall k}$, it can happen that reduced-entropy per-user input signals $\boldsymbol{\xi}_k$ with respect to $\mathcal{P}_{\mathrm{B}}$ are needed to achieve the whole rate region of the RoP MIMO BC-TIN. This statement holds for systems with and without zero-forcing constraints and for systems with and without (R)TS.*

Proof. Examples where this happens are given below in Propositions 7.4.1 and 7.4.3. □

In the remainder of this section, we study the complex multicarrier MIMO BC-TIN both with and without (R)TS, and we also consider the case of zero-forcing constraints. We demonstrate gains by improper signaling as well as by CC transmission, and we show that these different types of reduced-entropy transmission are not interchangeable, i.e., we find examples where one of them brings an improvement that cannot be obtained by the other one.[2]

The main challenge in proving these results is that a rigorous statement about a gain by reduced-entropy transmission is possible only if we can establish a *converse* for maximum-entropy transmission, i.e., if we know the globally optimal maximum-entropy TIN strategy (or an upper bound to it) for comparison. The converses we provide are based on the algorithmic solution from Section 7.3.1.2. This is a valid proof technique since the algorithm can compute the globally optimal solution up to an arbitrarily small error tolerance.

It is important to keep in mind that the above Theorem and the detailed results that follow state only that gains by reduced-entropy transmission can be possible. This does not mean

[2]Examples for further gains by improper signaling or CC transmission in the special case without (R)TS are provided in Section 7.5, where we also discuss the gains that were reported for this special case in [34, 173].

that such gains are obtained for each channel realization or for each choice of the system dimensions. Indeed, we also provide examples of special cases in which improper signaling or CC transmission cannot bring any improvements. Nevertheless, the fact that gains can be possible is still remarkable since the opposite was true in the systems considered in Chapters 4 through 6 (except Section 6.7). For these systems, it could be shown that reduced-entropy transmission can only be beneficial in case of reduced-entropy noise and in scenarios that violate the compatibility assumption.

7.4.1 Improper Signaling in the Complex Multicarrier MIMO BC-TIN

Let us first consider the power shaping spaces $\mathcal{P}_k = \grave{\mathcal{P}}_{\mathrm{U}_k},\ \forall k$ and $\mathcal{P}_{\mathrm{B}} = \grave{\mathcal{P}}_{\mathrm{B}}$, i.e., we study potential benefits of improper signaling.

7.4.1.1 Benefits of Improper Signaling

The following result is an extension of [16, Th. 1].

Proposition 7.4.1. *In the complex MIMO BC-TIN with proper noise and a sum power constraint* (3.4)*, proper per-user input signals do not always achieve the whole rate region. This statement holds with and without zero-forcing constraints and with and without (R)TS.*

Proof. Consider the combined real representation (3.37) of the complex three-user MISO BC-TIN with noise covariance matrices $\boldsymbol{C}_{\check{\boldsymbol{\eta}}_k} = \frac{1}{2}\mathbf{I}_2$, a sum power constraint with $Q = 5$, and the channel realization

$$\grave{\boldsymbol{H}}_1^{\mathrm{T}} = \begin{bmatrix} 1 & 0 & 0 & 0 \\ 0 & 0 & 1 & 0 \end{bmatrix}, \tag{7.50}$$

$$\grave{\boldsymbol{H}}_2^{\mathrm{T}} = \begin{bmatrix} \frac{1}{\sqrt{2}} & \frac{1}{\sqrt{2}} & 0 & 0 \\ 0 & 0 & \frac{1}{\sqrt{2}} & \frac{1}{\sqrt{2}} \end{bmatrix}, \tag{7.51}$$

$$\grave{\boldsymbol{H}}_3^{\mathrm{T}} = \begin{bmatrix} \frac{1}{\sqrt{2}} & 0 & 0 & -\frac{1}{\sqrt{2}} \\ 0 & \frac{1}{\sqrt{2}} & \frac{1}{\sqrt{2}} & 0 \end{bmatrix}. \tag{7.52}$$

Improper Signaling—Achievability: Let the transmit covariance matrices in the dual uplink be

$$\boldsymbol{C}_{\check{\boldsymbol{x}}_k} = \frac{Q}{3} \begin{bmatrix} \cos^2\varphi_k & \cos\varphi_k \sin\varphi_k \\ \cos\varphi_k \sin\varphi_k & \sin^2\varphi_k \end{bmatrix} \tag{7.53}$$

with $\varphi_1 = 0$, $\varphi_2 = -\frac{5\pi}{12}$, and $\varphi_3 = -\frac{7\pi}{12}$. These matrices fulfill the uplink power constraint $\sum_{k=1}^{K} \mathrm{tr}[\boldsymbol{C}_{\check{\boldsymbol{x}}_k}] \leq Q$. Using (7.14) with $\mu = \frac{1}{2}$, we can calculate that the rates $\rho_{\mathrm{improper},k} \approx 1.0237\ \forall k$ are achievable without zero-forcing, while (7.23) with $\mu = \frac{1}{2}$ yields that $\rho_{\mathrm{ZF,improper},k} \approx 1.0107\ \forall k$ is achievable with zero-forcing. These rates are of course still achievable if (R)TS is allowed.

Proper Signaling—Converse: The corresponding complex channels are row vectors

$$\boldsymbol{h}_1^{\mathrm{H}} = \begin{bmatrix} 1 & 0 \end{bmatrix} \qquad \boldsymbol{h}_2^{\mathrm{H}} = \begin{bmatrix} \frac{1}{\sqrt{2}} & \frac{1}{\sqrt{2}} \end{bmatrix} \qquad \boldsymbol{h}_3^{\mathrm{H}} = \begin{bmatrix} \frac{1}{\sqrt{2}} & \frac{\mathrm{j}}{\sqrt{2}} \end{bmatrix} \tag{7.54}$$

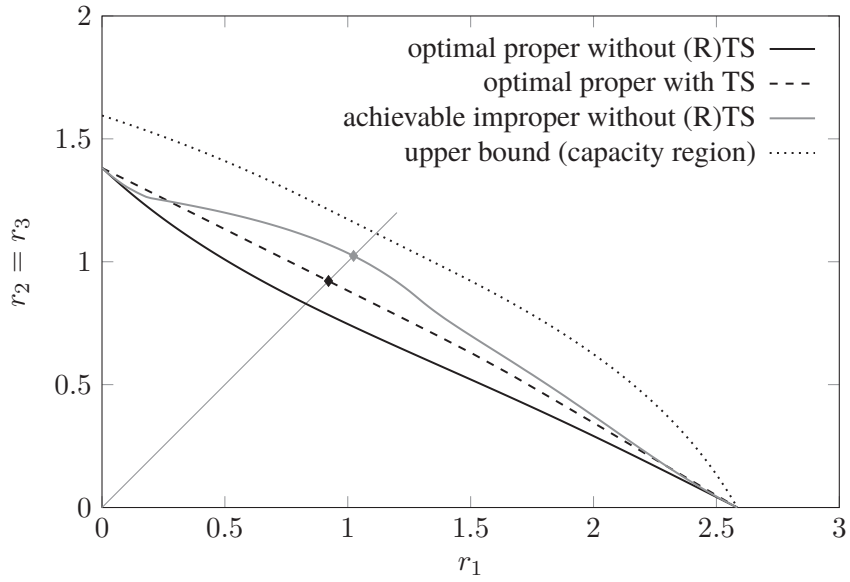

Figure 7.2: Achievable rates in the complex three-user MISO BC-TIN from the proof of Proposition 7.4.1 (intersections of the rate regions with the plane $r_2 = r_3$). The diamonds correspond to the values calculated in the proof of Proposition 7.4.1, and the gray diagonal line indicates the points where all users achieve the same rate.

and the proper noise of each user k is a scalar with variance $\boldsymbol{C}_{\boldsymbol{\eta}_k} = 1$. Consider a dual uplink transmission with three equal-length time slots, where a different pair of two users is served with equal power $\boldsymbol{C}_{\boldsymbol{x}_k} = \frac{Q}{2}$ in each time slot. Then, the overall rate of each user is $\frac{2}{3}$ of the per-slot rate, which we can calculate using (7.14) with $\mu = 1$. We obtain $\rho_{\mathrm{proper},k} \approx 0.92165\ \forall k$. By means of the method from Section 7.3.1.2, we can verify that this is indeed a Pareto-optimal TS solution. Thus, $\rho_{\mathrm{improper},k}$ from above is not achievable with proper signaling, and it of course stays unachievable if we introduce zero-forcing constraints and/or consider only strategies without TS (where either RTS is used or (R)TS is avoided completely). □

An illustration of the proof can be seen in Figure 7.2, where we have plotted intersections of various rate regions with the plane $r_2 = r_3$. Note that the upper left end of the Pareto boundary thus corresponds to a transmission to two users while the lower right point describes a single-user transmission, where all schemes have equal performance. The capacity region, which is achievable with DPC (see Chapter 6), is included as an upper bound. To obtain (potentially suboptimal) achievable solutions with improper signaling, we have applied the rate balancing algorithm from [9] in the combined real representation using random initializations.[3] Even without (R)TS, improper signaling brings a considerable improvement over the optimal proper strategy with TS nearly along the whole Pareto boundary. When combining improper signaling with TS, we could obtain a rate region that is at least as large as the convex hull of the gray curve.

7.4.1.2 Optimality of Proper Signaling in Special Cases

On the other hand, there are special cases of the MIMO BC-TIN, for which it can be shown that improper signaling can never bring a gain compared to proper signaling. One of them is given

[3] Algorithmic aspects are discussed in detail in Section 7.6.

in the following proposition.

Proposition 7.4.2. *In the complex two-user single-carrier MISO BC-TIN with proper noise, the whole TS rate region $\overline{\overline{\mathcal{R}}}_{\mathrm{TIN}}(Q)$ is achieved by proper per-user input signals.*

Proof. Let $\varrho_{1,1} \in \mathbb{R}$ and $\varrho_{1,2}, \varrho_{2,2} \in \mathbb{C}$ be the elements of $\boldsymbol{R}$ from the reduced QR decomposition $\boldsymbol{QR} = \boldsymbol{H} = [\boldsymbol{h}_{\mathrm{UL},1}, \boldsymbol{h}_{\mathrm{UL},2}] \in \mathbb{C}^{m\times 2}$. As the noise covariance matrix is an identity in the dual uplink, we can apply the following filter without changing the achievable rates:

$$\boldsymbol{y}' = \begin{bmatrix} 1 & \\ & \mathrm{e}^{\mathrm{j}\theta} \end{bmatrix} \boldsymbol{Q}^{\mathrm{H}} \boldsymbol{y} = \begin{bmatrix} 1 & \\ & \mathrm{e}^{\mathrm{j}\theta} \end{bmatrix} \boldsymbol{Q}^{\mathrm{H}} \left(\boldsymbol{H} \begin{bmatrix} x_1 \\ x_2 \end{bmatrix} + \boldsymbol{\eta} \right) = \underbrace{\begin{bmatrix} \varrho_{1,1} & \mathrm{e}^{\mathrm{j}\theta_2}\,\varrho_{1,2} \\ 0 & \mathrm{e}^{\mathrm{j}(\theta+\theta_2)}\,\varrho_{2,2} \end{bmatrix}}_{\boldsymbol{H}'} \begin{bmatrix} x_1' \\ x_2' \end{bmatrix} + \boldsymbol{\eta}' \tag{7.55}$$

where $x_1' = x_1$, $x_2' = \mathrm{e}^{-\mathrm{j}\theta_2} x_2$, and $\boldsymbol{\eta}'$ is proper Gaussian with covariance matrix $\boldsymbol{C}_{\boldsymbol{\eta}'} = \mathbf{I}_2$. The transformation $x_2' = \mathrm{e}^{-\mathrm{j}\theta_2} x_2$ does not change the transmit power, and x_2' is improper if and only if x_2 is improper. We may choose θ and θ_2 such that $\boldsymbol{H}' = [\boldsymbol{h}_1', \boldsymbol{h}_2'] \in \mathbb{R}^{2\times 2}$. The corresponding composite real channel matrices $\grave{\boldsymbol{H}}_1' = \grave{\Re}(\boldsymbol{h}_1')$ and $\grave{\boldsymbol{H}}_2' = \grave{\Re}(\boldsymbol{h}_2')$ are then block-diagonal with two equal blocks due to (2.46).

Any possible composite real uplink transmit covariance matrix can be parametrized as

$$\boldsymbol{C}_{\check{\boldsymbol{x}}_k'} = \frac{p_k}{2}\mathbf{I}_2 + \frac{n_k}{2} \begin{bmatrix} \cos\varphi_k & \sin\varphi_k \\ \sin\varphi_k & -\cos\varphi_k \end{bmatrix} \tag{7.56}$$

with $p_k \geq 0$, $n_k \geq 0$ and $\varphi_k \in \mathbb{R}$. For $\boldsymbol{X}$ and $\boldsymbol{X}_k$ from (7.15), we have

$$\boldsymbol{X} = \frac{1}{2}\mathbf{I}_4 + \grave{\boldsymbol{H}}_1' \boldsymbol{C}_{\check{\boldsymbol{x}}_1'} \grave{\boldsymbol{H}}_1'^{\mathrm{T}} + \grave{\boldsymbol{H}}_2' \boldsymbol{C}_{\check{\boldsymbol{x}}_2'} \grave{\boldsymbol{H}}_2'^{\mathrm{T}}, \qquad \boldsymbol{X}_k = \frac{1}{2}\mathbf{I}_4 + \grave{\boldsymbol{H}}_j' \boldsymbol{C}_{\check{\boldsymbol{x}}_j'} \grave{\boldsymbol{H}}_j'^{\mathrm{T}}, \tag{7.57}$$

with $j \neq k$. The following facts can be verified analytically (e.g., with the help of a software for symbolic calculations). The determinants $\det \boldsymbol{X}_k$, $k \in \{1, 2\}$ do not depend on φ_1 nor φ_2. The determinant $\det \boldsymbol{X}$ does not depend on φ_1 and φ_2 individually, but only on the difference $\Delta = \varphi_2 - \varphi_1$, and we have

$$\frac{\partial \det \boldsymbol{X}}{\partial \Delta} = \frac{1}{8}\varrho_{1,1}^2 |\varrho_{1,2}|^2 n_1 n_2 \sin\Delta. \tag{7.58}$$

Thus, both rates $r_k = \frac{1}{2}\log_2 \frac{\det \boldsymbol{X}}{\det \boldsymbol{X}_k}$, $k \in \{1, 2\}$ from (7.14) are maximized if $\varphi_2 = \Delta = \pi$, where we have chosen $\varphi_1 = 0$ without loss of generality. The intuition behind this result is that the impropriety of the intended signal and of the interference should point exactly in opposite directions (cf. Example 4.5.1 or a similar result for a one-sided interference channel in [38] and Theorem 8.3.1).

We can thus assume that $\boldsymbol{C}_{\check{\boldsymbol{x}}_k'}$, $\forall k$ in (7.56) are diagonal matrices. Together with the special structure of the channel matrices $\grave{\boldsymbol{H}}_k'$, we can interpret this as CN transmission in a real-valued two-carrier system with equal channel vectors on both carriers.

To optimize the CN transmission, we can apply the dual decomposition from Section 3.3.2. Since the channel vectors are equal on both carriers, the inner problem (3.33) is exactly the same on both carriers. Thus, for any given dual variable $\boldsymbol{\nu}$, there exists a solution to the inner problem that applies the same strategy on both carriers, i.e., it uses the same powers on both carriers. Since the primal recovery (3.23) combines such inner solutions to obtain an overall

transmit strategy, we can conclude that it is optimal to perform TS between operation points that apply the same powers on both carriers. This means that $\boldsymbol{C}_{\tilde{\boldsymbol{x}}'_k}$, $\forall k$ in (7.56) are scaled identity matrices, i.e., $n_k = 0$, $\forall k$, which corresponds to proper signaling in the original system. □

7.4.2 CC Transmission in the Complex Multicarrier MIMO BC-TIN

As a second example of reduced-entropy transmission, let us consider CC transmission in multicarrier systems.

7.4.2.1 Proper CN Transmission vs. Proper CC Transmission

In [1], it was shown that CN transmission not always achieves the complete rate region of the complex multicarrier MIMO BC-TIN with proper signaling, i.e., signals belonging to the power shaping spaces $\mathcal{P}'_k = \grave{\mathcal{P}}_{\mathrm{U}_k}$, $\forall k$ and $\mathcal{P}'_{\mathrm{B}} = \grave{\mathcal{P}}_{\mathrm{B}}$ can be beneficial compared to staying in the power shaping spaces $\mathcal{P}_k = \grave{\mathcal{P}}^{\mathrm{CN}}_{\mathrm{U}_k} \subset \grave{\mathcal{P}}_{\mathrm{U}_k}$, $\forall k$ and $\mathcal{P}_{\mathrm{B}} = \grave{\mathcal{P}}^{\mathrm{CN}}_{\mathrm{B}} \subset \grave{\mathcal{P}}_{\mathrm{B}}$. In [18], this result was extended to settings with zero-forcing constraints. Let us briefly summarize the example that was used in the proofs.

Example 7.4.1. *Consider the complex three-user two-carrier MISO BC-TIN with proper noise and* $C_{\eta_k^{(c)}} = 1$, $\forall k, \forall c$. *For all* k, *let* $\boldsymbol{h}_k^{(1)} = \boldsymbol{h}_k$ *and* $\boldsymbol{h}_k^{(2)} = \boldsymbol{h}_k^*$ *with* $\boldsymbol{h}_k$ *from* (7.54).

Proper CN Signaling—Converse: *According to [1], optimal proper CN transmission with TS can achieve the rates* $\rho_{\mathrm{CN},k} \approx 1\ \forall k$ *under a sum power constraint with* $Q = 3.5684$. *The optimal strategy consists of three equal-length time slots, where a different pair of two users is served over both carriers in each time slot. The optimality of this scheme can be verified by applying the method from Section 7.3.1.2 to the complex multicarrier formulation* (3.34).

Proper CC Signaling—Achievability: *In [1], a proper CC transmit strategy was constructed, which uses the combined complex transmit covariance matrices*

$$\boldsymbol{C}_{\boldsymbol{x}_k} = \frac{Q}{6} \begin{bmatrix} 1 & \mathrm{e}^{\mathrm{j}\varphi_k} \\ \mathrm{e}^{-\mathrm{j}\varphi_k} & 1 \end{bmatrix} \tag{7.59}$$

in the dual uplink. With $\varphi_1 = 0$, $\varphi_2 = -\frac{5\pi}{6}$, *and* $\varphi_3 = \frac{5\pi}{6}$, *we can calculate by means of* (7.14) *with* $\mu = 1$ *that the rates* $\rho_{\mathrm{CC},k} \approx 1.0986\ \forall k$ *are achievable using the same transmit power as before, i.e.,* $Q = 3.5684$. *From* (7.23) *with* $\mu = 1$, *we obtain that* $\rho_{\mathrm{ZF,CC},k} \approx 1.0648\ \forall k$ *is achievable with zero-forcing.*

7.4.2.2 Comparison of Proper CC Transmission and Improper CN Transmission

We might wonder whether such a rate gain due to CC transmission is still possible in this scenario if improper signaling is allowed, but the answer is negative. If we apply the improper transmit strategy from the proof of Proposition 7.4.1 independently on each carrier using the per-carrier transmit power $\frac{Q}{2} = 1.7842$, the per-carrier rates $\rho^{(c)}_{\mathrm{improper},k} = 0.54928\ \forall k, \forall c$ are achievable. Taking the sum over both carriers, we see that this improper CN scheme achieves exactly the same rate as the proper CC scheme from [1]. Similarly, we can show that the proper CC zero-forcing rates can instead be achieved with improper CN zero-forcing.

Does this mean that the two types of reduced-entropy transmission—improper signaling and CC transmission—can generally be substituted by each other? Obviously not, since CC

transmission is not a feasible approach in the single-carrier example from Proposition 7.4.1 or, e.g., in a multicarrier system where all carriers but one are negligibly weak. Thus, CC transmission is not a generally valid replacement of improper signaling. But what about the other direction? Improper signaling is always a feasible strategy in complex systems, and it is not obvious whether improper CN transmission can serve as a replacement of proper CC transmission in general.

7.4.2.3 Benefits of CC Transmission in Case of General Complex Signaling

When our aim is to demonstrate a gain by CC transmission that cannot be obtained by instead using improper CN transmission, the difficulty is that we need the globally optimal improper CN solution for comparison, but we are currently not aware of an algorithm to compute it. When optimizing such a strategy via the real-valued multicarrier formulation, we are always facing a true MIMO system with $M_{\mathrm{T}} > 1$ for all terminals T even if the original complex system has single-antenna terminals. This means that we have to optimize covariance matrices, and we cannot switch to an optimization of scalar powers, as we do in Section 7.3.1.2. Therefore, we have to go a different path. To this end, let us first introduce the following lemma, which turns out to be helpful.

Lemma 7.4.1. *In the RoP MIMO BC-TIN with a sum power constraint, let $\boldsymbol{H}_{\mathrm{UL},k} = \boldsymbol{H}_{\mathrm{UL},j}$ for some $j \neq k$. Then, the rate region with (R)TS can be achieved without serving users k and j simultaneously in any time slot.*

Proof. Consider a weighted sum rate maximization with weights $(w_k)_{\forall k}$, where we assume $w_k \geq w_j$ without loss of generality. For all other users, it does not matter how a given sum covariance matrix $\boldsymbol{Q} = \boldsymbol{C}_{\boldsymbol{x}_k} + \boldsymbol{C}_{\boldsymbol{x}_j}$ is split into $\boldsymbol{C}_{\boldsymbol{x}_k}$ and $\boldsymbol{C}_{\boldsymbol{x}_j}$ since $\boldsymbol{H}_{\mathrm{UL},k} = \boldsymbol{H}_{\mathrm{UL},j}$. For any such $\boldsymbol{Q}$, we can use the rate $r_{\boldsymbol{Q}}$ that is achievable when decoding users k and j jointly (as in Section 5.1) as an upper bound, i.e.,

$$w_k r_k + w_j r_j \leq w_k (r_k + r_j) \leq w_k r_{\boldsymbol{Q}} \quad \text{with} \quad r_{\boldsymbol{Q}} = \mu \log_2 \frac{\det \boldsymbol{X}}{\det \boldsymbol{X}_{k,j}} \tag{7.60}$$

where $\boldsymbol{X}_{k,j} = \boldsymbol{X} - \boldsymbol{H}_{\mathrm{UL},k} \boldsymbol{Q} \boldsymbol{H}_{\mathrm{UL},k}^{\mathrm{H}}$ is the covariance of the noise plus the interference from the other users $k' \notin \{k, j\}$. On the other hand, $w_k r_k = w_k r_{\boldsymbol{Q}}$ is obviously achievable with a TIN strategy by choosing $\boldsymbol{C}_{\boldsymbol{x}_k} = \boldsymbol{Q}$ and $\boldsymbol{C}_{\boldsymbol{x}_j} = \boldsymbol{0}$. By plugging in $w_k r_k = w_k r_{\boldsymbol{Q}}$ and $w_j r_j = 0$ as optimal strategy in (3.19) and (3.24), we obtain the desired result for TS and for RTS, respectively. □

We are now ready to demonstrate gains that cannot be obtained using improper signaling, but using CC transmission, i.e., reduced-entropy transmission with respect to the power shaping spaces $\mathcal{P}_k = \mathcal{P}_{\mathrm{U}_k}^{\mathrm{CN}}$, $\forall k$ and $\mathcal{P}_{\mathrm{B}} = \mathcal{P}_{\mathrm{B}}^{\mathrm{CN}}$.

Proposition 7.4.3. *In the complex multicarrier MIMO BC-TIN with CN noise and a sum power constraint* (3.4)*, CN per-user input signals do not always achieve the whole rate region. This statement holds for systems with and without (R)TS.*

Proof. Consider the combined complex representation (3.35) of the complex three-user two-carrier MISO BC-TIN with noise covariance matrices $\boldsymbol{C}_{\boldsymbol{\eta}_k} = \mathbf{I}_2$, a sum power constraint with

$Q = 3$, and the channel realization

$$\boldsymbol{H}_1^{\mathrm{H}} = \begin{bmatrix} 1 & 0 & 0 & 0 \\ 0 & 0 & 1 & 0 \end{bmatrix}, \tag{7.61}$$

$$\boldsymbol{H}_2^{\mathrm{H}} = \begin{bmatrix} \frac{1}{\sqrt{2}} & \frac{1}{\sqrt{2}} & 0 & 0 \\ 0 & 0 & 1 & 0 \end{bmatrix}, \tag{7.62}$$

$$\boldsymbol{H}_3^{\mathrm{H}} = \begin{bmatrix} 1 & 0 & 0 & 0 \\ 0 & 0 & \frac{1}{\sqrt{2}} & \frac{1}{\sqrt{2}} \end{bmatrix}. \tag{7.63}$$

CC Signaling—Achievability: Let the transmit signals in the dual uplink be proper with combined complex covariance matrices

$$\boldsymbol{C}_{\boldsymbol{x}_k} = p_k \begin{bmatrix} \cos^2 \varphi_k & \cos \varphi_k \sin \varphi_k \\ \cos \varphi_k \sin \varphi_k & \sin^2 \varphi_k \end{bmatrix} \tag{7.64}$$

with $\varphi_1 = \frac{45}{180}\pi$, $\varphi_2 = \frac{160}{180}\pi$, and $\varphi_3 = \frac{-70}{180}\pi$. Using $p_1 = 0.945$ and $p_2 = p_3 = 1.0275$, the uplink power constraint $\sum_{k=1}^{K} \mathrm{tr}[\boldsymbol{C}_{\boldsymbol{x}_k}] \leq Q$ is fulfilled. Using (7.14) with $\mu = 1$, we can calculate that the rates $\rho_{\mathrm{CC},k} \approx 0.91083 \ \forall k$ are achievable. These rates are of course still achievable if (R)TS is allowed.

CN Signaling—Converse: To obtain an optimal solution with TS, we apply the dual decomposition from Section 3.3.2 to the real-valued multicarrier formulation (3.36). On each carrier, there are two users with exactly the same composite real per-carrier channel matrices, which means that no more than two users need to be considered simultaneously when solving (3.33) due to Lemma 7.4.1. We thus have to optimize a complex two-user MISO BC-TIN on each carrier in each time slot, so that Proposition 7.4.2 applies, i.e., improper signaling cannot bring any gains. Plugging in the assumption of proper signals, the complex multicarrier formulation (3.34) becomes a RoP CN MISO system, and we can optimize the transmit signals as described in Section 7.3.1.2. The obtained globally optimal proper CN rates are $\rho_{\mathrm{CN},k} \approx 0.89117 \ \forall k$. This can be achieved with three equal-length time slots, where a pair of users is active on each carrier in each slot with per-user per-carrier transmit power $\frac{Q}{4}$. The rate $\rho_{\mathrm{CN},k}$ is then $\frac{4}{3}$ times the rate that an active user achieves on a carrier in a slot, which can be calculated using (7.14) with $\mu = 1$. Thus, $\rho_{\mathrm{CC},k}$ from above is not achievable with CN transmission, and it of course stays unachievable if we consider only strategies without TS (where either RTS is used or (R)TS is avoided completely). □

Note that the case of zero-forcing is not included in this proposition. However, this does not imply that improper signaling can always replace CC transmission if zero-forcing constraints are considered. It just means that we have not found a CC zero-forcing strategy that outperforms CN zero-forcing in this scenario. There might exist other examples in which gains that are only possible with CC transmission can be shown even though zero-forcing constraints are imposed. This question is left open for future research.

7.4.2.4 Optimality of CN Transmission in Special Cases

We can also find examples for which CN transmission is provably optimal. A particularly interesting example is the following result from [15], which does not depend on a certain channel realization.

Example 7.4.2. *Consider a complex two-user multicarrier MIMO BC-TIN with proper CN noise and proper signaling, and assume that $M \geq M_1 + M_2$, i.e., the number of base station antennas is at least as high as the total number of antennas at the user terminals. This case was called* full multiplexing *in [15, 150]. For this setting, CN transmission is optimal in the high-SNR regime, i.e., if the transmit power goes to infinity. This result was shown in [15] by applying the high-SNR rate balancing solution from [150] to the combined complex representation. The optimal combined complex transmit covariance matrices in the dual uplink then turn out to be block-diagonal, which corresponds to CN transmission.*

7.4.3 Discussion

We have shown that using improper signaling and CC transmission can bring gains compared to proper signaling and CN transmission, i.e., the rate region of the complex multicarrier MIMO BC-TIN is not always completely achievable with maximum-entropy transmission. This can happen no matter whether or not (R)TS is allowed. For the comparison of improper signaling to proper signaling, as well as for the comparison of proper CC transmission to proper CN transmission, we have shown that gains are also possible in the presence of zero-forcing constraints.

In some scenarios, the two considered types of entropy reduction—improper signaling and CC transmission—seem to be interchangeable, i.e., we have obtained the same gain when applying any of them. On the other hand, there are scenarios in which one of the techniques can bring a gain that is not achievable by the other one. Finally, there are also scenarios for which it can be shown that neither of the techniques can bring benefits.

Since we have demonstrated gains due to reduced-entropy transmission only for particular channel realizations, we could ask whether observing a channel realization for which such gains are possible is a measure-zero event. The answer is negative. For the comparison of proper CC transmission and proper CN transmission in the complex multicarrier MIMO BC-TIN, it was shown in [15] that there is in fact a large variety of channel realizations for which CC transmission can outperform CN transmission. In a similar way, we could construct further channel realizations for which improper signaling is beneficial. Therefore, the suboptimality of maximum-entropy transmission is an effect that can still play a role if more realistic channel realizations according to some channel model are considered instead of constructed channel matrices.

On the other hand, gains by reduced-entropy transmission are not possible for all channel realizations, i.e., it depends on the channel realization whether or not maximum-entropy transmission is suboptimal. The results presented in this section do not give a clear indication about which properties of the channel matrices are conducive to such a suboptimality. First approaches towards answering this question were presented in [15], but additional research would be necessary to better understand this aspect.

Moreover, the results in this section do not tell us anything about how large the gains by reduced-entropy transmission can be. In fact, the possible gains reported so far for the MIMO BC-TIN, e.g., in [1, 15, 16, 18], are all in a similar range as the ones presented above. However, as we will see in the following section, this can change drastically if we restrict our considerations to systems without (R)TS.

Finally, note that all configurations in which gains by reduced-entropy transmission could

be shown in this section consisted of three users. Conversely, for the complex two-user single-carrier MISO BC-TIN, we could show that improper signaling cannot bring any gains compared to proper signaling if TS is allowed. In addition, a special case of a two-user system where CC transmission cannot bring any gains was discussed in Example 7.4.2. For the general case of the two-user MIMO BC-TIN, we are not able to tell at the current point whether gains by any kind of reduced-entropy transmission can be possible. We will come back to this question later, at least for the case without (R)TS.

7.5 Further Aspects in Systems without (Rate-)Time-Sharing

Even though systems without (R)TS are also covered by the previous section, such systems merit some more attention for several reasons. First of all, many low-complexity algorithms for transceiver design do not account for the possibility of (R)TS (e.g., [2,91–94,156,159,161,162]). By studying the MIMO BC-TIN under the assumption that (R)TS is not allowed, we obtain insights about the behavior of such algorithms.

Secondly, if (R)TS is not allowed, the performance loss of maximum-entropy transmission compared to reduced-entropy transmission can be much larger than observed in the previous section. Moreover, we can then observe such a performance gap even in two-user systems, which is another difference to the previous section.

Finally, the question of quality of service (QoS) feasibility arises if (R)TS is not allowed, i.e., it can happen that a rate vector is never achievable in a system no matter how much transmit power is spent. We commence our analysis of systems without (R)TS by studying how maximum-entropy transmission and reduced-entropy transmission influence the QoS feasibility.

7.5.1 Quality of Service Feasibility

The *QoS feasibility region* contains all combinations of per-user QoS that are achievable in a system if we are ready to spend an arbitrarily high amount of transmit power. This region can be expressed in terms of various quality-of-services measures, e.g., as a feasible MMSE region [174] or feasible SINR region [175]. In the following, we concentrate on the feasible rate region (e.g., [176]), which is the most appropriate formulation in MIMO systems, where each user may be served with more than one data stream (see Section 1.3).

In a single-user system, we can achieve an arbitrarily high data rate if we do not limit the transmit power that may be invested. The same holds for the MIMO BC if dirty paper coding is applied [177], or if (R)TS is allowed [52]. However, if (R)TS is not allowed in the MIMO BC-TIN, it can happen that a rate vector is unachievable no matter how much transmit power we use (e.g., [5, 94, 174, 176]).

The feasible MMSE region of the MISO BC with linear transceivers and proper Gaussian signals was derived in [174], and the result was extended to the feasible rate region for the case of a MIMO system in [176]. As pointed out in [5], the derivation can be transferred to real-valued systems. We first consider the special case of the RoP MISO BC-TIN and generalize the result to the RoP MIMO BC-TIN afterwards.

Lemma 7.5.1. *In the RoP MISO BC-TIN, the rate vector* $[\rho_1, \ldots, \rho_K]^{\mathrm{T}} \geq \mathbf{0}$ *is feasible without*

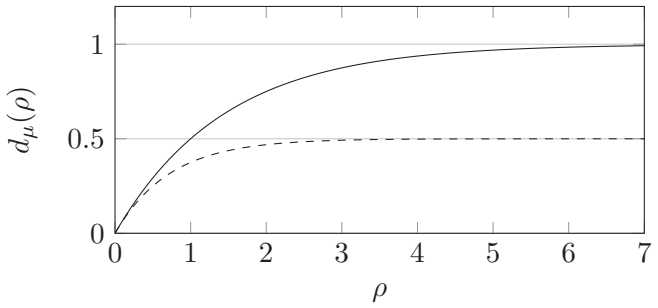

Figure 7.3: EDoF for rate requirement ρ with $\mu = 1$ (solid) and $\mu = \frac{1}{2}$ (dashed).

(R)TS if and only if

$$\sum_{k\in\mathcal{K}} 1 - 2^{-\frac{1}{\mu}\rho_k} < \operatorname{rank}\left[\boldsymbol{H}_{\mathcal{K}}\right], \quad \forall \mathcal{K} \subseteq \{1,\ldots,K\} \tag{7.65}$$

where $\boldsymbol{H}_{\mathcal{K}} \in \mathbb{C}^{M\times|\mathcal{K}|}$ ($\mathbb{R}$ for a real-valued system) is a matrix that comprises the nonzero uplink channel vectors $\boldsymbol{h}_{\mathrm{UL},k}$ of the users $k \in \mathcal{K}$ as a block row.

Sketch of Proof. The derivation of the QoS feasibility region of the complex MISO BC with linear transceivers and proper signaling given in [174, 176], which can be analogously applied to a real-valued system, leads to the condition $\sum_{k\in\mathcal{K}} \frac{\gamma_k^{\mathrm{UL}}}{1+\gamma_k^{\mathrm{UL}}} < \operatorname{rank}\left[\boldsymbol{H}_{\mathcal{K}}\right] \ \ \forall \mathcal{K} \subseteq \{1,\ldots,K\}$ on the uplink SINRs γ_k^{UL} after optimal receive filtering.[4] Since $r_k = \mu \log_2(1+\gamma_k^{\mathrm{UL}})$, we obtain the condition given in the lemma. □

For a more convenient description of the QoS feasibility region, the notion of effective degrees of freedom (EDoF) was introduced in [52]. The following definition extends this notion such that it can be used in the RoP MIMO BC-TIN. An illustration is given in Figure 7.3.

Definition 7.5.1. *We call*

$$d_\mu(\rho) = \mu(1 - 2^{-\frac{1}{\mu}\rho}) \in [0, \mu[\tag{7.66}$$

the effective degrees of freedom (EDoF) required for a rate ρ in the RoP MIMO BC-TIN.

For complex systems with $\mu = 1$, this is equivalent to the definition in [52]. By means of the EDoF requirements, (7.65) can be conveniently written as

$$\sum_{k\in\mathcal{K}} d_\mu(\rho_k) < \mu \operatorname{rank}\left[\boldsymbol{H}_{\mathcal{K}}\right], \quad \forall \mathcal{K} \subseteq \{1,\ldots,K\}. \tag{7.67}$$

In case of multiple antennas at the user terminals, i.e., in case of the RoP MIMO BC-TIN, we can assume that S_k streams are transmitted for user k, and that a decorrelation as in Lemma 7.2.1 is performed. We can then split the rate ρ_k into per-stream rate requirements $\rho_{k,s}$, which correspond to the summands in (7.21), and we can make the following observation.

[4] The SINR γ_k^{UL} corresponds to the fraction inside the logarithm in (7.21), where $S_k = 1$ in a MISO system. The original derivation in [174] is in terms of minimum mean square errors (MMSEs), but due to the one-to-one mapping $\mathrm{MMSE}_k = \frac{1}{1+\gamma_k}$ [174], we can equivalently express the result in terms of SINRs.

Lemma 7.5.2. *Given a rate requirement ρ_k, the sum EDoF requirement $\sum_{k=1}^{S_k} d_\mu(\rho_{k,s})$ of user k is minimized if $\rho_{k,\tilde{s}} = \rho_k$ for an arbitrary $\tilde{s} \in \{1, \ldots, S_k\}$ and $\rho_{k,s} = 0$ for $s \neq \tilde{s}$. Any other choice leads to a strictly larger sum EDoF requirement.*

Proof. Let $\boldsymbol{\rho}_k = [\rho_{k,1}, \ldots, \rho_{k,S_k}]$ such that $\mathbf{1}^{\mathrm{T}}\boldsymbol{\rho}_k = \rho_k$. Since $d_\mu(\rho)$ is strictly concave for $\rho \geq 0$ (see also Figure 7.3), the function $f(\boldsymbol{\rho}_k) = \sum_{s=1}^{S_k} d_\mu(\rho_{k,s})$ is strictly Schur-concave by Lemma 2.1.4. As $\boldsymbol{\rho}_k \prec \rho_k \mathbf{e}_{\tilde{s}}$ (Lemma 2.1.2), we thus have $f(\rho_k \mathbf{e}_{\tilde{s}}) \leq f(\boldsymbol{\rho}_k)$ for any $\boldsymbol{\rho}_k$ with equality if and only if $\boldsymbol{\rho}_k$ is a permuted version of $\rho_k \mathbf{e}_{\tilde{s}}$. □

We are now ready to extend Lemma 7.5.1 to the case of multiantenna users as in [176]. Since the obtained theorem is important as a basis for several results derived later on, we provide a proof that is more detailed than the argumentation given in [176].

Theorem 7.5.1. *In the RoP MIMO BC-TIN, the rate vector $[\rho_1, \ldots, \rho_K]^{\mathrm{T}} \geq \mathbf{0}$ is feasible without (R)TS if and only if*

$$\sum_{k \in \mathcal{K}} d_\mu(\rho_k) < \mu \operatorname{rank}\left[\boldsymbol{H}_{\mathcal{K}}\right], \quad \forall \mathcal{K} \subseteq \{1, \ldots, K\} \tag{7.68}$$

where $\boldsymbol{H}_{\mathcal{K}} \in \mathbb{C}^{M \times \sum_{k \in \mathcal{K}} M_k}$ ($\mathbb{R}$ for a real-valued system) is a matrix that comprises the nonzero uplink channel matrices $\boldsymbol{H}_{\mathrm{UL},k}$ of the users $k \in \mathcal{K}$ as a block row.

Proof. Let $\boldsymbol{t}_k = \boldsymbol{T}_k' \mathbf{e}_1$ be drawn independently for all users k from a continuous distribution, and let $\boldsymbol{H}_{\mathcal{K}}'$ be an $M \times |\mathcal{K}|$ matrix that comprises the effective uplink channel vectors $\boldsymbol{h}_{\mathrm{eff},k} = \boldsymbol{H}_{\mathrm{UL},k}\boldsymbol{t}_k$ of the users $k \in \mathcal{K}$ as a block row. We prove by induction that for any $(\rho_k)_{\forall k}$ complying to (7.68),

$$\sum_{k \in \mathcal{K}} d_\mu(\rho_k) < \mu \operatorname{rank}\left[\boldsymbol{H}_{\mathcal{K}}'\right], \quad \forall \mathcal{K} \subseteq \{1, \ldots, K\} \tag{7.69}$$

is fulfilled almost surely (a.s.). This statement then implies that there exists a set of transmit filters that achieves the QoS feasibility region stated in (7.68) with single-stream transmission.

The basis is that (7.69) holds for all sets with $|\mathcal{K}| = 1$ a.s. since $\boldsymbol{t}_k \notin \operatorname{null}[\boldsymbol{H}_{\mathrm{UL},k}]$ a.s. and $d_\mu(\rho_k) < \mu$ by definition. Assuming that (7.69) holds for all sets with $|\mathcal{K}| \leq N$ a.s., we prove the respective statement for $|\mathcal{K}| = N + 1$. For all sets for which $\operatorname{rank}[\boldsymbol{H}_{\mathcal{K}}'] = \min\{\operatorname{rank}[\boldsymbol{H}_{\mathcal{K}}], |\mathcal{K}|\}$, (7.69) is clearly fulfilled since $(\rho_k)_{\forall k}$ complies to (7.68) by assumption and $d_\mu(\rho_k) < \mu$. If this equality does not hold for a set $\mathcal{K}$, there must exist a $j \in \mathcal{K}$ such that $\operatorname{rank}[\,[\boldsymbol{H}_{\mathcal{K}}' \;\; \boldsymbol{H}_{\mathrm{UL},j}]\,] > \operatorname{rank}[\boldsymbol{H}_{\mathcal{K}}']$.

For this j, let $\mathcal{K}_j = \mathcal{K} \setminus \{j\}$, so that $\operatorname{rank}[\,[\boldsymbol{H}_{\mathcal{K}_j}' \;\; \boldsymbol{H}_{\mathrm{UL},j}]\,] = \operatorname{rank}[\,[\boldsymbol{H}_{\mathcal{K}}' \;\; \boldsymbol{H}_{\mathrm{UL},j}]\,] > \operatorname{rank}[\boldsymbol{H}_{\mathcal{K}}'] \geq \operatorname{rank}[\boldsymbol{H}_{\mathcal{K}_j}']$. Then, we have

$$\operatorname{rank}\left[\boldsymbol{H}_{\mathcal{K}}'\right] = \operatorname{rank}\left[[\boldsymbol{H}_{\mathcal{K}_j}' \;\; \boldsymbol{H}_{\mathrm{UL},j}\boldsymbol{t}_j]\right] = \operatorname{rank}\left[\boldsymbol{H}_{\mathcal{K}_j}'\right] + 1 \tag{7.70}$$

since $\boldsymbol{H}_{\mathrm{UL},j}\boldsymbol{t}_j \notin \operatorname{range}[\boldsymbol{H}_{\mathcal{K}_j}']$ a.s., which holds since $\boldsymbol{H}_{\mathrm{UL},j}\boldsymbol{t}_j$ lies in a randomly chosen subspace of $\operatorname{range}[\boldsymbol{H}_{\mathrm{UL},j}]$ and a.s. contains a contribution in the direction(s) causing the inequality $\operatorname{rank}[\,[\boldsymbol{H}_{\mathcal{K}_j}' \;\; \boldsymbol{H}_{\mathrm{UL},j}]\,] > \operatorname{rank}[\boldsymbol{H}_{\mathcal{K}_j}']$.

As $d_\mu(\rho_k) < \mu$, we have

$$\sum_{k \in \mathcal{K}} d_\mu(\rho_k) < \mu + \sum_{k \in \mathcal{K}_j} d_\mu(\rho_k) < \mu + \mu \operatorname{rank}\left[\boldsymbol{H}_{\mathcal{K}_j}'\right] = \mu \operatorname{rank}\left[\boldsymbol{H}_{\mathcal{K}}'\right] \tag{7.71}$$

where we could use (7.69) due to $|\mathcal{K}_j| = N$. This concludes the proof of achievability.

To show the converse statement that the QoS feasibility region is not larger than given in (7.68), assume that an additional data stream is added to a user k, which can be considered as a new virtual user k'. Since k and k' have the same channel matrix, adding k' to the set $\mathcal{K}$ cannot increase the right hand side of (7.68) if we already have $k \in \mathcal{K}$, but the left hand side is increased compared to the case of single-stream transmission due to Lemma 7.5.2. Therefore, multiple streams per user cannot enlarge the QoS feasibility region, and we can consider the setting as RoP MISO BC-TIN with effective uplink channel vectors $\boldsymbol{h}_{\mathrm{eff},k} = \boldsymbol{H}_{\mathrm{UL},k}\boldsymbol{t}_k$ for which the converse is shown in the proof of Lemma 7.5.1 in [174, 176]. □

The feasibility conditions can be simplified if the channel matrices fulfill a so-called *regularity condition* [174, 176].

Definition 7.5.2. *If the matrices $\boldsymbol{H}_{\mathcal{K}}$ satisfy*

$$\operatorname{rank}\left[\boldsymbol{H}_{\mathcal{K}}\right] \geq \min\{|\mathcal{K}|, M\}, \quad \forall \mathcal{K} \subseteq \{1, \ldots, K\} \tag{7.72}$$

we say that the regularity condition is fulfilled.

Corollary 7.5.1. *Assume that the regularity condition is fulfilled in the RoP MISO BC-TIN ($\boldsymbol{H}_{\mathcal{K}}$ from Lemma 7.5.1) or in the RoP MIMO BC-TIN ($\boldsymbol{H}_{\mathcal{K}}$ from Theorem 7.5.1). Then, the rate vector $[\rho_1, \ldots, \rho_K]^{\mathrm{T}} \geq \mathbf{0}$ is feasible without (R)TS if and only if*

$$\sum_{k=1}^{K} d_\mu(\rho_k) < \mu M. \tag{7.73}$$

From this inequality, we can understand the intuition behind the name effective degrees of freedom for the quantity $d_\mu(\rho_k)$. The base station in the complex MIMO BC-TIN can offer M degrees of freedom (DoF) in total and the transmission of a proper signal to user k reduces the DoF available to serve the other users with TIN strategies by $d_\mu(\rho_k)$ [52]. The factor of $\mu = \frac{1}{2}$ in the definition of $d_\mu(\rho_k)$ in a real-valued system corresponds to the interpretation that a real-valued data stream is half a complex data stream. Accordingly, the available DoF at the base station of the real-valued MIMO BC-TIN are divided by two on the right hand side of (7.73).

7.5.1.1 QoS Feasibility with Maximum-Entropy Signals

If we now restrict the users to perform maximum-entropy transmission with respect to the power shaping spaces $(\mathcal{P}_k)_{\forall k}$ (which corresponds to maximum-entropy transmission with respect to a power shaping space $\mathcal{P}_{\mathrm{B}}$ in the downlink), there are two effects that can occur. First of all, some power shaping spaces impose requirements on the rank of the covariance matrix $\boldsymbol{C}_{\boldsymbol{x}_k}$.

Example 7.5.1. *If we restrict the uplink transmit covariance matrices $\boldsymbol{C}_{\boldsymbol{x}_k}$ to lie in the power shaping space of scaled identity matrices (see Example 2.8.1), any $\boldsymbol{C}_{\boldsymbol{x}_k} \in \mathcal{P}_k$ has full rank M_k. However, single-stream transmission, which would be optimal in terms of feasibility (Lemma 7.5.2), corresponds to transmit covariance matrices with rank one.*

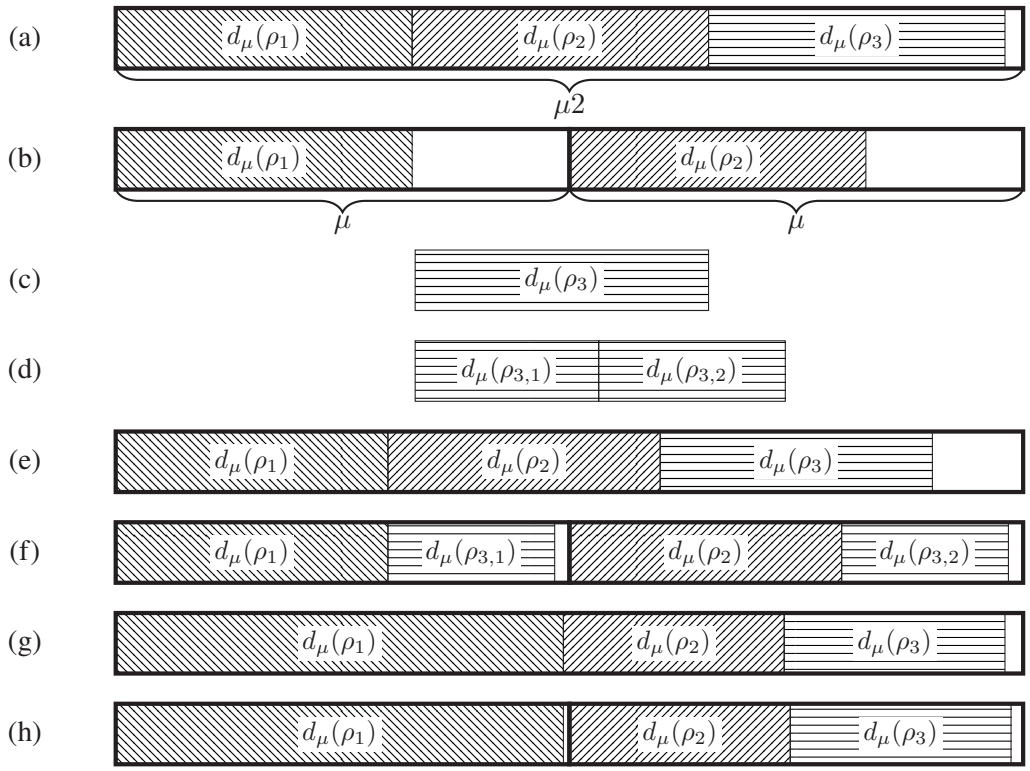

Figure 7.4: Visualizations of the various stream allocations in Example 7.5.2.

There is a second effect, which can occur even if we consider a power shaping space $\mathcal{P}_k$ that allows for single-stream transmission. Due to the structure that $\mathcal{P}_k$ imposes on $\boldsymbol{C}_{\boldsymbol{x}_k} = \boldsymbol{t}_k \boldsymbol{t}_k^{\mathrm{H}}$, it might be no longer possible to find transmit filters such that the effective channels $\boldsymbol{h}_{\mathrm{eff},k}$ in the proof of Theorem 7.5.1 fulfill the feasibility condition (7.69) in the resulting MISO system even if condition (7.68) in the MIMO system is satisfied.

Example 7.5.2. *Consider a three-user system with $M = 2$ and $\boldsymbol{H}_{\mathrm{UL},k} = \mathbf{I}_2,\ \forall k$. As the regularity condition is fulfilled, we can use* (7.73) *and obtain the condition*

$$\sum_{k=1}^{3} d_\mu(\rho_k) < \mu 2. \tag{7.74}$$

Let us now restrict the uplink transmit covariance matrices $\boldsymbol{C}_{\boldsymbol{x}_k}$ to lie in the power shaping space of diagonal matrices (see Example 2.8.2). For the case of single-stream transmission, the only possible uplink transmit filter vectors are then given by $\boldsymbol{t}_k \in \{\sqrt{p_k}\mathbf{e}_1, \sqrt{p_k}\mathbf{e}_2\}$, where $p_k \geq 0$ is the uplink transmit power of user k. Let $\mathcal{K}_c,\ c \in \{1,2\}$ contain the indices of the users that transmit by means of the filter vector $\boldsymbol{t}_k = \sqrt{p_k}\mathbf{e}_c$, so that $\{1,2,3\} = \mathcal{K}_1 \cup \mathcal{K}_2$. In the resulting MISO BC-TIN with uplink channel vectors $\boldsymbol{h}_{\mathrm{eff},k} = \boldsymbol{H}_{\mathrm{UL},k}\boldsymbol{t}_k$, the regularity condition is no longer fulfilled since there exists a set of at least two users with collinear effective channel vectors (both being a scaled version of $\mathbf{e}_c$ for some c). Therefore, we have to use (7.69)*. After removing redundant inequalities, we obtain the feasibility conditions*

$$\sum_{k \in \mathcal{K}_c} d_\mu(\rho_k) < \mu, \quad \forall c. \tag{7.75}$$

Regardless of how we choose the sets $\mathcal{K}_c$, these conditions are stricter than (7.74).

As a first scenario, consider a rate vector $\boldsymbol{\rho}$ such that $d_\mu(\rho_k) = \mu(\frac{2}{3} - \epsilon),\ \forall k$ with a small $\epsilon > 0$. This rate vector is achievable according to (7.74) *(Figure 7.4 a). However,* (7.75) *cannot be fulfilled with single-stream transmission since at least one of the sets would have to contain at least two users, yielding $2\mu(\frac{2}{3} - \epsilon) > \mu$ (Figure 7.4 b and c).*

We could now try to split one of the rates ρ_k into two per-stream rates $\rho_{k,1}$ and $\rho_{k,2}$ in order to serve user k partially via the transmit filter vector $\boldsymbol{t}_{k,1} = \sqrt{p_{k,1}}\mathbf{e}_1$ and partially via $\boldsymbol{t}_{k,2} = \sqrt{p_{k,2}}\mathbf{e}_2$, where $p_{k,s}$ are the respective per-stream powers. If we split, e.g., the rate requirement of user $k = 3$, the feasibility conditions for this maximum-entropy strategy read as

$$d_\mu(\rho_1) + d_\mu(\rho_{3,1}) < \mu \qquad\qquad d_\mu(\rho_2) + d_\mu(\rho_{3,2}) < \mu. \tag{7.76}$$

However, due to Lemma 7.5.2, we have $d_\mu(\rho_{k,1}) + d_\mu(\rho_{k,2}) > d_\mu(\rho_k)$ (Figure 7.4 c and d). For the sum EDoF requirement of all users, we thus obtain

$$d_\mu(\rho_{k,1}) + d_\mu(\rho_{k,2}) + \sum_{j\neq k} d_\mu(\rho_j) > \sum_{k=1}^{3} d_\mu(\rho_k) \overset{\epsilon\to 0}{\to} \mu 2 \tag{7.77}$$

i.e., if ϵ is sufficiently small, this sum EDoF requirement even violates the feasibility condition without the restriction to maximum-entropy transmission, i.e., for the example $k = 3$ the condition

$$d_\mu(\rho_1) + d_\mu(\rho_2) + d_\mu(\rho_{3,1}) + d_\mu(\rho_{3,2}) < \mu 2. \tag{7.78}$$

Thus, using multistream transmission does not help to achieve the rate vector $\boldsymbol{\rho}$ in case of the considered maximum-entropy transmission. Note that $\epsilon \to 0$ was used only for the sake of a simple argumentation without numerical computations. The infeasibility occurs already for a larger value of ϵ and is, thus, an effect that is not only of theoretical interest.

Let us now instead consider a scenario with smaller rate requirements[5] (i.e., with a larger ϵ), e.g., such that $d_\mu(\rho_k) = \mu 0.6,\ \forall k$ (Figure 7.4 e). It is then still impossible to fulfill (7.75) *with single-stream transmission, but it is possible to find a solution where one of the users is served with two streams as in* (7.76) *(Figure 7.4 f).*

As a final scenario, consider a rate vector $\boldsymbol{\rho}$ such that $d_\mu(\rho_1) = \mu(1 - \epsilon)$ and $d_\mu(\rho_2) = d_\mu(\rho_3) = \mu(\frac{1}{2} - \epsilon)$ (Figure 7.4 g). By choosing $\mathcal{K}_1 = \{1\}$ and $\mathcal{K}_2 = \{2, 3\}$, we can fulfill (7.75) *with single-stream transmission even for very small values of ϵ, i.e., even if we get close to the feasibility limit in terms of* (7.74) *(Figure 7.4 h). This shows that the limitation to the considered power shaping space is not always harmful, but only in case of an unsuitable combination of the individual rate requirements.*

Of course, we can also have combinations of the two effects described in Examples 7.5.1 and 7.5.2. In the next section, we see that the effects observed in these minimal examples also occur when studying proper signals and CN signals, respectively.

Unfortunately, there does not seem to be a simple way to describe the QoS feasibility region for maximum-entropy transmission in general. Unlike in Theorem 7.5.1, adequate transmit filters have to be constructed under structural constraints, and the two examples given above show that these constraints can be quite different in nature depending on which power shaping

[5] A similar example is mentioned in [52].

spaces are considered. It therefore seems to be more appropriate to study the QoS feasibility region separately for each kind of power shaping space we are interested in. In the following, we do so for the power shaping spaces that correspond to proper signaling, to CN transmission, and to the combination of both. Nevertheless, let us first summarize our observations as a general theorem.

Theorem 7.5.2. *Let $(\mathcal{P}_k = \mathcal{P}_{\mathrm{U}_k})_{\forall k}$ and $\mathcal{P}_{\mathrm{B}}$ be power shaping spaces fulfilling the compatibility assumption (Definition 3.1.3). Even if the noise vectors $\boldsymbol{\eta}_k$ are maximum-entropy signals with respect to $(\mathcal{P}_k)_{\forall k}$, it can happen that reduced-entropy per-user input signals $\boldsymbol{\xi}_k$ with respect to $\mathcal{P}_{\mathrm{B}}$ are needed to achieve the whole QoS feasibility region of the RoP MIMO BC-TIN.*

Proof. Examples where this happens are given above and below. □

7.5.1.2 QoS Feasibility in the Complex Multicarrier MIMO BC-TIN

In order to allow for an easy comparison of the various obtained results, we restrict the following study of QoS feasibility in the complex multicarrier MIMO BC-TIN to the case of proper CN noise. If the noise is improper or CC or both, we could still derive similar results, e.g., based on the combined real representation, but some of the following four descriptions of the uplink channel matrices would no longer exist (see Section 7.2.5). Let us define the following matrices, which contain the specified submatrices as a block row:

$$\grave{\boldsymbol{H}}_{\mathcal{K}} \in \mathbb{R}^{2Cm\times\sum_{k\in\mathcal{K}}2Cm_k} \quad \text{comprises} \quad \grave{\boldsymbol{H}}_{\mathrm{UL},k} \in \mathbb{R}^{2Cm\times 2Cm_k} \quad \text{for } k\in\mathcal{K}, \tag{7.79}$$

$$\boldsymbol{H}_{\mathcal{K}} \in \mathbb{C}^{Cm\times\sum_{k\in\mathcal{K}}Cm_k} \quad \text{comprises} \quad \boldsymbol{H}_{\mathrm{UL},k} \in \mathbb{C}^{Cm\times Cm_k} \quad \text{for } k\in\mathcal{K}, \tag{7.80}$$

$$\grave{\boldsymbol{H}}^{(c)}_{\mathcal{K}} \in \mathbb{R}^{2m\times\sum_{k\in\mathcal{K}}2m_k} \quad \text{comprises} \quad \grave{\boldsymbol{H}}^{(c)}_{\mathrm{UL},k} \in \mathbb{R}^{2m\times 2m_k} \quad \text{for } k\in\mathcal{K}, \tag{7.81}$$

$$\boldsymbol{H}^{(c)}_{\mathcal{K}} \in \mathbb{C}^{m\times\sum_{k\in\mathcal{K}}m_k} \quad \text{comprises} \quad \boldsymbol{H}^{(c)}_{\mathrm{UL},k} \in \mathbb{C}^{m\times m_k} \quad \text{for } k\in\mathcal{K}. \tag{7.82}$$

The matrices $\grave{\boldsymbol{H}}_{\mathrm{UL},k}$, $\boldsymbol{H}_{\mathrm{UL},k}$, $\grave{\boldsymbol{H}}^{(c)}_{\mathrm{UL},k}$, and $\boldsymbol{H}^{(c)}_{\mathrm{UL},k}$ correspond to the four representations from Table 3.1.

Note that the combined real representation of $\boldsymbol{H}^{(c)}_{\mathcal{K}}$ is not given by $\grave{\boldsymbol{H}}_{\mathcal{K}}$, but there exists a permutation matrix $\boldsymbol{\Pi}$ such that it is given by $\grave{\boldsymbol{H}}_{\mathcal{K}}\boldsymbol{\Pi}$. Accordingly, we can find permutation matrices to switch between the other representations. Since such permutations do not change the rank of a matrix, we can exploit (2.54) together with the fact that the rank of a block-diagonal matrix equals the sum of the ranks of the submatrices in order to obtain

$$\operatorname{rank}\left[\grave{\boldsymbol{H}}_{\mathcal{K}}\right] = 2\operatorname{rank}\left[\boldsymbol{H}_{\mathcal{K}}\right] = \sum_{c=1}^{C}\operatorname{rank}\left[\grave{\boldsymbol{H}}^{(c)}_{\mathcal{K}}\right] = 2\sum_{c=1}^{C}\operatorname{rank}\left[\boldsymbol{H}^{(c)}_{\mathcal{K}}\right]. \tag{7.83}$$

Without any restrictions on the transmit covariance matrices, we obtain the following QoS feasibility region.

Corollary 7.5.2. *Under the assumption of proper CN noise in the complex multicarrier MIMO BC-TIN, the rate vector $[\rho_1,\ldots,\rho_K]^{\mathrm{T}} \geq \mathbf{0}$ is feasible without (R)TS if and only if*

$$\sum_{k\in\mathcal{K}} d_{\frac{1}{2}}(\rho_k) < \sum_{c=1}^{C}\operatorname{rank}\left[\boldsymbol{H}^{(c)}_{\mathcal{K}}\right], \quad \forall\mathcal{K}\subseteq\{1,\ldots,K\}. \tag{7.84}$$

Proof. This directly follows from Theorem 7.5.1 applied to the combined real representation (3.37) with $\mu = \frac{1}{2}$ and $\grave{\boldsymbol{H}}_{\mathcal{K}}$ from (7.79). □

Corollary 7.5.3. *If the regularity condition is fulfilled in Corollary 7.5.2, the feasibility condition* (7.84) *reduces to*

$$\sum_{k=1}^{K} d_{\frac{1}{2}}(\rho_k) < Cm. \tag{7.85}$$

Proof. This directly follows from Corollary 7.5.1 applied to the combined real representation (3.37) with $\mu = \frac{1}{2}$ and $M = 2Cm$. □

In the following, we study the QoS feasibility region for various kinds of maximum-entropy transmission. If we restrict the combined real uplink transmit covariance matrices $\boldsymbol{C}_{\check{\boldsymbol{x}}_k}$ to lie in the power shaping spaces $\mathcal{P}_k = \grave{\mathcal{P}}_{\mathrm{U}_k}$, $\forall k$, which correspond to proper signaling, the rank of any $\boldsymbol{C}_{\check{\boldsymbol{x}}_k} \in \mathcal{P}_k$ is even due to Lemma 2.9.9. Similar as in Example 7.5.1, this means that single-stream transmission (i.e., a transmit covariance matrix with rank one) is impossible. It therefore is to be expected that a restriction to proper signaling reduces the QoS feasibility region. This effect is quantified in the following corollary.

Corollary 7.5.4. *Under the assumption of proper CN noise in the complex multicarrier MIMO BC-TIN, the rate vector* $[\rho_1, \ldots, \rho_K]^{\mathrm{T}} \geq \mathbf{0}$ *is feasible using proper per-user input signals without (R)TS if and only if*

$$\sum_{k\in\mathcal{K}} d_1(\rho_k) < \sum_{c=1}^{C} \operatorname{rank}\left[\boldsymbol{H}_{\mathcal{K}}^{(c)}\right], \quad \forall \mathcal{K} \subseteq \{1, \ldots, K\}. \tag{7.86}$$

Proof. Due to the assumption of proper signals and noise, the combined complex representation (3.35) is a RoP MIMO system (see Section 3.4.1) and Theorem 7.5.1 can be applied with $\mu = 1$ and $\boldsymbol{H}_{\mathcal{K}}$ from (7.80). □

Corollary 7.5.5. *If the regularity condition is fulfilled in Corollary 7.5.4, the feasibility condition for proper signaling* (7.86) *reduces to*

$$\sum_{k=1}^{K} d_1(\rho_k) < Cm. \tag{7.87}$$

Proof. This directly follows from Corollary 7.5.1 applied to the combined complex representation (3.35) with $\mu = 1$ and $M = Cm$. □

A comparison of the QoS feasibility regions with proper and improper signaling was first published in [5]. As pointed out therein, it holds that

$$d_1(\rho) - d_{\frac{1}{2}}(\rho) = (1 - 2^{-\rho}) - \frac{1}{2}(1 - 2^{-2\rho}) = \frac{1}{2}(1 - 2^{-\rho})^2 > 0 \tag{7.88}$$

for all $\rho > 0$ (see also Figure 7.3). Comparing (7.87) to (7.85) with the help of this inequality, we see that restricting all users to employ proper signaling makes the QoS feasibility region strictly smaller if there are more than Cm users in the system. In case of Cm users or less, arbitrary rate requirements can be fulfilled in both cases (see Section 7.5.2.2), but there may still be a difference in the transmit power that is required to do so (see Section 7.5.5).

Next, we turn our attention to the power shaping spaces $\mathcal{P}_k = \mathcal{P}_{\mathrm{U}_k}^{\mathrm{CN}}$, $\forall k$, which correspond to CN transmission. Example 7.5.2 can be considered as a minimal example for CN transmission, namely in a real-valued (or proper complex) single-antenna system with two carriers. It is reasonable to expect that similar effects as observed in the minimal example also happen in larger systems, i.e., that a restriction to CN transmission reduces the QoS feasibility region. This is studied in the following corollary.

Corollary 7.5.6. *Under the assumption of proper CN noise in the complex multicarrier MIMO BC-TIN, the rate vector* $[\rho_1, \ldots, \rho_K]^{\mathrm{T}} \geq \mathbf{0}$ *is feasible using CN per-user input signals without (R)TS if and only if there exist per-carrier rates* $\rho_k^{(c)} \geq 0$, $\forall k$ $\forall c$ *such that*

$$\sum_{c=1}^{C} \rho_k^{(c)} = \rho_k, \quad \forall k, \tag{7.89}$$

$$\sum_{k \in \mathcal{K}} d_{\frac{1}{2}}(\rho_k^{(c)}) < \operatorname{rank}\left[\boldsymbol{H}_{\mathcal{K}}^{(c)}\right], \quad \forall \mathcal{K} \subseteq \{1, \ldots, K\}, \quad \forall c. \tag{7.90}$$

Proof. Due to the assumption of CN signals and noise, the real-valued multicarrier formulation is a RoP CN MIMO system (see Section 3.4.1) and Theorem 7.5.1 can be applied separately on each carrier with $\mu = \frac{1}{2}$ and $\grave{\boldsymbol{H}}_{\mathcal{K}}^{(c)}$ from (7.81). While we have to consider the coupling of the per-carrier rates in (7.89), there is no coupling constraint on the per-carrier powers since arbitrarily high transmit powers are allowed when considering the QoS feasibility region. □

Corollary 7.5.7. *If the regularity condition is fulfilled in Corollary 7.5.6, the per-carrier feasibility condition* (7.90) *reduces to*

$$\sum_{k=1}^{K} d_{\frac{1}{2}}(\rho_k^{(c)}) < m, \quad \forall c. \tag{7.91}$$

Proof. This directly follows from Corollary 7.5.1 applied to each carrier of the real-valued multicarrier formulation (3.36) with $\mu = \frac{1}{2}$ and $M = 2m$. □

This result for general complex CN transmission is not contained in the existing literature, but it is similar to the corresponding result for proper CN transmission from [52], which we reproduce later on in Corollary 7.5.8. Due to this analogy, the following observations from [52] also apply in the case considered here.

If we assume single-stream transmission, the per-carrier constraints are stricter than the conditions in (7.84). Therefore, it may be necessary to activate multiple streams per user even though this increases the sum EDoF requirement in the system. A minimal example for this effect was discussed in detail in Example 7.5.2. Just like in this example, rate vectors with unsuitable combinations of the requirement sizes can be rendered infeasible by the restriction to CN transmission even if they are feasible with CC transmission. Consequently, the restriction to CN transmission reduces the size of the QoS feasibility region.

To test for feasibility in the case of CN transmission, we have to try to find a division of the rates ρ_k into per-stream rates and an allocation of the streams to carriers such that (7.90) is fulfilled. Just like in the case of proper complex CN transmission in [52], this decision problem is NP hard in general. An algorithm that can be used as sufficient feasibility test was proposed in [52] and can be transferred to the case of general complex CN transmission.

Finally, by combining both proper signaling and CN transmission, we expect a further reduction of the QoS feasibility region since the two effects observed above then occur simultaneously. In this case, we obtain the following feasibility region [52].

Corollary 7.5.8 ($\mathcal{P}_k = \grave{\mathcal{P}}_{\mathrm{U}_k}^{\mathrm{CN}},\ \forall k$ and $\mathcal{P}_{\mathrm{B}} = \grave{\mathcal{P}}_{\mathrm{B}}^{\mathrm{CN}}$)**.** *Under the assumption of proper CN noise in the complex multicarrier MIMO BC-TIN, the rate vector* $[\rho_1, \ldots, \rho_K]^{\mathrm{T}} \geq \mathbf{0}$ *is feasible using proper CN per-user input signals without (R)TS if and only if there exist per-carrier rates* $\rho_k^{(c)} \geq 0,\ \forall k\ \forall c$ *such that* (7.89) *holds and*

$$\sum_{k \in \mathcal{K}} d_1(\rho_k^{(c)}) < \operatorname{rank}\left[\boldsymbol{H}_{\mathcal{K}}^{(c)}\right], \quad \forall \mathcal{K} \subseteq \{1, \ldots, K\}, \quad \forall c. \tag{7.92}$$

Proof. Due to the assumption of proper CN signals and noise, the complex multicarrier formulation is a RoP CN MIMO system (see Section 3.4.1) and Theorem 7.5.1 can be applied separately on each carrier (in analogy to Corollary 7.5.6) with $\mu = 1$ and $\boldsymbol{H}_{\mathcal{K}}^{(c)}$ from (7.82). □

Corollary 7.5.9. *If the regularity condition is fulfilled in Corollary 7.5.8, the feasibility condition for CN transmission with proper signaling* (7.92) *reduces to*

$$\sum_{k=1}^{K} d_1(\rho_k^{(c)}) < m, \quad \forall c. \tag{7.93}$$

Proof. This directly follows from Corollary 7.5.1 applied to each carrier of the complex multicarrier formulation (3.34) with $\mu = 1$ and $M = m$. □

Due to (7.88), this QoS feasibility region is smaller than the one for general complex CN transmission in Corollaries 7.5.6 and 7.5.7. At the same time, this region is a subset of the one for proper complex CC transmission in Corollaries 7.5.4 and 7.5.5 since we can again use the argument that the per-carrier conditions are stricter than the original conditions (see Example 7.5.2 and [52]).

7.5.2 Feasibility of Zero-Forcing

In the presence of zero-forcing constraints, the question of feasibility becomes qualitatively different, but it turns out that the previously derived results are still helpful for the study of zero-forcing. In the RoP MISO BC-TIN, the number of users out of a group $\mathcal{K}$ that can be served simultaneously by a zero-forcing strategy is limited by the rank of the channel matrix $\boldsymbol{H}_{\mathcal{K}}$ (e.g., [124]). If this limitation is violated, the null space of the interference covariance matrix, which is necessary to construct the zero-forcing filters in (7.12) or (7.23), vanishes. We now formalize this for the RoP MIMO BC-TIN based of the previously stated feasibility results.

Theorem 7.5.3. *In the RoP MIMO BC-TIN with zero-forcing constraints, the rate vector* $[\rho_1, \ldots, \rho_K]^{\mathrm{T}} \geq \mathbf{0}$ *is feasible without (R)TS if and only if*

$$\left|\{k \in \mathcal{K} \mid \rho_k > 0\}\right| \leq \operatorname{rank}\left[\boldsymbol{H}_{\mathcal{K}}\right] \quad \forall \mathcal{K} \subseteq \{1, \ldots, K\}. \tag{7.94}$$

Proof. If a rate vector $\boldsymbol{\rho} = [\rho_1, \ldots, \rho_K]^{\mathrm{T}} \geq \mathbf{0}$ is achievable with zero-forcing, then the rate vector $\boldsymbol{\rho}_\infty = \lim_{\alpha \to \infty} \alpha \boldsymbol{\rho}$ is also achievable if an infinite amount of transmit power is invested.

The reason for this is that no interference is present and that the noise becomes negligible if the transmit power is sufficiently high. Conversely, the rate vector $\boldsymbol{\rho}_\infty$ is only achievable if zero-forcing is feasible because interference terms that grow together with the growing transmit powers prevent the SINRs from going to infinity (see the proof of [178, Theorem III.1]). Thus, $\boldsymbol{\rho}$ is feasible with zero-forcing if and only if $\boldsymbol{\rho}_\infty$ lies in the QoS feasibility region given in Theorem 7.5.1, i.e., if and only if

$$\sum_{k\in\mathcal{K}} d_{\mathrm{ZF},\mu}(\rho_k) \leq \mu \operatorname{rank}\left[\boldsymbol{H}_{\mathcal{K}}\right] \quad \forall \mathcal{K} \subseteq \{1,\ldots,K\} \tag{7.95}$$

with

$$d_{\mathrm{ZF},\mu}(\rho) = \lim_{\alpha\to\infty} d_\mu(\alpha\boldsymbol{\rho}) = \begin{cases} \mu & \text{if } \rho > 0 \\ 0 & \text{otherwise.} \end{cases} \tag{7.96}$$

The inequality in (7.95) is not strict since the bound in (7.68) can be reached with equality if the transmit powers tend to infinity (see [174, 176]). This means that we only need to count the number of users with nonzero rate requirements, which is compactly written in (7.94). □

Corollary 7.5.10. *If the regularity condition is fulfilled in Theorem 7.5.3, the feasibility condition* (7.94) *reduces to*

$$\Big|\{k \in \{1,\ldots,K\} \mid \rho_k > 0\}\Big| \leq M. \tag{7.97}$$

7.5.2.1 Feasibility of Zero-Forcing with Maximum-Entropy Signals

We are now interested in how this result changes if a restriction to maximum-entropy transmission is introduced.

Example 7.5.3. *Let us first consider the effect observed in Example 7.5.2, where a restriction to the power shaping space of diagonal matrices was imposed. In this case, individual feasibility conditions* (7.75) *corresponding to each of the diagonal elements had to be considered instead of an overall feasibility condition* (7.74)*. For unsuitable combinations of rate requirements ρ_k, it could then happen that there exists no choice of the transmit filters such that the individual conditions are satisfied, even though the overall criterion is fulfilled. However, such an effect is not possible for the case of zero-forcing because both sides of each inequality in* (7.94) *are integer multiples of μ.*

However, the situation is different when considering the effect observed in Example 7.5.1.

Example 7.5.4. *If the restriction to a power shaping space requires the rank of the transmit covariance matrices to be a multiple of $\beta > 1$, this means that at least β streams have to be transmitted if $\rho_k > 0$. The other users have to eliminate the interference of these streams by means of zero-forcing filters. We obtain a sum EDoF requirement of $\beta \mathrm{d}_{\mathrm{ZF},\mu}(\rho_k) = \mu\beta$ for each user k with $\rho_k > 0$. This leads to the stricter condition $\beta\Big|\{k \in \{1,\ldots,K\} \mid \rho_k > 0\}\Big| \leq M$ instead of* (7.97) *and reduces the set of rates that are feasible with zero-forcing.*

Before turning our attention to the complex multicarrier MIMO BC-TIN, let us formalize this finding in a general theorem.

Theorem 7.5.4. *The statement of Theorem 7.5.2 holds analogously if zero-forcing constraints are imposed.*

Proof. Examples where this happens are given above and below. □

7.5.2.2 Feasibility of Zero-Forcing in the Complex Multicarrier MIMO BC-TIN

From the proof of Theorem 7.5.3, we know an easy way to extend the results from Section 7.5.1.2 to the case of zero forcing constraints. We can simply replace d_μ by $d_{\mathrm{ZF},\mu}$ and $<$ by $\leq$ in Corollaries 7.5.2 through 7.5.9. By doing so, we obtain the following results. Just like in Section 7.5.1.2, we consider only the case of proper CN noise, but results for other types of noise could be derived as well.

Corollary 7.5.11 (see Corollary 7.5.2)**.** *Under the assumption of proper CN noise in the complex multicarrier MIMO BC-TIN with zero-forcing constraints, the rate vector* $[\rho_1, \ldots, \rho_K]^{\mathrm{T}} \geq \mathbf{0}$ *is feasible without (R)TS if and only if*

$$\frac{1}{2}\left|\{k \in \mathcal{K} \mid \rho_k > 0\}\right| \leq \sum_{c=1}^{C} \operatorname{rank}\left[\boldsymbol{H}_{\mathcal{K}}^{(c)}\right] \quad \forall \mathcal{K} \subseteq \{1, \ldots, K\}. \tag{7.98}$$

Corollary 7.5.12 (see Corollary 7.5.3)**.** *If the regularity condition is fulfilled in Corollary 7.5.11, the feasibility condition* (7.98) *reduces to*

$$\left|\{k \in \{1, \ldots, K\} \mid \rho_k > 0\}\right| \leq 2Cm. \tag{7.99}$$

Under a restriction to proper signaling, we obtain the following stricter feasibility condition.

Corollary 7.5.13 (see Corollary 7.5.4)**.** *Under the assumption of proper CN noise in the complex multicarrier MIMO BC-TIN with zero-forcing constraints, the rate vector* $[\rho_1, \ldots, \rho_K]^{\mathrm{T}} \geq \mathbf{0}$ *is feasible using proper per-user input signals without (R)TS if and only if*

$$\left|\{k \in \mathcal{K} \mid \rho_k > 0\}\right| \leq \sum_{c=1}^{C} \operatorname{rank}\left[\boldsymbol{H}_{\mathcal{K}}^{(c)}\right] \quad \forall \mathcal{K} \subseteq \{1, \ldots, K\}. \tag{7.100}$$

Corollary 7.5.14 (see Corollary 7.5.5)**.** *If the regularity condition is fulfilled in Corollary 7.5.13, the feasibility condition* (7.100) *reduces to*

$$\left|\{k \in \{1, \ldots, K\} \mid \rho_k > 0\}\right| \leq Cm. \tag{7.101}$$

In comparison to proper signaling (Corollary 7.5.14), improper signaling doubles the number of users that can be served in the complex multicarrier MIMO BC-TIN under zero-forcing constraints (Corollary 7.5.12). This result was published in [5] and can be found in a similar manner in [173], where a study based on bit error rates was performed instead of based on achievable rates. Note that the number of users given for proper signaling in Corollary 7.5.14 can be achieved with linear zero-forcing (see Proposition 7.1.1) while widely linear zero-forcing is necessary to achieve any higher number [5, 173].

Already in Section 7.5.1.2, we could notice a qualitative difference between the two kinds of reduced-entropy transmission that we consider, and we will see that this difference between CC transmission and improper signaling is even more pronounced in case of zero-forcing constraints. Let us first note the following difference between QoS feasibility (see Example 7.5.2) and the feasibility of zero-forcing constraints.

Lemma 7.5.3. *Under the assumption of proper CN noise in the complex multicarrier MIMO BC-TIN with zero-forcing constraints, the rate vector* $[\rho_1, \ldots, \rho_K]^{\mathrm{T}} \geq \mathbf{0}$ *is feasible using (proper or general complex) CN per-user input signals without (R)TS if and only if it is feasible with single-stream transmission (of proper or real-valued streams, respectively).*

Proof. When adding another stream to reduce the rate requirement $\rho_{k,1}$ of the first stream, this does not reduce the EDoF requirement $d_{\mathrm{ZF},\mu}(\rho_{k,1})$. □

Finding a feasible allocation of rate targets to carriers is still a combinatorial problem in the case of zero-forcing constraints, but due to Lemma 7.5.3, less possibilities than in the case of QoS feasibility (Corollaries 7.5.6 and 7.5.8) need to be considered.

Corollary 7.5.15 (see Corollary 7.5.6 and Lemma 7.5.3)**.** *Under the assumption of proper CN noise in the complex multicarrier MIMO BC-TIN with zero-forcing constraints, the rate vector* $[\rho_1,\ldots,\rho_K]^{\mathrm{T}} \geq \mathbf{0}$ *is feasible using CN per-user input signals without (R)TS if and only if we can find disjoint sets* $\mathcal{K}_c$, $\forall c$ *such that* $\bigcup_{c=1}^{C} \mathcal{K}_c = \{k \in \{1,\ldots,K\} \mid \rho_k > 0\}$ *and*

$$\frac{1}{2}|\mathcal{K}| \leq \operatorname{rank}\left[\boldsymbol{H}_{\mathcal{K}}^{(c)}\right] \quad \forall \mathcal{K} \subseteq \mathcal{K}_c, \quad \forall c. \tag{7.102}$$

Corollary 7.5.16 (see Corollary 7.5.8 and Lemma 7.5.3)**.** *Under the assumption of proper CN noise in the complex multicarrier MIMO BC-TIN with zero-forcing constraints, the rate vector* $[\rho_1,\ldots,\rho_K]^{\mathrm{T}} \geq \mathbf{0}$ *is feasible using proper CN per-user input signals without (R)TS if and only if we can find disjoint sets* $\mathcal{K}_c$, $\forall c$ *such that* $\bigcup_{c=1}^{C} \mathcal{K}_c = \{k \in \{1,\ldots,K\} \mid \rho_k > 0\}$ *and*

$$|\mathcal{K}| \leq \operatorname{rank}\left[\boldsymbol{H}_{\mathcal{K}}^{(c)}\right] \quad \forall \mathcal{K} \subseteq \mathcal{K}_c, \quad \forall c. \tag{7.103}$$

However, the combinatorial nature of the problem vanishes in case of regular channels, where we have the following result.

Proposition 7.5.1. *Under the assumption of regular channels and proper CN noise in the complex multicarrier MIMO BC-TIN with zero-forcing constraints without (R)TS, a restriction to CN transmission does not impair the feasibility of a rate vector* $\boldsymbol{\rho}$*.*

Proof. In this case, the sets $\mathcal{K}_c$ can be chosen arbitrarily as long as $|\mathcal{K}_c| \leq 2m$ in Corollary 7.5.15 and as long as $|\mathcal{K}_c| \leq m$ in Corollary 7.5.16. The resulting feasibility conditions are equivalent to the ones in Corollary 7.5.11 and Corollary 7.5.13, respectively. □

While improper signaling has the potential to double the number of users that can be served (Corollary 7.5.14 vs. Corollary 7.5.12) in scenarios with regular channels, CC transmission does not bring any gains in terms of the feasibility of zero-forcing constraints (Proposition 7.5.1). From the reasoning in the proof of Theorem 7.5.3 (see also [178, Theorem III.1]), we can infer that these observations are also valid for QoS feasibility in systems without zero-forcing constraints that operate in the high-rate regime. This statement is supported by Figure 7.3, which shows that the EDoF requirements $d_{\mu}(\rho)$ converge quickly to $d_{\mathrm{ZF},\mu}(\rho)$.

7.5.3 Reduced-Entropy Transmission in the Complex Two-User Multicarrier MIMO BC-TIN

A question that was left open in Section 7.4 is whether performance gains due to reduced-entropy transmission can occur in a two-user BC-TIN. If (R)TS is not allowed, this question can be easily answered by means of the QoS feasibility results presented above.

Example 7.5.5. *Consider the complex two-user single-carrier SISO BC with uplink channels* $h_{\mathrm{UL},k} = 1$, $\forall k$*. Due to Corollary 7.5.2, arbitrarily high rates are feasible since*

$\sum_{k=1}^{2} d_{\frac{1}{2}}(\rho_k) < 1$ *is satisfied for arbitrary* $\rho_k > 0,\ \forall k$. *However, if we restrict the users to apply proper signaling, the rates have to fulfill* $\sum_{k=1}^{2} 1 - 2^{-\rho_k} < 1$ *since* $\sum_{k=1}^{2} d_1(\rho_k) < 1$ *is required in Corollary 7.5.4.*

This is clearly a gain by reduced-entropy transmission in a two-user system without (R)TS, i.e., this example is sufficient to answer the question that was posed above. However, to get a better understanding of the effects that happen, it makes sense to also look at examples which not only show gains in terms of feasibility, but also for the case where QoS feasibility is not the limiting factor.

Example 7.5.6. *Consider the system from Example 7.5.5. With proper signaling, the only freedom of choice that we have in the uplink is the power allocation. Using* $\mathsf{C}_{\mathsf{x}_k} = p_k = \frac{1}{\sqrt{2}}\ \forall k$, *we can achieve the rates* $r_k = \log_2(1 + \frac{p_k}{1+p_j}) = \frac{1}{2}\ \forall k, j \neq k$ *due to* (7.14) *with* $\mu = 1$. *Using the framework from [179], it can be shown that the power allocation that is needed to achieve a particular rate vector in this setting is unique. Thus, the rate vector* $\boldsymbol{\rho} = \frac{1}{2}\mathbf{1}$ *cannot be achieved with a sum transmit power smaller than* $\sum_{k=1}^{2} \mathsf{C}_{\mathsf{x}_k} = \sqrt{2}$ *as long as we stick to proper signaling. Using improper signaling with the combined real transmit covariance matrices* $\boldsymbol{C}_{\check{\boldsymbol{x}}_k} = \frac{1}{2}\mathbf{e}_k\mathbf{e}_k^{\mathrm{T}}$, *we can calculate using* (7.14) *with* $\mu = \frac{1}{2}$ *and* $\boldsymbol{H}_{\mathrm{UL},k} = \grave{\boldsymbol{H}}_{\mathrm{UL},k} = \mathbf{I}_2,\ \forall k$ *that the same rate vector* $\boldsymbol{\rho} = \frac{1}{2}\mathbf{1}$ *is achievable at a reduced sum transmit power of* $\sum_{k=1}^{K} \mathrm{tr}[\boldsymbol{C}_{\check{\boldsymbol{x}}_k}] = 1$.

Note that we could apply zero-forcing receive filters $\boldsymbol{G}_{k,\mathrm{ZF}}^{\mathrm{H}} = \mathbf{e}_k^{\mathrm{T}}$ without changing the achievable rates of the improper strategy. On the other hand, if we impose zero-forcing constraints for the case of proper signaling, only one user can be served at a time in this example. This shows that gains by improper signaling occur as well if the same setting is considered under zero-forcing constraints.

The above example was constructed in a way that the (complex) degrees of freedom $Cm = 1$ available at the base station are less than the number of users $K = 2$, i.e., the system is overloaded if we stick to proper signaling. The additional flexibility of improper signaling, which can allocate streams that correspond to half a degree of freedom of the complex system, can resolve this issue. However, the same result could be obtained by instead exploiting the flexibility offered by (R)TS, which we assume to not be allowed throughout this section.

Let us now turn our attention to systems where the degrees of freedom at the base station are not the limiting factor. An example for this can be found in [34] where gains by improper signaling were demonstrated in the complex two-user single-carrier MISO BC-TIN. However, just like in Example 7.5.6, these gains did not persist when allowing (R)TS.

As a further example, we consider improper signaling and CC transmission in a complex multicarrier setting with zero-forcing constraints.

Example 7.5.7. *Consider the complex two-user two-carrier SISO BC with proper CN noise, where*

$$\mathsf{H}_k^{(1)} = 1,\ \forall k, \qquad \mathsf{H}_k^{(2)} = 0.1,\ \forall k, \qquad \mathsf{C}_{\boldsymbol{\eta}_k^{(c)}} = 1,\ \forall k,\ \forall c \tag{7.104}$$

i.e., both users have good channel conditions on the first carrier, but not on the second carrier. Such a situation was described with the term spectrally similar channels *in [4, 53]. When using proper CN signals, the setting can be studied in the complex multicarrier formulation, where*

the null space that is necessary to construct the zero-forcing filters vanishes as soon as the other user transmits. With zero-forcing constraints, we thus can only serve one user per carrier, i.e., we must have $C_{\xi_2^{(c)}} = 0$ *if* $C_{\xi_1^{(c)}} \neq 0$ *and vice versa. By scheduling only user* $k = c$ *on carrier* c*, we have from* (7.1) *with* $\mu = 1$ *that*

$$r_k = r_k^{(k)} = \log_2\left(1 + C_{\xi_k^{(k)}} \left|H_k^{(k)}\right|^2\right). \tag{7.105}$$

If the aim is to achieve the rate targets $\rho_k = 1,\ \forall k$*, we need a sum power of*

$$Q_{\mathrm{ZF,proper,CN}} = \sum_{k=1}^{2} C_{\xi_k^{(k)}} = \sum_{k=1}^{2} \frac{2^{\rho_k} - 1}{\left|H_k^{(k)}\right|^2} = 1 + \frac{1}{0.01} = 101. \tag{7.106}$$

If we instead impose the zero-forcing constraints in the real-valued multicarrier formulation (3.36)*, we can allow for improper signaling. We have*

$$\grave{\boldsymbol{H}}_k^{(1),\mathrm{T}} = \mathbf{I}_2,\ \forall k, \qquad \grave{\boldsymbol{H}}_k^{(2),\mathrm{T}} = 0.1\,\mathbf{I}_2,\ \forall k, \qquad \boldsymbol{C}_{\check{\boldsymbol{\eta}}_k^{(c)}} = \frac{1}{2}\mathbf{I}_2,\ \forall k,\ \forall c. \tag{7.107}$$

Using the transmit filters $\boldsymbol{B}_k^{(1)} = \sqrt{\frac{3}{2}}\mathbf{e}_k,\ \forall k$ *and* $\boldsymbol{B}_k^{(2)} = \mathbf{0},\ \forall k$ *together with the zero-forcing receive filters* $\boldsymbol{R}_k^{(1),\mathrm{T}} = \mathbf{e}_k^{\mathrm{T}},\ \forall k$*, we obtain from* (7.12) *with* $\mu = \frac{1}{2}$ *that the data rates* $r_k = r_k^{(1)} = \frac{1}{2}\log_2(1 + \frac{3}{2} \cdot \left(\frac{1}{2}\right)^{-1}) = 1,\ \forall k$ *are achievable at a sum transmit power of*

$$Q_{\mathrm{ZF,improper,CN}} = \sum_{c=1}^{2}\sum_{k=1}^{2} \mathrm{tr}[\boldsymbol{B}_k^{(c)}\boldsymbol{B}_k^{(c),\mathrm{T}}] = 3 < Q_{\mathrm{ZF,proper,CN}}. \tag{7.108}$$

This transmit strategy corresponds to improper CN transmission in the original complex system.

The relatively high transmit power in the case of proper CN transmission comes from the fact that only one user can be served via the strong carrier, so that a lot of transmit power is required to serve the second user via the weak carrier. Using improper signals, both users can share the strong carrier without violating the zero-forcing constraints. As pointed out in Section 7.5.2.2, this requires widely linear zero-forcing in the complex representation. An alternative method to avoid the competition for the strong carrier is using proper CC signals, as done in the following example from [4].

Example 7.5.8. *The combined complex representation* (3.35) *of the system from Example 7.5.7 reads as*

$$\boldsymbol{H}_k^{\mathrm{H}} = \mathrm{diag}(1,\ 0.1),\ \forall k, \qquad \boldsymbol{C}_{\boldsymbol{\eta}_k} = \mathbf{I}_2,\ \forall k. \tag{7.109}$$

Using the transmit and receive filters

$$\boldsymbol{B}_k = \sqrt{\frac{103}{12}}\begin{bmatrix}(-1)^k\\ \sqrt{3}\end{bmatrix},\ \forall k \qquad \boldsymbol{R}_k^{\mathrm{H}} = \frac{1}{\sqrt{103}}\begin{bmatrix}\sqrt{3} & 10(-1)^k\end{bmatrix},\ \forall k \tag{7.110}$$

the zero-forcing constraints $\boldsymbol{R}_k^{\mathrm{H}}\boldsymbol{H}_k^{\mathrm{H}}\boldsymbol{B}_j = 0,\ j \neq k$ *are fulfilled, and the achievable rates according to* (7.12) *with* $\mu = 1$ *are*

$$\begin{aligned} r_k &= \log_2\left(1 + (\boldsymbol{R}_k^{\mathrm{H}}\boldsymbol{C}_{\boldsymbol{\eta}_k}\boldsymbol{R}_k)^{-1}\boldsymbol{R}_k^{\mathrm{H}}\boldsymbol{H}_k^{\mathrm{H}}\boldsymbol{B}_k\boldsymbol{B}_k^{\mathrm{H}}\boldsymbol{H}_k\boldsymbol{R}_k\right)\\ &= \log_2\left(1 + \left(\frac{1}{\sqrt{103}}\sqrt{\frac{103}{12}}\,2\sqrt{3}\right)^2\right) = 1,\ \forall k \end{aligned} \tag{7.111}$$

using a sum transmit power of

$$Q_{\mathrm{ZF,proper,CC}} = \sum_{k=1}^{2} \mathrm{tr}[\boldsymbol{B}_k \boldsymbol{B}_k^{\mathrm{H}}] = \frac{206}{3} < Q_{\mathrm{ZF,proper,CN}}. \tag{7.112}$$

In this transmit strategy, both users are served via a combination of the strong and the weak carrier, which leads to a moderate transmit power for both users. The resulting sum power is lower than in the case of proper CN transmission, where the users compete for the best carrier. Note that an even lower transmit power can be achieved by optimizing the CC strategy as in [4]. Moreover, [4] established conditions on the channel coefficients that lead to the described competition for the strong carrier and, thus, to gains by CC transmission (as long as neither (R)TS nor improper signaling is used). Similar results were presented for systems with higher numbers of users, carriers, and antennas in [53]. In [18], the system from Example 7.5.8 was studied without zero-forcing constraints, and it was observed that proper CC transmission outperforms proper CN transmission in this case as well.

Note that we could also employ (R)TS in all these examples in order to avoid a competition for strong carriers. However, as long as (R)TS is not allowed, reduced-entropy transmission (in the form of CC transmission or improper signals) can apparently be necessary to achieve the whole rate region of a two-user BC-TIN. If (R)TS is allowed, it remains an open question whether we can find an example of a two-user BC-TIN where reduced-entropy transmission is beneficial.

7.5.4 Excursus to DPC Zero-Forcing

In Section 6.7, we considered the combination of zero-forcing and nonlinear interference cancellation using DPC. While maximum-entropy transmission was shown to achieve the complete rate region in case of optimal DPC (Theorem 6.3.1), we claimed in Section 6.7 that reduced-entropy transmission can be beneficial if a suboptimal DPC scheme is employed. Based on the above examples, we can give a simple proof of this claim.

Proof of Theorem 6.7.1. As an example for a suboptimal DPC scheme in the sense of Theorem 6.7.1, let us consider DPC zero-forcing without (R)TS (see, e.g., [50, 91, 124]). Consider the system from Example 7.5.7. Due to DPC, we only need to consider one-sided interference for the zero-forcing constraints, but it is still impossible to serve more than one user per carrier using proper CN transmission. Thus, we still need $Q_{\mathrm{ZF,proper,CN}} = 101$ to achieve the rates $\rho_k = 1,\ \forall k$. On the other hand, canceling part of the interference by means of DPC cannot increase the required transmit power compared to TIN zero-forcing. Thus, a transmit power of at most $Q_{\mathrm{ZF,proper,CC}} = \frac{206}{3}$ (see Example 7.5.8) is sufficient for DPC zero-forcing with proper CC signals, and a transmit power of at most $Q_{\mathrm{ZF,improper,CN}} = 3$ (see Example 7.5.7) is sufficient for DPC zero-forcing with improper CN signals. Each of these examples is enough to establish Theorem 6.7.1. □

7.5.5 Numerical Results

For systems with more than two users, we have shown in Section 7.4 that reduced-entropy transmission can be beneficial even if (R)TS is allowed. However, when analyzing such settings

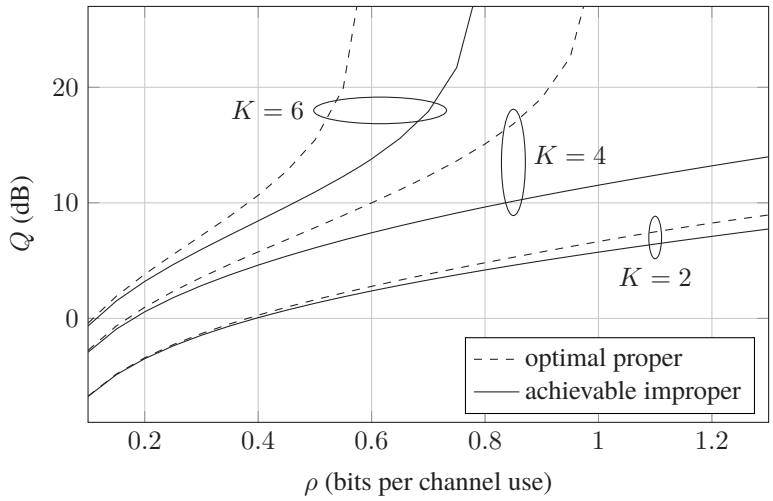

Figure 7.5: Transmit power Q needed to serve K users with data rate $\rho_k = \rho$, $\forall k$ in the complex single-carrier MISO BC-TIN without (R)TS.

for the case without (R)TS, we can observe gains that are significantly higher than the ones in Section 7.4.

As an example, we study the complex single-carrier MISO BC-TIN. Instead of rate balancing, we consider the inverse problem of power minimization under QoS constraints, i.e., we do not search for Pareto-optimal rate vectors for a given transmit power, but we instead ask how large the transmit power has to be such that a given rate vector lies on the Pareto-boundary of the rate region. This approach enables us to plot the necessary transmit power over the requested per-user rate, so that the numerical results can also serve as an illustration of the feasibility study in Sections 7.5.1.2 and 7.5.2.2.

Under the assumption of proper noise and signals, the power minimization problem without (R)TS can be efficiently solved in a globally optimal manner by means of the methods proposed in [94, 162, 164] (see also Section 7.3.1). To obtain an achievable strategy with improper signaling, we apply the power minimization algorithm from [2] to the combined real representation (3.37). In Section 7.6, we discuss in detail how algorithms that have originally been developed for proper signaling in the MIMO BC-TIN (such as the one from [2]) can be applied to optimize improper signaling strategies.

We consider a setting with $m = 2$ base station antennas and $K \in \{2, 4, 6\}$ users with rate requirements $\rho_k = \rho$, $\forall k$. The results in Figure 7.5 are averaged (in the dB domain) over 1000 channel realizations with independent and identically distributed proper Gaussian channel coefficients with zero mean and variance $\frac{1}{m}$. These channels fulfill the regularity condition (Definition 7.5.2) almost surely. Note that a similar setting was studied in [5].

For all numbers of users and all rate requirements considered in Figure 7.5, the improper transmit scheme brings a power saving or, conversely, can achieve higher rates at the same power. As we have applied a globally optimal algorithm to solve the optimization for the case of proper signals, it is clear that the observed performance loss is inherent to the restriction to proper signaling. On the other hand, the optimization for improper signaling has not been solved in a globally optimal manner, meaning that the gap between optimal proper signaling and optimal improper signaling might even be larger.

For $K = 6$ users, the curves tend to infinity at certain values of ρ. This is in compliance

with Corollary 7.5.5 and Corollary 7.5.3, from which we can calculate that transmission with equal rates $\rho_k = \rho,\ k = 1, \ldots, 6$ in a system with $m = 2$ base station antennas becomes infeasible at $\rho_{\mathrm{proper}} \approx 0.58496$ and $\rho_{\mathrm{improper}} \approx 0.79248$, respectively.

For a four-user system, we can directly see from Corollary 7.5.12 that arbitrary rate requirements are feasible with improper signals (since the feasibility of zero-forcing implies that arbitrarily high rates can be achieved, see the proof of Theorem 7.5.3). For proper signaling, we obtain from Corollary 7.5.5 that infeasibility of the requirements $\rho_k = \rho,\ k = 1, \ldots, 4$ occurs for $\rho \geq 1$, which is again in compliance with the numerical result. Finally, for $K = 2$ users, arbitrary rate requirements are feasible with both proper and improper signaling (see Corollary 7.5.14 and Corollary 7.5.12).

Note that the fundamental limitations imposed by the QoS feasibility results do not depend on the particular channel realization as long as the regularity condition is fulfilled. Therefore, the values of ρ where the curves diverge to infinity are independent of the chosen channel model, and this divergence is not an average behavior, but rather happens for every channel realization.

Similar numerical results can be found in [23] for multiantenna users, i.e., for proper and improper signaling in the complex MIMO BC-TIN. For entropy reduction by means of CC transmission, numerical results are provided in [11, 20] for the complex multicarrier MISO BC-TIN, and in [20, 53] for the complex multicarrier MIMO BC-TIN. In all these numerical studies, gains by proper CC transmission compared to proper CN transmission were observed.

7.6 Algorithmic Aspects

From the previous chapters, we are already familiar with the method of optimizing a complex multicarrier MIMO system via its combined real representation or combined complex representation. In the system models considered so far, the main motivation for doing so was the possibility of treating reduced-entropy noise appropriately. In the MIMO BC-TIN, there is an additional motivation: even in case of maximum-entropy noise, reduced-entropy transmission can be beneficial when using TIN strategies (Theorem 7.4.1). The combined real representation provides us with a simple way to analyze and optimize transmit strategies involving reduced-entropy signals.

However, there is an important difference to the previous chapters that we have to consider. Whenever we have discussed the optimization of reduced-entropy transmit strategies so far, we have used the argument that the covariance matrices of reduced-entropy noise vectors do not lie in a particular power shaping space, so that the resulting optimized transmit covariance matrices lie outside the considered power shaping space as well. If we aim at obtaining reduced-entropy input signals even though we have maximum-entropy noise, this argument cannot be used, and it needs to be studied in detail whether the applied optimization algorithms are able to deliver the desired reduced-entropy solutions.

Due to the large variety of optimization methods that can be found in the literature, it is of course impossible to provide a detailed study that covers every possible approach. Instead, we concentrate on some fundamental procedures that are contained in many algorithms for transceiver optimization. Even though the procedures that we analyze can only be understood as exemplary representatives, they already give us a good impression of typical pitfalls that we should keep in mind. Algorithms that are not covered by the examples provided in this section

could be analyzed in a similar manner.

Each of the procedures is first studied in the RoP MIMO BC-TIN, and the results can then be specialized to the cases of improper signaling and CC transmission in the complex multicarrier MIMO BC-TIN. Throughout this section, we assume that the noise is proper and CN, and we restrict ourselves to the following two special cases for the sake of a simple presentation.

The first special case we consider is the optimization of improper signaling strategies in the single-carrier MIMO BC-TIN, which can be studied by means of the combined real representation (3.37) and the power shaping spaces $\grave{\mathcal{P}}_{\mathrm{U}_k},\ \forall k$ and $\grave{\mathcal{P}}_{\mathrm{B}}$ from Proposition 3.4.2.

As a second example, we study the optimization of proper CC transmit strategies in the complex multicarrier MIMO BC-TIN via the combined complex representation (3.35). To this end, we let $\underline{\mathcal{P}}_{\mathrm{U}_k}^{\mathrm{CN}} = \mathbb{H}^{(m_{\mathrm{U}_k})_{\forall c}},\ \forall k$ and $\underline{\mathcal{P}}_{\mathrm{B}}^{\mathrm{CN}} = \mathbb{H}^{(m_{\mathrm{B}})_{\forall c}}$ denote the power shaping spaces of block-diagonal Hermitian matrices of appropriate dimensions throughout this section (see Examples 2.8.5 and 3.4.2). Note that the combined complex channel matrices $\boldsymbol{H}_k^{\mathrm{H}} = \boldsymbol{H}_{\mathrm{U}_k\mathrm{B}}$ are compatible with $(\underline{\mathcal{P}}_{\mathrm{U}_k}^{\mathrm{CN}}, \underline{\mathcal{P}}_{\mathrm{B}}^{\mathrm{CN}})$ (see Example 2.8.6). For the sake of a simple presentation, we use the notation of a RoP MIMO BC-TIN throughout, and it becomes clear from the context whether we apply the results to the combined complex representation (3.35) or to the combined real representation (3.37).

7.6.1 Iterative Algorithms

We commence our analysis with steps that are typically applied in iterative algorithms, namely gradient steps, alternating filter updates, and power control steps.

7.6.1.1 Gradient-Based Filter Updates

As an example for gradient-based methods, we consider a gradient-projection update of the uplink transmit filter matrices $\boldsymbol{T}_k$ as proposed in [123, 126, 178] for weighted sum rate maximization under a sum power constraint and in [19] for optimizing the energy efficiency. We concentrate on the weighted sum rate maximization

$$\max_{(\boldsymbol{T}_k)_{\forall k}} \sum_{k=1}^{K} w_k r_k \qquad \text{s. t.} \quad \sum_{k=1}^{K} \mathrm{tr}[\boldsymbol{T}_k \boldsymbol{T}_k^{\mathrm{H}}] \leq Q \tag{7.113}$$

and we apply the formulation that was originally derived for the complex MIMO BC-TIN with proper signaling in [123, 126, 178] to the RoP MIMO BC-TIN.

Using r_k from (7.14) with $\boldsymbol{C}_{\boldsymbol{x}_k} = \boldsymbol{T}_k \boldsymbol{T}_k^{\mathrm{H}}$, the update rule reads as

$$\boldsymbol{T}_{k,\mathrm{new}} = a \left(\boldsymbol{T}_k + b \frac{\partial \left(\sum_{k=1}^{K} w_k r_k \right)}{\partial \boldsymbol{T}_k^*} \right) = \boldsymbol{A}_k \boldsymbol{T}_k \tag{7.114}$$

where [178]

$$\boldsymbol{A}_k = a \mathbf{I}_{M_k} + ab \frac{\mu}{\ln 2} \boldsymbol{H}_{\mathrm{UL},k} \left(\sum_{\ell=1}^{K} w_\ell \boldsymbol{X}^{-1} - \sum_{\ell \neq k} w_\ell \boldsymbol{X}_\ell^{-1} \right) \boldsymbol{H}_{\mathrm{UL},k}^{\mathrm{H}} \tag{7.115}$$

with $\boldsymbol{X}$ and $\boldsymbol{X}_k$ from (7.15) and $\boldsymbol{H}_{\mathrm{UL},k}$ from (7.13). The scalar $b > 0$ is the step size, and $a > 0$ is chosen such that the power constraint is fulfilled, which corresponds to a projection to the constraint set.

Proposition 7.6.1. *Let $(\mathcal{P}_k = \mathcal{P}_{\mathrm{U}_k})_{\forall k}$ and $\mathcal{P}_{\mathrm{B}}$ be power shaping spaces fulfilling the compatibility assumption (Definition 3.1.3), and assume that the noise vectors $\boldsymbol{\eta}_k$ are maximum-entropy signals with respect to $(\mathcal{P}_k)_{\forall k}$. If the uplink transmit filters $(\boldsymbol{T}_k)_{\forall k}$ correspond to maximum-entropy transmission with respect to $(\mathcal{P}_k)_{\forall k}$, i.e., $\boldsymbol{T}_k\boldsymbol{T}_k^{\mathrm{H}} \in \mathcal{P}_k,\ \forall k$, the filters $(\boldsymbol{T}_{k,\mathrm{new}})_{\forall k}$ after the gradient-projection update* (7.114) *correspond to maximum-entropy transmission with respect to $(\mathcal{P}_k)_{\forall k}$ as well.*

Proof. First note that $\boldsymbol{H}_{\mathrm{UL},k}$ is compatible with $(\mathcal{P}_{\mathrm{B}}, \mathcal{P}_k)$ for all k (see the proof of Theorem 7.2.1). If $\boldsymbol{C}_{\boldsymbol{x}_k} = \boldsymbol{T}_k\boldsymbol{T}_k^{\mathrm{H}} \in \mathcal{P}_k$ for all k, we have $\boldsymbol{X} \in \mathcal{P}_{\mathrm{B}}$ and $\boldsymbol{X}_k \in \mathcal{P}_{\mathrm{B}},\ \forall k$. Then, $\boldsymbol{A}_k \in \mathcal{P}_k,\ \forall k$ due to Corollary 2.4.2, so that $\boldsymbol{T}_{k,\mathrm{new}}\boldsymbol{T}_{k,\mathrm{new}}^{\mathrm{H}} = \boldsymbol{A}_k\boldsymbol{C}_{\boldsymbol{x}_k}\boldsymbol{A}_k \in \mathcal{P}_k$. □

Due to this result, an algorithm based on this gradient-projection update converges to a solution with maximum-entropy transmission if we use an initialization that corresponds to maximum-entropy transmission.

We have the following two specializations of this result. Considering the combined complex representation and the power shaping spaces $\mathcal{P}_k = \underline{\mathcal{P}}_{\mathrm{U}_k}^{\mathrm{CN}},\ \forall k$ and $\mathcal{P}_{\mathrm{B}} = \underline{\mathcal{P}}_{\mathrm{B}}^{\mathrm{CN}}$, we get the result from [11], namely that a CN solution is obtained if the algorithm is initialized with a CN strategy. With the combined real representation and the power shaping spaces $\mathcal{P}_k = \grave{\mathcal{P}}_{\mathrm{U}_k},\ \forall k$ and $\mathcal{P}_{\mathrm{B}} = \grave{\mathcal{P}}_{\mathrm{B}}$, we obtain that an initialization that corresponds to proper signaling leads to a solution with proper signaling, as already reported in [7, 23].

However, recall that this is not the intended outcome since the aim of this section is to find methods for optimizing reduced-entropy strategies. Thus, Proposition 7.6.1 reveals that it is necessary to study which of the usually employed initializations lead to transmit covariance matrices that lie outside the power shaping spaces of interest. Before we do so in Section 7.6.2, let us consider further examples of iterative optimization methods.

7.6.1.2 Alternating Filter Updates

Many iterative algorithms for transceiver optimization are based on alternating updates of the transmit and receive filters. While it is easy to find the optimal receive filters for fixed transmit filters by calculating the MMSE filter for each user separately, optimizing the transmit filters is a problem that is coupled across all users and therefore more involved. Thus, it has been proposed to either resort to an equivalent weighted MSE formulation [180] or to optimize the uplink receive filters as a vehicle to obtain improved downlink transmit filters and vice versa.

In the following analysis, we concentrate on the latter approach, which was applied in the form of alternating filter updates, e.g., in [93, 159, 160] for weighted sum rate maximization, in [159] for sum MSE minimization and SINR balancing, in [9, 93, 161] for rate balancing, and in [2, 93, 159] for power minimization. These publications assume complex systems with linear filters and proper signals, and we can apply the concept to the RoP MIMO BC-TIN.

The method of alternating filter updates in the uplink and downlink is based on the observation that the downlink receive filters (7.25) obtained from the uplink-to-downlink transformation in Lemma 7.2.2 are in general not equal to the optimal MMSE receive filters. Thus, by keeping the downlink transmit filters (7.25) obtained in the transformation, but replacing the downlink receive filters by the MMSE filters (7.7), we obtain increased per-user rates. The resulting transmit strategy can then be transformed back to the uplink, where the same reasoning applies, i.e., replacing the obtained uplink receive filters by the MMSE filters

(7.19) leads to a further increase of the rates. This procedure can be repeated until convergence, and we can show the following behavior.

Proposition 7.6.2. *Let $(\mathcal{P}_k = \mathcal{P}_{\mathrm{U}_k})_{\forall k}$ and $\mathcal{P}_{\mathrm{B}}$ be power shaping spaces fulfilling the compatibility assumption (Definition 3.1.3), and assume that the noise vectors $\boldsymbol{\eta}_k$ are maximum-entropy signals with respect to $(\mathcal{P}_k)_{\forall k}$. If the uplink transmit filters $(\boldsymbol{T}_k)_{\forall k}$ correspond to maximum-entropy transmission with respect to $(\mathcal{P}_k)_{\forall k}$ and the modal matrices $\boldsymbol{W}_k$ in* (7.20) *are chosen such that the projections $\mathrm{proj}_{\mathcal{P}'_k}$ and $\mathrm{proj}_{\mathrm{diag}}$ in the proof of Theorem 7.2.1 commute, the obtained downlink transmit filters $(\boldsymbol{B}_k)_{\forall k}$ correspond to maximum-entropy transmission with respect to $\mathcal{P}_{\mathrm{B}}$. This statement holds analogously with downlink and uplink interchanged.*

Proof. This statement is proven in the proof of Theorem 7.2.1. □

The critical step that merits special attention is the choice of the modal matrix $\boldsymbol{W}_k$ in (7.20) and (7.8). In the proof of Theorem 7.2.1, this matrix is used to define a new power shaping space $\mathcal{P}'_k$. The assumption that the projections $\mathrm{proj}_{\mathcal{P}'_k}$ and $\mathrm{proj}_{\mathrm{diag}}$ commute is necessary to show that the individual scaling of the columns of the filter matrices in (7.25) preserves maximum-entropy transmission.

Due to Corollary 2.6.4, a modal matrix that satisfies this condition always exists, which was sufficient to prove Theorem 7.2.1. However, this does not mean that any arbitrarily chosen modal matrix in a numerical algorithm complies to the assumption. Will this particularity of the method allow the algorithm to deviate from maximum-entropy strategies? The answer is negative under mild assumptions.

As matrices with repeated eigenvalues are a set of measure zero within the set of Hermitian (or real symmetric) matrices (e.g., [181, Sec. A.37]), we should assume that repeated eigenvalues do not occur by hazard, but only for structural reasons—namely if the power shaping space under consideration requires the eigenvalues to have a multiplicity larger than one. This means that we assume the MSE matrices ($\boldsymbol{G}^{\mathrm{H}}_{k,\mathrm{MMSE}}\boldsymbol{H}_{\mathrm{UL},k}\boldsymbol{T}_k$ and $\boldsymbol{R}^{\mathrm{H}}_{k,\mathrm{MMSE}}\boldsymbol{H}^{\mathrm{H}}_k\boldsymbol{B}_k$ in the uplink and in the downlink, respectively) to have the highest number of distinct eigenvalues that is possible for matrices from the considered power shaping spaces. We then obtain from Theorem 2.6.1 that any modal matrix fulfills the requirement of Proposition 7.6.2.

The power shaping spaces $\mathcal{P}_k = \grave{\mathcal{P}}_{\mathrm{U}_k}$, $\forall k$ and $\mathcal{P}_{\mathrm{B}} = \grave{\mathcal{P}}_{\mathrm{B}}$, which model proper signaling, require all eigenvalues to have even multiplicity (see Lemma 2.9.9). Assuming that all eigenvalues of the MSE matrices have multiplicity two, we obtain from Proposition 7.6.2 (using Theorem 2.6.1) that the uplink transmit filters after an iteration of the alternating filter update method correspond to proper signaling if all previous uplink transmit filters correspond to proper signaling. This behavior was first reported in [23].

When considering the combined complex representation and the power shaping spaces $\mathcal{P}_k = \underline{\mathcal{P}}^{\mathrm{CN}}_{\mathrm{U}_k}$, $\forall k$ and $\mathcal{P}_{\mathrm{B}} = \underline{\mathcal{P}}^{\mathrm{CN}}_{\mathrm{B}}$, which model CN transmission, there is no structural requirement for repeated eigenvalues. Our assumption is thus that all eigenvalues have multiplicity one, and we obtain from Proposition 7.6.2 (using Theorem 2.6.1) that the uplink transmit filters after an iteration of the alternating filter update method correspond to CN transmission if all previous uplink transmit filters correspond to CN transmission. A similar observation was described in [11].

In the unlikely event that we have eigenvalues with a higher multiplicity than enforced by the considered power shaping spaces, the assumption in Proposition 7.6.2 might be violated.

As can be verified numerically by constructing an adequate example, it can then happen that we obtain, e.g., an improper signaling strategy in the downlink even though we start with uplink transmit filters that correspond to proper signaling.

However, as we cannot expect this to happen by chance, the conclusion is again that already the initialization has to correspond to reduced-entropy transmission if our aim is to obtain a solution with reduced-entropy signals.

7.6.1.3 Power Control

Many algorithms for transceiver optimization contain so-called power control steps, in which the transmit powers of individual data streams are adapted, e.g., in order to achieve given rate targets [2, 93] or to balance the per-user rates [9, 93, 161]. The scaling factors can be chosen, for instance, by solving an inner optimization (e.g., a geometric program in [93, 161]) or by performing a single improving step of an inner optimization (e.g., a gradient-projection step for a vector of per-stream rate targets in [2, 9]).

In the following, we consider power control steps that consist in scaling the columns of the uplink transmit filter matrices $\boldsymbol{T}_k$ by individual factors, i.e., we replace $\boldsymbol{T}_k$ by $\boldsymbol{T}_k\boldsymbol{D}$, where $\boldsymbol{D}$ is a real diagonal matrix. For an exhaustive analysis, the same reasoning can be applied in the downlink. The question to consider is whether $\boldsymbol{T}_k\boldsymbol{T}_k^{\mathrm{H}} \in \mathcal{P}_k$ implies that $\boldsymbol{T}_k\boldsymbol{D}^2\boldsymbol{T}_k^{\mathrm{H}} \in \mathcal{P}_k$ for any real diagonal matrix $\boldsymbol{D}$. However, there is no general answer to this question.

For a given transmit covariance matrix $\boldsymbol{C}_{\boldsymbol{x}_k} = \boldsymbol{T}_k\boldsymbol{T}_k^{\mathrm{H}}$, the matrix square root $\boldsymbol{T}_k$ of $\boldsymbol{T}_k\boldsymbol{T}_k^{\mathrm{H}}$ is not unique, and $\boldsymbol{T}_k\boldsymbol{D}^2\boldsymbol{T}_k^{\mathrm{H}} \in \mathcal{P}_k$ is not fulfilled for arbitrary choices of the matrix square root $\boldsymbol{T}_k$ and arbitrary scaling matrices $\boldsymbol{D}$. To see this, consider the power shaping space $\underline{\mathcal{P}}_{\mathrm{U}_k}^{\mathrm{CN}}$, which contains block-diagonal matrices. If $\boldsymbol{C}_{\boldsymbol{x}_k}$ is block-diagonal, there exists a block-diagonal $\boldsymbol{T}_k$ such that $\boldsymbol{T}_k\boldsymbol{T}_k^{\mathrm{H}} = \boldsymbol{C}_{\boldsymbol{x}_k}$. However, $\boldsymbol{T}_k' = \boldsymbol{T}_k\boldsymbol{U}$ with an arbitrary unitary matrix $\boldsymbol{U}$ would be a valid choice as well. While $\boldsymbol{T}_k\boldsymbol{D}^2\boldsymbol{T}_k^{\mathrm{H}}$ is block-diagonal for any diagonal matrix $\boldsymbol{D}$, this is not true for $\boldsymbol{T}_k'\boldsymbol{D}^2\boldsymbol{T}_k'^{\mathrm{H}}$.

We thus need to study which special situations lead to choices of $\boldsymbol{T}_k$ that fulfill $\boldsymbol{T}_k\boldsymbol{D}^2\boldsymbol{T}_k^{\mathrm{H}} \in \mathcal{P}_k$. It turns out that we have to distinguish between two kinds of power shaping spaces for this analysis. The first kind is covered by the following proposition.

Proposition 7.6.3. *Let $\mathcal{P}_k$ be a power shaping space in which there exist matrices whose eigenvalues all have multiplicity one, and let $\boldsymbol{D}$ be a real diagonal matrix of appropriate dimension. Then, $\boldsymbol{T}_k\boldsymbol{T}_k^{\mathrm{H}} \in \mathcal{P}_k$ implies that $\boldsymbol{T}_k\boldsymbol{D}^2\boldsymbol{T}_k^{\mathrm{H}} \in \mathcal{P}_k$ if one of the following cases applies.*

1. *All nonzero eigenvalues of $\boldsymbol{T}_k\boldsymbol{T}_k^{\mathrm{H}}$ have multiplicity one, and $\boldsymbol{T}_k$ is obtained by performing an eigenvalue decomposition $\boldsymbol{U}\boldsymbol{\Lambda}\boldsymbol{U}^{\mathrm{H}} = \boldsymbol{T}_k\boldsymbol{T}_k^{\mathrm{H}}$ and setting $\boldsymbol{T}_k = \boldsymbol{U}\boldsymbol{\Lambda}^{\frac{1}{2}}$, where $\boldsymbol{\Lambda}^{\frac{1}{2}}$ is the positive semidefinite square root of $\boldsymbol{\Lambda}$.*
2. *$\boldsymbol{T}_k$ is a transmit filter for which stream-wise decoding is optimal, i.e., it is chosen like $\boldsymbol{T}_k'$ in* (7.20)*, and all eigenvalues of the MSE matrix $\boldsymbol{G}_{k,\mathrm{MMSE}}^{\mathrm{H}}\boldsymbol{H}_{\mathrm{UL},k}\boldsymbol{T}_k$ have multiplicity one.*
3. *$\operatorname{rank}\left[\boldsymbol{T}_k\boldsymbol{T}_k^{\mathrm{H}}\right] = 1$.*
4. *The considered algorithm treats all streams of a user separately as virtual users, and $\boldsymbol{T}_k\boldsymbol{T}_k^{\mathrm{H}}$ is the transmit covariance matrix of a virtual user.*
5. *$\mathcal{P}_k = \underline{\mathcal{P}}_{\mathrm{U}_k}^{\mathrm{CN}}$, and only one of the submatrices of $\boldsymbol{T}_k\boldsymbol{T}_k^{\mathrm{H}}$ is nonzero.*

6. $\mathcal{P}_k = \underline{\mathcal{P}}^{\mathrm{CN}}_{\mathrm{U}_k}$, *and the numerical method used to calculate* $\boldsymbol{T}_k$ *from* $\boldsymbol{T}_k\boldsymbol{T}_k^{\mathrm{H}}$ *delivers a block-diagonal output when the input is block-diagonal.*

Proof. 1. If all eigenvalues have multiplicity one, $\boldsymbol{D} \in \mathcal{P}'_k = \{\boldsymbol{P}' \mid \boldsymbol{P}' = \boldsymbol{U}^{\mathrm{H}}\boldsymbol{P}\boldsymbol{U},\ \boldsymbol{P} \in \mathcal{P}_k\}$ due to Corollary 2.6.3, and the chosen $\boldsymbol{T}_k$ is compatible with $(\mathcal{P}'_k, \mathcal{P}_k)$. As the choice of eigenvectors corresponding to the eigenvalue zero does not matter for $\boldsymbol{T}_k\boldsymbol{D} = \boldsymbol{U}\boldsymbol{\Lambda}^{\frac{1}{2}}\boldsymbol{D}$, it suffices to apply the reasoning from Corollary 2.6.3 to the nonzero eigenvalues, which are distinct by assumption.
2. Define $\mathcal{P}'_k$ as in the proof of Theorem 7.2.1. Then, $\boldsymbol{D} \in \mathcal{P}'_k$ due to Corollary 2.6.3, and the chosen $\boldsymbol{T}_k$ is compatible with $(\mathcal{P}'_k, \mathcal{P}_k)$ as shown in the proof of Theorem 7.2.1.
3. Since $\mathrm{range}[\boldsymbol{T}_k\boldsymbol{D}] \subseteq \mathrm{range}[\boldsymbol{T}_k]$, we obtain $\boldsymbol{T}_k\boldsymbol{D}^2\boldsymbol{T}_k^{\mathrm{H}} = \alpha\boldsymbol{T}_k\boldsymbol{T}_k^{\mathrm{H}}$ for some $\alpha \in \mathbb{R}$.
4. In this case, $\boldsymbol{T}_k\boldsymbol{T}_k^{\mathrm{H}}$ has rank one, so that Item 3 applies.
5. Since $\mathrm{range}[\boldsymbol{T}_k\boldsymbol{D}] \subseteq \mathrm{range}[\boldsymbol{T}_k]$, we obtain that $\boldsymbol{T}_k\boldsymbol{D}^2\boldsymbol{T}_k^{\mathrm{H}}$ is nonzero only in the same submatrix as $\boldsymbol{T}_k\boldsymbol{T}_k^{\mathrm{H}}$.
6. This case is obvious, but it shall be remarked that this condition is often fulfilled by software for numerical computations. □

Note that calculating uplink MMSE receive filters (7.19) (without the diagonalization from Lemma 7.2.1) can be considered as an operation in the sense of Proposition 7.6.3 Item 4 since each row of the resulting receive filter corresponds to a column of the transmit filter. The same is true for a stream-wise uplink-downlink duality as used, e.g., in [93, 161]. This means that power control steps that are combined with these kinds of operations in an algorithm can be analyzed by means of Proposition 7.6.3 Item 4. Consequently, the above proposition can be applied both to algorithms based on optimal stream-wise decoding in terms of Lemma 7.2.1 (e.g., [2, 9]) and to algorithms with simple stream-wise decoding, where streams are always treated separately (e.g., [93, 161]). Moreover, it would cover approaches to perform power control by rescaling the eigenvalues of the transmit covariance matrices.

As discussed in Section 7.6.1.2, the assumption that all eigenvalues of the MSE matrix have multiplicity one is sensible in practice. It seems that the same argument can be applied for the nonzero eigenvalues of $\boldsymbol{T}_k\boldsymbol{T}_k^{\mathrm{H}}$ in Proposition 7.6.3 Item 1 during the execution of an optimization algorithm unless we speak about the initialization (see Section 7.6.2), where eigenvalues with higher multiplicity might have been created artificially.

All in all, Proposition 7.6.3 indicates that power control steps behave similar to the other considered iterative update methods as long as we consider power shaping spaces that do not impose restrictions on the multiplicity of the eigenvalues. Even if the scaling factors contained in $\boldsymbol{D}$ are chosen arbitrarily, the resulting transmit covariance matrix after the power control step corresponds to maximum-entropy transmission if the previous covariance matrix does so. In particular, when considering the combined complex representation and the power shaping spaces $\mathcal{P}_k = \underline{\mathcal{P}}^{\mathrm{CN}}_{\mathrm{U}_k}$, $\forall k$ and $\mathcal{P}_{\mathrm{B}} = \underline{\mathcal{P}}^{\mathrm{CN}}_{\mathrm{B}}$, power control steps preserve CN strategies, and the conclusion that we have to account for CC transmission already in the initialization of iterative methods stays valid.[6]

[6]Note that the study of power control steps is simplified if the analysis is not based on the covariance matrices, but directly on the transmit filters as in [11]. On the other hand, the analysis of various iterative update methods based on covariance matrices and power shaping spaces allows for a more general treatment in which the optimization of CC transmission considered in [11] is only a special case.

However, the situation is different for power shaping spaces which do not allow for eigenvalues with multiplicity one.

Example 7.6.1. *Let $\mathcal{P}_k$ be a power shaping space which restricts the multiplicity of all eigenvalues to be a multiple of $\beta > 1$. Note that this violates the assumption of Proposition 7.6.3. Then, for any nonzero $\boldsymbol{T}_k\boldsymbol{T}_k^{\mathrm{H}} \in \mathcal{P}_k$ and regardless of the choice of $\boldsymbol{T}_k$, there exists a real diagonal matrix $\boldsymbol{D}$ such that $\boldsymbol{T}_k\boldsymbol{D}^2\boldsymbol{T}_k^{\mathrm{H}} \notin \mathcal{P}_k$. For instance, we can set $\boldsymbol{D} = \mathbf{e}_i\mathbf{e}_i^{\mathrm{T}}$ where i is such that $\boldsymbol{T}_k\mathbf{e}_i \neq \mathbf{0}$, which leads to a matrix with rank one.*

This means that power control steps could lead to reduced-entropy transmission with respect to this second kind of power shaping spaces. In particular, when modeling proper signaling by means of $\mathcal{P}_k = \grave{\mathcal{P}}_{\mathrm{U}_k},\ \forall k$ and $\mathcal{P}_{\mathrm{B}} = \grave{\mathcal{P}}_{\mathrm{B}}$, we might obtain an improper signaling strategy even if the transmit strategy corresponds to proper signaling before performing the power control step. Whether or not this happens depends on the choice of the matrix square root $\boldsymbol{T}_k$ and of the scaling factors contained in $\boldsymbol{D}$. However, it again turns out that the choices made by typical algorithms preserve maximum-entropy signals.

Proposition 7.6.4. *Let $\mathcal{P}_k$ be a power shaping space, and let $\boldsymbol{D}$ be a real diagonal matrix of appropriate dimension. Then, $\boldsymbol{T}_k\boldsymbol{T}_k^{\mathrm{H}} \in \mathcal{P}_k$ implies $\boldsymbol{T}_k\boldsymbol{D}^2\boldsymbol{T}_k^{\mathrm{H}} \in \mathcal{P}_k$ if one of the following cases applies.*

1. *$\boldsymbol{T}_k$ is obtained from an eigenvalue decomposition as in Proposition 7.6.3 Item 1, and $\boldsymbol{D}$ has repeated diagonal elements at the positions corresponding to the repeated eigenvalues.*
2. *$\boldsymbol{T}_k$ is a transmit filter for which stream-wise decoding is optimal as in Proposition 7.6.3 Item 2, and $\boldsymbol{D}$ has repeated diagonal elements at the positions corresponding to the repeated eigenvalues of the MSE matrix.*
3. *$\mathcal{P}_k = \grave{\mathcal{P}}_{\mathrm{U}_k}$, $\boldsymbol{D}$ is a diagonal $\mathcal{BSC}_2$ matrix, and the numerical method used to calculate $\boldsymbol{T}_k$ from $\boldsymbol{T}_k\boldsymbol{T}_k^{\mathrm{H}}$ delivers a $\mathcal{BSC}_2$ output when the input is $\mathcal{BSC}_2$.*

Proof. The proof for the first two items is in analogy to the proof of Proposition 7.6.3 since $\boldsymbol{D}$ is chosen such that Corollary 2.6.5 can be applied instead of Corollary 2.6.3. The last item follows from Lemma 2.9.3. □

Even though the requirements on $\boldsymbol{D}$ in Proposition 7.6.4 may sound quite demanding, they are indeed often fulfilled in practice. The reason for this is that a routine that decides for the scaling factors contained in $\boldsymbol{D}$ will tend to produce a symmetric output with equal scaling factors if it is provided with a symmetric input that corresponds to maximum-entropy transmission (see [23] for the example of proper signaling). Clearly, this has to be investigated separately for any applied power control algorithm. However, Proposition 7.6.4 reveals that even in the case of power shaping spaces that require repeated eigenvalues, we cannot expect power control steps to turn maximum-entropy strategies into reduced-entropy strategies.

7.6.1.4 Effects Caused by Numerical Inaccuracies

As remarked in [23] for the special case of the power shaping spaces $\mathcal{P}_k = \grave{\mathcal{P}}_{\mathrm{U}_k},\ \forall k$ and $\mathcal{P}_{\mathrm{B}} = \grave{\mathcal{P}}_{\mathrm{B}}$, numerical inaccuracies may also have an influence on the behavior of iterative methods

for transceiver design. In particular, a function that theoretically delivers an output $\boldsymbol{P} \in \mathcal{P}_k$ might yield a result with a small, but nonzero entropy reduction component $\mathrm{proj}_{\mathcal{N}_k}(\boldsymbol{P}) \neq \boldsymbol{0}$ in case of finite precision arithmetic. It is not obvious how large this deviation needs to be in order to interrupt the line of argumentation of Sections 7.6.1.1 through 7.6.1.3. However, it was reported in [23] that the algorithm from [2], which is a combination of alternating filter updates and power control steps, can indeed leave the neighborhood of $\mathcal{P}_k = \grave{\mathcal{P}}_{\mathrm{U}_k}$ and converge to an improper signaling solution due to numerical inaccuracies. If our aim is to obtain a reduced-entropy strategy, we should of course not base an algorithm on this effect, but we should rather leave the respective power shaping space $\mathcal{P}_k$ explicitly—e.g., by means of an appropriate initialization as discussed in the following section.

7.6.2 Initialization of Iterative Algorithms

The previous observations indicate that iterative algorithms tend to preserve matrix structures that correspond to maximum-entropy transmission. If we aim at obtaining a solution that corresponds to reduced-entropy transmission, we should therefore account for this already in the initialization of the iterative procedure.

The initializations discussed in the following can again only serve as examples, but they cover a wide range of possibilities. We discuss all examples in the uplink, but the reasoning applies analogously for algorithms that are initialized in the downlink.

7.6.2.1 Scaled and Truncated Identity Matrices

A particularly simple initialization are identity matrices. Since the filter matrices to be initialized are rectangular in many cases, it has been proposed to truncate an identity matrix to the required size (e.g., [2, 123, 178]). Moreover, a scaling may be done, e.g., in order to fulfill a power constraint.

While $\boldsymbol{T}_k = \alpha \mathbf{I}_{M_k},\ \alpha \in \mathbb{R}$ always corresponds to maximum-entropy transmission due to (2.13), no matter which power shaping space is considered, the situation is different for a truncated identity $\boldsymbol{T}_k = \alpha[\mathbf{e}_1 \ \ \ldots \ \ \mathbf{e}_{s_k}] \in \mathbb{R}^{M_k \times s_k}$ with $s_k < M_k$. In the latter case, $\boldsymbol{C}_{\boldsymbol{x}_k} = \boldsymbol{T}_k \boldsymbol{T}_k^{\mathrm{H}}$ is a diagonal matrix whose first s_k diagonal elements equal α^2 while the remaining ones are zero. It has to be verified whether $\boldsymbol{C}_{\boldsymbol{x}_k}$ lies in the power shaping space of interest.

Obviously, we have $\boldsymbol{C}_{\boldsymbol{x}_k} \in \underline{\mathcal{P}}_{\mathrm{U}_k}^{\mathrm{CN}}$, which is the power shaping space of block-diagonal matrices, i.e., the initialization corresponds to CN transmission and is therefore not appropriate when the aim is to optimize a CC strategy via the combined complex representation [11]. However, $\boldsymbol{C}_{\boldsymbol{x}_k} \notin \grave{\mathcal{P}}_{\mathrm{U}_k}$ as long as $s_k < M_k$ since $\boldsymbol{C}_{\boldsymbol{x}_k}$ does not have $\mathcal{BSC}_2$ structure in this case. Thus, an initialization based on truncated identity matrices can be applied when the aim is to obtain a solution based on improper signaling via the combined real representation. In case of a square matrix with $s_k = M_k$, an individual scaling of the columns could be applied to break the $\mathcal{BSC}_2$ structure (see also [23]), but not to break block-diagonal structures.

7.6.2.2 Singular Value Decomposition

Another method proposed in the literature is to initialize the columns of $\boldsymbol{T}_k$ with the (possibly scaled) right singular vectors of the uplink channel matrices $\boldsymbol{H}_{\mathrm{UL},k}$ (e.g., [93, 160, 161]). We

then have $\boldsymbol{C}_{\boldsymbol{x}_k} = \boldsymbol{T}_k \boldsymbol{T}_k^{\mathrm{H}} = \boldsymbol{U}\boldsymbol{D}^2\boldsymbol{U}^{\mathrm{H}}$ where $\boldsymbol{U}$ is obtained from the eigenvalue decomposition $\boldsymbol{U}\boldsymbol{\Lambda}\boldsymbol{U}^{\mathrm{H}} = \boldsymbol{H}_{\mathrm{UL},k}^{\mathrm{H}}\boldsymbol{H}_{\mathrm{UL},k}$ and $\boldsymbol{D}$ is a real diagonal matrix containing scaling factors. Of course, $\boldsymbol{T}_k$ can also consist of only a subset of the columns of $\boldsymbol{U}$. This possibility is contained in the following discussion implicitly in terms of the equivalent operation of setting some scaling factors in $\boldsymbol{D}$ to zero.

Since $\boldsymbol{H}_{\mathrm{UL},k}^{\mathrm{H}}$ is compatible with $(\mathcal{P}_k, \mathcal{P}_{\mathrm{B}})$ for all k (see the proof of Theorem 7.2.1 and Proposition 2.7.1), we have $\boldsymbol{H}_{\mathrm{UL},k}^{\mathrm{H}}\boldsymbol{H}_{\mathrm{UL},k} \in \mathcal{P}_k$. It is reasonable to assume that the nonzero eigenvalues of $\boldsymbol{H}_{\mathrm{UL},k}^{\mathrm{H}}\boldsymbol{H}_{\mathrm{UL},k}$ have the lowest multiplicity that is possible in $\mathcal{P}_k$ (since matrices with repeated eigenvalues are a set of measure zero, see Section 7.6.1.2). When choosing $\boldsymbol{T}_k = \boldsymbol{U}\boldsymbol{D}$, we have the same situation as in Proposition 7.6.3 Item 1 or as in Proposition 7.6.4 Item 1 (depending on which kind of power shaping space we consider). Arguing only based on the nonzero eigenvalues of $\boldsymbol{H}_{\mathrm{UL},k}^{\mathrm{H}}\boldsymbol{H}_{\mathrm{UL},k}$ is sufficient since filter vectors inside the null space of $\boldsymbol{H}_{\mathrm{UL},k}$ do not have an influence on whether or not $\boldsymbol{H}_{\mathrm{UL},k}\boldsymbol{T}_k\boldsymbol{T}_k^{\mathrm{H}}\boldsymbol{H}_{\mathrm{UL},k}^{\mathrm{H}} \in \mathcal{P}_{\mathrm{B}}$, which is the relevant question for the study of iterative methods in Section 7.6.1.

As a result, any choice of $\boldsymbol{D}$ leads to $\boldsymbol{C}_{\boldsymbol{x}_k} \in \mathcal{P}_k$ if $\mathcal{P}_k$ is a power shaping space without a restriction on the multiplicity of the eigenvalues. For the special case of $\mathcal{P}_k = \underline{\mathcal{P}}_{\mathrm{U}_k}^{\mathrm{CN}}$ (CN signals), this was observed in [11]. The result changes if the power shaping space $\mathcal{P}_k$ imposes restrictions on the multiplicity of the eigenvalues, such as the special case $\mathcal{P}_k = \dot{\mathcal{P}}_{\mathrm{U}_k}$ (proper signals). Whether $\boldsymbol{C}_{\boldsymbol{x}_k}$ lies in $\dot{\mathcal{P}}_{\mathrm{U}_k}$ depends on the choice of the scaling factors contained in $\boldsymbol{D}$ [23]. In any case, we obtain $\boldsymbol{C}_{\boldsymbol{x}_k} \in \mathcal{P}_k$ if $\boldsymbol{D}$ is a scaled identity matrix.

7.6.2.3 Initialization based on Zero-Forcing

As mentioned earlier, there are many low-complexity algorithms that can find good zero-forcing transmit strategies quite efficiently (see Section 7.1.2), e.g., by means of successive allocation. To further improve the obtained system performance, we could subsequently drop the zero-forcing constraints and use the zero-forcing solution as the initialization of an iterative algorithm, which then further improves this solution, e.g., by means of the procedures discussed in Section 7.6.1. This approach was pursued, e.g., in [2].

Zero-forcing strategies are usually obtained either using block-diagonalization [151], which is based on the singular value decomposition of a joint channel matrix, or on successive allocation (e.g., [91, 152, 154, 155]). Therefore, to verify whether or not an initialization based on zero-forcing corresponds to reduced-entropy transmission, we can use the arguments from Section 7.6.2.2 and Section 7.6.3, respectively. For the special case of $\underline{\mathcal{P}}_{\mathrm{U}_k}^{\mathrm{CN}}$ (CN signals), it turns out that the commonly used zero-forcing schemes do not lead to CC initializations. This aspect was discussed in more detail in [11].

7.6.2.4 Random Initialization

Though not necessarily satisfactory from a theoretical point of view, it is also possible to choose the initial transmit filters randomly as proposed, e.g., in [2, 53, 159]. As long as the resulting random transmit covariance matrix $\boldsymbol{C}_{\boldsymbol{x}_k}$ follows a continuous distribution, it has a nonzero entropy reduction component almost surely since any strict subspace $\mathcal{P}_k$ of the space of Hermitian (or real symmetric) matrices is a set of measure zero.

Random initializations were discussed for optimizing CC strategies in [11, 20] and for

optimizing improper signaling in [23]. An example given in these papers is that the columns of $\boldsymbol{T}_k$ could be initialized with columns of a Haar matrix $\boldsymbol{U}$, i.e., a random unitary matrix (e.g., [182]). This does not lead to the desired behavior if $s_k = M_k$, i.e., if we use the square matrix $\boldsymbol{T}_k = \boldsymbol{U}$, so that $\boldsymbol{C}_{\boldsymbol{x}_k} = \boldsymbol{T}_k \boldsymbol{T}_k^{\mathrm{H}} = \mathbf{I}_{M_k} \in \mathcal{P}_k$. However, if $\boldsymbol{T}_k$ is rectangular or if we scale the columns individually, i.e., we set $\boldsymbol{T}_k = \boldsymbol{U}\boldsymbol{D}$ where $\boldsymbol{D}$ is a diagonal matrix containing scaling factors, we obtain an initialization that is appropriate for optimizing reduced-entropy transmission with respect to an arbitrary power shaping space. Note that a special case of a rectangular $\boldsymbol{T}_k$ can be found in algorithms that treat all streams separately as virtual users, so that all transmit filters are vectors.

7.6.2.5 Fourier Matrix

We have already identified several methods how a strategy with improper signaling can be obtained. However, among the initializations discussed so far, the random initialization is the only one that is appropriate for optimizing CC transmission. As a deterministic initialization for the special case of $\underline{\mathcal{P}}_{\mathrm{U}_k}^{\mathrm{CN}}$ (CN signals), it was proposed in [20] to use the columns of the Fourier matrix (DFT matrix, e.g., [183, Section 6.12]) as initial filter vectors. This is a deterministic alternative to the matrix $\boldsymbol{U}$ in Section 7.6.2.4, and it can be shown that this choice is appropriate for optimizing CC transmission in the combined complex representation [20] (unless we use $\boldsymbol{T}_k = \boldsymbol{U}$, see Section 7.6.2.4).

7.6.3 Successive Allocation Algorithms

Let us finally briefly discuss algorithms that optimize zero-forcing strategies by successively allocating data streams to the users (e.g., [91, 152, 154, 155]). It was shown in [11] that such algorithms tend to yield CN solutions when applied to the combined complex representation of the complex multicarrier MIMO BC-TIN. In [53], it was demonstrated that CC zero-forcing solutions delivered by an iterative method with random initialization can indeed lead to better performance than the CN solutions obtained with successive allocation (yet at a higher computational complexity). It is still an open question how to optimize CC zero-forcing by means of a purely successive method.

On the other hand, successive allocation schemes are a strong candidate for optimizing improper signaling. When applied to the combined real representation, they allocate one real-valued data stream after another, which clearly corresponds to improper signaling with widely linear zero-forcing. It then depends on the allocation rule whether or not the final solution corresponds to improper per-user input signals.

7.6.4 Summary and Discussion

The analysis in this section has shown that many procedures that are applied in algorithms for transceiver design tend to preserve matrix structures that correspond to maximum-entropy transmission. If the aim is to obtain a reduced-entropy strategy, such as improper signaling or CC transmission, by means of an iterative algorithm, it is thus necessary to account for this already in the initialization. Note that there is then still no guarantee that the obtained solutions always correspond to reduced-entropy transmission, but this is not a problem. We have to recall that reduced-entropy signals are not always beneficial, but it rather depends on

the scenario and on the channel realization. It is thus only important to avoid an inherent restriction to maximum-entropy transmission in order to obtain an algorithm that is able to converge to reduced-entropy or maximum-entropy strategies depending on the particular channel realizations. Numerical experiments reveal that such a convergence to reduced-entropy strategies is indeed possible (see, e.g., the simulation results in Section 7.5.5 and in [11, 20, 23, 53]).

While we have identified several initializations of combined real transmit filters that correspond to improper signaling, finding initializations that correspond to CC transmission is less obvious. An initialization that is appropriate no matter which power shaping space is considered is a random initialization, but even then it is necessary to know about the possible pitfalls (e.g., the case where $\boldsymbol{T}_k \boldsymbol{T}_k^{\mathrm{H}} = \mathbf{I}_{M_k}$ in Section 7.6.2.4).

In summary, we can say that the combined representations from Table 3.1 enable us to optimize improper signaling and CC transmission by means of algorithms that have originally been developed, e.g., for proper signaling in single-carrier systems. However, we usually do not obtain the intended reduced-entropy solutions when we apply such methods thoughtlessly. Instead, it is necessary to adapt the initializations carefully.

A final remark is in order concerning algorithms that have been designed for SISO and MISO systems. The combined representations in Table 3.1 always correspond to a true MIMO system with $M_{\mathrm{T}} > 1$ for all terminals T, no matter how many antennas the original complex multicarrier system has. Thus, the approach pursued in this section is possible only with algorithms that are able to handle such true MIMO systems. If the aim is, e.g., to extend an algorithm that was developed for proper signaling in a MISO system to the case of improper signaling, different approaches are necessary. An example of such an extension can be found in [34].

7.7 Worst-Case Noise

Just like in the previous chapters, let us conclude our study of the MIMO BC-TIN by analyzing the worst-case noise. Theorem 6.5.1 for the RoP MIMO BC with DPC can be easily extended to the case of TIN strategies.

Theorem 7.7.1. *Let $(\mathcal{P}_k = \mathcal{P}_{\mathrm{U}_k})_{\forall k}$ and $\mathcal{P}_{\mathrm{B}}$ be power shaping spaces fulfilling the compatibility assumption (Definition 3.1.3), and let the constraint $(\boldsymbol{C}_{\boldsymbol{\eta}_k})_{\forall k} \in \mathcal{Q}_{\mathrm{noise}}$ be compatible with $\bigotimes_{k=1}^{K} \mathcal{P}_k$ (in the sense of Definition 3.1.2). If it holds for all per-user input signals in the RoP MIMO BC-TIN that $\boldsymbol{\xi}_k$ is an arbitrary maximum-entropy signal with respect to $\mathcal{P}_{\mathrm{B}}$, maximum-entropy noise with respect to $(\mathcal{P}_k)_{\forall k}$ minimizes the achievable rates of all users simultaneously.*

Proof. We can consider $\boldsymbol{C}_{\boldsymbol{z}_k}$ from (7.2) as effective noise covariance matrix and apply the same argumentation as in Theorem 6.5.1. □

Even though this worst-case noise theorem, which applies for the case that the input signals are maximum-entropy signals, can be obtained using the same proof technique as before, the situation changes if we are interested in the case of optimized transmit strategies. Unlike for the MIMO BC with DPC, optimal transmit strategies in the MIMO BC-TIN do not necessarily consist of maximum-entropy input signals even if we have maximum-entropy noise (Theorem 7.4.1). Therefore, we cannot easily obtain a corollary for the case of optimized

transmission. Some further comments on this aspect are given when we discuss the worst-case noise in interference channels in Section 8.4.

For the complex multicarrier MIMO BC-TIN, we have the following specializations based on the power shaping spaces from Proposition 3.4.2. Note that the case of optimized transmit strategies is missing in the corollaries as well.

Corollary 7.7.1 ($\mathcal{P}_k = \grave{\mathcal{P}}^{\mathrm{CN}}_{\mathrm{U}_k},\ \forall k$ and $\mathcal{P}_{\mathrm{B}} = \grave{\mathcal{P}}^{\mathrm{CN}}_{\mathrm{B}}$)**.** *In the complex multicarrier MIMO BC-TIN with constraints on the complex per-carrier noise covariance matrices, the worst-case noise is proper and CN if the per-user input signals are proper and CN.*

Corollary 7.7.2 ($\mathcal{P}_k = \grave{\mathcal{P}}_{\mathrm{U}_k},\ \forall k$ and $\mathcal{P}_{\mathrm{B}} = \grave{\mathcal{P}}_{\mathrm{B}}$)**.** *In the complex (multicarrier) MIMO BC-TIN with constraints on the combined complex noise covariance matrices, the worst-case noise is proper if the per-user input signals are proper.*

Corollary 7.7.3 ($\mathcal{P}_k = \mathcal{P}^{\mathrm{CN}}_{\mathrm{U}_k},\ \forall k$ and $\mathcal{P}_{\mathrm{B}} = \mathcal{P}^{\mathrm{CN}}_{\mathrm{B}}$)**.** *In the complex multicarrier MIMO BC-TIN with constraints on the per-carrier noise properties, the worst-case noise is CN if the per-user input signals are CN.*

Chapter 8

Gaussian MIMO Interference Channels

Up to this point, we have considered systems with either only a single transmitter or only a single receiver. By instead considering configurations where both the number of transmitters and the number of receivers are larger than one, we arrive at so-called interference networks. We restrict the following considerations to the special case where each receiver is only interested in the data from a particular transmitter and each transmitter has data for only one receiver, so that the involved terminals can be grouped into transmitter-receiver pairs, which are also referred to as users (see Figure 8.1). This setting is called (Gaussian) K-user MIMO interference channel (IFC) [184].

After introducing the system model, we summarize results from the literature which show that reduced-entropy transmission can be beneficial in the K-user MIMO IFC. As a special case, we consider the so-called MIMO Z-interference channel (ZIFC), where only partial interference is present. In this setting, we study proper and improper signaling both for systems with and without TS. Finally, we compare the results obtained in the K-user MIMO IFC and the MIMO ZIFC to our observations from the previous chapters.

8.1 System Model and Achievable Rates

From the general model (3.1), we obtain the model for the K-user RoP MIMO IFC as

$$\boldsymbol{y}_k = \sum_{j=1}^{K} \boldsymbol{H}_{k,j}\boldsymbol{x}_j + \boldsymbol{\eta}_k,\ \forall k \tag{8.1}$$

with a covariance constraint $(\boldsymbol{C}_{\boldsymbol{x}_k})_{\forall k} \in \mathcal{Q}$ as given by (3.3). We have introduced the abbreviations $\boldsymbol{y}_k = \boldsymbol{y}_{\mathrm{D}_k}$, $\boldsymbol{H}_{k,j} = \boldsymbol{H}_{\mathrm{D}_k\mathrm{S}_j}$, $\boldsymbol{x}_k = \boldsymbol{x}_{\mathrm{S}_k}$, and $\boldsymbol{\eta}_k = \boldsymbol{\eta}_{\mathrm{D}_k}$. The system model for the complex K-user multicarrier MIMO IFC can be obtained in an analogous manner from the general model in (3.34).

The capacity region of the K-user MIMO IFC is still an open problem apart from some special cases. Therefore, it is assumed in many publications (e.g., [32, 34, 35, 170] and the references therein) that interference is treated as noise, i.e., TIN strategies are applied, and that all transmit signals are Gaussian, even though this is not necessarily the optimal input

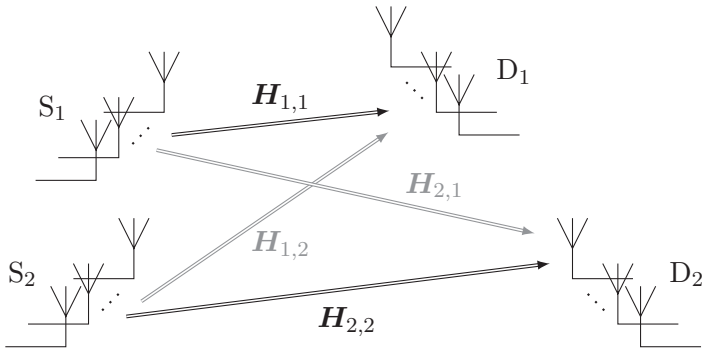

Figure 8.1: Example of the MIMO interference channel with $K = 2$ transmitter-receiver pairs. The unintended channels are drawn in gray.

distribution (see Chapter 10). We refer to the system model with these two restrictions as K-user MIMO IFC-TIN.

In the K-user RoP MIMO IFC-TIN, we can achieve the per-user rates

$$r_k = \mu \log_2 \frac{\det \boldsymbol{C}_{\boldsymbol{y}_k}}{\det \boldsymbol{C}_{\boldsymbol{z}_k}} \tag{8.2}$$

with

$$\boldsymbol{C}_{\boldsymbol{y}_k} = \boldsymbol{C}_{\boldsymbol{\eta}_k} + \sum_{j=1}^{K} \boldsymbol{H}_{k,j} \boldsymbol{C}_{\boldsymbol{x}_j} \boldsymbol{H}_{k,j}^{\mathrm{H}} \qquad \text{and} \qquad \boldsymbol{C}_{\boldsymbol{z}_k} = \boldsymbol{C}_{\boldsymbol{y}_k} - \boldsymbol{H}_{k,k} \boldsymbol{C}_{\boldsymbol{x}_k} \boldsymbol{H}_{k,k}^{\mathrm{H}}. \tag{8.3}$$

The corresponding achievable rate region is

$$\mathcal{R}_{\mathrm{TIN}} = \bigcup_{\substack{(\boldsymbol{C}_{\boldsymbol{x}_k} \succeq \boldsymbol{0})_{\forall k} \\ (\boldsymbol{C}_{\boldsymbol{x}_k})_{\forall k} \in \mathcal{Q}}} \left\{ \boldsymbol{\rho} \in \mathbb{R}_{0,+}^{K} \;\middle|\; \rho_k \leq r_k, \;\; \forall k \right\} \tag{8.4}$$

with r_k from (8.2). As this rate region is nonconvex in general (see, e.g., the plots in [33]), allowing (R)TS (see Section 3.2.1) can lead to enlarged rate regions $\overline{\mathcal{R}}_{\mathrm{TIN}}$ (with RTS) and $\overline{\overline{\mathcal{R}}}_{\mathrm{TIN}}$ (with TS).

8.1.1 Symbol Extensions

Several results in the literature on interference channels are based on so-called symbol extensions (e.g., [30, 184, 185]), where multiple subsequent channel uses are grouped together as a single channel use of a higher-dimensional system. Recalling that we use the term *carriers* as a synonym for orthogonal resources (see Section 1.2), no matter whether these resources are, e.g., disjoint frequency bands or disjoint time intervals, we can interpret coding across the elements of an extended symbol vector as a form of CC transmission.

Note that such a coding across time intervals shall not be confused with time-sharing (TS) in the sense of Section 3.2.1. On the one hand, TS is more restrictive in the sense that the transmission in each time slot is independent, i.e., we do not code across time slots. On the other hand, TS brings additional flexibility as it allows for variable-length time slots as compared to symbol extensions where each of the underlying individual symbols has the same duration.

If the channel stays constant over time as considered, e.g., in [30, 184], and we interpret symbol extensions as multicarrier transmission, we obtain the special case of equal channel conditions on all carriers, i.e., $\boldsymbol{C}_{\boldsymbol{\eta}_k^{(c)}}$ is the same for all c, and analogously for $\boldsymbol{H}_{k,j}^{(c)}$. In the combined complex representation, this leads to block-diagonal matrices where all submatrices are equal. Therefore, the following comment is in order.

For given block size, the space of Hermitian block-diagonal matrices consisting of equal submatrices complies to the definition of a power shaping space (Definition 2.3.1), and the noise described above can be considered as maximum-entropy noise with respect to this power shaping space $\mathcal{P}_{\mathrm{D}_k}$. Accordingly, we can define an analogous power shaping space $\mathcal{P}_{\mathrm{S}_j}$ at the transmitter, and the combined complex channel matrices $\boldsymbol{H}_{k,j}$ are compatible with $(\mathcal{P}_{\mathrm{D}_k}, \mathcal{P}_{\mathrm{S}_j})$. This means that the framework established in Chapter 2 could also be applied for a detailed study of this special case using a stricter notion of maximum-entropy signals: we could decide to count only CN signals with equal covariance matrices on all carriers as maximum-entropy signals.

However, for the considerations that follow, it is sufficient to take the more general perspective, where any CN signal is considered as maximum-entropy signal no matter whether the per-carrier covariance matrices are equal. We therefore formulate the examples given below in terms of the power shaping spaces from Proposition 3.4.2 and refrain from defining further special cases of power shaping spaces.

8.1.2 Degrees of Freedom

In Section 7.5.1, we have used the concept of effective degrees of freedom for a study with finite data rates. For some of the discussions in this chapter, we instead need the conventional notion of *degrees of freedom*, which describe the behavior of a system when the SNR and the achievable rates tend to infinity. The achievable (sum) DoF in an IFC are given by (see, e.g., [30])

$$D = \lim_{Q \to \infty} \frac{r(Q)}{\log_2(Q)} \tag{8.5}$$

where $r(Q)$ is the achievable sum rate with sum power Q. For a given $D \geq 0$, this means that the sum rate $r(Q)$ scales linearly with $\log_2 Q$ in the high-SNR regime (i.e., for high values of Q), and D is the slope of this linear relationship. It is easy to verify[1] that we obtain $D = \mu$ in a single-user SISO system (e.g., [184]), and this is clearly an achievable value in the K-user SISO IFC (e.g., by shutting off all users but one).

Recall that allowing for RTS does not bring any gains for sum rate maximization (see Section 3.2.2). Moreover, the high-SNR approximation $r(Q) \approx D \log_2 Q + R_0$, where R_0 is a constant, is concave in Q. Therefore, averaging over rates achieved with different values of Q cannot bring benefits in the high-SNR regime, i.e., TS cannot improve the achievable DoF. Therefore, results based on DoF hold independently of whether or not (R)TS is allowed.

8.2 Benefits of Reduced-Entropy Transmission

In the literature, we find several results on, e.g., coding across carriers (e.g., [40–42, 186]), symbol extensions (e.g., [30, 184, 185]), and improper signaling (e.g., [30–34, 187–193]) in

[1] This could be calculated from (4.4) by plugging in the special case $M_{\mathrm{D}} = M_{\mathrm{S}} = 1$ with $C_x = Q$.

interference channels. When interpreting them in terms of the nomenclature that we use here, these results can be summarized in the following general theorem.

Theorem 8.2.1. *Let $(\mathcal{P}_{\mathrm{S}_k})_{\forall k}$ and $(\mathcal{P}_{\mathrm{D}_k})_{\forall k}$ be power shaping spaces fulfilling the compatibility assumption (Definition 3.1.3). Even if the noise vectors $\boldsymbol{\eta}_k$ are maximum-entropy signals with respect to $(\mathcal{P}_{\mathrm{D}_k})_{\forall k}$, it can happen that reduced-entropy transmit signals $\boldsymbol{x}_k$ with respect to $(\mathcal{P}_{\mathrm{S}_k})_{\forall k}$ are needed to achieve the whole capacity region of the K-user RoP MIMO IFC or the whole rate region of the K-user RoP MIMO IFC-TIN. This statement holds for systems with and without (R)TS.*

Proof. Examples where this happens are given below. □

Just like in Chapter 7, the examples to establish the theorem can be special cases with relatively small system dimensions. Some examples from the literature are revisited below, and references to further examples are provided.

Example 8.2.1. *In [40], the three-user two-carrier SISO IFC was considered. For a particular channel realization, it was shown that joint coding across carriers achieves a sum rate that is higher than the sum of the individual per-carrier sum capacities. In the achievable scheme that was used for joint coding, each user transmits exactly the same signal on both carriers, and the signals are combined by a linear filter at the receiver, while the interference coming from the two other users aligns in the nullspace of the receive filter. This is clearly an application of CC transmission, i.e., an example for a gain by reduced-entropy transmission, where the combined real transmit covariance matrices lie outside of the power shaping spaces $(\mathcal{P}_{\mathrm{S}_k}^{\mathrm{CN}})_{\forall k}$. It is remarkable that this TIN strategy outperforms the best separate coding scheme that utilizes optimal multiuser detection [40]. Therefore, this example suffices as a proof both in terms of the capacity region and in terms of the TIN rate region.*

In [41], it was shown that such an *inseparability* can occur in more complicated single-antenna interference networks, where transmitters may have messages for multiple receivers, and receivers may be interested in messages from multiple transmitters. Indeed, it was shown that only a very special class of interference networks with a so-called *MAC-Z-BC* structure is always separable in the sense that the sum capacity can be achieved without joint coding. However, when the aim is to achieve not only the sum capacity, but the whole capacity region, coding across carriers can be necessary even in this kind of network. This was shown in [42, 186] along with some further results on cases in which coding across carriers is necessary to achieve the capacity of interference networks.

Example 8.2.2. *A technique called interference alignment was studied in [184] for the K-user (MIMO) IFC. The idea behind this method is to design the transmit signals such that several interfering signals arriving at a receiver fall into the same lower-dimensional subspace and can easily be canceled by linear zero-forcing as the remaining space stays interference-free (see [184] for more details). Note that a similar effect was exploited in Example 8.2.1. To achieve the sum capacity at high SNR, i.e., the maximum DoF, in the K-user SISO IFC with time-varying channels, the authors of [184] apply interference alignment in combination with symbol extensions. As stated above (see Section 8.1.1), the latter can be considered as a form of CC transmission.*

Interference alignment and signal extensions have also been studied in many further publications, e.g., for a more general interference network called MIMO X channel in [185], and the concept of interference alignment is particularly promising in the K-user MIMO IFC with multiple antennas at all terminals (see, e.g., [184]). Moreover, interference alignment and symbol extensions form the basis of the following example.

Example 8.2.3. *In [30], it was proposed to combine improper transmit signals and symbol extensions in order to achieve interference alignment in the three-user SISO IFC. The resulting transmit scheme is a TIN strategy with widely linear zero-forcing and achieves $D = 1.2$ DoF, while proper Gaussian transmit signals can achieve only $D = 1$ DoF in this setting [30]. This combination of CC transmission (due to symbol extensions, see Section 8.1.1) and improper signaling is clearly an example for a gain by reduced-entropy transmission. The combined real transmit covariance matrices lie neither in $(\mathcal{P}_{\mathrm{S}_k}^{\mathrm{CN}})_{\forall k}$ nor in $(\grave{\mathcal{P}}_{\mathrm{S}_k})_{\forall k}$. As the study is based on DoF, the result holds irrespective of whether (R)TS is allowed (see Section 8.1.2).*

This result was extended to the four-user SISO IFC in [187], where $D = \frac{4}{3}$ DoF were shown to be achievable with improper signaling. Moreover, we can find several examples of improper signaling at finite SNR in the literature.

Example 8.2.4. *The complex two-user SISO IFC-TIN was studied in [189], and the results were generalized to a SISO system with $K > 2$ users in [33] and to the complex K-user MISO IFC-TIN in [34, 190]. In these papers, suboptimal algorithms for rate balancing with improper signaling were proposed, and it was demonstrated that the achieved solutions enlarge the rate region compared to optimized TIN strategies with proper signals, both in the case without (R)TS and in the case with RTS. However, the application of TS was not considered in these papers.*

In two earlier papers [31, 188], the complex two-user SISO IFC-TIN was studied from a game theoretic perspective and the cooperative solutions based on improper signaling were shown to outperform the noncooperative Nash equilibrium with proper signaling. Moreover, a parametrization of the Pareto boundary of the achievable rate region with maximally improper signals (corresponding to one-dimensional real-valued signals) was derived. Further algorithms that can be applied for transceiver design without (R)TS in the SISO IFC-TIN with improper signaling were presented in [32, 191]. In [192], it was demonstrated that gains by improper signaling are possible for a large range of channel realizations.

The complex K-user MIMO IFC-TIN, i.e., the case of multiple antennas at transmitters and receivers, was studied in [35, 193], and a suboptimal algorithm for widely linear transceiver design was derived based on the weighted MSE method [180]. Note that it was discussed in [26] how the algorithm from [35, 193], which is based on the complex formulation, can be related to the application of a previously existing algorithm for linear transceivers [194] in the composite real representation. In numerical studies in [35, 193], it was shown that the solutions obtained with widely linear transceivers and improper signals lead to higher achievable rates than the solutions with linear transceivers and proper signals. However, as this is a numerical comparison between two suboptimal schemes, a more rigorous or even analytical comparison of the achievable rate regions of the complex K-user MIMO IFC-TIN with proper signals and with improper signals is still an open problem.

Finally, benefits of improper signaling have recently been studied in several closely related system models, e.g., in interfering BCs [195, 196], in interfering MACs with TIN strategies

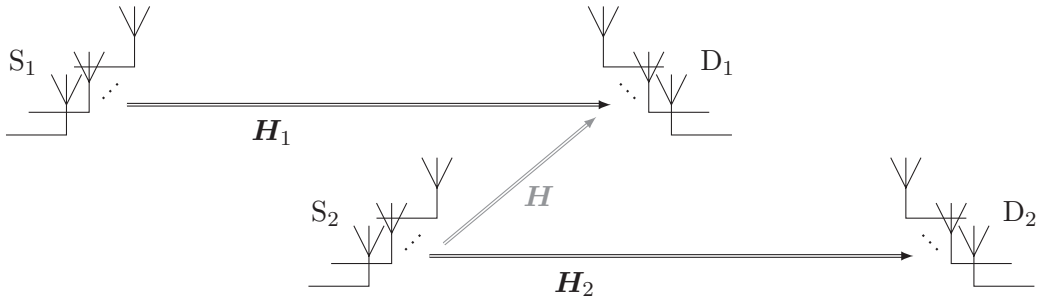

Figure 8.2: Illustration of the MIMO ZIFC, where one of the unintended channels is negligible due to the positioning of the terminals.

[197], in the K-user IFC with practical coding and modulation schemes [198], in cognitive radio systems [199–205], and in heterogeneous cellular networks [36].

All these examples show that reduced-entropy transmission can bring gains in the complex K-user multicarrier MIMO IFC and in special cases thereof, as well as in other interference networks. However, the overview also makes clear that there is a large variety of interference networks that can be studied and, accordingly, a large variety of open research questions, especially in MIMO settings with multiple antennas at all transmitters and receivers.

8.3 Improper Signaling in the Complex MIMO Z-Interference Channel

The MIMO ZIFC (or one-sided MIMO IFC) is a special case of the two-user MIMO IFC, where only one of the receivers is disturbed by interference from the other user. The system model of the K-user RoP MIMO IFC (8.1) then simplifies to

$$\boldsymbol{y}_1 = \boldsymbol{H}_1\boldsymbol{x}_1 + \boldsymbol{H}\boldsymbol{x}_2 + \boldsymbol{\eta}_1 \tag{8.6}$$

$$\boldsymbol{y}_2 = \boldsymbol{H}_2\boldsymbol{x}_2 + \boldsymbol{\eta}_2 \tag{8.7}$$

with the abbreviations $\boldsymbol{H}_k = \boldsymbol{H}_{k,k}$ and $\boldsymbol{H} = \boldsymbol{H}_{1,2}$. For the achievable rates with TIN strategies (8.2), we obtain

$$r_1 = \mu \log_2 \frac{\det\left(\boldsymbol{C}_{\boldsymbol{\eta}_1} + \boldsymbol{H}_1\boldsymbol{C}_{\boldsymbol{x}_1}\boldsymbol{H}_1^{\mathrm{H}} + \boldsymbol{H}\boldsymbol{C}_{\boldsymbol{x}_2}\boldsymbol{H}^{\mathrm{H}}\right)}{\det\left(\boldsymbol{C}_{\boldsymbol{\eta}_1} + \boldsymbol{H}\boldsymbol{C}_{\boldsymbol{x}_2}\boldsymbol{H}^{\mathrm{H}}\right)}, \tag{8.8}$$

$$r_2 = \mu \log_2 \frac{\det\left(\boldsymbol{C}_{\boldsymbol{\eta}_2} + \boldsymbol{H}_2\boldsymbol{C}_{\boldsymbol{x}_2}\boldsymbol{H}_2^{\mathrm{H}}\right)}{\det \boldsymbol{C}_{\boldsymbol{\eta}_2}}. \tag{8.9}$$

From a practical perspective, such a scenario could arise when the transmitting and receiving nodes are positioned in a way that one of the unintended links is negligibly weak (see, e.g., [36, 206] and Figure 8.2). From a theoretical point of view, the ZIFC is an important starting point for analytical studies since it is easier to analyze due to the one-sided interference. The hope is then that fundamental insights gained in this simpler scenario also help to understand more complicated interference networks.

In this section, we discuss the application of improper signaling in the complex ZIFC. We restrict our considerations to TIN strategies with Gaussian transmit signals in a single-carrier single-antenna setting with individual power constraints. From the analysis of the resulting

SISO ZIFC-TIN, we obtain an insight on the interplay between TS and improper signaling, and we discuss possible implications for other systems at the end of this section.

8.3.1 Previous Results

From the literature on the capacity of the (MIMO) ZIFC (e.g., [42, 186, 207–210]), it is known that treating the interference as noise is in general not the optimal strategy in this type of system. Nevertheless, TIN strategies have still attracted the interest of researchers due to their simplicity, and several recent publications have studied possible benefits of improper signaling in the (MIMO) ZIFC-TIN.

In [36, 206], improper signaling was compared to proper signaling in the complex MIMO ZIFC-TIN. However, as the numerical analysis was based on heuristic transmit schemes, the observed gains do not allow conclusions about whether improper signaling can also outperform the (unknown) globally optimal proper transmit strategy. Despite the simplification due to one-sided interference, the MIMO case still does not seem to be easily tractable in an analytical study.

Analytical expressions for the achievable sum rate in the complex SISO ZIFC-TIN with improper signaling were derived in [37], and an extension to the whole Pareto-boundary of the rate region was presented in [38]. The obtained results show that the rate region with improper signaling is in general larger than with proper signaling, but the studies in [37, 38] do not consider the possibility of TS (i.e., they apply only to systems where either RTS is used or (R)TS is avoided completely). We study the case with TS in the following.

8.3.2 Standard Form of the Complex SISO ZIFC

As noted in [37, 38], the SISO ZIFC

$$y_1 = |h_1|\mathrm{e}^{\mathrm{j}\theta_1}x_1 + |h|\mathrm{e}^{\mathrm{j}\theta}x_2 + \eta_1 \tag{8.10}$$

$$y_2 = |h_2|\mathrm{e}^{\mathrm{j}\theta_2}x_2 + \eta_2 \tag{8.11}$$

with proper Gaussian noise and power constraints $C_{x_k} \leq Q_k,\ \forall k$ can always be transformed to a standard form

$$y_1' = x_1' + \sqrt{a}\,x_2' + \eta_1' \tag{8.12}$$

$$y_2' = x_2' + \eta_2' \tag{8.13}$$

where we have chosen

$$y_1' = \mathrm{e}^{-\mathrm{j}\theta_1} C_{\eta_1}^{-\frac{1}{2}} y_1, \qquad x_1' = |h_1| C_{\eta_1}^{-\frac{1}{2}} x_1, \qquad \eta_1' = \mathrm{e}^{-\mathrm{j}\theta_1} C_{\eta_1}^{-\frac{1}{2}} \eta_1, \tag{8.14}$$

$$y_2' = \mathrm{e}^{\mathrm{j}(\theta-\theta_1-\theta_2)} C_{\eta_2}^{-\frac{1}{2}} y_2, \quad x_2' = |h_2|\mathrm{e}^{\mathrm{j}(\theta-\theta_1)} C_{\eta_2}^{-\frac{1}{2}} x_2, \quad \eta_2' = \mathrm{e}^{\mathrm{j}(\theta-\theta_1-\theta_2)} C_{\eta_2}^{-\frac{1}{2}} \eta_2. \tag{8.15}$$

We can identify that $a = |h|^2|h_2|^{-2} C_{\eta_2} C_{\eta_1}^{-1} \geq 0$ and that η_k' is proper Gaussian noise with unit variance for all k. The transmit signals $x_k',\ \forall k$ are (possibly improper) complex Gaussian with power constraints $C_{x_k'} \leq Q_k' = |h_k|^2 C_{\eta_k}^{-1} Q_k,\ \forall k$. In the following, we use the standard form, but we omit the prime symbols for the ease of notation.

8.3.3 Optimal Transmit Strategy with Time-Sharing in the Complex SISO ZIFC-TIN

When allowing TS as introduced in Section 3.2.1, we obtain the following result, which is also shown in [8].

Theorem 8.3.1. *In the complex SISO ZIFC-TIN, the whole TS rate region is achieved by proper transmit signals.*

Proof. We perform the proof in the standard form (8.12)–(8.13). When writing the transmit pseudovariances as $\tilde{C}_{x_k} = |\tilde{C}_{x_k}| \mathrm{e}^{\mathrm{j}\varphi_k}$, it can be shown that it is optimal to choose $\varphi_1 = \varphi_2 + \pi$ and that $\varphi_1 = 0$ can be chosen without loss of generality (see [38]). This means, we can assume $\tilde{C}_{x_k}$ to be real-valued for all k. Note that this complies to our observations in Example 4.5.1 and in the proof of Proposition 7.4.2.

For the corresponding composite real transmit covariance matrices, we obtain from (2.34)

$$\boldsymbol{C}_{\breve{\boldsymbol{x}}'_k} = \frac{1}{2} \begin{bmatrix} C_{x_k} + \tilde{C}_{x_k} & \\ & C_{x_k} - \tilde{C}_{x_k} \end{bmatrix} = \begin{bmatrix} p_k^{(1)} & \\ & p_k^{(2)} \end{bmatrix} \tag{8.16}$$

where we have introduced the abbreviations $p_k^{(1)} = \frac{1}{2}(C_{x_k} + \tilde{C}_{x_k})$ and $p_k^{(2)} = \frac{1}{2}(C_{x_k} - \tilde{C}_{x_k})$. To establish the theorem, we have to show that we can use $p_k^{(1)} = p_k^{(2)}$ in each time slot of the optimal TS solution (which is equivalent to $\tilde{C}_{x_k} = 0$).

The combined real representations (2.46) of $h_k = 1,\ \forall k$ and $h = \sqrt{a}$ are given by $\grave{\boldsymbol{H}}_k = \mathbf{I}_2,\ \forall k$ and $\grave{\boldsymbol{H}} = \sqrt{a}\mathbf{I}_2$, respectively. For the combined real noise covariance matrices, we obtain $\boldsymbol{C}_{\breve{\boldsymbol{\eta}}_k} = \frac{1}{2}\mathbf{I}_2$ from (2.34) since the complex noise is proper with unit variance. As all these matrices are scaled identities, we can interpret (8.16) as CN transmission in a real-valued two-carrier system with equal channel conditions on both carriers. By applying (8.8)–(8.9) with $\mu = \frac{1}{2}$ on each carrier, we obtain the same rate equations

$$r_1^{(c)} = \frac{1}{2}\log_2\left(1 + 2p_1^{(c)}(1 + 2ap_2^{(c)})^{-1}\right), \qquad r_2^{(c)} = \frac{1}{2}\log_2\left(1 + 2p_2^{(c)}\right) \tag{8.17}$$

on both carriers, so that the solution to the inner problem (3.33) is exactly the same on both carriers when we apply the dual decomposition from Section 3.3.2. Thus, the primal recovery (3.23) performs time-sharing between solutions for which it holds that $p_k^{(1)} = p_k^{(2)},\ \forall k$ (see also the argumentation in the proof of Proposition 7.4.2). □

8.3.4 Numerical Examples and Discussion

The above result might seem surprising since a gain by improper signaling was shown in terms of the sum rate in [37] and in terms the rate region in [38]. However, the difference comes from the fact that TS was not considered in these two publications. Instead, convex hulls of the rate regions were taken in [38], which corresponds to an application of RTS.

The more flexible TS not only renders improper signaling unnecessary, but even leads to a larger rate region than the one obtained in [38]. This can be seen from Figure 8.3, where we reproduce one of the examples from [38] along with an additional curve for proper signaling with TS.[2] To obtain this curve, we have adapted the branch-and-bound approach discussed in

[2]This simulation result was presented in a similar manner in [8].

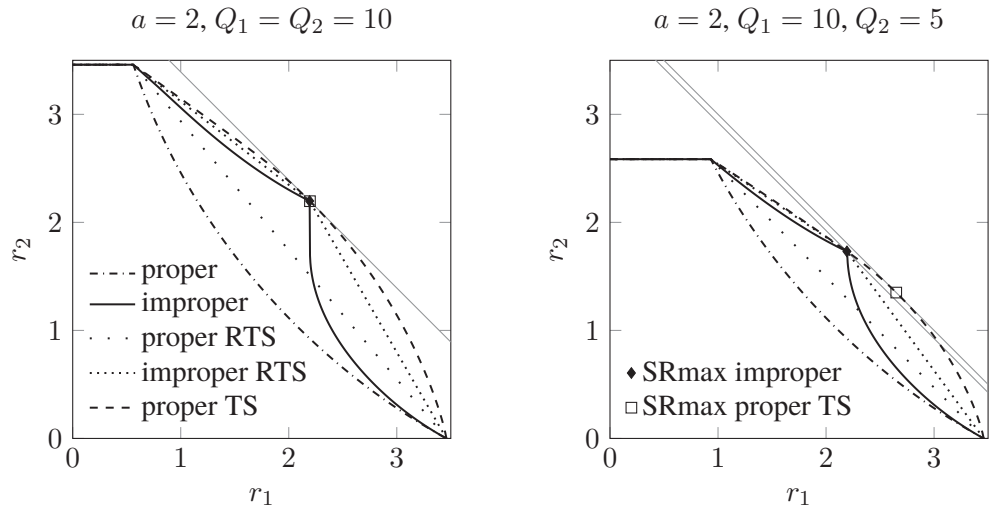

Figure 8.3: Achievable rate regions of the SISO ZIFC-TIN without (R)TS, with RTS and with TS. The solid gray lines are the tangents with slope -1 at the sum rate points.

Section 7.3.1.2 to the considered scenario. In addition, we plot the rate region for a scenario with asymmetric power constraints $Q_1 \neq Q_2$, where it can be observed that proper signaling with TS can also improve the sum rate (SRmax) compared to the one obtained with improper signaling in [37, 38].

The bad performance of proper signaling with RTS compared to improper signaling with RTS can be understood by considering the complex transmission of the second user as two real-valued data streams. When reducing the power of one of the real-valued streams, we do not only reduce the interference that this stream causes to the first user, but we can also increase the transmit power of the other real-valued stream without violating the power constraint. Accordingly, we can redistribute power between the two real-valued streams of the first user in order to invest more power in the dimension where the interference is weaker (according to the waterfilling solution (4.10) with the noise covariance matrix replaced by the composite real interference-plus-noise covariance matrix).

When trying to achieve the same effect by considering two time slots in a transmit scheme with proper signals and RTS, we encounter the problem that reducing the power in one time slot does not allow us to increase the power in the other one. However, TS gives us this possibility (since the powers are averaged over the slots in case of TS, see Section 3.2.1), and it provides us with an even more flexible way of redistributing the power, namely by varying the length of the time slots in addition. As a result, proper signaling with TS can even outperform improper signaling with RTS.

It shall be noted that this argumentation is only possible due to the special structure of the combined real transmit covariance matrices in (8.16), where improper signaling boils down to a nonuniform power allocation between two real-valued streams. Thus, this justification of the optimality of proper signals is based on the fact that the system can be transformed to a standard model with purely real-valued channel coefficients. This is similar to Proposition 7.4.2, where the complex two-user MISO BC-TIN was transformed to a description with real-valued channel coefficients. On the other hand, such a transformation is not possible in the three-user examples in Proposition 7.4.1 and Example 8.2.3, where improper signaling was shown to be beneficial

even in case that TS is allowed.

It is therefore an interesting question whether or not Theorem 8.3.1 can be extended to the two-user IFC-TIN, where both users disturb each other. On the one hand, the improvements due to improper signaling reported for the two-user SISO IFC-TIN and the two-user MISO IFC-TIN in [31–34, 188–192] (see Example 8.2.4) were all obtained in comparison to proper signaling with RTS (or without any form of (R)TS), and TS was not considered in these publications. On the other hand, when transforming this scenario to a standard form, at least one complex coefficient remains, so that we cannot easily transfer the argumentation from the proof of Theorem 8.3.1 to these scenarios. A further study of this question is left open for future research.

Another aspect that is left open is the extension to the MIMO ZIFC-TIN and the two-user MIMO IFC-TIN (e.g., [35, 36, 193, 206]). The step from scalar variances to covariance matrices makes it more difficult to obtain analytical results, and it does not seem to be possible to transform these systems to a standard form with real-valued coefficients, even if the considerations are restricted to one-sided interference. It is therefore again not clear whether Theorem 8.3.1 can be extended to these scenarios.

8.4 Worst-Case Noise

Just like in the MIMO BC-TIN, a difficulty when studying the worst-case noise in the K-user MIMO IFC is that the optimal transmit strategy is not known. In [66, 67], it was shown that Gaussian noise is the worst-case noise in arbitrary networks with multiple nodes, but this, e.g., does not allow direct conclusions about proper or improper noise since a real-valued setting was considered in [66, 67]. It might be possible to extend the proof technique from [66, 67], which does not require knowledge of the optimal transmit strategy, to complex systems in order to answer this question. At least from an intuitive point of view, it is to be expected that a disturbance with the highest differential entropy should always be the worst case. While we leave a proof of this aspect open for future research, we can at the current point at least state a worst-case noise theorem for the K-user MIMO IFC-TIN under the assumption that the transmit signals are fixed to be maximum-entropy signals.

Theorem 8.4.1. *Let $(\mathcal{P}_{\mathrm{S}_k})_{\forall k}$ and $(\mathcal{P}_{\mathrm{D}_k})_{\forall k}$ be power shaping spaces fulfilling the compatibility assumption (Definition 3.1.3), and let the constraint $(\boldsymbol{C}_{\boldsymbol{\eta}_k})_{\forall k} \in \mathcal{Q}_{\mathrm{noise}}$ be compatible with $\bigotimes_{k=1}^{K} \mathcal{P}_{\mathrm{D}_k}$ (in the sense of Definition 3.1.2). If it holds for all transmit signals in the K-user RoP MIMO IFC-TIN that $\boldsymbol{x}_k$ is an arbitrary maximum-entropy signal with respect to $\mathcal{P}_{\mathrm{S}_k}$, maximum-entropy noise with respect to $(\mathcal{P}_{\mathrm{D}_k})_{\forall k}$ minimizes the achievable rates of all users simultaneously.*

Proof. We can consider $\boldsymbol{C}_{\boldsymbol{z}_k}$ from (8.3) as effective noise covariance matrix and apply the same argumentation as in Theorem 6.5.1. □

Using the power shaping spaces from Proposition 3.4.2, we obtain the following corollaries for the complex K-user multicarrier MIMO IFC-TIN. The statement of Corollary 8.4.2 can also be found in [28].

Corollary 8.4.1 ($\mathcal{P}_{\mathrm{S}_k} = \grave{\mathcal{P}}^{\mathrm{CN}}_{\mathrm{S}_k}$, $\forall k$ and $\mathcal{P}_{\mathrm{D}_k} = \grave{\mathcal{P}}^{\mathrm{CN}}_{\mathrm{D}_k}$)**.** *In the complex K-user multicarrier MIMO IFC-TIN with constraints on the complex per-carrier noise covariance matrices, the worst-case noise is proper and CN if the transmit signals are proper and CN.*

Corollary 8.4.2 ($\mathcal{P}_{\mathrm{S}_k} = \grave{\mathcal{P}}_{\mathrm{S}_k}$, $\forall k$ and $\mathcal{P}_{\mathrm{D}_k} = \grave{\mathcal{P}}_{\mathrm{D}_k}$)**.** *In the complex K-user (multicarrier) MIMO IFC-TIN with constraints on the combined complex noise covariance matrices, the worst-case noise is proper if the transmit signals are proper.*

Corollary 8.4.3 ($\mathcal{P}_{\mathrm{S}_k} = \mathcal{P}_{\mathrm{S}_k}^{\mathrm{CN}}$, $\forall k$ and $\mathcal{P}_{\mathrm{D}_k} = \mathcal{P}_{\mathrm{D}_k}^{\mathrm{CN}}$)**.** *In the complex K-user multicarrier MIMO IFC-TIN with constraints on the per-carrier noise properties, the worst-case noise is CN if the transmit signals are CN.*

8.5 Comparison to the MIMO Multiple Access Channel and to the MIMO Broadcast Channel

Having studied potential benefits of reduced-entropy transmission in various MIMO communication systems with interference, a comparison of the observations is in order. While there is clearly room for further interpretations and discussions, we have two main objectives in this section. Firstly, we compare findings in the MIMO MAC with SIC, the MIMO BC with DPC, and the MIMO ZIFC-TIN, which can all be considered as systems with one-sided interference. Secondly, we briefly discuss differences and common points of the K-user MIMO IFC-TIN and the MIMO BC-TIN, which are both systems with mutual interference between all users.

8.5.1 Systems with One-Sided Interference

When looking at the rate equations of the RoP MIMO ZIFC-TIN given in (8.8)–(8.9), one might be reminded of the SIC rates in the RoP MIMO MAC (5.7) or the DPC rates in the RoP MIMO BC (6.2). Indeed, the partial interference cancellation by means of SIC and DPC, respectively, turn the MIMO MAC and the MIMO BC into systems with one-sided interference.

Note that the one-sided interference in the ZIFC was assumed as part of the channel model, and we might try to implement a multiuser coding scheme to further reduce the interference (e.g., [207]). However, when restricting our considerations to the MIMO ZIFC-TIN, we can ask why this model behaves differently from the MIMO MAC and the MIMO BC despite the similarities in the rate equations. For the MIMO MAC and the MIMO BC, employing RTS is sufficient, i.e., no gain can be obtained by allowing TS instead (see Sections 5.1.1 and 6.1), and it can be shown that maximum-entropy transmission is the optimal choice (when RTS is allowed and maximum-entropy noise is assumed). By contrast, we have seen in the previous section that TS can be necessary to exploit the full potential of the ZIFC-TIN, and we have observed that reduced-entropy transmission can bring gains under the assumption of RTS.

The first important difference when comparing (8.8)–(8.9) to, e.g., the SIC rate in the RoP MIMO MAC (5.7) is that the signal $\boldsymbol{x}_2$ travels over two different channels in the ZIFC-TIN while it travels only over the channel $\boldsymbol{H}_2$ in the MAC. Note that the unique feature of the MIMO MAC that the weighted sum rate can be rewritten as a concave function (5.11) of the transmit covariance matrices relies exactly on this property. Therefore, if we want to obtain a MIMO ZIFC-TIN that behaves similarly to the MIMO MAC, we have to restrict our considerations to the special case where $\boldsymbol{H} = \boldsymbol{H}_2$ in (8.6), or to $a = 1$ in (8.12) in the special case of a SISO system.

However, we then still do not obtain the same situation as in the MAC with SIC. While the decoding order can be chosen arbitrarily in the MAC, meaning that we can design which

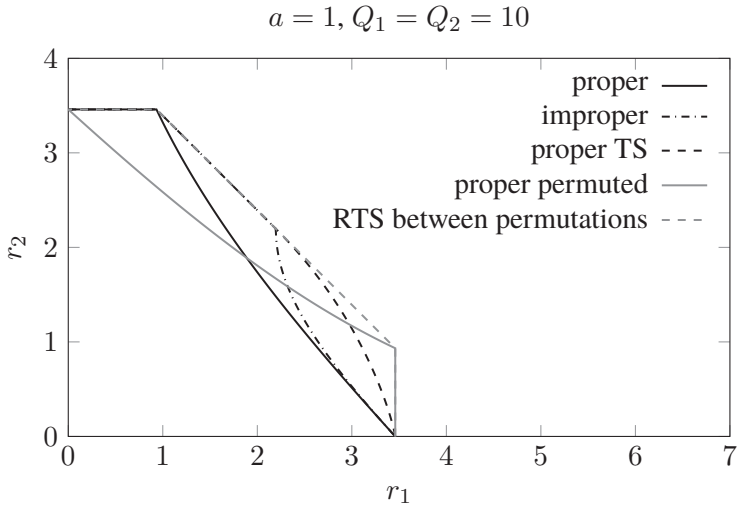

Figure 8.4: Achievable rate regions of the SISO ZIFC-TIN without (R)TS and with TS, along with the rate region of the SISO ZIFC-TIN obtained by permuting the users.

of the users is disturbed by the other one, the direction of the one-sided interference in the ZIFC-TIN is dictated by the channel model. The effect of this restriction can be observed in Figure 8.4, which shows the rate region of the SISO ZIFC-TIN with $a = 1$ along with the rate region that we obtain when permuting the users such that the first user is the one that receives in an interference-free manner. If we could perform RTS between these two permutations, we would achieve the well-known pentagonal capacity region of the two-user SISO MAC (e.g., [48]), which is larger than the TS rate region of the original SISO ZIFC-TIN.

This minimal example demonstrates the following. Even if we consider the special case where the unintended channel is equal to the intended channel, the ZIFC-TIN suffers from the fixed direction of the interference. Methods such as improper signaling and TS can compensate this at least partially. In the MAC with SIC, where the direction of the interference can be modified by switching to a different decoding order, it suffices to perform RTS between strategies with maximum-entropy transmission (see Section 5.1.1 and Theorem 5.2.1). In a similar manner, we could compare the MIMO ZIFC-TIN to the MIMO BC with DPC, where we in addition would have to consider the difference that the power constraint in the MIMO BC acts on the sum of the input covariance matrices $\boldsymbol{C}_{\boldsymbol{x}} = \sum_{k=1}^{K} \boldsymbol{C}_{\boldsymbol{\xi}_k}$ while we have considered individual power constraints in the examples of the ZIFC-TIN.

The above comparison shows that we need to be careful with intuitive argumentations such as the following one. In each of the three systems considered above, there is a user that does not see any interference, so that it seems sensible to use a maximum-entropy signal for this user (in case of maximum-entropy noise). As this leads to maximum-entropy interference for the other users, we could continue the same reasoning successively to justify that all users should use maximum-entropy signals. However, the results for the ZIFC-TIN demonstrate that this is not a valid argumentation when our aim is to achieve a Pareto-optimal solution. In fact, this line of argumentation would instead fit in case of selfish behavior of the users (cf., e.g., [31, 188]).

This underlines how particular the structure of the residual interference in the MIMO MAC with SIC and in the MIMO BC with DPC is. The properties discussed in Chapters 5 and 6 including the optimality of maximum-entropy signals cannot be easily justified by an intuitive

argument as the one given above, but they are apparently directly linked to this special structure in combination with the possibility of performing RTS between different decoding orders or encoding orders, respectively. The latter is in line with Theorem 6.7.1, where we have observed that the optimality of maximum-entropy signals no longer holds, e.g., for DPC zero-forcing without (R)TS.

8.5.2 Systems with Mutual Interference

Another apparent similarity between rate equations belonging to different system models can be found when comparing the achievable rates of the RoP MIMO BC-TIN (7.1) and the K-user RoP MIMO IFC-TIN (8.2). Indeed, some similar effects have been observed in both settings, e.g., the fact that maximum-entropy transmission is not always optimal (see Theorems 7.4.1 and 8.2.1). Moreover, algorithms for transceiver design have been transferred from the MIMO BC-TIN to the K-user MIMO IFC-TIN (e.g., the weighted MSE formulation [180] applied to the IFC in [35, 193, 194]) and vice versa (e.g., the separate covariance and pseudocovariance optimization from [34, 190] applied to the BC-TIN in [34]). Note that the algorithmic considerations for the MIMO BC-TIN given in Section 7.6 carry over to interference channel scenarios as well. For instance, the approach of accounting for reduced-entropy transmission already in the initialization was adopted by [35].

Unlike in the discussion in Section 8.5.1, there is no need to consider decoding orders or encoding orders when comparing two systems with TIN strategies. However, there is again an important difference between the systems we compare due to the fact that the intended signals and the unintended signals travel over different channels in the IFC. As pointed out in [30], the key to interference alignment is the so-called relativity of alignment, meaning that a set of signals can align at one receiver while remaining distinct at another one. This is not possible if the intended signal and the interference travel over the same channel, so that interference alignment is not an option in the MIMO BC-TIN.

However, as it is known that linear transceivers with proper signals are able to achieve the maximum possible DoF of the MIMO BC [211, 212], there would anyway be nothing to gain in terms of DoF in the MIMO BC-TIN. This is another difference to the K-user MIMO IFC. The tremendous improvements of the high-SNR rates that reduced-entropy transmission can provide in the K-user MIMO IFC by obtaining a higher number of DoF are therefore not possible in the MIMO BC-TIN. Nevertheless, when considering achievable rate regions at finite SNR or in systems that do not allow for (R)TS, we have seen that reduced-entropy transmission can bring remarkable benefits in the MIMO BC-TIN as well.

From this point of view, the highest similarity between the MIMO IFC-TIN and the MIMO BC-TIN can be observed for the two-user IFC-TIN, where interference alignment is not an option either since the interference at each receiver comes from a single source (e.g., [213]). An example where reduced-entropy transmission in the MISO IFC-TIN and in the MISO BC-TIN are studied jointly in one publication is [34].

Despite all the differences between the MIMO communication systems with interference that we considered in Chapters 5 through 8, there is a fundamental insight that we can summarize. While maximum-entropy transmission is clearly the optimal choice in an interference-free system with maximum-entropy noise (Theorem 4.2.1), reduced-entropy transmission might bring benefits whenever we have interference in the system—apart from cases with a very

particular one-sided interference structure occurring in the MIMO MAC with SIC and in the MIMO BC with DPC, for which maximum-entropy transmission stays the optimal choice.

Chapter 9

The Gaussian MIMO Relay Channel with (Partial) Decode-and-Forward

By adding terminals that do not act as conventional transmitters or receivers, but instead as relays that forward information they have received [214], we can construct a large variety of further system models, where the information reaches its intended destination via multihop transmission. Of course, the question whether or not we should transmit maximum-entropy signals can be posed in such MIMO relaying networks as well. We study the simplest possible example, namely the MIMO relay channel (RC) [215], which consists of a source S, a destination D, and a relay R, whose only aim is to assist the data transmission from S to D (see Figure 9.1).

The capacity of relay networks in general and of the MIMO RC in particular is still an open problem (see, e.g., [216]) except for special cases, but several upper bounds and achievable schemes can be found in the literature. Important examples are the cut-set (upper) bound [215, 217–221] and the coding schemes amplify-and-forward [218, 222–225], compress-and-forward [217, 218, 220, 226], and decode-and-forward [215, 217–221], as well as combinations of these schemes [217].

In this chapter, we concentrate on the decode-and-forward (DF) scheme and on a generalization called partial decode-and-forward (PDF) [6, 216, 218, 227–232], [54, Sec. 9.4.1], [55, Sec. 16.6]. Further coding schemes are briefly discussed as an outlook in Section 9.6.

Even though we have a single-user system in the sense that data has to be transmitted only from a single source to a single destination, we have to deal with interference when studying relay networks with in-band relaying, i.e., if we assume that all transmissions take place in the same spectrum. For the MIMO RC, this applies especially in cases where the relay does not decode the received data or decodes it only partially. For the PDF scheme considered in this chapter, it turns out that the interference has a very particular structure, which entails that maximum-entropy signals are optimal under the assumption of maximum-entropy noise (Section 9.2). However, for other coding schemes or under modified system assumptions, the results can be quite different (see Section 9.6).

We first study (P)DF in the RoP MIMO RC and extend our results to the complex multicarrier MIMO RC afterwards. We present results on the optimality of maximum-entropy transmission

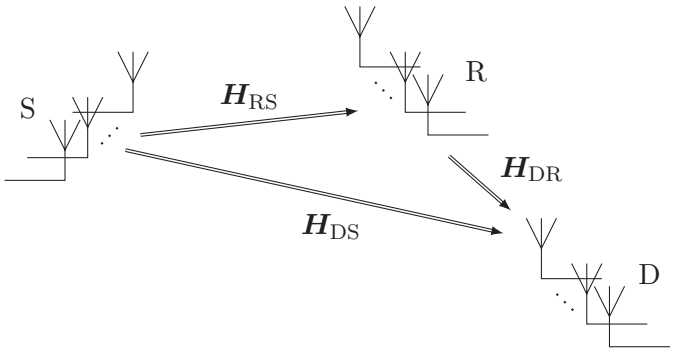

Figure 9.1: Illustration of the MIMO relay channel.

as well as a worst-case noise theorem, and we comment on methods to compute the optimal input covariance matrices. There are several new aspects that have to be taken into account due to the multihop transmission. In particular, we have to find ways to treat correlations between transmit signals at different nodes (see Section 9.5.1), and we have to be careful with the exact meaning of the terms CC transmission and coding across carriers (see Section 9.5.2).

9.1 System Model and Coding Scheme

We consider a system with a source node S, a destination D, and a relay R. The relay operates in full-duplex mode with perfect self-interference cancellation, i.e., it can transmit and receive at the same time without being disturbed by its own transmit signal. From the general model in (3.1), we obtain the description of the RoP MIMO RC as

$$\boldsymbol{y}_{\mathrm{R}} = \boldsymbol{H}_{\mathrm{RS}}\boldsymbol{x}_{\mathrm{S}} + \boldsymbol{\eta}_{\mathrm{R}} \tag{9.1}$$

$$\boldsymbol{y}_{\mathrm{D}} = \boldsymbol{H}_{\mathrm{DS}}\boldsymbol{x}_{\mathrm{S}} + \boldsymbol{H}_{\mathrm{DR}}\boldsymbol{x}_{\mathrm{R}} + \boldsymbol{\eta}_{\mathrm{D}}. \tag{9.2}$$

Even though we have multiple terminals, there is only one data rate of interest since the only purpose of the relay is to assist the transmission from the source to the destination. The aim is to find achievable values of this rate under a general covariance constraint

$$(\boldsymbol{C}_{\boldsymbol{x}_{\mathrm{S}}}, \boldsymbol{C}_{\boldsymbol{x}_{\mathrm{R}}}) \in \mathcal{Q} \tag{9.3}$$

where $\mathcal{Q}$ is as in (3.3).

In the decode-and-forward protocol, the relay is required to decode all new information that is transmitted by the source, in order to then retransmit it jointly with the source in a coherent manner. The resulting achievable DF rate is [215, 217]

$$r_{\mathrm{DF}} = \min\{\mathrm{I}\left(\boldsymbol{x}_{\mathrm{S}}; \boldsymbol{y}_{\mathrm{R}} \,|\, \boldsymbol{x}_{\mathrm{R}}\right),\ \mathrm{I}\left((\boldsymbol{x}_{\mathrm{S}}, \boldsymbol{x}_{\mathrm{R}}); \boldsymbol{y}_{\mathrm{D}}\right)\}. \tag{9.4}$$

The first mutual information expression represents the transmission from the source to the relay, while the second one describes the coherent transmission from the source and the relay to the destination.

The DF protocol can be capacity-achieving in case of a strong source-relay channel [218]. However, as the relay has to decode the whole information transmitted by the source, a weak

source-relay link can become a bottleneck in this protocol [218], [54, Sec. 9.2.1]. It can thus make sense to introduce a message portion that is not decoded by the relay, i.e., that is transmitted directly from the source to the destination without any help of the relay. Even though this signal then acts as interference at the relay, the resulting partial decode-and-forward (PDF) protocol [6, 218, 227–230, 232], [54, Sec. 9.4.1], [55, Sec. 16.6] can significantly improve the data rate compared to DF. The PDF scheme has recently been shown to perform close to the (generally unknown) capacity of the MIMO RC [216], and it is capacity-achieving in some special cases in which the capacity is known [231].

The achievable rate of this protocol is given by [54, Sec. 9.4.1], [55, Sec. 16.6]

$$r_{\mathrm{PDF}} = \min\{\underbrace{\mathrm{I}\left(\boldsymbol{u};\boldsymbol{y}_{\mathrm{R}} \,|\, \boldsymbol{x}_{\mathrm{R}}\right) + \mathrm{I}\left(\boldsymbol{x}_{\mathrm{S}};\boldsymbol{y}_{\mathrm{D}} \,|\, (\boldsymbol{u},\boldsymbol{x}_{\mathrm{R}})\right)}_{r_{\mathrm{A}}}, \underbrace{\mathrm{I}\left((\boldsymbol{x}_{\mathrm{S}},\boldsymbol{x}_{\mathrm{R}});\boldsymbol{y}_{\mathrm{D}}\right)}_{r_{\mathrm{B}}}\} \tag{9.5}$$

where it must hold that $\boldsymbol{u} - (\boldsymbol{x}_{\mathrm{S}}, \boldsymbol{x}_{\mathrm{R}}) - (\boldsymbol{y}_{\mathrm{R}}, \boldsymbol{y}_{\mathrm{D}})$ is a Markov chain. The auxiliary random variable $\boldsymbol{u}$ represents the part of the source signal that is intended for coherent transmission, i.e., the part that is decoded by the relay. While the second mutual information expression is the same as in (9.4), the first one is now a sum of a term describing the transmission from the source to the relay and a term describing the direct transmission to the destination.

The DF rate is maximized by jointly Gaussian input signals [215], and the same has recently been shown for the PDF rate [232]. The proofs can be transferred to real-valued settings, but for the sake of brevity, we do not reproduce them here. These properties were shown under individual power constraints (3.5), but an extension to general covariance constraints does not pose any problems [232, Footnote 1]. For a complex setting, note that Remark 4.1.1 applies accordingly to the current chapter.

9.2 Optimality of Maximum-Entropy Transmission

In this section, we study the properties of the optimal input signals for DF and for PDF under the assumption of maximum-entropy noise. The result is stated in the following theorem. Parts of the proof are similar to derivations in [6, 22], but we consider a more general formulation here.

Theorem 9.2.1. *Let $\mathcal{P}_{\mathrm{S}}$, $\mathcal{P}_{\mathrm{R}}$, and $\mathcal{P}_{\mathrm{D}}$ be power shaping spaces fulfilling the compatibility assumption (Definition 3.1.3), and let $\mathcal{P} \subseteq \mathbb{H}^{M_{\mathrm{S}}+M_{\mathrm{R}}}$ (with $\mathbb{S}$ instead of $\mathbb{H}$ in case of a real-valued system) be a power shaping space such that*

- $\begin{bmatrix}\boldsymbol{H}_{\mathrm{DS}} & \boldsymbol{H}_{\mathrm{DR}}\end{bmatrix}$ *is compatible with* $(\mathcal{P}_{\mathrm{D}}, \mathcal{P})$,
- $\begin{bmatrix}\mathbf{I}_{M_{\mathrm{S}}} & \mathbf{0}\end{bmatrix}$ *is compatible with* $(\mathcal{P}_{\mathrm{S}}, \mathcal{P})$, *and*
- $\begin{bmatrix}\mathbf{0} & \mathbf{I}_{M_{\mathrm{R}}}\end{bmatrix}$ *is compatible with* $(\mathcal{P}_{\mathrm{R}}, \mathcal{P})$.

If the noise vectors $\boldsymbol{\eta}_{\mathrm{R}}$ and $\boldsymbol{\eta}_{\mathrm{D}}$ are maximum-entropy signals with respect to $\mathcal{P}_{\mathrm{R}}$ and $\mathcal{P}_{\mathrm{D}}$, respectively, the DF rate r_{DF} and the PDF rate r_{PDF} are maximized by strategies where $[\boldsymbol{x}_{\mathrm{S}}^{\mathrm{T}} \;\; \boldsymbol{x}_{\mathrm{R}}^{\mathrm{T}}]^{\mathrm{T}}$ is a maximum-entropy signal with respect to $\mathcal{P}$, $\boldsymbol{x}_{\mathrm{S}}$ conditioned on $\boldsymbol{x}_{\mathrm{R}}$ is a maximum-entropy signal with respect to $\mathcal{P}_{\mathrm{S}}$, and, in case of PDF, $[\boldsymbol{u}^{\mathrm{T}} \;\; \boldsymbol{x}_{\mathrm{R}}^{\mathrm{T}}]^{\mathrm{T}}$ is a maximum-entropy signal with respect to $\mathcal{P}$.

Proof. The PDF rate can be achieved by superposition coding (e.g., [227], [54, Sec. 9.4.1]), i.e., a source signal $\boldsymbol{x}_{\mathrm{S}} = \boldsymbol{u} + \boldsymbol{v}$ is created from $\boldsymbol{u}$ and from a signal $\boldsymbol{v}$ that is intended for direct transmission (see [228]). While $\boldsymbol{v}$ and $\boldsymbol{u}$ as well as $\boldsymbol{v}$ and $\boldsymbol{x}_{\mathrm{R}}$ are statistically independent, this is in general not true for $\boldsymbol{u}$ and $\boldsymbol{x}_{\mathrm{R}}$. Let us decompose $\boldsymbol{x}_{\mathrm{S}}$ further as

$$\boldsymbol{x}_{\mathrm{S}} = \boldsymbol{v} + \boldsymbol{u} = \boldsymbol{v} + \boldsymbol{w} + \boldsymbol{z} \quad \text{with} \quad \boldsymbol{z} = \boldsymbol{A}\boldsymbol{x}_{\mathrm{R}} \tag{9.6}$$

where $\boldsymbol{A}$ is chosen such that it completely captures the correlations between $\boldsymbol{u}$ and $\boldsymbol{x}_{\mathrm{R}}$, i.e., we can assume $\boldsymbol{w}$ and $\boldsymbol{x}_{\mathrm{R}}$ to be uncorrelated. Since all signals are (real-valued or proper) Gaussian, this implies that $\boldsymbol{w}$ and $\boldsymbol{x}_{\mathrm{R}}$ are independent.[1]

Similar as in [6, 22, 114], we can write the optimization of the PDF rate by means of an auxiliary variable $\boldsymbol{P}_{\boldsymbol{v}+\boldsymbol{w}}$ as

$$\begin{aligned} \max_{\boldsymbol{P}_{\boldsymbol{v}+\boldsymbol{w}} \succeq \boldsymbol{0}} \; \max_{\boldsymbol{C}_{\boldsymbol{v}} \succeq \boldsymbol{0}, \boldsymbol{C}_{\boldsymbol{w}} \succeq \boldsymbol{0}, \boldsymbol{R} \succeq \boldsymbol{0}} \; & \min\{r_{\mathrm{A}},\, r_{\mathrm{B}}\} \\ \text{s.t.} \quad & \operatorname{proj}_{\mathcal{P}_{\mathrm{S}}}(\boldsymbol{C}_{\boldsymbol{v}}) + \operatorname{proj}_{\mathcal{P}_{\mathrm{S}}}(\boldsymbol{C}_{\boldsymbol{w}}) = \boldsymbol{P}_{\boldsymbol{v}+\boldsymbol{w}} \\ & (\boldsymbol{P}_{\boldsymbol{v}+\boldsymbol{w}} + \boldsymbol{P}_{\boldsymbol{z}}, \boldsymbol{P}_{\boldsymbol{x}_{\mathrm{R}}}) \in \mathcal{Q} \cap (\mathcal{P}_{\mathrm{S}} \times \mathcal{P}_{\mathrm{R}}) \end{aligned} \tag{9.7}$$

with r_{A} and r_{B} from (9.5). We have exploited that the covariance constraint is compatible with $\mathcal{P}_{\mathrm{S}} \times \mathcal{P}_{\mathrm{R}}$, and we have used the abbreviations $\boldsymbol{R} = \boldsymbol{C}_{\left[\begin{smallmatrix}\boldsymbol{z}\\ \boldsymbol{x}_{\mathrm{R}}\end{smallmatrix}\right]}$ and

$$\boldsymbol{P}_{\boldsymbol{z}} = \operatorname{proj}_{\mathcal{P}_{\mathrm{S}}}(\boldsymbol{C}_{\boldsymbol{z}}) = \operatorname{proj}_{\mathcal{P}_{\mathrm{S}}}([\mathbf{I}_{M_{\mathrm{S}}} \;\; \boldsymbol{0}]\boldsymbol{R}\,[\mathbf{I}_{M_{\mathrm{S}}} \;\; \boldsymbol{0}]^{\mathrm{T}}) = [\mathbf{I}_{M_{\mathrm{S}}} \;\; \boldsymbol{0}]\operatorname{proj}_{\mathcal{P}}(\boldsymbol{R})[\mathbf{I}_{M_{\mathrm{S}}} \;\; \boldsymbol{0}]^{\mathrm{T}}, \tag{9.8}$$

$$\boldsymbol{P}_{\boldsymbol{x}_{\mathrm{R}}} = \operatorname{proj}_{\mathcal{P}_{\mathrm{R}}}(\boldsymbol{C}_{\boldsymbol{x}_{\mathrm{R}}}) = \operatorname{proj}_{\mathcal{P}_{\mathrm{R}}}([\boldsymbol{0} \;\; \mathbf{I}_{M_{\mathrm{R}}}]\boldsymbol{R}\,[\boldsymbol{0} \;\; \mathbf{I}_{M_{\mathrm{R}}}]^{\mathrm{T}}) = [\boldsymbol{0} \;\; \mathbf{I}_{M_{\mathrm{R}}}]\operatorname{proj}_{\mathcal{P}}(\boldsymbol{R})[\boldsymbol{0} \;\; \mathbf{I}_{M_{\mathrm{R}}}]^{\mathrm{T}}. \tag{9.9}$$

The multiplications and the projections can be swapped since the matrices are compatible with the respective power shaping spaces by assumption. To ensure that $\boldsymbol{z}$ can be expressed as $\boldsymbol{A}\boldsymbol{x}_{\mathrm{R}}$, we would need an additional structural constraint on the joint covariance matrix $\boldsymbol{R}$ of $\boldsymbol{z}$ and $\boldsymbol{x}_{\mathrm{R}}$. However, since redistributing power from $\boldsymbol{z}$ to $\boldsymbol{w}$ improves r_{A} without reducing r_{B}, this constraint is automatically fulfilled in the optimum and can thus be neglected (see [114]). As in [6, 22], we now fix $\boldsymbol{P}_{\boldsymbol{v}+\boldsymbol{w}}$ to an arbitrary value and derive a strategy that simultaneously maximizes r_{A} and r_{B}.

By exploiting that $\boldsymbol{v}$ and $\boldsymbol{w}$ are independent of $\boldsymbol{x}_{\mathrm{R}}$, we rewrite r_{A} as

$$\begin{aligned} r_{\mathrm{A}} &= \mathrm{h}\left(\boldsymbol{y}_{\mathrm{R}} \,|\, \boldsymbol{x}_{\mathrm{R}}\right) - \mathrm{h}\left(\boldsymbol{y}_{\mathrm{R}} \,|\, (\boldsymbol{x}_{\mathrm{R}}, \boldsymbol{u})\right) + \mathrm{h}\left(\boldsymbol{y}_{\mathrm{D}} \,|\, (\boldsymbol{u}, \boldsymbol{x}_{\mathrm{R}})\right) - \mathrm{h}\left(\boldsymbol{y}_{\mathrm{D}} \,|\, (\boldsymbol{u}, \boldsymbol{x}_{\mathrm{R}}, \boldsymbol{x}_{\mathrm{S}})\right) \\ &= \mathrm{h}\left(\boldsymbol{H}_{\mathrm{RS}}(\boldsymbol{v} + \boldsymbol{w}) + \boldsymbol{\eta}_{\mathrm{R}}\right) - \mathrm{h}\left(\boldsymbol{H}_{\mathrm{RS}}\boldsymbol{v} + \boldsymbol{\eta}_{\mathrm{R}}\right) + \mathrm{h}\left(\boldsymbol{H}_{\mathrm{DS}}\boldsymbol{v} + \boldsymbol{\eta}_{\mathrm{D}}\right) - \mathrm{h}\left(\boldsymbol{\eta}_{\mathrm{D}}\right) \\ &= \log_2 \frac{\det\left(\boldsymbol{C}_{\boldsymbol{\eta}_{\mathrm{R}}} + \boldsymbol{H}_{\mathrm{RS}}(\boldsymbol{C}_{\boldsymbol{v}} + \boldsymbol{C}_{\boldsymbol{w}})\boldsymbol{H}_{\mathrm{RS}}^{\mathrm{H}}\right)}{\det\left(\boldsymbol{C}_{\boldsymbol{\eta}_{\mathrm{R}}} + \boldsymbol{H}_{\mathrm{RS}}\boldsymbol{C}_{\boldsymbol{v}}\boldsymbol{H}_{\mathrm{RS}}^{\mathrm{H}}\right)} + \log_2 \frac{\det\left(\boldsymbol{C}_{\boldsymbol{\eta}_{\mathrm{D}}} + \boldsymbol{H}_{\mathrm{DS}}\boldsymbol{C}_{\boldsymbol{v}}\boldsymbol{H}_{\mathrm{DS}}^{\mathrm{H}}\right)}{\det \boldsymbol{C}_{\boldsymbol{\eta}_{\mathrm{D}}}} \end{aligned} \tag{9.10}$$

Therefore, the optimization of r_{A} while ignoring r_{B} only depends on the covariance matrices $\boldsymbol{C}_{\boldsymbol{v}}$ and $\boldsymbol{C}_{\boldsymbol{w}}$, i.e.,

$$\max_{\boldsymbol{C}_{\boldsymbol{v}} \succeq \boldsymbol{0}, \boldsymbol{C}_{\boldsymbol{w}} \succeq \boldsymbol{0}} \; r_{\mathrm{A}} \quad \text{s.t.} \quad \operatorname{proj}_{\mathcal{P}_{\mathrm{S}}}(\boldsymbol{C}_{\boldsymbol{v}}) + \operatorname{proj}_{\mathcal{P}_{\mathrm{S}}}(\boldsymbol{C}_{\boldsymbol{w}}) = \boldsymbol{P}_{\boldsymbol{v}+\boldsymbol{w}} \tag{9.11}$$

[1] This decomposition is similar to the one in [6, 22, 114, 232], but we do not assume any particular structure of $\boldsymbol{A}$. Therefore, we can directly assume $\boldsymbol{w}$ and $\boldsymbol{x}_{\mathrm{R}}$ to be independent, which is different from [6, 22]. An illustration of the three signal portions is given later on in Figure 9.2 and is discussed in Section 9.5.2.

where we have dropped the second constraint of (9.7), which does not restrict $\boldsymbol{C}_{\boldsymbol{v}}$ nor $\boldsymbol{C}_{\boldsymbol{w}}$. As observed in [6], the expression in (9.10) is mathematically equivalent to the sum rate $r_1 + r_2$ in a two-user RoP MIMO BC with DPC, see (6.2). In particular, we have $\mathcal{P}_{\mathrm{B}} = \mathcal{P}_{\mathrm{S}}$, $\mathcal{P}_1 = \mathcal{P}_{\mathrm{R}}$, $\mathcal{P}_2 = \mathcal{P}_{\mathrm{D}}$, $\boldsymbol{\xi}_1 = \boldsymbol{w}$, $\boldsymbol{\xi}_2 = \boldsymbol{v}$, $\boldsymbol{\eta}_1 = \boldsymbol{\eta}_{\mathrm{R}}$, $\boldsymbol{\eta}_2 = \boldsymbol{\eta}_{\mathrm{D}}$, $\boldsymbol{H}_1^{\mathrm{H}} = \boldsymbol{H}_{\mathrm{RS}}$, and $\boldsymbol{H}_2^{\mathrm{H}} = \boldsymbol{H}_{\mathrm{DS}}$. The rate expression in (9.10) corresponds to a fixed DPC encoding order in the equivalent MIMO BC (similar as discussed for the comparison with the MIMO ZIFC-TIN in Section 8.5.1). However, this does not pose any problems since we are only interested in the sum rate, which can be achieved using any encoding order.[2] It thus follows from Theorem 6.3.1 that using $\boldsymbol{C}_{\boldsymbol{v}} \in \mathcal{P}_{\mathrm{S}}$ and $\boldsymbol{C}_{\boldsymbol{w}} \in \mathcal{P}_{\mathrm{S}}$ is optimal in (9.11), i.e., we have

$$\boldsymbol{C}_{\boldsymbol{v}} + \boldsymbol{C}_{\boldsymbol{w}} = \mathrm{proj}_{\mathcal{P}_{\mathrm{S}}}(\boldsymbol{C}_{\boldsymbol{v}}) + \mathrm{proj}_{\mathcal{P}_{\mathrm{S}}}(\boldsymbol{C}_{\boldsymbol{w}}) = \boldsymbol{P}_{\boldsymbol{v}+\boldsymbol{w}}. \tag{9.12}$$

The second rate r_{B} is given by

$$\begin{aligned} r_{\mathrm{B}} &= \mathrm{h}\left(\boldsymbol{y}_{\mathrm{D}}\right) - \mathrm{h}\left(\boldsymbol{y}_{\mathrm{D}} \,|\, (\boldsymbol{x}_{\mathrm{S}}, \boldsymbol{x}_{\mathrm{R}})\right) \\ &= \mathrm{h}\left(\boldsymbol{H}_{\mathrm{DS}}(\boldsymbol{v}+\boldsymbol{w}) + \begin{bmatrix} \boldsymbol{H}_{\mathrm{DS}} & \boldsymbol{H}_{\mathrm{DR}} \end{bmatrix} \begin{bmatrix} \boldsymbol{z} \\ \boldsymbol{x}_{\mathrm{R}} \end{bmatrix} + \boldsymbol{\eta}_{\mathrm{D}}\right) - \mathrm{h}\left(\boldsymbol{\eta}_{\mathrm{D}}\right). \end{aligned} \tag{9.13}$$

By introducing the auxiliary covariance matrix $\boldsymbol{C}_{\boldsymbol{v}+\boldsymbol{w}} = \boldsymbol{C}_{\boldsymbol{v}} + \boldsymbol{C}_{\boldsymbol{w}}$, the optimization of r_{B} while ignoring r_{A} can be written as

$$\begin{aligned} \max_{\boldsymbol{C}_{\boldsymbol{v}+\boldsymbol{w}} \succeq \boldsymbol{0}, \boldsymbol{R} \succeq \boldsymbol{0}} \; & r_{\mathrm{B}} \quad \text{s.t.} \quad \mathrm{proj}_{\mathcal{P}_{\mathrm{S}}}(\boldsymbol{C}_{\boldsymbol{v}+\boldsymbol{w}}) = \boldsymbol{P}_{\boldsymbol{v}+\boldsymbol{w}} \\ & \qquad\qquad (\boldsymbol{P}_{\boldsymbol{v}+\boldsymbol{w}} + \boldsymbol{P}_{\boldsymbol{z}}, \boldsymbol{P}_{\boldsymbol{x}_{\mathrm{R}}}) \in \mathcal{Q} \cap (\mathcal{P}_{\mathrm{S}} \times \mathcal{P}_{\mathrm{R}}) \end{aligned} \tag{9.14}$$

with the abbreviations $\boldsymbol{R}$, $\boldsymbol{P}_{\boldsymbol{z}}$, and $\boldsymbol{P}_{\boldsymbol{x}_{\mathrm{R}}}$ as in (9.7). This is mathematically equivalent to the maximization of the sum rate $r_1 + r_2$ in a two-user RoP MIMO MAC, see (5.2), where $\mathcal{P}_{\mathrm{B}} = \mathcal{P}_{\mathrm{D}}$, $\mathcal{P}_1 = \mathcal{P}_{\mathrm{S}}$, $\mathcal{P}_2 = \mathcal{P}$, $\boldsymbol{x}_1 = \boldsymbol{v} + \boldsymbol{w}$, $\boldsymbol{x}_2 = \begin{bmatrix} \boldsymbol{z}^{\mathrm{T}} & \boldsymbol{x}_{\mathrm{R}}^{\mathrm{T}} \end{bmatrix}^{\mathrm{T}}$, $\boldsymbol{\eta} = \boldsymbol{\eta}_{\mathrm{D}}$, $\boldsymbol{H}_1 = \boldsymbol{H}_{\mathrm{DS}}$, and $\boldsymbol{H}_2 = \begin{bmatrix} \boldsymbol{H}_{\mathrm{DS}} & \boldsymbol{H}_{\mathrm{DR}} \end{bmatrix}$. Moreover, as can be seen in combination with (9.8) and (9.9), the constraints act only on the power shaping components of $\boldsymbol{C}_{\boldsymbol{v}+\boldsymbol{w}}$ and $\boldsymbol{R}$. It thus follows from Theorem 5.2.1 that choosing $\boldsymbol{C}_{\boldsymbol{v}+\boldsymbol{w}} \in \mathcal{P}_{\mathrm{S}}$ and $\boldsymbol{R} \in \mathcal{P}$ is optimal in (9.14), i.e., we have

$$\boldsymbol{C}_{\boldsymbol{v}} + \boldsymbol{C}_{\boldsymbol{w}} = \boldsymbol{C}_{\boldsymbol{v}+\boldsymbol{w}} = \mathrm{proj}_{\mathcal{P}_{\mathrm{S}}}(\boldsymbol{C}_{\boldsymbol{v}+\boldsymbol{w}}) = \boldsymbol{P}_{\boldsymbol{v}+\boldsymbol{w}}. \tag{9.15}$$

Note that this solution is in compliance with (9.12). Moreover, (9.11) does not depend on the value of $\boldsymbol{R}$, and for (9.14), it does not matter how $\boldsymbol{C}_{\boldsymbol{v}+\boldsymbol{w}}$ is split into $\boldsymbol{C}_{\boldsymbol{v}}$ and $\boldsymbol{C}_{\boldsymbol{w}}$. Thus, we can combine the solutions of (9.11) and (9.14) in order to obtain a maximizer of the inner optimization in (9.7). Since the derivation holds for any given $\boldsymbol{P}_{\boldsymbol{v}+\boldsymbol{w}}$ for which the constraint set of the inner problem is nonempty, it also holds for the optimal $\boldsymbol{P}_{\boldsymbol{v}+\boldsymbol{w}}$.

Using Proposition 2.7.1, we have $\boldsymbol{C}_{\left[\begin{smallmatrix} \boldsymbol{x}_{\mathrm{S}} \\ \boldsymbol{x}_{\mathrm{R}} \end{smallmatrix}\right]} = [\mathbf{I}_{M_{\mathrm{S}}} \;\; \boldsymbol{0}]^{\mathrm{T}} \boldsymbol{C}_{\boldsymbol{v}+\boldsymbol{w}} [\mathbf{I}_{M_{\mathrm{S}}} \;\; \boldsymbol{0}] + \boldsymbol{R} \in \mathcal{P}$ and $\boldsymbol{C}_{\left[\begin{smallmatrix} \boldsymbol{u} \\ \boldsymbol{x}_{\mathrm{R}} \end{smallmatrix}\right]} = [\mathbf{I}_{M_{\mathrm{S}}} \;\; \boldsymbol{0}]^{\mathrm{T}} \boldsymbol{C}_{\boldsymbol{w}} [\mathbf{I}_{M_{\mathrm{S}}} \;\; \boldsymbol{0}] + \boldsymbol{R} \in \mathcal{P}$. The conditional covariance matrix of $\boldsymbol{x}_{\mathrm{S}}$ conditioned on $\boldsymbol{x}_{\mathrm{R}}$ is given by $\boldsymbol{C}_{\boldsymbol{v}+\boldsymbol{w}} \in \mathcal{P}_{\mathrm{S}}$. This concludes the proof for the PDF rate.

To optimize the DF rate, we can introduce the additional constraint $\boldsymbol{C}_{\boldsymbol{v}} = \boldsymbol{0}$, which is equivalent to $\mathrm{proj}_{\mathcal{P}_{\mathrm{S}}}(\boldsymbol{C}_{\boldsymbol{v}}) = \boldsymbol{0}$ due to Proposition 2.5.1. This additional constraint has no influence on (9.14). Problem (9.11) with the added constraint $\mathrm{proj}_{\mathcal{P}_{\mathrm{S}}}(\boldsymbol{C}_{\boldsymbol{v}}) = \boldsymbol{0}$ still complies to the assumptions of Theorem 6.3.1, i.e., the argumentation used above is still valid. □

[2] To see that this is true, note that the weighted sum rate maximization in the MIMO MAC (Section 5.3) can be performed with an arbitrary decoding order if all weights are equal. This translates to the MIMO BC via the duality in Lemma 6.2.1.

9.3 Optimal Transmit Covariance Matrices

For the special case of DF, it was shown in [220, 221] that the rate maximization can be rewritten as a convex optimization. However, such a reformulation has not yet been found for the PDF protocol.

An approach that comes quite close to this aim is the method from [114], which restricts the matrix $\boldsymbol{P}_{\boldsymbol{v}+\boldsymbol{w}}$ introduced in (9.7) to be strictly positive-definite instead of being positive-semidefinite. The optimization with this modified constraint set can then be reformulated as a convex program, and it was conjectured in [114] that the modification introduces only a small deviation from the globally optimal solution. The method uses a similar formulation as in (9.7), and it applies an algorithm developed for the MIMO BC in [120] to solve the subproblem (9.11). Other algorithmic approaches to optimize the PDF rate are either based on local methods, e.g., the inner approximation algorithm from [230], or on heuristics such as introducing zero-forcing constraints [229].

Also note that the algorithms mentioned above have been derived for power constraints (3.5), but not for general covariance constraints. In summary, it can be said that the optimization of the PDF rate is a field of ongoing research. We therefore refrain from a more detailed analysis of algorithmic aspects, which would go beyond the scope of this work.

It shall only be noted that similar arguments and methods as in Sections 5.3.1, 6.4, and 7.6 could be used to study the behavior of the abovementioned algorithms. It is to be expected that these algorithms converge to solutions with maximum-entropy signals if the assumptions of Theorem 9.2.1 are fulfilled and an initialization corresponding to maximum-entropy transmission is used. The reason for stating the latter condition is that the solution of local methods for nonconvex problems can depend on the initialization (see, e.g., Section 7.6.1).

Unlike in the MIMO BC with TIN strategies considered in Section 7.6, obtaining a solution that corresponds to maximum-entropy transmission is now a desirable property due to Theorem 9.2.1. Thus, using a maximum-entropy initialization (cf. Section 7.6.2) is a reasonable choice.

On the other hand, if the assumptions of Theorem 9.2.1 are violated, e.g., due to reduced-entropy noise, the arguments from Sections 5.3.1, 6.4, and 7.6 do not apply. In this case, we expect the outcomes of the abovementioned algorithms to correspond to reduced-entropy transmission.

9.4 Worst-Case Noise

Due to the reformulation of the two mutual information expressions r_{A} and r_{B} in the (P)DF rate as the sum rates of the MIMO BC and MIMO MAC, respectively, we can use the previously derived worst-case noise theorems for the MIMO BC (Theorem 6.5.1) and the MIMO MAC (Theorem 5.4.1), to prove a worst-case noise theorem for (P)DF in the MIMO RC.

Theorem 9.4.1. *Let $\mathcal{P}_{\mathrm{S}}$, $\mathcal{P}_{\mathrm{R}}$, $\mathcal{P}_{\mathrm{D}}$, and $\mathcal{P}$ be as in Theorem 9.2.1, and let the constraint $(\boldsymbol{C}_{\boldsymbol{\eta}_{\mathrm{R}}}, \boldsymbol{C}_{\boldsymbol{\eta}_{\mathrm{D}}}) \in \mathcal{Q}_{\mathrm{noise}}$ be compatible with $\mathcal{P}_{\mathrm{R}} \times \mathcal{P}_{\mathrm{D}}$ (in the sense of Definition 3.1.2). If $[\boldsymbol{x}_{\mathrm{S}}^{\mathrm{T}} \ \boldsymbol{x}_{\mathrm{R}}^{\mathrm{T}}]^{\mathrm{T}}$ is a maximum-entropy signal with respect to $\mathcal{P}$, $\boldsymbol{x}_{\mathrm{S}}$ conditioned on $\boldsymbol{x}_{\mathrm{R}}$ is a maximum-entropy signal with respect to $\mathcal{P}_{\mathrm{S}}$, and, in case of PDF, $[\boldsymbol{u}^{\mathrm{T}} \ \boldsymbol{x}_{\mathrm{R}}^{\mathrm{T}}]^{\mathrm{T}}$ is a maximum-entropy signal*

with respect to $\mathcal{P}$, maximum-entropy noise vectors $\boldsymbol{\eta}_{\mathrm{R}}$ and $\boldsymbol{\eta}_{\mathrm{D}}$ with respect to $\mathcal{P}_{\mathrm{R}}$ and $\mathcal{P}_{\mathrm{D}}$, respectively, minimize the (P)DF rate.

Proof. For any given $\boldsymbol{P}_{\boldsymbol{\eta}_{\mathrm{R}}} = \mathrm{proj}_{\mathcal{P}_{\mathrm{R}}}(\boldsymbol{C}_{\boldsymbol{\eta}_{\mathrm{R}}})$ and given $\boldsymbol{P}_{\boldsymbol{\eta}_{\mathrm{D}}} = \mathrm{proj}_{\mathcal{P}_{\mathrm{D}}}(\boldsymbol{C}_{\boldsymbol{\eta}_{\mathrm{D}}})$, the rate r_{A} in (9.10) and r_{B} in (9.13) are simultaneously minimized by maximum-entropy noise due to Theorem 6.5.1 and Theorem 5.4.1, respectively. □

As we have previously shown maximum-entropy transmission to be optimal for (P)DF in the MIMO RC with maximum-entropy noise, the following extension is possible.

Corollary 9.4.1. *Let $\mathcal{P}_{\mathrm{S}}$, $\mathcal{P}_{\mathrm{R}}$, $\mathcal{P}_{\mathrm{D}}$, $\mathcal{P}$, and $\mathcal{Q}_{\mathrm{noise}}$ be as in Theorem 9.4.1, but assume that the input signals are optimized (for given $\boldsymbol{C}_{\boldsymbol{\eta}_{\mathrm{R}}}$ and $\boldsymbol{C}_{\boldsymbol{\eta}_{\mathrm{D}}}$) under a constraint $(\boldsymbol{C}_{\boldsymbol{x}_{\mathrm{S}}}, \boldsymbol{C}_{\boldsymbol{x}_{\mathrm{R}}}) \in \mathcal{Q}$ that is compatible with $\mathcal{P}_{\mathrm{S}} \times \mathcal{P}_{\mathrm{R}}$. Then, maximum-entropy noise vectors $\boldsymbol{\eta}_{\mathrm{R}}$ and $\boldsymbol{\eta}_{\mathrm{D}}$ with respect to $\mathcal{P}_{\mathrm{R}}$ and $\mathcal{P}_{\mathrm{D}}$, respectively, minimize the (P)DF rate.*

Proof. This is a consequence of Theorem 9.2.1 combined with Theorem 9.4.1 following the same line of argumentation as Corollary 4.4.1. □

9.5 Complex Multicarrier MIMO RC

From the general model (3.34), we obtain the description of the complex multicarrier MIMO RC

$$\boldsymbol{y}_{\mathrm{R}}^{(c)} = \boldsymbol{H}_{\mathrm{RS}}^{(c)} \boldsymbol{x}_{\mathrm{S}}^{(c)} + \boldsymbol{\eta}_{\mathrm{R}}^{(c)}, \qquad c = 1, \ldots, C \tag{9.16}$$

$$\boldsymbol{y}_{\mathrm{D}}^{(c)} = \boldsymbol{H}_{\mathrm{DS}}^{(c)} \boldsymbol{x}_{\mathrm{S}}^{(c)} + \boldsymbol{H}_{\mathrm{DR}}^{(c)} \boldsymbol{x}_{\mathrm{R}}^{(c)} + \boldsymbol{\eta}_{\mathrm{D}}^{(c)}, \qquad c = 1, \ldots, C \tag{9.17}$$

with a covariance constraint

$$\left(\left(\boldsymbol{C}_{\boldsymbol{x}_{\mathrm{S}}^{(c)}} \right)_{\forall c}, \left(\boldsymbol{C}_{\boldsymbol{x}_{\mathrm{R}}^{(c)}} \right)_{\forall c} \right) \in \bar{\mathcal{Q}} \tag{9.18}$$

where $\bar{\mathcal{Q}}$ is as in (3.38). Using the combined real representation (3.37), we obtain the RoP MIMO RC (9.1)–(9.2) with $\boldsymbol{H}_{\mathrm{RS}} = \grave{\boldsymbol{H}}_{\mathrm{RS}}$, $\boldsymbol{H}_{\mathrm{DS}} = \grave{\boldsymbol{H}}_{\mathrm{DS}}$, and $\boldsymbol{H}_{\mathrm{DR}} = \grave{\boldsymbol{H}}_{\mathrm{DR}}$.

9.5.1 Optimality of Maximum-Entropy Transmission

For the case of power constraints (3.5) and proper Gaussian noise, several results on optimal input distributions for (P)DF can be found in the literature. According to [215], proper Gaussian signals maximize the DF rate in this case. For PDF under power constraints, it was shown in [6] that proper Gaussian signals are optimal among all Gaussian signals. An extension of this statement was later obtained in [232], where the optimality of proper Gaussian signals among all possible input distributions was shown. Assuming proper Gaussian signals and noise in a multicarrier setting, CN transmission was shown to be optimal for PDF under power constraints in case of CN noise in [22]. The corollaries of Theorem 9.2.1 presented in this section extend these results to more general covariance constraints.

Unlike in, e.g., the MIMO MAC, the transmit signals of the source and of the relay are correlated in the MIMO RC. Therefore, it is relevant to show that the optimal input signals are not only proper and/or CN, but even jointly proper/CN. The term *jointly proper* was introduced in Definition 2.9.3, and we define the term *jointly CN* as follows.

Definition 9.5.1. *We call the signals $\boldsymbol{x}_n,\ n \in \{1,\dots,N\}$ consisting of the per-carrier signals $\boldsymbol{x}_n^{(c)}$* jointly CN *if the signal $\boldsymbol{x}$ consisting of the per-carrier signals $\boldsymbol{x}^{(c)} = \begin{bmatrix}\boldsymbol{x}_1^{(c),\mathrm{H}} & \dots & \boldsymbol{x}_N^{(c),\mathrm{H}}\end{bmatrix}^{\mathrm{H}}$ is CN.*

For the signals to be jointly proper/CN, a certain structure of the cross-covariance matrix of the combined real signals $\check{\boldsymbol{x}}_{\mathrm{S}}$ and $\check{\boldsymbol{x}}_{\mathrm{R}}$ is required. In Theorem 9.2.1, we avoided an explicit definition of such a structure by instead defining an abstract power shaping space $\mathcal{P}$ in which the joint covariance matrix $\boldsymbol{C}_{\begin{bmatrix}\boldsymbol{x}_{\mathrm{S}}\\ \boldsymbol{x}_{\mathrm{R}}\end{bmatrix}}$ of $\boldsymbol{x}_{\mathrm{S}}$ and $\boldsymbol{x}_{\mathrm{R}}$ finally lies.

When choosing a concrete $\mathcal{P}$ in the following corollaries, we can no longer avoid specifying the structure of the submatrix that corresponds to the cross-covariance matrix. To write this down formally, we need to consider that the combined real representation of the concatenated per-carrier vectors $\begin{bmatrix}\boldsymbol{x}_{\mathrm{S}}^{(c),\mathrm{H}} & \boldsymbol{x}_{\mathrm{R}}^{(c),\mathrm{H}}\end{bmatrix}^{\mathrm{H}}$ is not equal to the concatenated vector $\begin{bmatrix}\check{\boldsymbol{x}}_{\mathrm{S}}^{\mathrm{T}} & \check{\boldsymbol{x}}_{\mathrm{R}}^{\mathrm{T}}\end{bmatrix}^{\mathrm{T}}$, but to a permuted version of it. In the proofs of the corollaries, we account for this by introducing an appropriate permutation matrix. The other power shaping spaces that occur in the corollaries are known from Proposition 3.4.2.

Corollary 9.5.1 ($\mathcal{P}_{\mathrm{S}} = \grave{\mathcal{P}}_{\mathrm{S}}$, $\mathcal{P}_{\mathrm{R}} = \grave{\mathcal{P}}_{\mathrm{R}}$, and $\mathcal{P}_{\mathrm{D}} = \grave{\mathcal{P}}_{\mathrm{D}}$)**.** *In the complex (multicarrier) MIMO RC* (9.16)–(9.17) *with a covariance constraint* (9.18)*, the (P)DF rate is maximized by input signals that are jointly proper (but possibly CC) if the noise is proper (but possibly CC).*

Proof. Using Lemma 2.9.3, we can verify that

$$\mathcal{P} = \left\{ \boldsymbol{P} = \begin{bmatrix}\boldsymbol{A} & \boldsymbol{B}\\ \boldsymbol{B}^{\mathrm{T}} & \boldsymbol{C}\end{bmatrix} \;\middle|\; \boldsymbol{A} \in \grave{\mathcal{P}}_{\mathrm{S}}, \boldsymbol{C} \in \grave{\mathcal{P}}_{\mathrm{R}}, \boldsymbol{B} \in \mathcal{BSC}_2^{Cm_{\mathrm{S}} \times Cm_{\mathrm{R}}} \right\}. \tag{9.19}$$

fulfills the assumptions of Theorem 9.2.1. To see that $\mathcal{P}$ is a power shaping space and that it corresponds to jointly proper signals, let $\boldsymbol{\Pi}$ be a permutation matrix such that the combined real representation of the concatenated per-carrier vectors $\begin{bmatrix}\boldsymbol{x}_{\mathrm{S}}^{(c),\mathrm{H}} & \boldsymbol{x}_{\mathrm{R}}^{(c),\mathrm{H}}\end{bmatrix}^{\mathrm{H}}$ equals $\boldsymbol{\Pi}\begin{bmatrix}\check{\boldsymbol{x}}_{\mathrm{S}}^{\mathrm{T}} & \check{\boldsymbol{x}}_{\mathrm{R}}^{\mathrm{T}}\end{bmatrix}^{\mathrm{T}}$. Then, $\boldsymbol{\Pi}\boldsymbol{P}\boldsymbol{\Pi}^{\mathrm{T}} \in \mathcal{SBSC}_2^{C(m_{\mathrm{S}}+m_{\mathrm{R}})}$ for $\boldsymbol{P} \in \mathcal{P}$, which corresponds to the combined real covariance matrix of a proper random vector of length $C(m_{\mathrm{S}} + m_{\mathrm{R}})$. Moreover, $\mathcal{P}$ is a power shaping space due to Corollary 2.6.1. □

Corollary 9.5.2 ($\mathcal{P}_{\mathrm{S}} = \mathcal{P}_{\mathrm{S}}^{\mathrm{CN}}$, $\mathcal{P}_{\mathrm{R}} = \mathcal{P}_{\mathrm{R}}^{\mathrm{CN}}$, and $\mathcal{P}_{\mathrm{D}} = \mathcal{P}_{\mathrm{D}}^{\mathrm{CN}}$)**.** *In the complex multicarrier MIMO RC* (9.16)–(9.17) *with a covariance constraint* (9.18)*, the (P)DF rate is maximized by input signals that are jointly CN (but possibly improper) if the noise is CN (but possibly improper).*

Proof. To obtain the result, we use

$$\mathcal{P} = \left\{ \boldsymbol{P} = \begin{bmatrix}\boldsymbol{A} & \boldsymbol{B}\\ \boldsymbol{B}^{\mathrm{T}} & \boldsymbol{C}\end{bmatrix} \;\middle|\; \boldsymbol{A} \in \mathcal{P}_{\mathrm{S}}^{\mathrm{CN}}, \boldsymbol{C} \in \mathcal{P}_{\mathrm{R}}^{\mathrm{CN}}, \boldsymbol{B} \in \mathcal{H}_{\mathrm{SR}} \right\} \tag{9.20}$$

where $\mathcal{H}_{\mathrm{SR}}$ is the set of matrices that contain block-diagonal submatrices of appropriate dimensions, i.e.,

$$\mathcal{H}_{\mathrm{SR}} = \left\{ \boldsymbol{H} = \begin{bmatrix}\boldsymbol{D} & \boldsymbol{E}\\ \boldsymbol{F} & \boldsymbol{G}\end{bmatrix} \;\middle|\; \boldsymbol{D}, \boldsymbol{E}, \boldsymbol{F}, \boldsymbol{G} \in \mathbb{R}^{\mathcal{M}_{\mathrm{S}} \times \mathcal{M}_{\mathrm{R}}} \right\} \tag{9.21}$$

with $\mathcal{M}_{\mathrm{S}} = (m_{\mathrm{S}})_{\forall c}$, and $\mathcal{M}_{\mathrm{R}} = (m_{\mathrm{R}})_{\forall c}$. The assumptions of Theorem 9.2.1 can be verified by exploiting that the block-diagonal structures are preserved in matrix products. To see that $\mathcal{P}$ is a power shaping space and that it corresponds to jointly CN signals, let $\boldsymbol{\Pi}$ be as in the proof of Corollary 9.5.1. Then, $\{\boldsymbol{P}' \mid \boldsymbol{P}' = \boldsymbol{\Pi}\boldsymbol{P}\boldsymbol{\Pi}^{\mathrm{T}},\ \boldsymbol{P} \in \mathcal{P}\}$ is equivalent to $\mathcal{P}_{\mathrm{T}}^{\mathrm{CN}}$ of a terminal with $m_{\mathrm{T}} = m_{\mathrm{S}} + m_{\mathrm{R}}$ antennas (see Definition 3.4.1). Moreover, $\mathcal{P}$ is a power shaping space due to Corollary 2.6.1. □

Corollary 9.5.3 ($\mathcal{P}_{\mathrm{S}} = \grave{\mathcal{P}}_{\mathrm{S}}^{\mathrm{CN}}$, $\mathcal{P}_{\mathrm{R}} = \grave{\mathcal{P}}_{\mathrm{R}}^{\mathrm{CN}}$, and $\mathcal{P}_{\mathrm{D}} = \grave{\mathcal{P}}_{\mathrm{D}}^{\mathrm{CN}}$)**.** *In the complex multicarrier MIMO RC* (9.16)–(9.17) *with a covariance constraint* (9.18)*, the (P)DF rate is maximized by input signals that are jointly proper and jointly CN if the noise is proper and CN.*

Proof. Let $\mathcal{P}$ be the intersection of the spaces in (9.19) and (9.20), which is a power shaping space due to Proposition 2.4.3. The assumptions of Theorem 9.2.1 can be verified by combining the arguments from Corollaries 9.5.1 and 9.5.2. □

9.5.2 CC Transmission vs. Coding Across Carriers in Multihop Systems

It is known that coding separately on each carrier is not always capacity-achieving in multicarrier relay channels [233]. To get an intuition about this fact, let us consider an extreme case. Let $\boldsymbol{H}_{\mathrm{RS}}^{(1)} = \mathbf{0}$ and $\boldsymbol{H}_{\mathrm{DR}}^{(2)} = \mathbf{0}$ in a relay channel with $C = 2$ carriers. In this scenario, the relay can assist the transmission only if information received on carrier 2 may be forwarded to the destination via carrier 1. If we additionally assume that the direct link between source and destination is negligibly weak, i.e., $\boldsymbol{H}_{\mathrm{DS}}^{(1)} = \boldsymbol{H}_{\mathrm{DS}}^{(2)} = \mathbf{0}$, the capacity on each carrier is zero when treating the carriers separately. However, by coding jointly across both carriers, a nonzero rate is achievable.

Clearly, this observation also applies to PDF, i.e., joint coding can be necessary to achieve the optimal PDF rate. However, we have shown above that CN signals are optimal for the PDF protocol in the complex multicarrier MIMO RC with CN noise. To understand this seeming contradiction, we have to look closer into the applied coding scheme.

The PDF rate can be achieved by a so-called block-Markov coding scheme [54, Sec. 9.4.1], where the time is divided into blocks. In each block, the relay can, for reasons of causality, only forward information that it has received in an earlier block. In the decomposition (9.6), $\boldsymbol{w}$ represents the information that is provided to the relay in order to allow for coherent transmission in a future block while the joint signal $\begin{bmatrix}\boldsymbol{z}^{\mathrm{H}} & \boldsymbol{x}_{\mathrm{R}}^{\mathrm{H}}\end{bmatrix}^{\mathrm{H}}$ describes the coherent transmission that is currently taking place [6]. This is illustrated in Figure 9.2.

From Theorem 9.2.1, we obtain that the three independent signal portions $\boldsymbol{w}$, $\begin{bmatrix}\boldsymbol{z}^{\mathrm{H}} & \boldsymbol{x}_{\mathrm{R}}^{\mathrm{H}}\end{bmatrix}^{\mathrm{H}}$, and $\boldsymbol{v}$ (direct transmission without the relay) are maximum-entropy signals in the optimal solution. Applying this to the complex multicarrier MIMO RC via Corollary 9.5.2, we obtain that the optimal signals $\boldsymbol{w}$, $\begin{bmatrix}\boldsymbol{x}_{\mathrm{S}}^{\mathrm{H}} & \boldsymbol{x}_{\mathrm{R}}^{\mathrm{H}}\end{bmatrix}^{\mathrm{H}}$, and $\boldsymbol{v}$ are jointly CN, i.e., there are no correlations across carriers.

However, this perspective is only a snapshot for a single block. To make the protocol work, it is of course necessary that $\begin{bmatrix}\boldsymbol{z}^{\mathrm{H}} & \boldsymbol{x}_{\mathrm{R}}^{\mathrm{H}}\end{bmatrix}^{\mathrm{H}}$ is correlated with the signals that correspond to $\boldsymbol{w}$ in earlier blocks and these correlations may also span across carriers [22] without violating Theorem 9.2.1. Unfortunately, this does not become visible in the single-letter representations on which our analysis is based.

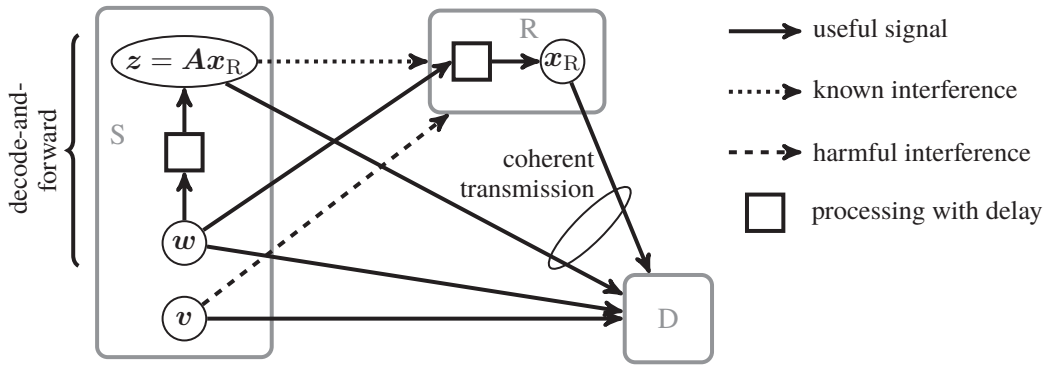

Figure 9.2: Visualization of the various signal portions in (9.6) *and of the time offset between* $\boldsymbol{w}$ *and* $\boldsymbol{z}$ *(see Section 9.5.2). Figure adapted from [6, 22].*

In order to still capture this particularity of block coding schemes, the following distinction was proposed in [22].

- *Separate coding:* messages are split into chunks that are then processed individually, each on a different carrier.
- *Joint coding:* there are signals in the system that are transmitted on different carriers, but depend on the same message portion.
- *CN transmission:* within each time block, the signals are not correlated across carriers (CN signals).
- *CC transmission:* correlations across carriers (CC signals) occur within the time blocks.

As pointed out in [22], transmitting CC signals only makes sense in combination with joint coding, but conversely, joint coding does not imply that CC signals are used.

For the example of PDF in the complex multicarrier MIMO RC with proper CN noise, the distinction becomes clear in the following comparison. By plugging in proper CN signals (due to Corollary 9.5.3) into (9.5), we obtain

$$r_{\mathrm{PDF}} = \min\{\mathrm{I}\left(\boldsymbol{u};\boldsymbol{y}_{\mathrm{R}} \,|\, \boldsymbol{x}_{\mathrm{R}}\right) + \mathrm{I}\left(\boldsymbol{x}_{\mathrm{S}};\boldsymbol{y}_{\mathrm{D}} \,|\, (\boldsymbol{u},\boldsymbol{x}_{\mathrm{R}})\right),\ \mathrm{I}\left((\boldsymbol{x}_{\mathrm{S}},\boldsymbol{x}_{\mathrm{R}});\boldsymbol{y}_{\mathrm{D}}\right)\} \tag{9.22}$$

$$= \min\left\{\sum_{c=1}^{C} r_{\mathrm{A}}^{(c)},\ \sum_{c=1}^{C} r_{\mathrm{B}}^{(c)}\right\} \tag{9.23}$$

with

$$r_{\mathrm{A}}^{(c)} = \mathrm{I}\left(\boldsymbol{u}^{(c)};\boldsymbol{y}_{\mathrm{R}}^{(c)} \,|\, \boldsymbol{x}_{\mathrm{R}}^{(c)}\right) + \mathrm{I}\left(\boldsymbol{x}_{\mathrm{S}}^{(c)};\boldsymbol{y}_{\mathrm{D}}^{(c)} \,|\, (\boldsymbol{u}^{(c)},\boldsymbol{x}_{\mathrm{R}}^{(c)})\right) \tag{9.24}$$

$$r_{\mathrm{B}}^{(c)} = \mathrm{I}\left((\boldsymbol{x}_{\mathrm{S}}^{(c)},\boldsymbol{x}_{\mathrm{R}}^{(c)});\boldsymbol{y}_{\mathrm{D}}^{(c)}\right) \tag{9.25}$$

i.e., r_{A} and r_{B} can be considered as sums over per-carrier rates $r_{\mathrm{A}}^{(c)}$ and $r_{\mathrm{B}}^{(c)}$, respectively. To obtain this result, we can use similar arguments as in Proposition 3.4.5 since all signals are Gaussian.

Under the assumption of separate coding, we would instead obtain $r_{\mathrm{PDF,sep}}$ as the sum of individual PDF rates $r_{\mathrm{PDF}}^{(c)}$ on each carrier. For any given input distribution, the comparison of both approaches yields

$$r_{\mathrm{PDF,sep}} = \sum_{c=1}^{C} r_{\mathrm{PDF}}^{(c)} = \sum_{c=1}^{C} \min\left\{r_{\mathrm{A}}^{(c)},\, r_{\mathrm{B}}^{(c)}\right\} \leq \min\left\{\sum_{c=1}^{C} r_{\mathrm{A}}^{(c)},\, \sum_{c=1}^{C} r_{\mathrm{B}}^{(c)}\right\} = r_{\mathrm{PDF}}. \quad (9.26)$$

It is easy to show mathematically that the sum of the minima never exceeds the minimum of the sums, but we can also give a technical interpretation [22]. For $r_{\mathrm{PDF,sep}}$, the rate of information leaving the source (towards relay and destination) on any carrier has to be balanced with the rate of information arriving at the destination (from the source and the relay) on the same carrier. By contrast, on the right hand side of the inequality in (9.26), this balance has to hold only for the overall system, but not on each carrier. This is clearly less restrictive, and can lead to a higher achievable rate.

Even though the functioning of PDF and of amplify-and-forward (AF) is quite different, a similar observation was reported for the AF protocol in [234].[3] Therein, it was pointed out that allowing the relay to forward information in new spatial directions and on different carriers leads to a so-called space-frequency pairing gain that is in general higher than the space-only pairing gain obtained by forwarding information in new spatial directions on the same carriers. This benefit of joint processing is, just like the one in (9.26), not related to CC transmission in the sense of the definition proposed above, i.e., it is not a gain obtained by reduced-entropy transmission in a system with interference. It is instead based on the simple fact that the variation of channel conditions across carriers is in general different for the source-relay channel and for the relay-destination channel.

9.5.3 Optimal Transmit Covariance Matrices

A numerical optimization of the input covariance matrices for (P)DF in the complex multicarrier MIMO RC can be performed by applying the methods described in Section 9.3 to the combined real formulation (3.37). Under the assumption of proper noise and signals, we can instead use the formulation in (9.22), which corresponds to the combined complex representation (3.35).

For (P)DF in the complex multicarrier MIMO RC with CN noise and signals, it seems that there are currently no dedicated algorithms that exploit the block-diagonal structures or operate directly on the formulation in (9.23). A paper that explicitly considers PDF in a multicarrier RC is [235]. However, this paper is restricted to a single-antenna system and mainly treats the case where the relay and the source are not able to transmit in a coherent manner, i.e., $\boldsymbol{z} = \mathbf{0}$. For the general case, no convex reformulation is found, and an optimal solution to the PDF rate maximization is not obtained.

When designing a specialized algorithm for PDF with CN signals based on a dual decomposition (Section 3.3.2), two aspects have to be taken into account. Firstly, it is necessary to decompose the expressions for r_{A} and r_{B} rather then the overall PDF rate (see Section 9.5.2). The second aspect arises when choosing a solver for the inner problem (3.33).

[3] Note that the authors of [234] use a different nomenclature. The solution they derive for what they call a subcarrier-cooperative MIMO relay system would fall into the category of joint coding without CC transmission when using the nomenclature proposed above.

When maximizing the DF rate, we could, e.g., use a modified version of the formulation in [221] to solve the inner problem by means of convex programming techniques. For PDF, however, there is currently no solver available that could solve (3.33) in a globally optimal manner. Since such a globally optimal solution was assumed in the derivation of the dual decomposition approach, it would be necessary to study how local or approximate solutions (as in [114, 230]) influence the behavior of the overall algorithm.

To overcome this problem, we could instead apply one of the algorithms presented in Section 9.3 directly to the combined representation and perform dual decompositions for the arising subproblems. For instance, the inner approximation algorithm from [230] solves a series of approximated optimization problems. Each of these problems can be solved in a globally optimal manner, and the dual decomposition approach could be applied to each of them. This idea was pursued in [236] to optimize the PDF rate in a half duplex MIMO RC, and it could be applied in a similar manner to optimize CN transmission. An alternative is the method from [114], which reformulates the PDF rate maximization in a way that an arising subproblem is equivalent to a sum rate maximization in the MIMO BC. When applying the overall algorithm to the combined formulation, the CN structure could then be exploited by a dual decomposition of the BC subproblem. The question which of the sketched approaches is most adequate and most efficient for maximizing the PDF rate in case of CN noise and CN signals is left open for future research.

9.5.4 Worst-Case Noise

For the complex multicarrier MIMO RC, we obtain the following specializations of the worst-case noise result from Theorem 9.4.1 using the power shaping spaces from Proposition 3.4.2. The term *optimized* is always understood in the sense of maximizing the (P)DF rate under a transmit covariance constraint (9.18).

Corollary 9.5.4 (power shaping spaces as in Corollary 9.5.3)**.** *For (P)DF in the complex multicarrier MIMO RC* (9.16)–(9.17) *with constraints on the complex per-carrier noise covariance matrices, the worst-case noise is proper and CN if the input signals are either fixed to be jointly proper and jointly CN or optimized based on the noise properties.*

Corollary 9.5.5 (power shaping spaces as in Corollary 9.5.1)**.** *For (P)DF in the complex (multicarrier) MIMO RC* (9.16)–(9.17) *with constraints on the combined complex noise covariance matrices, the worst-case noise is proper if the input signals are either fixed to be jointly proper or optimized based on the noise properties.*

Corollary 9.5.6 (power shaping spaces as in Corollary 9.5.2)**.** *For (P)DF in the complex multicarrier MIMO RC* (9.16)–(9.17) *with constraints on the per-carrier noise properties, the worst-case noise is CN if the input signals are either fixed to be jointly CN or optimized based on the noise properties.*

9.6 Results on Reduced-Entropy Signals in Relay Networks

In this chapter, we have focused on (P)DF in the full-duplex MIMO RC with perfect self-interference cancellation. For this setting, we have shown that maximum-entropy transmit

signals are optimal under the assumption of maximum-entropy noise. However, the considered setting is only an example among many possible configurations of relay networks, and PDF and DF are only two examples out of many possible coding schemes. For any other setting or coding scheme, the question whether maximum-entropy signals are optimal can be asked again, and it turns out that there are many situations in which the response is different.

In [237, 238], the DF scheme was considered in a full-duplex RC under the assumption of imperfect self-interference cancellation. It was proposed to employ improper signaling in order to mitigate the negative impact of the residual self-interference, and it was shown that this indeed has the potential to reduce the outage probability compared to proper signaling. This result was extended to relay networks with two relays in [239–241], where improper signaling was shown to be helpful to combat inter-relay interference.

A larger relay network was studied in [43] by not only increasing the number of relays, but also the number of source nodes and destination nodes. In the resulting relay-assisted interference channel, benefits of CC transmission were reported for a suboptimal amplify-and-forward (AF) scheme. A part of the performance gain can be attributed to channel pairing [43], i.e., to the pairing gain described at the end of Section 9.5.2. However, our previous discussion of interference channels in Section 8.5.2 suggests that another part of the observed gain due to CC transmission is related to the fact that maximum-entropy transmission is not always optimal in systems with interference—in this case between the multiple source-destination pairs.

An example of gains by reduced-entropy transmission that are clearly related to multiuser interference can be found in [242]. Therein, a single-carrier relay-assisted interference channel was considered, and it was observed that the same per-user rates can be achieved with lower transmit power when improper signaling instead of proper signaling is applied.

Relay-assisted interference channels have also been studied from the perspective of physical layer security, and gains by reduced-entropy transmission have been reported. According to [44], CC transmission can be beneficial for the secrecy rate in a multicarrier setting. In [135], improper signals were applied in combination with a widely linear relaying scheme to achieve a higher number of secure degrees of freedom than with linear processing at the relay.

Finally, it shall be noted that there are several publications on relaying scenarios that do not ask whether improper signaling is beneficial when compared to proper signaling, but take impropriety of the transmit signals as a given fact and investigate how AF relay processing can be optimized in this case (see [136, 243] as well as [137] and the references therein). This question arises since many modulation schemes that are applied in practice, such as binary phase shift keying (BPSK), amplitude shift keying (ASK), and Gaussian minimum-shift keying (GMSK), lead to improper transmit signals (e.g., [243]). In a similar manner, the authors of [142] studied AF transceiver design for the case of improper noise.

On the one hand, these various examples show that reduced-entropy transmission in relay networks and relay-assisted interference networks is a field of ongoing research. Indeed, there are many more possible combinations of system configurations and coding schemes than the ones studied in the abovementioned references. This leads to a manifold of open question that need to be considered in future research. On the other hand, the above summary illustrates that the interference that is introduced in the PDF scheme due to partial decoding at the relay—described by the signal $\boldsymbol{v}$ in (9.6)—is quite different from the residual self-interference in [237, 238], the inter-relay interference in [239–241], and the inter-user interference or leakage

in [43, 44, 135, 242]. Unlike these other kinds of interference, the interference caused by partial decoding in the MIMO RC exhibits the same special structure as the residual inter-user interference in the MIMO BC with dirty paper coding or the MIMO MAC with successive interference cancellation. As discussed in Section 8.5.1, it is remarkable that this particular interference structure does not give rise to gains by reduced-entropy transmission even though other kinds of interference do so.

Chapter 10

Conclusion and Outlook

The various recent results on carrier-cooperative transmission (coding across carriers) and improper signaling (asymmetric complex signaling) can be considered as small pieces of a larger picture. To get a better impression of this overall picture, we have used the notion of reduced-entropy signals, which we have formally defined based on the new mathematical framework of power shaping spaces. Improper signaling and carrier-cooperative transmission are then just two examples of transmit strategies where the differential entropy of the input signals is intentionally chosen lower than what would be allowed by the constraints on the transmit covariance matrices.

The reason why these two kinds of entropy reduction merit special attention is connected to the channel models that are typically considered in information theoretic studies. This connection can be seen based on the notion of compatibility that we have introduced in the context of power shaping spaces. While (strictly) linear channels are compatible with the power shaping spaces that we use to study improper signaling, channels where all carriers are orthogonal to each other are compatible with the power shaping spaces used for the analysis of carrier-cooperative transmission. If different channel models were studied, other power shaping spaces and, thus, other types of reduced-entropy signals would be of interest. The framework of power shaping spaces is general enough to derive results about maximum-entropy transmission and reduced-entropy transmission that are valid no matter which type of entropy reduction is finally considered.

Using this framework, we have reviewed various recently published results from a more general perspective, and we have derived new statements about maximum-entropy transmission and reduced-entropy transmission in various MIMO communication systems. The main question in all considered system models is whether maximum-entropy transmission is the optimal transmit strategy under the assumption of maximum-entropy noise or, conversely, whether reduced-entropy transmission can bring any gains. Maximum-entropy transmission turns out to be optimal in interference-free systems and in systems where the interference has a very particular structure that occurs in the MIMO broadcast channel with dirty paper coding and in the MIMO multiple access channel with successive interference cancellation. By contrast, maximum-entropy signals are in general not the best choice in the presence of other kinds of

interference.

The nature of the possible benefits of using reduced-entropy signals instead can be quite different in the various considered communication systems. For example, an improvement in terms of the degrees of freedom, which are the decisive figure of merit for the high SNR regime, is possible in some systems while there are only gains in terms of achievable rate regions at finite SNR in others. However, we have also seen that insights obtained in one system model can sometimes be transferred to other, qualitatively different systems. An important example is the design of algorithms for transceiver optimization in the MIMO broadcast channel and the MIMO interference channel, both with interference treated as noise, where the similarity of the rate equations calls for similar algorithmic solutions.

We have also observed that the performance gap between maximum-entropy transmission and reduced-entropy transmission can depend significantly on whether or not we allow the use of time-sharing, and whether this time-sharing averages only over the achievable rates or also over the employed transmit covariance matrices. Some of our results indicate that time-sharing (including the possibility of averaging over the transmit covariance matrices) can enlarge the considered rate regions and it can sometimes even render reduced-entropy transmission unnecessary, or at least lead to situations where the performance loss resulting from maximum-entropy transmission is much less pronounced. Therefore, when trying to incorporate recent information theoretic insights into future practical systems, reduced-entropy transmission is not the only interesting candidate, but the application of time-sharing should be evaluated as well—despite disadvantages such as possible fluctuations of the transmit powers and the signaling overhead that arises when allowing time slots with arbitrary lengths.

An additional remark on the topic of time-sharing is in order for the MIMO broadcast channel with interference treated as noise. Many publications on this setting exclude the possibility of time-sharing while time-sharing between different encoding orders (at least in terms of averaging over the rates) is an integral part of the optimal transmit strategy based on dirty paper coding. For a fair comparison, it then needs to be considered that only a part of the performance degradation compared to the capacity region comes from treating interference as noise while another part can come from excluding the use of time-sharing. This should be kept in mind since time-sharing might, despite its disadvantages, still be easier to implement than complicated multiuser coding schemes that are meant to approximate dirty paper coding. Combining the various approaches that improve the performance of strategies where interference is treated as noise, namely improper signaling, carrier-cooperative transmission, and time-sharing, might help to make the performance gap to optimal dirty paper coding significantly smaller in many situations, without the need of such multiuser coding schemes.

Finally, there is another piece of the puzzle of optimal transmission in communication systems with interference, which should be considered. Throughout all chapters, we have sticked to the assumption that all signals are Gaussian. This can be shown to be an optimal choice (under the assumption of Gaussian noise) for single users systems, for the MIMO multiple access channel (with joint decoding or successive interference cancellation), for the MIMO broadcast channel with dirty paper coding, and for the MIMO relay channel with (partial) decode-and-forward. When recapitulating the results that we derived in the respective chapters, it is striking that these are exactly the system models for which we could show that maximum-entropy transmission in the sense of the framework of power shaping spaces is

optimal. On the other hand, Gaussian signals have not been proven to be optimal in MIMO interference channels nor in the MIMO broadcast channel with interference treated as noise. These are the system models, for which reduced-entropy transmission with respect to the considered power shaping spaces turned out to bring benefits.

In fact, it was shown that non-Gaussian signals can indeed be beneficial in interference channel scenarios with Gaussian noise [56], and it was observed that interference that follows a Gaussian distribution does not feature a favorable structure that could be exploited for efficient interference management [213]. There do not seem to be similar statements for the MIMO broadcast channel with interference treated as noise in the existing literature. However, continuing the above line of argumentation, we can conclude that it would not be surprising if similar proofs could be found for this case as well. The Gaussian distribution is the one that maximizes the differential entropy for given second-order properties, and it would make sense that *reduced-entropy transmission by using non-Gaussian signals* can bring gains in the same system models as *reduced-entropy transmission in terms of the framework of power shaping spaces*.

This aspect could also be interesting from a practical perspective since the entropy-maximizing Gaussian codebooks are anyway replaced by discrete constellations in real-world communication systems. It is remarkable that non-Gaussian signals, which are employed for practical reasons, might have advantages even from a theoretical point of view due to the fact that maximizing the entropy is not always the best option. Nevertheless, bringing such theoretical observations to practical use is of course a long way to go, where many additional aspects such as imperfect channel knowledge, more elaborated channel models including time-varying and frequency-selective channels, limitations of practical error correcting codes, and many more need to be considered. For practical codes, it shall also be remarked that coding across carriers can bring further benefits in case of a short block length, even in systems without interference [39, Sec. 5.3].

The aim of studies that are based on achievable rates in the sense of Shannon and on further idealistic assumptions is to shed light on fundamental aspects and to point out possible directions that could be pursued in the design of future communication systems. This is the spirit in which the presented results on benefits of reduced-entropy signals and on the optimization of reduced-entropy transmit strategies need to be understood.

Bibliography

[1] C. Hellings and W. Utschick, "On the inseparability of parallel MIMO broadcast channels with linear transceivers," *IEEE Trans. Signal Process.*, vol. 59, no. 12, pp. 6273–6278, Dec. 2011.

[2] C. Hellings, M. Joham, and W. Utschick, "Gradient-based power minimization in MIMO broadcast channels with linear precoding," *IEEE Trans. Signal Process.*, vol. 60, no. 2, pp. 877–890, Feb. 2012.

[3] C. Hellings, M. Joham, M. Riemensberger, and W. Utschick, "Minimal transmit power in parallel vector broadcast channels with linear precoding," *IEEE Trans. Signal Process.*, vol. 60, no. 4, pp. 1890–1898, Apr. 2012.

[4] C. Hellings, S. Herrmannn, and W. Utschick, "Carrier cooperation can reduce the transmit power in parallel MIMO broadcast channels with zero-forcing," *IEEE Trans. Signal Process.*, vol. 61, no. 12, pp. 3021–3027, Jun. 2013.

[5] C. Hellings, M. Joham, and W. Utschick, "QoS feasibility in MIMO broadcast channels with widely linear transceivers," *IEEE Signal Process. Lett.*, vol. 20, no. 11, pp. 1134–1137, Nov. 2013.

[6] C. Hellings, L. Gerdes, L. Weiland, and W. Utschick, "On optimal Gaussian signaling in MIMO relay channels with partial decode-and-forward," *IEEE Trans. Signal Process.*, vol. 62, no. 12, pp. 3153–3164, Jun. 2014.

[7] C. Hellings and W. Utschick, "Block-skew-circulant matrices in complex-valued signal processing," *IEEE Trans. Signal Process.*, vol. 63, no. 8, pp. 2093–2107, Apr. 2015.

[8] ——, "Improper signaling versus time-sharing in the SISO Z-interference channel," *IEEE Commun. Lett.*, vol. 21, no. 11, pp. 2432–2435, Nov. 2017.

[9] C. Hellings, M. Joham, and W. Utschick, "Gradient-based rate balancing for MIMO broadcast channels with linear precoding," presented at the Int. ITG Workshop on Smart Antennas (WSA) 2011, Aachen, Germany, Feb. 24–25, 2011.

[10] C. Hellings, W. Utschick, and M. Joham, "Power minimization in parallel vector broadcast channels with separate linear precoding," in *Proc. 19th European Signal Process. Conf. (EUSIPCO)*, Aug./Sep. 2011, pp. 1834–1838.

[11] C. Hellings and W. Utschick, "Carrier-cooperative transmission in parallel MIMO broadcast channels: Potential gains and algorithms," in *Proc. 8th Int. Symp. Wireless Commun. Syst. (ISWCS)*, Nov. 2011, pp. 774–778.

[12] C. Hellings, N. Damak, and W. Utschick, "Energy-efficient zero-forcing with user selection in parallel vector broadcast channels," in *Proc. Int. ITG Workshop on Smart Antennas (WSA) 2012*, Mar. 2012, pp. 168–175.

[13] C. Hellings, P. Kiefer, and W. Utschick, "Rate prediction and receding horizon power minimization in block-fading broadcast channels," in *Proc. IEEE 13th Int. Workshop Signal Process. Adv. Wireless Commun. (SPAWC)*, Jun. 2012, pp. 30–34.

[14] C. Hellings and W. Utschick, "Energy-efficient rate balancing in vector broadcast channels with linear transceivers," in *Proc. 9th Int. Symp. Wireless Commun. Syst. (ISWCS)*, Aug. 2012, pp. 1044–1048.

[15] ——, "Linear precoding in parallel MIMO broadcast channels: Separable and inseparable scenarios," presented at the Int. ITG Workshop on Smart Antennas (WSA) 2013, Stuttgart, Germany, Mar., 13–14, 2013.

[16] ——, "Performance gains due to improper signals in MIMO broadcast channels with widely linear transceivers," in *Proc. Int. Conf. Acoust., Speech, and Signal Process. (ICASSP) 2013*, May 2013, pp. 4379–4383.

[17] ——, "Energy efficiency optimization in MIMO broadcast channels with fairness constraints," in *Proc. IEEE 14th Int. Workshop Signal Process. Adv. Wireless Commun. (SPAWC)*, Jun. 2013, pp. 594–598.

[18] ——, "Three kinds of inseparability in parallel MIMO broadcast channels with linear transceivers," in *Proc. 10th Int. Symp. Wireless Commun. Syst. (ISWCS)*, Aug. 2013, pp. 557–561.

[19] ——, "Energy efficiency optimization in the multiantenna downlink with linear transceivers," in *Proc. IEEE 24th Annual Int. Symp. Personal, Indoor, and Mobile Radio Commun. (PIMRC)*, Sep. 2013, pp. 414–418.

[20] C. Hellings, S. Herrmann, and W. Utschick, "A deterministic initialization for optimizing carrier-cooperative transmit strategies," presented at the Int. ITG Workshop on Smart Antennas (WSA) 2014, Erlangen, Germany, Mar., 12–13, 2014.

[21] C. Hellings, L. Weiland, and W. Utschick, "Optimality of proper signaling in Gaussian MIMO broadcast channels with shaping constraints," in *Proc. Int. Conf. Acoust., Speech, and Signal Process. (ICASSP) 2014*, May 2014, pp. 3498–3502.

[22] C. Hellings and W. Utschick, "On carrier-cooperation in parallel Gaussian MIMO relay channels with partial decode-and-forward," presented at the 48th Asilomar Conf. Signals, Syst., and Comput. (ACSSC), Pacific Grove, CA, USA, Nov. 2–5, 2014.

[23] ——, "Iterative algorithms for transceiver design in MIMO broadcast channels with improper signaling," presented at the 10th Int. ITG Conf. Syst., Commun., and Coding (SCC), Hamburg, Germany, 2–5 Feb. 2015.

[24] C. Hellings, M. Koller, and W. Utschick, "An impropriety test based on block-skew-circulant matrices," presented at the Int. ITG Workshop on Smart Antennas (WSA) 2015, Ilmenau, Germany, Mar., 3–5 2015.

[25] C. Hellings and W. Utschick, "Separability of parallel Gaussian MIMO broadcast channels with shaping constraints," in *Proc. IEEE 16th Int. Workshop Signal Process. Adv. Wireless Commun. (SPAWC)*, Jun. 2015, pp. 126–130.

[26] ——, "Two different real representations of complex matrices for describing widely linear systems," in *Proc. 12th Int. Symp. Wireless Commun. Syst. (ISWCS)*, Aug. 2015, pp. 641–645.

[27] C. Hellings, P. Gögler, and W. Utschick, "Composite real principal component analysis of complex signals," in *Proc. 23rd European Signal Process. Conf. (EUSIPCO)*, Aug. 2015, pp. 2216–2220.

[28] C. Hellings and W. Utschick, "On the worst-case noise in Gaussian MIMO systems with proper and with improper signaling," presented at the Int. ITG Workshop on Smart Antennas (WSA) 2017, Berlin, Germany, Mar. 15–17, 2017.

[29] I. E. Telatar, "Capacity of multi-antenna Gaussian channels," *European Trans. Telecommun.*, vol. 10, no. 6, pp. 585–595, Nov./Dec. 1999.

[30] V. R. Cadambe, S. A. Jafar, and C. Wang, "Interference alignment with asymmetric complex signaling—settling the Høst-Madsen–Nosratinia conjecture," *IEEE Trans. Inf. Theory*, vol. 56, no. 9, pp. 4552–4565, Sep. 2010.

[31] Z. K. M. Ho and E. Jorswieck, "Improper Gaussian signaling on the two-user SISO interference channel," *IEEE Trans. Wireless Commun.*, vol. 11, no. 9, pp. 3194–3203, Sep. 2012.

[32] H. Park, S. H. Park, J. S. Kim, and I. Lee, "SINR balancing techniques in coordinated multi-cell downlink systems," *IEEE Trans. Wireless Commun.*, vol. 12, no. 2, pp. 626–635, Feb. 2013.

[33] Y. Zeng, C. M. Yetis, E. Gunawan, Y. L. Guan, and R. Zhang, "Transmit optimization with improper Gaussian signaling for interference channels," *IEEE Trans. Signal Process.*, vol. 61, no. 11, pp. 2899–2913, Jun. 2013.

[34] Y. Zeng, R. Zhang, E. Gunawan, and Y. L. Guan, "Optimized transmission with improper Gaussian signaling in the K-user MISO interference channel," *IEEE Trans. Wireless Commun.*, vol. 12, no. 12, pp. 6303–6313, Dec. 2013.

[35] S. Lagen, A. Agustin, and J. Vidal, "Coexisting linear and widely linear transceivers in the MIMO interference channel," *IEEE Trans. Signal Process.*, vol. 64, no. 3, pp. 652–664, Feb. 2016.

[36] ——, "On the superiority of improper Gaussian signaling in wireless interference MIMO scenarios," *IEEE Trans. Commun.*, vol. 64, no. 8, pp. 3350–3368, Aug. 2016.

[37] E. Kurniawan and S. Sun, "Improper Gaussian signaling scheme for the Z-interference channel," *IEEE Trans. Wireless Commun.*, vol. 14, no. 7, pp. 3912–3923, Jul. 2015.

[38] C. Lameiro, I. Santamaría, and P. J. Schreier, "Rate region boundary of the SISO Z-interference channel with improper signaling," *IEEE Trans. Commun.*, vol. 65, no. 3, pp. 1022–1034, Mar. 2017.

[39] D. Tse and P. Viswanath, *Fundamentals of Wireless Communication*. Cambridge, UK: Cambridge University Press, 2005.

[40] V. R. Cadambe and S. A. Jafar, "Parallel Gaussian interference channels are not always separable," *IEEE Trans. Inf. Theory*, vol. 55, no. 9, pp. 3983–3990, Sep. 2009.

[41] ——, "Sum-capacity and the unique separability of the parallel Gaussian MAC-Z-BC network," in *Proc. Int. Symp. Inf. Theory (ISIT) 2010*, Jun. 2010, pp. 2318–2322.

[42] L. Sankar, X. Shang, E. Erkip, and H. V. Poor, "Ergodic fading interference channels: Sum-capacity and separability," *IEEE Trans. Inf. Theory*, vol. 57, no. 5, pp. 2605–2626, May 2011.

[43] R. T. L. Rolny, M. Kuhn, A. Amah, and A. Wittneben, "Multi-cell cooperation using subcarrier-cooperative two-way amplify-and-forward relaying," in *Proc. 10th Int. Symp. Wireless Commun. Syst. (ISWCS)*, Aug. 2013, pp. 259–263.

[44] Z. Ho, E. Jorswieck, and S. Engelmann, "Information leakage neutralization for the multi-antenna non-regenerative relay-assisted multi-carrier interference channel," *IEEE J. Sel. Areas Commun.*, vol. 31, no. 9, pp. 1672–1686, Sep. 2013.

[45] P. Viswanath and D. N. C. Tse, "Sum capacity of the vector Gaussian broadcast channel and uplink-downlink duality," *IEEE Trans. Inf. Theory*, vol. 49, no. 8, pp. 1912–1921, Aug. 2003.

[46] S. Vishwanath, N. Jindal, and A. Goldsmith, "Duality, achievable rates, and sum-rate capacity of Gaussian MIMO broadcast channels," *IEEE Trans. Inf. Theory*, vol. 49, no. 10, pp. 2658–2668, Oct. 2003.

[47] D. N. Tse, "Optimal power allocation over parallel Gaussian broadcast channels," presented at the Int. Symp. Inf. Theory (ISIT) 1997, Ulm, Germany, Jun. 29–Jul. 4, 1997.

[48] D. N. C. Tse and S. V. Hanly, "Multi-access fading channels—part I: Polymatroid structure, optimal resource allocation and throughput capacities," *IEEE Trans. Inf. Theory*, vol. 44, no. 7, pp. 2796–2815, Nov. 1998.

[49] M. Mohseni, R. Zhang, and J. Cioffi, "Optimized transmission for fading multiple-access and broadcast channels with multiple antennas," *IEEE J. Sel. Areas Commun.*, vol. 24, no. 8, pp. 1627–1639, Aug. 2006.

[50] P. Tejera, W. Utschick, J. Nossek, and G. Bauch, "Rate balancing in multiuser MIMO OFDM systems," *IEEE Trans. Commun.*, vol. 57, no. 5, pp. 1370–1380, May 2009.

[51] R. Hunger and M. Joham, "A general rate duality of the MIMO multiple access channel and the MIMO broadcast channel," presented at the IEEE GLOBECOM 2008, New Orleans, LA, USA, Nov. 30–Dec. 4, 2008.

[52] M. Joham, C. Hellings, and R. Hunger, "QoS feasibility for the MIMO broadcast channel: Robust formulation and multi-carrier systems," in *Proc. 8th Int. Symp. Modeling and Optim. Mobile, Ad Hoc, and Wireless Netw. (WiOpt)*, May 2010, pp. 610–614.

[53] S. Herrmann, C. Hellings, and W. Utschick, "Carrier-cooperative zero-forcing for power minimization in parallel MIMO broadcast channels," presented at the 46th Asilomar Conf. Signals, Syst., and Comput. (ACSSC), Pacific Grove, CA, USA, Nov. 4–7, 2012.

[54] G. Kramer, "Topics in multi-user information theory," *Foundations and Trends® Commun. and Inf. Theory*, vol. 4, no. 4–5, pp. 265–444, 2007.

[55] A. E. Gamal and Y.-H. Kim, *Network Information Theory*. Cambridge University Press, 2011.

[56] E. Abbe and L. Zheng, "Coding along Hermite polynomials for interference channels," in *Proc. IEEE Inf. Theory Workshop (ITW) 2009*, Oct. 2009, pp. 584–588.

[57] W. Yu, W. Rhee, S. Boyd, and J. M. Cioffi, "Iterative water-filling for Gaussian vector multiple-access channels," *IEEE Trans. Inf. Theory*, vol. 50, no. 1, pp. 145–152, Jan. 2004.

[58] R. Ahlswede, "Multi-way communication channels," in *Proc. 2nd Int. Symp. Inf. Theory (ISIT)*, 1971, pp. 23—52.

[59] C. E. Shannon, "A mathematical theory of communication," *The Bell System Technical J.*, vol. 27, pp. 379–423 and 623–656, Jul./Oct. 1948.

[60] J. Cioffi, "A multicarrier primer," Committee Contribution, Nov. 1991, ANSI T1E1.4/91-157.

[61] D. P. Palomar and Y. Jiang, "MIMO transceiver design via majorization theory," *Foundations and Trends® Commun. and Inf. Theory*, vol. 3, no. 4–5, pp. 331–551, 2006.

[62] T. Cover and J. Thomas, *Elements of Information Theory*, 2nd ed. Hoboken, NJ: Wiley-Interscience, 2006.

[63] F. D. Neeser and J. L. Massey, "Proper complex random processes with applications to information theory," *IEEE Trans. Inf. Theory*, vol. 39, no. 4, pp. 1293–1302, Jul. 1993.

[64] P. J. Schreier and L. L. Scharf, *Statistical Signal Processing of Complex-Valued Data: The Theory of Improper and Noncircular Signals*. Cambridge, UK: Cambridge University Press, 2010.

[65] D. P. Palomar, M. A. Lagunas, and J. M. Cioffi, "Optimum linear joint transmit-receive processing for MIMO channels with QoS constraints," *IEEE Trans. Signal Process.*, vol. 52, no. 5, pp. 1179–1197, May 2004.

[66] I. Shomorony and A. S. Avestimehr, "Is Gaussian noise the worst-case additive noise in wireless networks?" in *Proc. Int. Symp. Inf. Theory (ISIT) 2012*, Jul. 2012, pp. 214–218.

[67] ——, "Worst-case additive noise in wireless networks," *IEEE Trans. Inf. Theory*, vol. 59, no. 6, pp. 3833–3847, Jun. 2013.

[68] R. A. Horn and C. R. Johnson, *Matrix Analysis*, 2nd ed. Cambridge, UK: Cambridge University Press, 2013.

[69] E. Jorswieck and H. Boche, "Majorization and matrix-monotone functions in wireless communications," *Foundations and Trends® Commun. and Inf. Theory*, vol. 3, no. 6, pp. 553–701, 2007.

[70] A. Marshall, I. Olkin, and B. Arnold, *Inequalities: Theory of Majorization and its Applications*. New York, NY, USA: Springer, 2011.

[71] R. Bhatia, *Matrix Analysis*, ser. Graduate Texts in Mathematics. Springer, 1997, vol. 169.

[72] D. P. Palomar, "Unified framework for linear MIMO transceivers with shaping constraints," *IEEE Commun. Lett.*, vol. 8, no. 12, pp. 697–699, Dec. 2004.

[73] T. S. Blyth and E. F. Robertson, *Further Linear Algebra*. London: Springer, 2002.

[74] B. Picinbono and P. Chevalier, "Widely linear estimation with complex data," *IEEE Trans. Signal Process.*, vol. 43, no. 8, pp. 2030–2033, Aug. 1995.

[75] B. Picinbono, "Second-order complex random vectors and normal distributions," *IEEE Trans. Signal Process.*, vol. 44, no. 10, pp. 2637–2640, Oct. 1996.

[76] P. J. Schreier and L. L. Scharf, "Second-order analysis of improper complex random vectors and processes," *IEEE Trans. Signal Process.*, vol. 51, no. 3, pp. 714–725, Mar. 2003.

[77] T. Adalı, P. J. Schreier, and L. L. Scharf, "Complex-valued signal processing: The proper way to deal with impropriety," *IEEE Trans. Signal Process.*, vol. 59, no. 11, pp. 5101–5125, Nov. 2011.

[78] D. P. Mandic and S. L. Goh, *Complex Valued Nonlinear Adaptive Filters: Noncircularity, Widely Linear and Neural Models*. West Sussex, UK: John Wiley & Sons, 2009.

[79] G. Tauböck, "Complex-valued random vectors and channels: Entropy, divergence, and capacity," *IEEE Trans. Inf. Theory*, vol. 58, no. 5, pp. 2729–2744, May 2012.

[80] H. Karner, J. Schneid, and C. W. Ueberhuber, "Spectral decomposition of real circulant matrices," *Linear Algebra and its Appl.*, vol. 367, pp. 301–311, Jul. 2003.

[81] S. T. Flammia, N. C. Menicucci, and O. Pfister, "The optical frequency comb as a one-way quantum computer," *J. Physics B: Atomic, Molecular and Optical Physics*, vol. 42, no. 114009, pp. 1–12, May 2009.

[82] S. A. Andersson and M. D. Perlman, "Two testing problems relating the real and complex multivariate normal distributions," *J. Multivariate Anal.*, vol. 15, no. 1, pp. 21–51, 1984.

[83] S. A. Andersson, H. K. Brons, and S. T. Jensen, "Distribution of eigenvalues in multivariate statistical analysis," *Ann. Statist.*, vol. 11, no. 2, pp. 392–415, Jun. 1983.

[84] A. T. Walden and P. Rubin-Delanchy, "On testing for impropriety of complex-valued Gaussian vectors," *IEEE Trans. Signal Process.*, vol. 57, no. 3, pp. 825–834, Mar. 2009.

[85] A. Böttcher and I. Spitkovsky, "A gentle guide to the basics of two projections theory," *Linear Algebra and its Appl.*, vol. 432, no. 6, pp. 1412–1459, Mar. 2010.

[86] A. Dotzler, M. Riemensberger, W. Utschick, and G. Dietl, "Interference robustness for cellular MIMO networks," in *Proc. IEEE 13th Int. Workshop Signal Process. Adv. Wireless Commun. (SPAWC)*, Jun. 2012, pp. 229–233.

[87] T. Han and K. Kobayashi, "A new achievable rate region for the interference channel," *IEEE Trans. Inf. Theory*, vol. 27, no. 1, pp. 49–60, Jan. 1981.

[88] N. Hassan and M. Assaad, "Margin adaptive resource allocation in downlink multiuser MIMO-OFDMA system with multiuser eigenmode transmission," in *Proc. IEEE 9th Int. Workshop Signal Process. Adv. Wireless Commun. (SPAWC)*, Jul. 2008, pp. 545–549.

[89] ——, "Low complexity margin adaptive resource allocation in downlink MIMO-OFDMA system," *IEEE Trans. Wireless Commun.*, vol. 8, no. 7, pp. 3365–3371, Jul. 2009.

[90] W. Yu and R. Lui, "Dual methods for nonconvex spectrum optimization of multicarrier systems," *IEEE Trans. Commun.*, vol. 54, no. 7, pp. 1310–1322, Jul. 2006.

[91] C. Guthy, W. Utschick, and G. Dietl, "Spatial resource allocation for the multiuser multicarrier MIMO broadcast channel – a QoS optimization perspective," in *Proc. Int. Conf. Acoust., Speech, and Signal Process. (ICASSP) 2010*, Mar. 2010, pp. 3166–3169.

[92] Q. H. Spencer, A. L. Swindlehurst, and M. Haardt, "Fast power minimization with QoS constraints in multi-user MIMO downlinks," in *Proc. Int. Conf. Acoust., Speech, and Signal Process. (ICASSP) 2003*, vol. 4, Apr. 2003, pp. IV–816–IV–819.

[93] S. Shi, M. Schubert, and H. Boche, "Rate optimization for multiuser MIMO systems with linear processing," *IEEE Trans. Signal Process.*, vol. 56, no. 8, pp. 4020–4030, Aug. 2008.

[94] M. Schubert and H. Boche, "Solution of the multiuser downlink beamforming problem with individual SINR constraints," *IEEE Trans. Veh. Technol.*, vol. 53, no. 1, pp. 18–28, Jan. 2004.

[95] A. Khachan, A. Tenenbaum, and R. Adve, "Linear processing for the downlink in multiuser MIMO systems with multiple data streams," in *Proc. Int. Conf. Commun. (ICC) 2006*, vol. 9, Jun. 2006, pp. 4113–4118.

[96] G. Zheng, K.-K. Wong, and T.-S. Ng, "Throughput maximization in linear multiuser MIMO-OFDM downlink systems," *IEEE Trans. Veh. Technol.*, vol. 57, no. 3, pp. 1993–1998, May 2008.

[97] J. Brehmer, *Utility Maximization in Nonconvex Wireless Systems*, ser. Foundations in Signal Processing, Communications and Networking, W. Utschick, H. Boche, and R. Mathar, Eds. Berlin, Germany: Springer, 2012, vol. 5.

[98] E. Jorswieck and H. Boche, "Rate balancing for the multi-antenna Gaussian broadcast channel," in *Proc. Int. Symp. Spread Spectrum Tech. and Appl. (ISSSTA) 2002*, vol. 2, Sep. 2002, pp. 545–549.

[99] R. Zhang and S. Cui, "Cooperative interference management with MISO beamforming," *IEEE Trans. Signal Process.*, vol. 58, no. 10, pp. 5450–5458, Oct. 2010.

[100] S. Boyd and L. Vandenberghe, *Convex Optimization*. Cambridge, UK: Cambridge University Press, 2009, 7th printing with corrections.

[101] M. S. Bazaraa, H. D. Sherali, and C. M. Shetty, *Nonlinear Programming: Theory and Algorithms*, 3rd ed. Hoboken, NJ, USA: Wiley-Interscience, 2006.

[102] J. E. Kelley, Jr., "The cutting-plane method for solving convex programs," *J. Soc. Indust. and Appl. Math.*, vol. 8, no. 4, pp. 703–712, 1960.

[103] A. Lapidoth, "Nearest neighbor decoding for additive non-Gaussian noise channels," *IEEE Trans. Inf. Theory*, vol. 42, no. 5, pp. 1520–1529, Sep. 1996.

[104] H. Boche and E. Jorswieck, "Multiuser MIMO systems, worst case noise and transmitter cooperation," in *Proc. 3rd IEEE Int. Symp. Signal Process. Inf. Technol. (ISSPIT)*, Dec. 2003, pp. 166–169.

[105] E. Jorswieck and H. Boche, "Performance analysis of capacity of MIMO systems under multiuser interference based on worst-case noise behavior," *EURASIP J. Wireless Commun. and Networking*, vol. 2004, no. 2, pp. 1–13, 2004.

[106] A. Dotzler, M. Riemensberger, and W. Utschick, "Minimax duality for MIMO interference networks," *Information*, vol. 7, no. 2, p. 19, Jun. 2016.

[107] Y. C. Yoon and H. Leib, "Maximizing SNR in improper complex noise and applications to CDMA," *IEEE Commun. Lett.*, vol. 1, no. 1, pp. 5–8, Jan. 1997.

[108] D. Mattera, L. Paura, and F. Sterle, "MMSE WL equalizer in presence of receiver IQ imbalance," *IEEE Trans. Signal Process.*, vol. 56, no. 4, pp. 1735–1740, Apr. 2008.

[109] L. Anttila, M. Valkama, and M. Renfors, "Circularity-based I/Q imbalance compensation in wideband direct-conversion receivers," *IEEE Trans. Veh. Technol.*, vol. 57, no. 4, pp. 2099–2113, Jul. 2008.

[110] W. Zhang, R. C. de Lamare, C. Pan, M. Chen, J. Dai, B. Wu, and X. Bao, "Widely linear precoding for large-scale MIMO with IQI: Algorithms and performance analysis," *IEEE Trans. Wireless Commun.*, vol. 16, no. 5, pp. 3298–3312, May 2017.

[111] H. Liao, "Multiple access channels," Ph.D. Dissertation, Dep. Elec. Eng., Univ. Hawaii, Honlulu, 1972.

[112] A. Goldsmith, *Wireless Communications*. Cambridge, UK: Cambridge University Press, 2005.

[113] E. Biglieri, R. Calderbank, A. Constantinides, A. Goldsmith, A. Paulraj, and H. V. Poor, Eds., *MIMO Wireless Communications*. Cambridge, UK: Cambridge University Press, 2007.

[114] T. Wiegart, C. Hellings, and W. Utschick, "Close-to-optimal partial decode-and-forward rate in the MIMO relay channel via convex programming," in *Proc. 20th Int. ITG Workshop on Smart Antennas (WSA)*, Mar. 2016, pp. 581–588.

[115] E. A. Jorswieck, "Transmission strategies for the MIMO MAC," in *Smart Antennas - State of the Art*, ser. EURASIP Book Series on Signal Processing and Communications, Volume 3, T. Kaiser, A. Bourdoux, H. Boche, J. R. Fonollosa, J. B. Andersen, and W. Utschick, Eds. New York, NY, USA: Hindawi Publishing Corporation, 2005, vol. 3, ch. 21, pp. 423–441.

[116] N. Jindal, W. Rhee, S. Vishwanath, S. Jafar, and A. Goldsmith, "Sum power iterative water-filling for multi-antenna Gaussian broadcast channels," *IEEE Trans. Inf. Theory*, vol. 51, no. 4, pp. 1570–1580, Apr. 2005.

[117] M. Kobayashi and G. Caire, "Iterative waterfilling for weighted rate sum maximization in MIMO-MAC," presented at the IEEE 7th Int. Workshop Signal Process. Adv. Wireless Commun. (SPAWC), Cannes, France, Jul. 2–5, 2006.

[118] ——, "An iterative water-filling algorithm for maximum weighted sum-rate of Gaussian MIMO-BC," *IEEE J. Sel. Areas Commun.*, vol. 24, no. 8, pp. 1640–1646, Aug. 2006.

[119] R. Hunger, D. Schmidt, M. Joham, and W. Utschick, "A general covariance-based optimization framework using orthogonal projections," in *Proc. IEEE 9th Int. Workshop Signal Process. Adv. Wireless Commun. (SPAWC)*, Jul. 2008, pp. 76–80.

[120] H. H. Brunner, A. Dotzler, W. Utschick, and J. A. Nossek, "Weighted sum rate maximization with multiple linear conic constraints," in *Proc. Int. Conf. Commun. (ICC) 2015*, Jun. 2015, pp. 4635–4640.

[121] H. Weingarten, Y. Steinberg, and S. Shamai, "The capacity region of the Gaussian multiple-input multiple-output broadcast channel," *IEEE Trans. Inf. Theory*, vol. 52, no. 9, pp. 3936–3964, Sep. 2006.

[122] M. Costa, "Writing on dirty paper (Corresp.)," *IEEE Trans. Inf. Theory*, vol. 29, no. 3, pp. 439–441, May 1983.

[123] R. Böhnke and K.-D. Kammeyer, "Weighted sum rate maximization for MIMO-OFDM systems with linear and dirty paper precoding," presented at the 7th Int. ITG Conf. Source and Channel Coding (SCC), Ulm, Germany, Jan. 14–16, 2008.

[124] G. Caire and S. Shamai, "On the achievable throughput of a multiantenna Gaussian broadcast channel," *IEEE Trans. Inf. Theory*, vol. 49, no. 7, pp. 1691–1706, Jul. 2003.

[125] G. Dimic and N. Sidiropoulos, "On downlink beamforming with greedy user selection: performance analysis and a simple new algorithm," *IEEE Trans. Signal Process.*, vol. 53, no. 10, pp. 3857–3868, Oct. 2005.

[126] R. Hunger, *Analysis and transceiver design for the MIMO broadcast channel*, ser. Foundations in Signal Processing, Communications and Networking. Berlin: Springer, 2013, vol. 8.

[127] W. H. Gerstacker, R. Schober, and A. Lampe, "Receivers with widely linear processing for frequency-selective channels," *IEEE Trans. Commun.*, vol. 51, no. 9, pp. 1512–1523, Sep. 2003.

[128] D. Mattera, L. Paura, and F. Sterle, "Widely linear MMSE transceiver for real-valued sequences over MIMO channel," presented at the 14th European Signal Process. Conf. (EUSIPCO), Florence, Italy, Sep. 4–8, 2006.

[129] S. Buzzi, M. Lops, and S. Sardellitti, "Widely linear reception strategies for layered space-time wireless communications," *IEEE Trans. Signal Process.*, vol. 54, no. 6, pp. 2252–2262, Jun. 2006.

[130] A. Mirbagheri, K. N. Plataniotis, and S. Pasupathy, "An enhanced widely linear CDMA receiver with OQPSK modulation," *IEEE Trans. Commun.*, vol. 54, no. 2, pp. 261–272, Feb. 2006.

[131] D. Darsena, G. Gelli, and F. Verde, "Universal linear precoding for NBI-proof widely linear equalization in MC systems," *EURASIP J. Wireless Commun. and Networking*, vol. 2008, pp. 8:1–8:11, Jan. 2008.

[132] P. Xiao and M. Sellathurai, "Iterative receiver design for MIMO systems with improper signal constellations," presented at the Int. Conf. Commun. (ICC) 2009, Dresden, Germany, Jun. 14–18, 2009.

[133] ——, "Improved linear transmit processing for single-user and multi-user MIMO communications systems," *IEEE Trans. Signal Process.*, vol. 58, no. 3, pp. 1768–1779, Mar. 2010.

[134] J. Steinwandt, R. C. de Lamare, L. Wang, N. Song, and M. Haardt, "Widely linear adaptive beamforming algorithm based on the conjugate gradient method," presented at the Int. ITG Workshop on Smart Antennas (WSA) 2011, Aachen, Germany, Feb. 24–25, 2011.

[135] Z. Ho and E. Jorswieck, "Secure degrees of freedom on widely linear instantaneous relay-assisted interference channel," in *Proc. IEEE 14th Int. Workshop Signal Process. Adv. Wireless Commun. (SPAWC)*, Jun. 2013, pp. 684–688.

[136] J. Zhang and M. Haardt, "Widely linear signal processing for two-way relaying with MIMO amplify and forward relays," in *Proc. 10th Int. Symp. Wireless Commun. Syst. (ISWCS)*, Aug. 2013, pp. 264–268.

[137] J. Steinwandt, V. Radhakrishnan, and M. Haardt, "Distributed beamforming for cooperative networks with widely-linear processing at the relays and the receiver," in *Proc. Int. Conf. Acoust., Speech, and Signal Process. (ICASSP) 2015*, Apr. 2015, pp. 2714–2718.

[138] B. Hassibi and B. M. Hochwald, "High-rate codes that are linear in space and time," *IEEE Trans. Inf. Theory*, vol. 48, no. 7, pp. 1804–1824, Jul. 2002.

[139] W. H. Gerstacker, F. Obernosterer, R. Schober, A. T. Lehmann, A. Lampe, and P. Gunreben, "Equalization concepts for Alamouti's space-time block code," *IEEE Trans. Commun.*, vol. 52, no. 7, pp. 1178–1190, Jul. 2004.

[140] A. S. Aghaei, K. N. Plataniotis, and S. Pasupathy, "Widely linear MMSE receivers for linear dispersion space-time block-codes," *IEEE Trans. Wireless Commun.*, vol. 9, no. 1, pp. 8–13, Jan. 2010.

[141] P. Chevalier and F. Dupuy, "Widely linear Alamouti receiver for the reception of real-valued constellations corrupted by interferences—the Alamouti-SAIC/MAIC concept," *IEEE Trans. Signal Process.*, vol. 59, no. 7, pp. 3339–3354, Jul. 2011.

[142] D. Darsena, G. Gelli, I. Iudice, and F. Verde, "Widely-linear transceiver design for amplify-and-forward MIMO relaying," presented at the 2016 IEEE Sensor Array Multichannel Signal Process. Workshop (SAM), Rio de Janerio, Brazil, Jul. 10–13, 2016.

[143] U. Erez and S. ten Brink, "A close-to-capacity dirty paper coding scheme," *IEEE Trans. Inf. Theory*, vol. 51, no. 10, pp. 3417–3432, October 2005.

[144] W. Yu, D. P. Varodayan, and J. M. Cioffi, "Trellis and convolutional precoding for transmitter-based interference presubtraction," *IEEE Trans. Commun.*, vol. 53, no. 7, pp. 1220–1230, Jul. 2005.

[145] T. Yoo and A. Goldsmith, "On the optimality of multiantenna broadcast scheduling using zero-forcing beamforming," *IEEE J. Sel. Areas Commun.*, vol. 24, no. 3, pp. 528–541, Mar. 2006.

[146] P. Marsch and D. Tse, "Information-theoretic basics," in *Coordinated Multi-Point in Mobile Communications: From Theory to Practice*, P. Marsch and G. P. Fettweis, Eds. Cambridge, UK: Cambridge University Press, 2011.

[147] R. F. H. Fischer, *Precoding and Signal Shaping for Digital Transmission*. John Wiley & Sons, 2002.

[148] G. D. Forney, Jr, "Trellis shaping," *IEEE Trans. Inf. Theory*, vol. 38, no. 2, pp. 281–300, 1992.

[149] R. D. Wesel and J. M. Cioffi, "Achievable rates for Tomlinson-Harashima precoding," *IEEE Trans. Inf. Theory*, vol. 44, no. 2, pp. 824–831, 1998.

[150] P. de Kerret, R. Hunger, M. Joham, W. Utschick, and R. Mathar, "MIMO broadcast channel rate region with linear filtering at high SNR: Full multiplexing," presented at the Int. Conf. Commun. (ICC) 2011, Kyoto, Japan, Jun. 5–9, 2011.

[151] Q. H. Spencer, A. L. Swindlehurst, and M. Haardt, "Zero-forcing methods for downlink spatial multiplexing in multiuser MIMO channels," *IEEE Trans. Signal Process.*, vol. 52, no. 2, pp. 461–471, Feb. 2004.

[152] F. Boccardi and H. Huang, "A near-optimum technique using linear precoding for the MIMO broadcast channel," in *Proc. Int. Conf. Acoust., Speech, and Signal Process. (ICASSP) 2007*, vol. 3, Apr. 2007, pp. III–17–III–20.

[153] A. D. Dabbagh and D. J. Love, "Precoding for multiple antenna Gaussian broadcast channels with successive zero-forcing," *IEEE Trans. Signal Process.*, vol. 55, no. 7, pp. 3837–3850, Jul. 2007.

[154] C. Guthy, W. Utschick, G. Dietl, and P. Tejera, "Efficient linear successive allocation for the MIMO broadcast channel," in *Conf. Record 42nd Asilomar Conf. Signals, Syst., and Comput. (ACSSC)*, Oct. 2008, pp. 336–340.

[155] C. Guthy, W. Utschick, R. Hunger, and M. Joham, "Efficient weighted sum rate maximization with linear precoding," *IEEE Trans. Signal Process.*, vol. 58, no. 4, pp. 2284–2297, Apr. 2010.

[156] C. Hellings, M. Joham, and W. Utschick, "Power minimization in parallel vector broadcast channels with zero-forcing beamforming," presented at the IEEE GLOBECOM 2010, Miami, FL, USA, Dec. 6–10, 2010.

[157] A. Berman and R. J. Plemmons, *Nonnegative Matrices in the Mathematical Sciences*, ser. Classics in Applied Mathematics. SIAM, 1994, no. 9.

[158] M. Kobayashi and G. Caire, "A practical approach for weighted rate sum maximization in MIMO-OFDM broadcast channels," in *Conf. Record 41st Asilomar Conf. Signals, Syst., and Comput. (ACSSC)*, Nov. 2007, pp. 1591–1595.

[159] M. Codreanu, A. Tölli, M. Juntti, and M. Latva-aho, "Joint design of Tx-Rx beamformers in MIMO downlink channel," *IEEE Trans. Signal Process.*, vol. 55, no. 9, pp. 4639–4655, Sep. 2007.

[160] S. Shi, M. Schubert, and H. Boche, "Weighted sum-rate optimization for multiuser MIMO systems," in *Proc. 41st Annual Conf. Inf. Sci. and Syst. (CISS)*, Mar. 2007, pp. 425–430.

[161] ——, "Capacity balancing for multiuser MIMO systems," in *Proc. Int. Conf. Acoust., Speech, and Signal Process. (ICASSP) 2007*, vol. 3, Apr. 2007, pp. III–397–III–400.

[162] A. Mezghani, M. Joham, R. Hunger, and W. Utschick, "Transceiver design for multi-user MIMO systems," presented at the Int. ITG Workshop on Smart Antennas (WSA) 2006, Ulm, Germany, Mar. 13–14, 2006.

[163] J. Brehmer and W. Utschick, "Utility maximization in the multi-user MISO downlink with linear precoding," presented at the Int. Conf. Commun. (ICC) 2009, Dresden, Germany, Jun. 14–18, 2009.

[164] M. Schubert and H. Boche, "A generic approach to QoS-based transceiver optimization," *IEEE Trans. Commun.*, vol. 55, no. 8, pp. 1557–1566, Aug. 2007.

[165] H. Tuy, *Convex Analysis and Global Optimization*, 2nd ed., ser. Springer Optimization and Its Applications. Springer, 2016, vol. 110.

[166] H. Tuy, F. Al-Khayyal, and P. Thach, "Monotonic optimization: Branch and cut methods," in *Essays and Surveys in Global Optimization*. New York, NY, USA: Springer, 2005, ch. 2, pp. 39–78.

[167] A. Gründinger, M. Joham, and W. Utschick, "Feasibility test and globally optimal beamformer design in the satellite downlink based on instantaneous and ergodic rates," in *Proc. Int. ITG Workshop on Smart Antennas (WSA) 2012*, Mar. 2012, pp. 217–224.

[168] E. A. Jorswieck and E. G. Larsson, "Linear precoding in multiple antenna broadcast channels: Efficient computation of the achievable rate region," in *Proc. Int. ITG Workshop on Smart Antennas (WSA) 2008*, Feb. 2008, pp. 21–28.

[169] ——, "Monotonic optimization framework for the MISO IFC," in *Proc. Int. Conf. Acoust., Speech, and Signal Process. (ICASSP) 2009*, Apr. 2009, pp. 3633–3636.

[170] ——, "Monotonic Optimization Framework for the Two-User MISO Interference Channel," *IEEE Trans. Commun.*, vol. 58, no. 7, pp. 2159–2168, Jul. 2010.

[171] L. P. Qian, Y. J. Zhang, and J. Huang, "MAPEL: Achieving global optimality for a non-convex wireless power control problem," *IEEE Trans. Wireless Commun.*, vol. 8, no. 3, pp. 1553–1563, Mar. 2009.

[172] S. A. Vavasis, "Complexity Issues in Global Optimization: A Survey," Cornell University, Ithaca, NY, USA, Tech. Rep., Jan. 1993.

[173] J. C. D. L. Ducoing, N. Yi, Y. Ma, and R. Tafazolli, "Using real constellations in fully- and over-loaded large MU-MIMO systems with simple detection," *IEEE Commun. Lett.*, vol. 5, no. 1, pp. 92–95, Feb. 2016.

[174] R. Hunger and M. Joham, "A complete description of the QoS feasibility region in the vector broadcast channel," *IEEE Trans. Signal Process.*, vol. 58, no. 7, pp. 3870–3878, Jul. 2010.

[175] H. Boche and M. Schubert, "A general theory for SIR balancing," *EURASIP J. Wireless Commun. and Networking*, vol. 2006, no. 2, pp. 1–18, Apr. 2006.

[176] M. Joham and R. Hunger, "Feasible rate region of the MIMO broadcast channel with linear transceivers," in *Proc. Int. ITG Workshop on Smart Antennas (WSA) 2010*, Feb. 2010, pp. 342–349.

[177] M. Schubert and H. Boche, "Iterative multiuser uplink and downlink beamforming under SINR constraints," *IEEE Trans. Signal Process.*, vol. 53, no. 7, pp. 2324–2334, Jul. 2005.

[178] R. Hunger, D. Schmidt, and M. Joham, "A combinatorial approach to maximizing the sum rate in the MIMO BC with linear precoding," in *Conf. Record 42nd Asilomar Conf. Signals, Syst., and Comput. (ACSSC)*, Oct. 2008, pp. 316–320.

[179] R. Yates, "A framework for uplink power control in cellular radio systems," *IEEE J. Sel. Areas Commun.*, vol. 13, no. 7, pp. 1341–1347, Sep. 1995.

[180] S. S. Christensen, R. Agarwal, E. D. Carvalho, and J. M. Cioffi, "Weighted sum-rate maximization using weighted MMSE for MIMO-BC beamforming design," *IEEE Trans. Wireless Commun.*, vol. 7, no. 12, pp. 4792–4799, Dec. 2008.

[181] M. L. Mehta, *Random Matrices*, 3rd ed. Amsterdam, The Netherlands: Elsevier, 2004.

[182] A. M. Tulino and S. Verdú, "Random matrix theory and wireless communications," *Commun. Inf. Theory*, vol. 1, no. 1, pp. 1–182, 2004.

[183] J. O. Smith III, *Mathematics of the Discrete Fourier Transform: With Audio Applications*. W3K Publishing, 2006.

[184] V. R. Cadambe and S. A. Jafar, "Interference alignment and degrees of freedom of the K-user interference channel," *IEEE Trans. Inf. Theory*, vol. 54, no. 8, pp. 3425–3441, Aug. 2008.

[185] S. Jafar and S. Shamai, "Degrees of freedom region of the MIMO X channel," *IEEE Trans. Inf. Theory*, vol. 54, no. 1, pp. 151–170, Jan. 2008.

[186] L. Sankar, X. Shang, E. Erkip, and H. V. Poor, "Ergodic two-user interference channels: Is separability optimal?" in *Proc. 46th Annu. Allerton Conf. Commun., Control, and Comput.*, Sep. 2008, pp. 723–729.

[187] C. Lameiro and I. Santamaría, "Degrees-of-freedom for the 4-user SISO interference channel with improper signaling," in *Proc. Int. Conf. Commun. (ICC) 2013*, Jun. 2013, pp. 1646–1650.

[188] Z. K. M. Ho and E. Jorswieck, "Improper Gaussian signaling on the two-user SISO interference channel," in *Proc. 8th Int. Symp. Wireless Commun. Syst. (ISWCS)*, Nov. 2011, pp. 824–828.

[189] Y. Zeng, C. M. Yetis, E. Gunawan, Y. L. Guan, and R. Zhang, "Improving achievable rate for the two-user SISO interference channel with improper Gaussian signaling," Nov. 2012, invited paper at the Forty-Sixth Asilomar Conference on Signals, Systems and Computers (ACSSC 2012).

[190] Y. Zeng, R. Zhang, E. Gunawan, and Y. L. Guan, "MISO interference channel with improper Gaussian signaling," in *Proc. Int. Conf. Acoust., Speech, and Signal Process. (ICASSP) 2013*, May 2013, pp. 4374–4378.

[191] S. H. Park, H. Park, and I. Lee, "Coordinated SINR balancing techniques for multi-cell downlink transmission," presented at the IEEE 72nd Veh. Technol. Conf. 2010-Fall, Ottawa, ON, Canada, Sep. 6–9, 2010.

[192] J. Kim, J. Yeo, and J. H. Cho, "Potential of improper-complex signaling in communications over two-user interference channel," in *6th Int. Workshop Signal Design Appl. Commun. (IWSDA)*, Oct. 2013, pp. 4–7.

[193] S. Lagen, A. Agustin, and J. Vidal, "Decentralized widely linear precoding design for the MIMO interference channel," in *Globecom Workshops 2014*, Dec. 2014, pp. 771–776.

[194] ——, "Distributed inter-cluster interference management for CoMP-based cellular networks," in *Proc. IEEE GLOBECOM 2013*, Dec. 2013, pp. 4204–4209.

[195] H.-Y. Shin, S.-H. Park, H. Park, and I. Lee, "Interference alignment with asymmetric complex signaling and multiuser diversity," presented at the IEEE GLOBECOM 2010, Miami, FL, USA, Dec. 6–10, 2010.

[196] ——, "A new approach of interference alignment through asymmetric complex signaling and multiuser diversity," *IEEE Trans. Wireless Commun.*, vol. 11, no. 3, pp. 880–884, Mar. 2012.

[197] A. Kariminezhad, A. Chaaban, and A. Sezgin, "Improper signaling and symbol extensions: How far can we go with Gaussian P2P codebooks in the interfering MAC with TIN?" unpublished. Preprint at https://arxiv.org/abs/1607.01995.

[198] H. D. Nguyen, R. Zhang, and S. Sun, "Improper signaling for symbol error rate minimization in K-user interference channel," *IEEE Trans. Commun.*, vol. 63, no. 3, pp. 857–869, Mar. 2015.

[199] C. Lameiro, I. Santamaría, W. Utschick, and P. J. Schreier, "Maximally improper interference in underlay cognitive radio networks," in *Proc. Int. Conf. Acoust., Speech, and Signal Process. (ICASSP) 2016*, Mar. 2016, pp. 3666–3670.

[200] C. Lameiro, I. Santamaría, and P. J. Schreier, "Benefits of improper signaling for underlay cognitive radio," *IEEE Wireless Commun. Lett.*, vol. 4, no. 1, pp. 22–25, Feb. 2015.

[201] ——, "Analysis of maximally improper signaling schemes for underlay cognitive radio networks," in *Proc. Int. Conf. Commun. (ICC) 2015*, Jun. 2015, pp. 1398–1403.

[202] O. Amin, W. Abediseid, and M. S. Alouini, "Underlay cognitive radio systems with improper Gaussian signaling: Outage performance analysis," *IEEE Trans. Wireless Commun.*, vol. 15, no. 7, pp. 4875–4887, Jul. 2016.

[203] ——, "Overlay spectrum sharing using improper Gaussian signaling," *IEEE J. Sel. Areas Commun.*, vol. 35, no. 1, pp. 50–62, Jan. 2017.

[204] M. Gaafar, O. Amin, W. Abediseid, and M. S. Alouini, "Sharing the licensed spectrum of full-duplex systems using improper Gaussian signaling," presented at the IEEE GLOBECOM 2015, San Diego, CA, USA, Dec. 6–10, 2015.

[205] ——, "Underlay spectrum sharing techniques with in-band full-duplex systems using improper Gaussian signaling," *IEEE Trans. Wireless Commun.*, vol. 16, no. 1, pp. 235–249, Jan. 2017.

[206] S. Lagen, A. Agustin, and J. Vidal, "Improper Gaussian signaling for the Z-interference channel," in *Proc. Int. Conf. Acoust., Speech, and Signal Process. (ICASSP) 2014*, May 2014, pp. 1140–1144.

[207] C. W. Sung, K. W. K. Lui, K. W. Shum, and H. C. So, "Sum capacity of one-sided parallel Gaussian interference channels," *IEEE Trans. Inf. Theory*, vol. 54, no. 1, pp. 468–472, Jan. 2008.

[208] X. Shang, B. Chen, G. Kramer, and H. V. Poor, "MIMO Z-interference channels: Capacity under strong and noisy interference," in *Conf. Record 43rd Asilomar Conf. Signals, Syst., and Comput. (ACSSC)*, Nov. 2009, pp. 667–671.

[209] ——, "Capacity regions and sum-rate capacities of vector Gaussian interference channels," *IEEE Trans. Inf. Theory*, vol. 56, no. 10, pp. 5030–5044, Oct. 2010.

[210] X. Shang and H. V. Poor, "Noisy-interference sum-rate capacity for vector Gaussian interference channels," *IEEE Trans. Inf. Theory*, vol. 59, no. 1, pp. 132–153, Jan. 2013.

[211] J. Lee and N. Jindal, "High SNR analysis for MIMO broadcast channels: Dirty paper coding versus linear precoding," *IEEE Trans. Inf. Theory*, vol. 53, no. 12, pp. 4787–4792, Dec. 2007.

[212] R. Hunger and M. Joham, "An asymptotic analysis of the MIMO broadcast channel under linear filtering," in *Proc. 43rd Annual Conf. Inf. Sci. and Syst. (CISS)*, Mar. 2009, pp. 494–499.

[213] A. S. Motahari, S. Oveis-Gharan, M. A. Maddah-Ali, and A. K. Khandani, "Real interference alignment: Exploiting the potential of single antenna systems," *IEEE Trans. Inf. Theory*, vol. 60, no. 8, pp. 4799–4810, Aug. 2014.

[214] E. C. van der Meulen, "Three-terminal communication channels," *Advances in Applied Probability*, vol. 3, no. 1, pp. 120–154, 1971.

[215] B. Wang, J. Zhang, and A. Høst-Madsen, "On the capacity of MIMO relay channels," *IEEE Trans. Inf. Theory*, vol. 51, no. 1, pp. 29–43, Jan. 2005.

[216] X. Jin and Y.-H. Kim, "The approximate capacity of the MIMO relay channel," *IEEE Trans. Inf. Theory*, vol. 63, no. 2, pp. 1167–1176, Feb. 2017.

[217] T. Cover and A. El Gamal, "Capacity theorems for the relay channel," *IEEE Trans. Inf. Theory*, vol. 25, no. 5, pp. 572–584, Sep. 1979.

[218] G. Kramer, M. Gastpar, and P. Gupta, "Cooperative strategies and capacity theorems for relay networks," *IEEE Trans. Inf. Theory*, vol. 51, no. 9, pp. 3037–3063, Sep. 2005.

[219] S. Simoens, O. Muñoz-Medina, J. Vidal, and A. del Coso, "On the Gaussian MIMO relay channel with full channel state information," *IEEE Trans. Signal Process.*, vol. 57, no. 9, pp. 3588–3599, Sep. 2009.

[220] C. T. K. Ng and G. J. Foschini, "Transmit signal and bandwidth optimization in multiple-antenna relay channels," *IEEE Trans. Commun.*, vol. 59, no. 11, pp. 2987–2992, Jul. 2011.

[221] L. Gerdes and W. Utschick, "Optimized capacity bounds for the MIMO relay channel," in *Proc. Int. Conf. Acoust., Speech, and Signal Process. (ICASSP) 2011*, May 2011, pp. 3336–3339.

[222] J. N. Laneman, D. N. C. Tse, and G. W. Wornell, "Cooperative diversity in wireless networks: Efficient protocols and outage behavior," *IEEE Trans. Inf. Theory*, vol. 50, no. 12, pp. 3062–3080, Dec. 2004.

[223] A. El Gamal, M. Mohseni, and S. Zahedi, "Bounds on capacity and minimum energy-per-bit for AWGN relay channels," *IEEE Trans. Inf. Theory*, vol. 52, no. 4, pp. 1545–1561, Apr. 2006.

[224] Y. Fan and J. Thompson, "MIMO configurations for relay channels: Theory and practice," *IEEE Trans. Wireless Commun.*, vol. 6, no. 5, pp. 1774–1786, May 2007.

[225] Y. Rong and F. Gao, "Optimal beamforming for non-regenerative MIMO relays with direct link," *IEEE Commun. Lett.*, vol. 13, no. 12, pp. 926–928, 2009.

[226] S. Simoens, O. Muñoz-Medina, J. Vidal, and A. del Coso, "Compress-and-forward cooperative MIMO relaying with full channel state information," *IEEE Trans. Signal Process.*, vol. 58, no. 2, pp. 781–791, Feb. 2010.

[227] A. El Gamal and M. Aref, "The capacity of the semideterministic relay channel," *IEEE Trans. Inf. Theory*, vol. 28, no. 3, pp. 536–536, May 1982.

[228] C. K. Lo, S. Vishwanath, and R. W. Heath, "Rate bounds for MIMO relay channels," *J. Commun. Netw.*, vol. 10, no. 2, pp. 194–203, Jun. 2008.

[229] L. Gerdes, L. Weiland, and W. Utschick, "A zero-forcing partial decode-and-forward scheme for the Gaussian MIMO relay channel," in *Proc. Int. Conf. Commun. (ICC) 2013*, Jun. 2013, pp. 1942–1947.

[230] L. Weiland, L. Gerdes, and W. Utschick, "Partial decode-and-forward rates for the Gaussian MIMO relay channel: Inner approximation of non-convex rate constraints," in *Proc. IEEE 14th Int. Workshop Signal Process. Adv. Wireless Commun. (SPAWC)*, Jun. 2013, pp. 540–544.

[231] L. Gerdes, L. Weiland, M. Riemensberger, and W. Utschick, "Optimal partial decode-and-forward rates for stochastically degraded Gaussian relay channels," presented at the 48th Annual Conf. Inf. Sci. and Syst. (CISS), Princeton, NJ, USA., Mar. 2014.

[232] L. Gerdes, C. Hellings, L. Weiland, and W. Utschick, "On the maximum achievable partial decode-and-forward rate for the Gaussian MIMO relay channel," *IEEE Trans. Inf. Theory*, vol. 61, no. 12, pp. 6751–6758, Dec. 2015.

[233] Y. Liang and G. Kramer, "Rate regions for relay broadcast channels," *IEEE Trans. Inf. Theory*, vol. 53, no. 10, pp. 3517–3535, Oct. 2007.

[234] Y. Rong, X. Tang, and Y. Hua, "A unified framework for optimizing linear nonregenerative multicarrier MIMO relay communication systems," *IEEE Trans. Signal Process.*, vol. 57, no. 12, pp. 4837–4851, Dec. 2009.

[235] Y. Liang, V. Veeravalli, and H. Poor, "Resource allocation for wireless fading relay channels: Max-min solution," *IEEE Trans. Inf. Theory*, vol. 53, no. 10, pp. 3432–3453, Oct. 2007.

[236] L. Gerdes, "Capacity bounds and achievable rates for the Gaussian MIMO relay channel," Ph.D. Dissertation, Fachgebiet Methoden der Signalverarbeitung, Technische Universität München, 2016.

[237] M. G. M. Khafagy, "On the performance of in-band full-duplex cooperative communications," Ph.D. Dissertation, King Abdullah University of Science and Technology (KAUST), Thuwal, Saudi Arabia, 2016.

[238] M. Gaafar, M. G. Khafagy, O. Amin, and M. S. Alouini, "Improper Gaussian signaling in full-duplex relay channels with residual self-interference," presented at the Int. Conf. Commun. (ICC) 2016, Kuala Lumpur, Malaysia, May 22–27, 2016.

[239] M. Gaafar, O. Amin, A. Ikhlef, A. Chaaban, and M. S. Alouini, "On alternate relaying with improper Gaussian signaling," *IEEE Commun. Lett.*, vol. 20, no. 8, pp. 1683–1686, Aug. 2016.

[240] M. Gaafar, O. Amin, R. F. Schaefer, and M.-S. Alouini, "Improper signaling for virtual full-duplex relay systems," presented at the Int. ITG Workshop on Smart Antennas (WSA) 2017, Berlin, Germany, Mar. 15–17, 2017.

[241] ——, "Improper signaling in two-path relay channels," presented at the Int. Conf. Commun. (ICC) Workshops 2017, Paris, France, May 21–25, 2017.

[242] A. Kariminezhad, A. Sezgin, and M. Pesavento, "Power efficiency of improper signaling in MIMO full-duplex relaying for K-user interference networks," presented at the Int. Conf. Commun. (ICC) 2017, Paris, France, May 21–25, 2017.

[243] Z. Ho, A. Zappone, and E. Jorswieck, "Optimal non-regenerative relay processing with improper signals," in *Proc. 10th Int. Symp. Wireless Commun. Syst. (ISWCS)*, Aug. 2013, pp. 567–571.